ROCK BREAKAGE IN PERCUSSIVE DRILLING

CLAUDE DROUIN, Ph. D. Thesis

July 1971

AUTEUR : CLAUDE DROUIN

TITRE DE LA THESE : Fragmentation de la Roche dans la Foration Percutante

DEPARTEMENT : Génie Minier et Géophysique Appliquée

GRADE : Philisophiae Doctor

EXTRAIT

La foration percutante de la roche est une opération poussiéreuse, dangereuse pour la santé des mineurs. Les méthodes actuelles d'élimination des poussières faillissent à procurer un environnement de travail sain; c'est pourquoi l'objectif de cette recherche était la compréhension du mécanisme de formation des poussières afin de pouvoir les éliminer à la source. Cette recherche était fondée sur les théories de la foration percutante et de la fragmentation des roches. L'étude fut exécutée en laboratoire au moyen d'un marteau à impact simple.

Une méthode de fragmentation en laboratoire a été trouvée satisfaisante pour simuler le broyage en foration percutante à partir de laquelle l'auteur a pu calculer la quantité de roche cassée par cisaillement, la quantité par la première onde incidente d'énergie et celle par la première onde réfléchie lors de l'application du coup de marteau. L'auteur démontre que l'onde réfléchie ne fait aucun travail utile et que son énergie sert exclusivement à pulvériser du matériel déjà broyé et à engendrer de la poussière. Enfin l'auteur conclut qu'une foreuse à percussion devrait avoir un système indépendant de rotation et une

forte fréquence de frappes relativement faibles pour pénétrer rapidement dans la roche et produire le minimum de poussière. La préparation de taillants asymétriques apparaît comme désirable.

ROCK BREAKAGE IN PERCUSSIVE DRILLING

A Thesis

Submitted to the Faculty of

Graduate Studies and Research

by

CLAUDE DROUIN

In partial fulfilment of the

requirements for the Degree of

DOCTOR OF PHILOSOPHY

Department of Mining Engineering
and Applied Geophysics,
McGill University,
Montreal

July 1971

TABLE OF CONTENTS

AUTHOR : Claude Drouin

TITLE OF THESIS : Rock Breakage in Percussive Drilling

DEPARTMENT : Mining Engineering and Applied Geophysics

DEGREE : Doctor of Philosophy

ABSTRACT

Percussive rock drilling is a dusty operation creating a health hazard for the miners. Since the current methods of dust control fail to provide a sanitary environment, this research was planned to explain the mechanism of dust formation in view of its elimination at the source. The theories of comminution and percussive drilling were used in this project to study the drilling process by means of a laboratory single-blow rock-drill.

A comminution test was found to represent rock breakage in percussive drilling from which it was possible to calculate the amount of rock broken by chipping during a bit impact, the amount of rock broken by the first incident stress wave and the rock broken by the first reflected stress wave. It was found that no useful work is performed by the reflected stress wave and that its energy is used exclusively in pulverizing already broken rock. The test also permits the determination of the number of fracture events per single impact blow; these small fracture events have been called

micro-events. If the objective is to produce the least amount of dust, it is concluded that a percussive rock drill should have an independent rotation, a high blow rate and a low blow energy in order to enjoy a high penetration rate. The design of non-symmetrical bits appear desirable.

ACKNOWLEDGMENTS

The author is most grateful to the many people who have made contributions to this investigation,

Professor F.T.M. White for his guidance and encouragement throughout this work;

Professor W. Bardswick, Dr. J.E.G. Schwellnus and Dr. K.J. Reid for their advice and helpful suggestions;

L'Université de Montréal and Dr. Maurice Panisset, Dean of the School of Public Health, for allowing this research work to be done while employed by them;

The technicians from the Institute for Mineral Industry Research at Mont St-Hilaire for assistance in the design and construction of the testing equipment;

Mr. Michel Gagnon for his help with figure preparation;

Fellow graduate students, particularly Mr. C.G. Ong, for their interest and assistance; and

My wife Mimi and children who provided the necessary environment to permit the successful completion of this work.

GLOSSARY

Bit	In this thesis, unless otherwise specified, bit refers to a tungsten carbide chisel bit with an included angle of 110° between faces of the wedge.
Bit Cutting Angle	This is the included angle between the two faces of the chisel bit. The term is used interchangeably with wedge angle or bit included angle.
Crater	The hole made by the bit impact on the rock surface.
Crater Area	The cross-sectional area of the crater measured at right angle to the longitudinal central axis of the bit.
Dispersion	This is the extent of the scatter or dispersion of particle size around the average (Herdan (57)). An assembly of particles is monodispersed if all particles belong to the same class size, otherwise, it is heterodispersed.
Dust	As this term is loosely defined and must include respirable particles as well as a certain amount of coarser particles, it was decided in this thesis to consider as dust, particles passing through the 325 mesh sieve.
History Factors	An expression used by Bennett, Brown and Crone (7) to represent the sum of weakness planes present in a mass of rock at a given time due to its geological history as well as its previous mining and milling history.
IBULCE	An abbreviation used by Irving (62) to represent the Intensity of Blow per Unit Length of Cutting Edge.
Index Angle	The angle turned by a drill steel between successive blows. Theoretically, the rock between the position of two successive blows is completely removed to the bottom of the crater when there is indexed fracture.
Indexed Fracture	This is described by Simon (81) as the complete removal of rock between the position of two successive blows when the blow energy is sufficient.

Indexing Distance	This is defined by Simon (81) as the distance between successive impacts, when dealing with parallel blows on the surface of a rock and when indexed fracture occurs.
Rock Drilling	In this thesis, unless otherwise specified, this expression means pneumatic percussive rock drilling.
Rock Drill	In this thesis, pneumatic percussive rock drills available on the market were sometimes referred to as actual drills, conventional drills, commercial drills, standard drills or rock drills.
Size Distribution	This expression was used to represent the cumulative size distribution of particles passing through a sieve of a given size opening.
Specific Energy	This is the energy used per unit volume of rock broken in a given process. In this thesis, specific energy was calculated per unit weight of rock broken per blow.

LIST OF FIGURES

LIST OF FIGURES (continued)

LIST OF FIGURES (continued)

LIST OF FIGURES (continued)

LIST OF TABLES

LIST OF SYMBOLS

a	drill steel cross-sectional area
A	parameter in Charles' Law (Equation 3.8)
b	bit diameter
B	breakage matrix
B_e	blow energy
B_F	blow frequency
c	stress wave velocity in drill steel
C	parameter in Gilliland's Law (Equation 3.7)
d	drill steel diameter
d	derivative symbol
D	piston diameter
D	matrix describing the machine operation
E_η	energy level
E	Young's modulus
f	feed size distribution vector
F	force acting on bit (fig. 2.1)
F_s	feed size - Bond's Law
F_j	instantaneous value of the force acting on a bit (fig. 2.1)
F_o	initial force on drill steel
F_T	forward thrust
H	depth of crater
i_η	optimum index angle for energy level E_η
I	unit matrix

k	proportionality factor in Irving's relation (Equation 2.13)
k	size modulus in Gaudin-Schuhmann's equation
K	average slope of the force-penetration diagram (fig. 2.1)
K_j	slope of a given segment on the force-penetration diagram (fig. 2.1)
L	length of drill rod
m	mass of drill steel
M	mass of piston
n	number of blows per half revolution
n	exponent in Gilliland's equation
N	exponent in Hartman's relation for depth of crater (Equation 2.15)
N	tensile stress normal to plane of crack
P	product size distribution vector
P_s	product size - Bond's Law
P	point on the force-penetration diagram corresponding to coordinates (U, F) (fig. 2.1)
P_1	point of maximum force on the force-penetration diagram (fig. 2.1)
P_j	a specific point on the force-penetration diagram located by the coordinates (U_j, F_j)
r	radius of drill rod
S	selection matrix
t	time; independent variable in the fundamental model of percussive drilling
U	penetration corresponding to force F (fig. 2.1)
U_j	penetration corresponding to force F_j (fig. 2.1)
v	particle velocity in drill rod

V	piston velocity
W_i	work index
W_p	weight of the piston
X	size of particle
Y	percentage of material in weight passing through sieve of size X
a	size distribution factor in Gaudin-Schuhmann model
α	constant index angle
β	variable index angle
β_c	corrected exponent in Charles' Law (Equation 3.11)
γ	decay factor
δ	stem rigidity factor
ζ	fraction of incident energy
θ	total bit included angle
λ	thickness of crack (Griffith's equation 3.1)
ν	radius at the tip of a crack (Griffith's relation 3.1)
ρ	density of the drill steel
ρ_b	bit radius
σ	instantaneous value of stress in drill rod
σ_i	incident stress in drill steel
σ	reflected stress in drill steel
σ_t	stress at time t
τ	duration of energy transfer
Υ	volume of crater

ϕ angle made by a segment of the force-penetration diagram and the penetration axis (fig. 2.1)

ψ angle made by the line estimating the average force-penetration relation and the penetration axis (fig. 2.1)

Ψ breaking stress in Griffith's equation 3.1

ω total index angle

I - INTRODUCTION

The author is primarily interested in the control of the mining environment for the prevention of industrial pneumoconiosis. Rock drilling is a well-known occupation leading to dangerous dust exposure and hygienists are still searching for an efficient method of dust control during this operation. A logical approach to the solution of this problem is the elimination of the dust at the source but this is possible only if the dust formation process is correctly understood.

In this research, rock drilling was considered as a comminution process, and conclusions were drawn from the study of particle size distributions. An attempt was made to establish a comminution model of rock drilling which would permit the understanding of dust formation during the process. This knowledge would lead to the statement of the necessary conditions for the design of more efficient and less dusty equipment.

A very large number of publications were consulted during this research but the key authors behind this work are Epstein (33), Broadbent & Callcott (16), Brown et al (6, 7, 8, 19), Reid et al (63), Kinasevich et al (29), Harris (50), Hustrulid (60), Simon (81, 82, 83), Fairhurst (36, 37, 38), Hartman (53, 54, 55) and Cheatham et al (24, 25, 61).

This thesis constitutes a link between the theories of comminution and percussion drilling.

II - REVIEW OF PERCUSSIVE DRILLING THEORIES

A - INTRODUCTION

Mechanical rock drills were first introduced in 1855 and the general principles of the machine designed by George Leyner in 1897 can still be found in the present rock drill. A rock drill consists of a simple chamber in which a piston moves freely back and forth. Compressed air, which is admitted at the rear end of the piston by means of a valve, moves the piston forward towards the end of the chamber where it comes in contact with the end of a length of drill steel. Rebound from the drill steel as well as the action of a valve return the piston to its original position. The piston is so designed that a rifle bar engages a nut which rotates the machine chuck and hence, the drill steel; a ratchet system limits rotation of the drill steel to the return stroke (Fig. 2.8).

The literature on percussive drilling comprises facets of highly empirical work and/or sophisticated theoretical analysis. The recent doctoral dissertation on percussive drilling by Hustrulid (60) is probably the most up-to-date document on the subject. From the environmental point of view, reference must be made to the contributions of Hartman (53), Cheatham and Inett (24) and Inett (61). At present, there is no document available to explain the mechanism of dust formation by percussive drills. One of the objects of this dissertation is to develop a theory to explain rock breakage in percussive drilling and eventually dust

formation.

The purpose of this literature review on percussive drilling is to present and discuss some of the pertinent theories related to the objectives of the author. The fundamental theories of percussive drilling developed by Drilling Research Incorporated (81) and The University of Minnesota (38,60) are first reviewed and then, the findings of various researchers on the influence of specific rock drilling variables are studied.

B - THE PROCESS OF ROCK DRILLING

A rock drill converts the potential energy of compressed air into piston kinetic energy which is most efficiently transmitted when the drill steel is in contact with the rock at the instant when the piston strikes the end of the drill steel. Penetration rate will depend upon machine design, drill steel properties, rock properties and the thrust which keeps the drill steel in contact with the rock. In the first part of this section, attention will be focused upon Hustrulid's drilling model.

1 - Drill Bit Penetration Into Rock

Attemps (54, 37, 78) to explain the sequence of events in bit penetration agree fairly well and the findings may be summarized as follows:

(i) surface irregularities are crushed upon impact;

(ii) energy transmitted to the rock below the wedge of the drill bit causes the rock to deform elastically and plastically;

(iii) a major crack develops below the tip of the wedge;

(iv) two converging cracks propagate axially from the perimeter of the indent. The rock contained between these cracks (Fig 6.10) is pulverized and rock porosity controls its degree of compaction;

(v) a quasi-hydrostatic pressure which builds up within the crushed wedge of rock produces a series of radial cracks in the rock originating from the wedge. The cracks which occur nearer the surface of the rock curve upward due to the low pressure of the free face and result in large spall fragments;

(vi) the removal of the larger fragments on either side of the bit permits the crumbling of the upper part of the crushed wedge. This causes the bit suddenly to penetrate the rock. The above process is repeated as long as energy is available;

(vii) in this thesis, each cycle as described above is called a micro-event.

The sequence of events described above is shown in the force-penetration diagram (Fig. 2.1). Here, the positive slope sections represent elastic and plastic deformation and

crushing (38). The change of slope to a negative value occurs when chipping begins and the negative slope represents the sudden penetration due to the crumbling of the central wedge. The return to the positive slope occurs when the load is reapplied. The steeper slope of subsequent sections is attributed to the different bottom conditions (60) and the contact of the inclined faces of the bit with the rock surface (54).

Mathematically, the position of any point on the Force-Penetration curve (Fig. 2.1) may be expressed by the relationship from Hustrulid (60):

$$F = F_j + K_j(U - U_j) \qquad (2.1)$$

where U = penetration corresponding to the force F

K_j = slope of segment originating at the point P_j

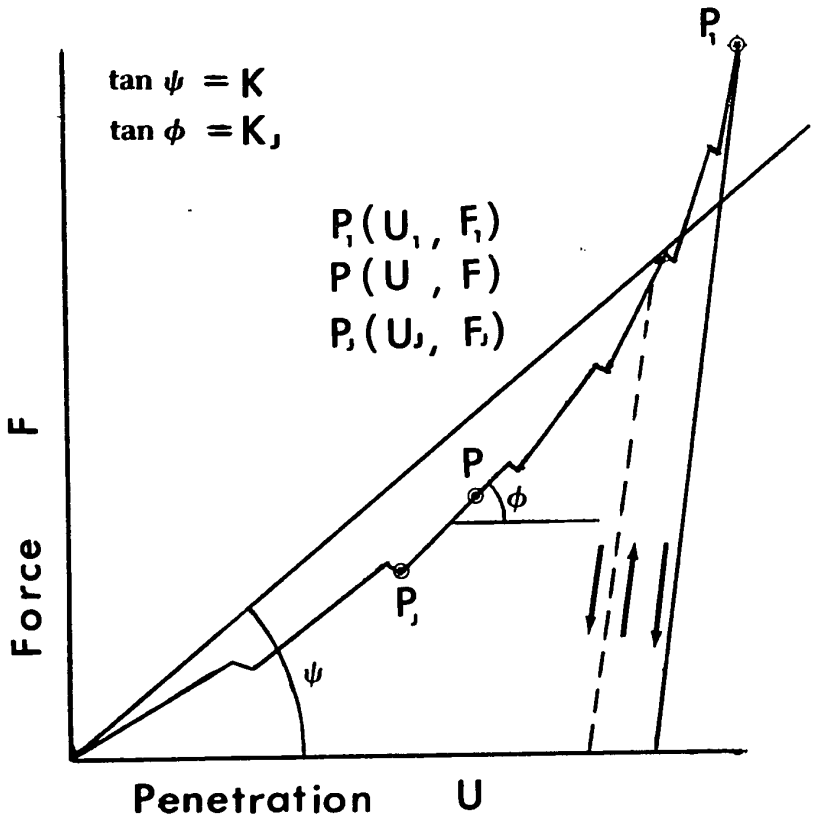

Fig. 2.1

Theoretically, if the energy were released at P, Fig. 2.1, the bit would move upward due to elastic rock deformation and particle movement. If the load was reapplied, the force-penetration curve would follow the same line as the previous unloading curve. Additional penetration would occur if the applied force at P_1 is larger than that at P. Unloading at P_1 would follow a line parallel to the original unloading at P. The average slope K of the jagged line represents the resistance of the rock to penetration (Fig. 2.1).

2 - Static Versus Dynamic Loading

Several researchers (78, 60) have found that the properties of rocks differ under static and dynamic conditions. It is well-recognized that the static resistance to penetration is half that of dynamic resistance and consequently, the specific energy of rock fracture in the dynamic formation of craters is twice that obtained under static conditions. However, there is evidence that the value K is related to the bit cutting angle. Rock mechanics researchers are satisfied with the results obtained under dynamic conditions because they claim that the range of values found by these methods is comparable to those met with in rock drilling (36).

Cheatham (25) developed a series of equations to describe the static force-penetration relations for a smooth tooth and a dull tooth into an idealized rock. His theories apply to rocks under high confining pressure and are intended for rotary drilling. Gnirk (45) and Garner (40) tested the theories

experimentally and found that the jagged F-U penetration curve (Fig. 2.1) becomes smooth under heavy confining pressures.

The confusion concerning the effect of blow velocity is particularly apparent when the geometry of the crater is considered. It is generally accepted that the volume of the crater is proportional to the energy of the blow, but the shape of the crater varies with velocity. According to Hartman (54), high velocity blows will have a tendency to produce shallow craters of wide area while low velocity blows cut deep craters of relatively smaller area. Experiments carried out with impacting bullets (71) led to the same conclusions.

3 - Indexing

Indexed fracture (Fig. 2.4) of rock occurs when the blow is powerful enough to remove completely the material located between two consecutive blows (Fig. 2.2). If the indexing distance is too large, the crater formed by the blow will be a function of the energy of the blow and of the shape of the bit. Simon (81) and Hartman (55) made detailed studies of indexing and a review of the present knowledge on the subject is presented by Hustrulid (60).

Simon presented a theory of rock drilling based upon experiments with parallel blows (Fig. 2.2). He arrived at a bell-shaped curve (Fig. 2.3) relating the indexing distance with the cross-sectional area (Fig. 2.4) of the indexed crater. Hartman obtained similar results and idealized the plot of his data as shown in Fig. 2.5. Both curve plots illustrate the same

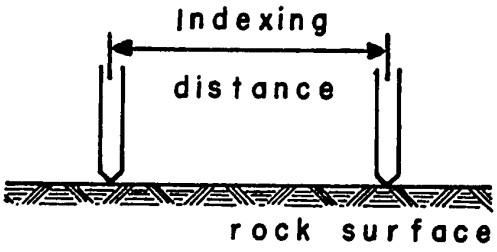

Fig. 2.2

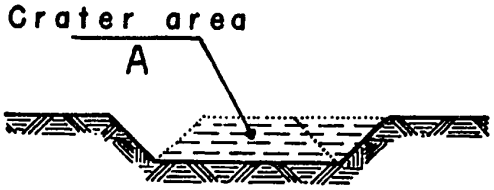

Fig. 2.4

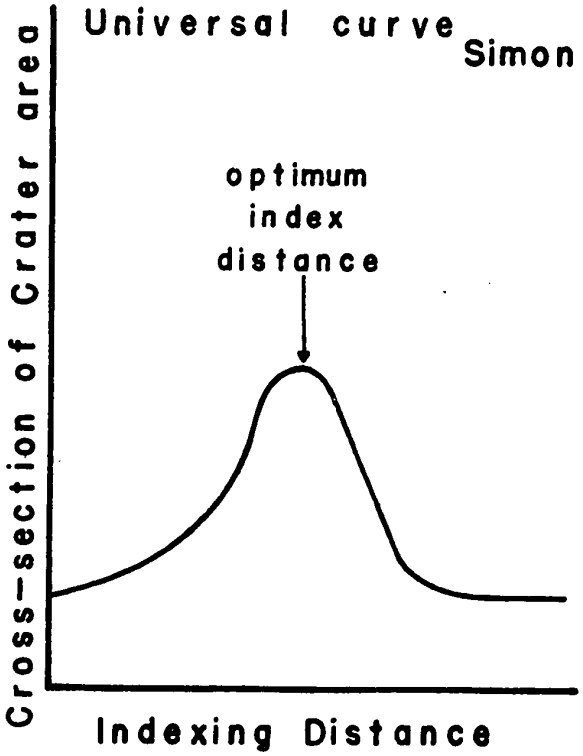

Fig. 2.3

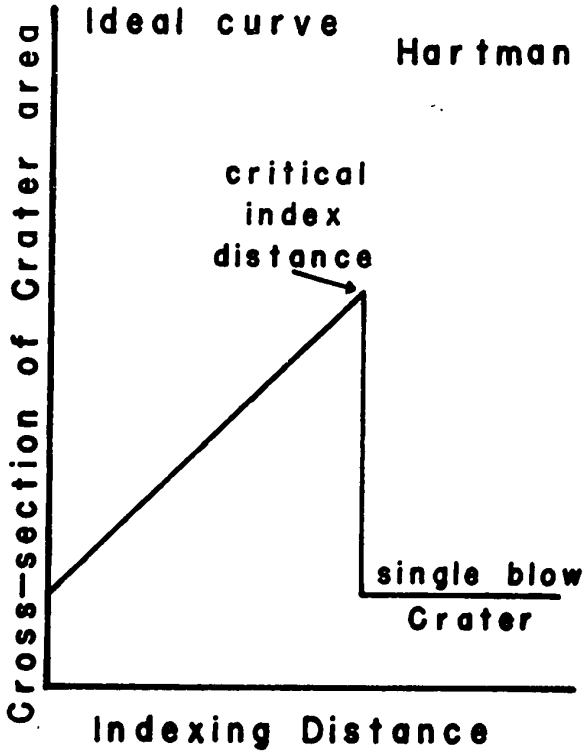

Fig. 2.5

phenomenon. The section at the left of the maximum shows that, if the indexing distance is kept below a critical value for a given energy, the material located between any two parallel blows will be completely removed. Furthermore, a decrease in specific energy will result when the indexing distance is increased. Further increases in indexing distance beyond a critical distance will present a series of individual craters of equal volume, as shown by the flat section to the right of the maximum (Fig. 2.3).

Both Simon and Hartman used parallel blows on the surface of rocks to study indexing, but their results do not necessarily pertain to a drill hole at a depth beyond the influence of the collar. Neither Simon's Universal curve nor Hartman's Ideal curve represents the actual index-angle-crater-area curve in a borehole. The latter curve is believed to be as shown in Fig. 2.6, but the specific energy curve will have a reverse shape. It is on this basis that Hartman (55) provides little incentive for the design of percussion drill with independent rotation. The writer will present a different view concerning indexing.

The current results of research to date supports the following conclusions (81, 37, 54, 55, 60).

(i) parallel blows of any given energy level will have an indexing distance for which the specific energy is a minimum. This minimum specific energy value is constant for a given combination of bit and rock type (Fig. 2.7);

Variation of Rock Breakage Specific Energy with the Index Angle

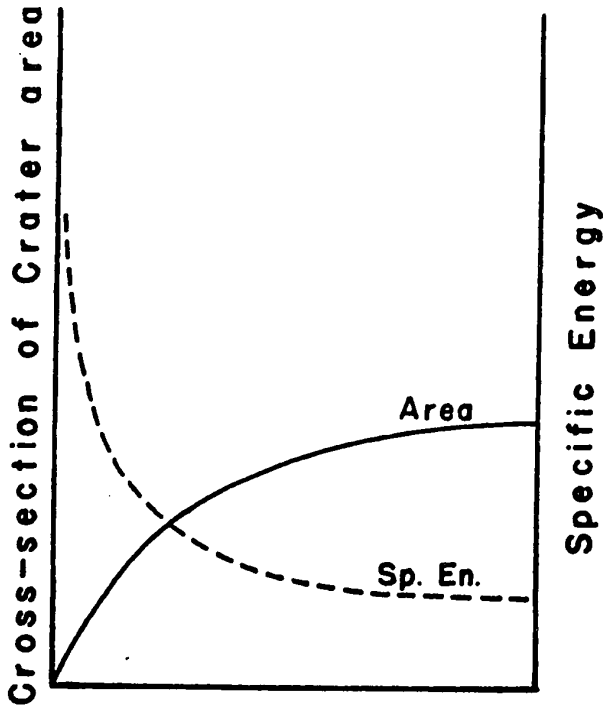

Fig. 2.6

(ii) the specific energy of rock breaking with an impacting drill bit depends upon the energy of the blow and the index angle;

(iii) there is a minimum value of specific energy for a given bit-rock combination which is independent of the blow energy. It appears probable that the following relation may be used to predict the optimum index angle for a given energy (60);

$$\frac{i_1}{i_2} = \frac{E_1}{E_2} \qquad (2.2)$$

i_η = Optimum index angle for energy level E_η

(iv) to date, it has not been possible to correlate data on single crater volume and indexed fracture.

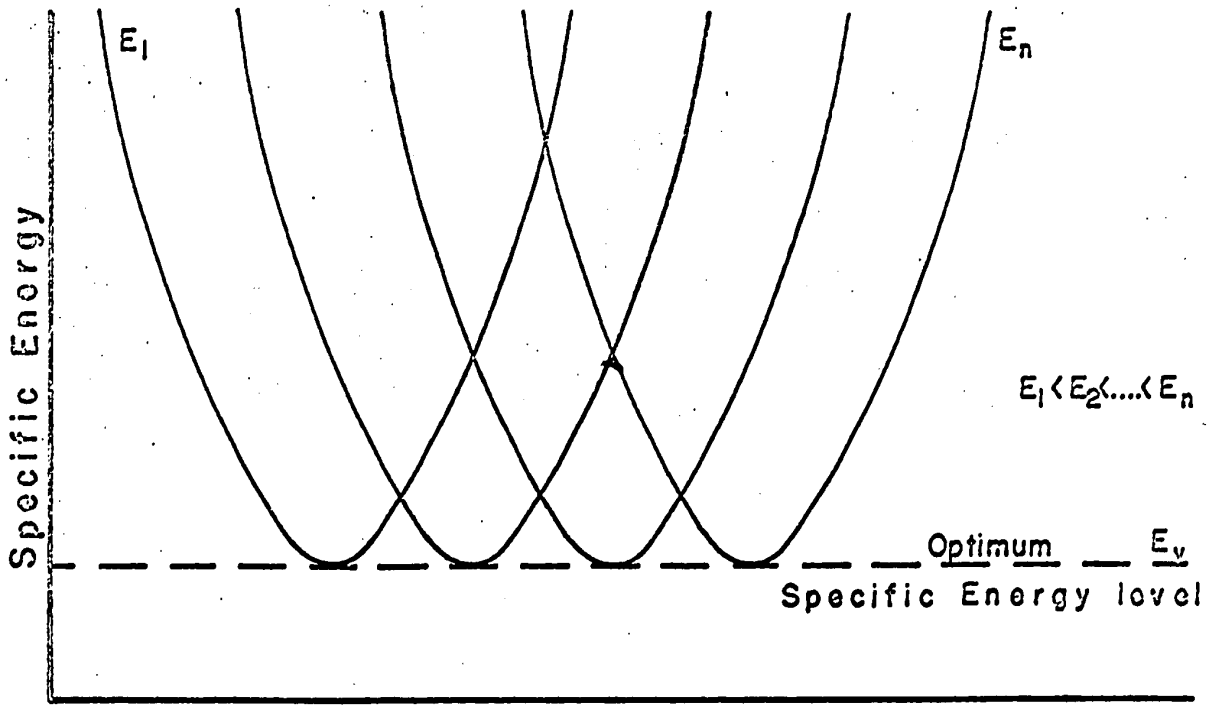

Fig. 2.7

Similarly, bit shape data and single crater geometry do not provide any satisfactory correlation rule.

4 - Theory of Percussive Drilling (60)

Schematically, the rock drill operation may be illustrated as shown in Fig. 2.8. The drilling cycle is initiated by the introduction of compressed air at the rear end of the piston which is accelerated towards the drill steel. If the drill steel collar is in contact with the machine when the piston reaches its forward limit, energy will be transmitted to the drill steel; similarly, if the drill bit is in contact with the rock at the time of arrival of the stress wave, energy will be

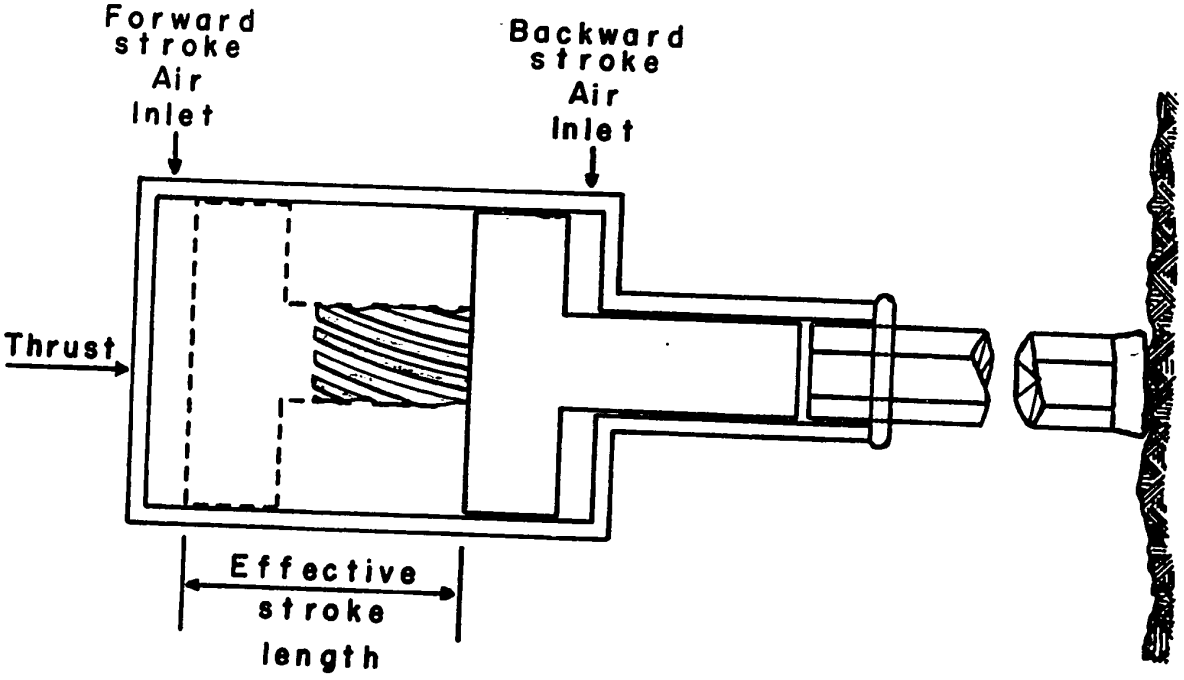

Percussive Drill Principle
Fig. 2.8

transmitted to the rock and penetration will occur. However, as there is elastic deformation in the rock as well as in the drill steel, a fraction of the incident energy is returned to the drill steel and travels back to the piston.

The instantaneous force F at one point of the drill steel at a specific time is then given by the relation

$$F = \left(\sigma_i + \sigma_R\right)a + F_0 \qquad (2.3)$$

where σ_i = incident stress, instantaneous;

σ_R = reflected stress, instantaneous;

a = drill steel cross-sectional area;

F_0 = force between bit and rock before arrival of incident stress wave, (considered to be negligible).

The theories of elasticity have shown that the particle velocity in a bar struck axially is given by the relation

$$\frac{v}{c} = \frac{\sigma}{E} \qquad (2.4)$$

where v = particle velocity, or velocity of the bar after impact $v = \frac{dU}{dt}$;

c = wave velocity in the drill steel;

E = Young's Modulus of the drill steel;

σ = instantaneous value of the stress at a given point in the drill steel; as the incident wave σ_i, and the reflected wave σ_R are travelling in opposite directions, we can write in this particular case

$$\sigma = \sigma_i - \sigma_R$$

Therefore, the actual particle velocity equation may be written as follows:

$$\frac{dU}{dt} = \frac{c}{E}\left(\sigma_i - \sigma_R\right) + v_0 \qquad (2.5)$$

v_0 = velocity of drill steel before the piston impact, considered to be negligible.

Equations 2.3 and 2.5 indicate that the shape of the stress waves determines the penetration rate of the drill steel when the necessary thrust is maintained.

Equations 2.1, 2.3 and 2.5 were combined by Hustrulid (60) to obtain the fundamental model of percussive drilling.

$$\frac{dU}{dt} + \frac{K_1 c}{a E} U = \frac{2c}{E}\sigma_i - \frac{F_1 c}{a E} + \frac{K_1 c}{a E} U_1 \qquad (2.6)$$

The above equation emphasizes the following points:

(i) the solution of this differential equation is complex and requires the use of a digital computer for the calculation of concrete situations;

(ii) the reflected stress wave does not appear in the equation; this implies that the shape of the reflected stress wave is controlled by the shape of the incident stress wave;

(iii) experimental work is required to determine the values of K_1, U_1 and F_1; this is performed by indexed drop tests, but the results so obtained are applicable only to comparable drilling conditions;

(iv) there is clear evidence that the shape of the incident stress wave controls the performance of a given drilling assembly. The wave shape may be determined experimentally or it can be calculated from piston geometry;

(v) the drill steel characteristics are extremely important, as indicated by the equation because all of the fixed parameters are those of the drill steel (This will be studied later);

(vi) it can be concluded that the theoretical performance of percussive drills may be predicted from the knowledge of the force-penetration curve and the shape of the incident stress wave.

5 - Energy Balance (83, 36, 60)

It is believed that, within certain ratios of drill steel mass and piston mass, 100% of the piston energy is transferred to the drill steel when the necessary thrust is applied. This energy propagates along the drill steel down to the drill bit where a portion is absorbed by the rock and the remainder is reflected towards the piston. Upon arrival of the reflected wave at the piston, a fraction of this energy is absorbed by the piston to separate it from the drill steel and the balance is sent back to the bit as a second incident stress wave. A similar reflection occurs again at the bit-rock contact but, as the piston is now separated from the steel, the bit is pulled away from the rock when the second reflection hits the piston end

of the drill rod. Accordingly, as long as the thrust is sufficient, energy will be transferred to the rock in two separate events for every piston blow. Hustrulid claims that 70% to 80% of the incident piston energy is transferred to the rock on the first impact. The remainder is reflected and is distributed between the piston and the second incident wave. This research will show that only the first incident wave produces effective penetration and the reflected wave is the most important factor in dust production.

The ratio of energy transferred from steel to rock was found by Simon to depend upon the decay factor (83, 36);

$$\gamma = \frac{\pi^2 d^4 E \rho}{16 W_p} \qquad (2.7)$$

γ = decay factor;

d = drill steel diameter;

ρ = density of the drill steel;

W_p = weight of the piston.

Experimentally, Simon found that energy transfer reached a maximum of about 60% when the ratio γ/K was about equal to unity, K being the average slope of the F-U curve (Fig. 2.9).

Energy losses in drill steel are most important, as will be seen later; detachable bits and sectional steels are especially large consumers of energy. A large amount of energy is also lost in flexural waves especially in smaller diameter steels(93, 62, 70, 61).

For over a century, comminution researchers believed that all of the grinding energy was used in creating new surfaces. The mechanical efficiency of the process calculated on this basis appeared to be of the order of 1% to 3%. Simon (82) recognized the same performance in rock drilling. It is believed that most of the drilling energy is used in elastic deformation, crack propagation due to dissipation of strain energy in the form of stress waves, pulverization in triaxial compression favored by porosity and finally, heat dissipation.

6 - Penetration Rate

There are at least a dozen formulae that have been advanced to estimate the penetration rate, but they generally fall into two categories: (93, 26, 84, 54, 60, 89)

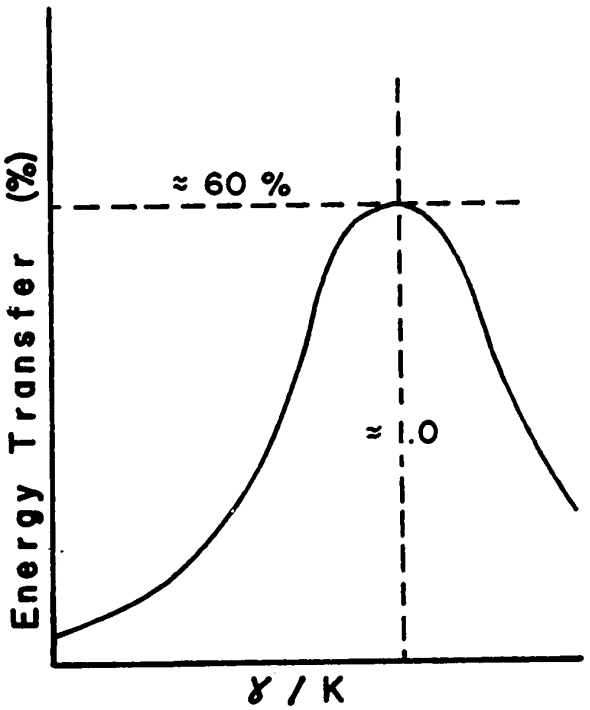

Fig. 2.9. Energy Transfer from Steel to Rock.

(i) those of the first category are suitably illustrated by Simon, Wells and others who devised methods to evaluate the volume of rock removed per blow or per cutting wing; knowing the blow rate, the penetration rate may be estimated;

(ii) the second group of penetration rate calculation formulae is well-represented by Hustrulid. The method consists of measuring the total energy available, the efficiency of energy transfer and the specific energy for a specific indexing condition. The knowledge of these three factors permits the calculation of the volume of rock broken per blow and, if the blow rate is known, the penetration rate can be calculated.

Both categories provide formulae offering little practical value since they call for the use of data which are usually not available in field work, and mine operators must rely on testing methods to estimate the average performance of a given drilling assembly.

C - ROCK DRILLING VARIABLES

The number of variables in rock drilling is so numerous that theoretical optimization of the process by mathematical analysis is an impossible task. In this review of current knowledge on rock drilling, penetration rate and dust formation will be used as the most important dependent variables.

In addition to the variables just mentioned, the complexity of the percussive drilling process is illustrated by the list of variables, shown in Table 2.1.

Table 2.1

ROCK DRILLING VARIABLES

Groups of Variables	Independent Variables	Dependent Variables
External Variables	Compressed air Water supply Lubrication Thrust	Penetration rate Indexing Corrosion Wear
Machines	Characteristics	
	Piston geometry Cylinder bore	
		Operation
		Energy transfer Blow energy Blow velocity Blow rate Indexing Penetration rate Wear
Tools	Drill steels	Energy losses
	Diameter Length Accessories	
	Bits	Wear Penetration rate Indexing
	Diameter Cutting angle Shape, Design	
Comminution	Rock properties	Type of fracture Particle size Particle shape

D - EXTERNAL VARIABLES

The performance of a rock drill depends upon the drilling practice of a given installation. The operating air and water pressure are fixed parameters at a given working place and their values govern the drilling conditions; adequate lubrication of the drilling equipment is a function of the quality of lubricants supplied and of the efficiency of lubricators; machine mounting equipment determines the thrust that must be applied to control the machine. These variables are considered to be external because they can be acted upon independently and they fix the limits of any given piece of drilling equipment or of any given drilling unit.

1 - Air Pressure

Wells (93) found empirically that:

$$\text{Blow energy} \approx \text{Air pressure}$$

$$\text{Penetration rate} \approx (\text{Air pressure})^{1.5}$$

It is observed that, as air pressure increases, blow energy, blow velocity and rotation all increase but, the machine becomes unbalanced and higher thrusts are required in order to maintain bit-rock contact. The consequences of these conditions are that:

(i) considerable increase in air pressure results in a disproportionately small increase in penetration rate (Fig. 2.10);

(ii) wear and tear of machine parts is considerably increased and is evident in the plastic deformation

at the shank end of the drill steel and in the frequent failure of drill rods (24);

(iii) higher air pressure requires higher thrust, maximum possible thrust is dependent upon rock properties, bit design and equipment.

It can be therefore concluded from empirical research that there is an optimum operating air pressure for a given combination of rock and drilling system.

The consumption of compressed air varies almost arithmetically with the operating air pressure (24).

Dust formation, specific energy and air pressure appear to be interrelated and trends in the variation of each of these can be obtained from Cheatham and Inett (24). Their

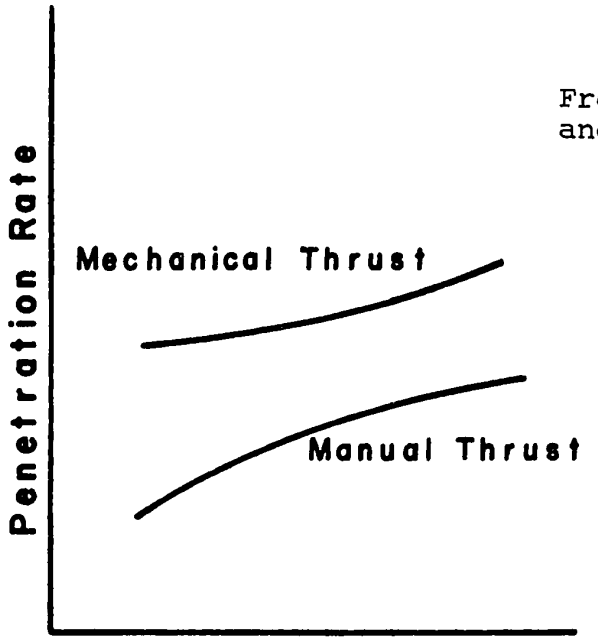

From Simpson and Parry (84)

Fig. 2.10

results, shown in Fig. 2.11 and 2.12, lead to the conclusion that above a certain air pressure, dust formation decreases with higher air pressure, the specific energy peak being located around 50 psi. On the other hand, Hartman (53) has shown that higher air pressures produce more dust. However, the increase in dust is partially offset by a coarser mean particle size. The author's results substantiate Hartman's views.

2 - Water

Prior to the introduction of tungsten carbide bits, the penetration rate with steel bits was lower in wet drilling than in dry drilled holes because bit wear and loss of gauge were more severe under wet conditions. This gauge loss is related to increased rotation in wet drilling due to inertia of the piston.

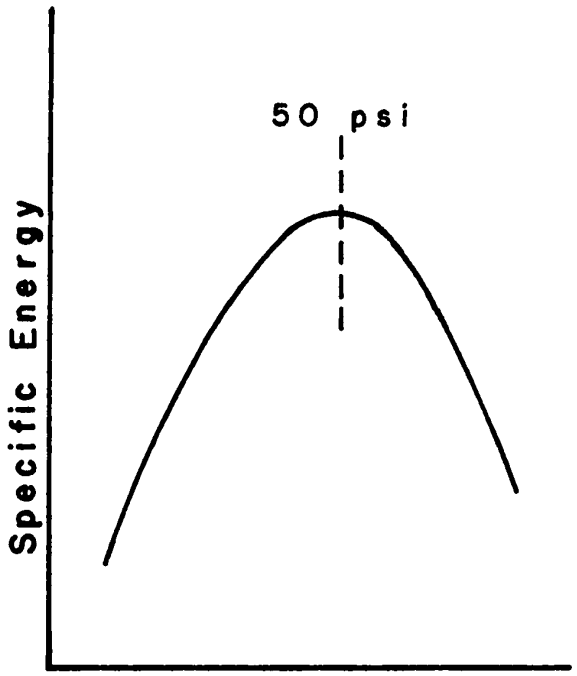

Fig. 2.11

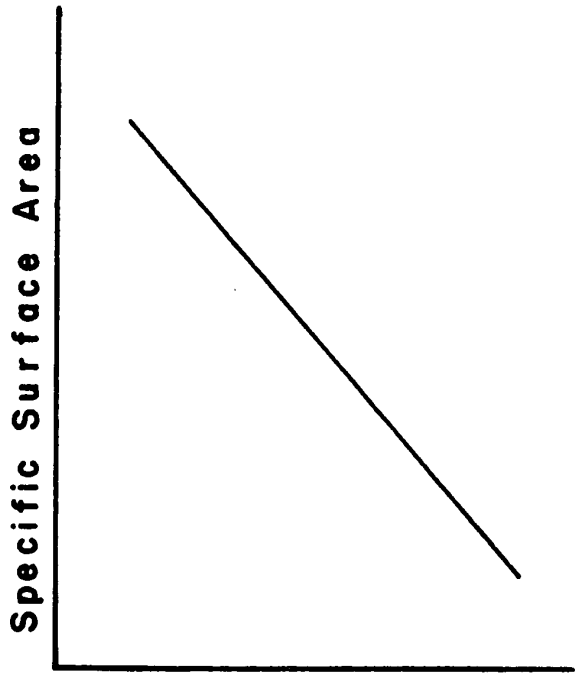

Fig. 2.12

From empirical work (26, 70, 24), it appears that a lack of water due either to low pressure or to poor bit design will cause sludging of the drill hole but, once a certain water pressure is obtained, whatever the thrust or the air pressure, machine performance will be sensibly the same. It follows that water requirements appear to be based upon machine design. It is believed that excessive water will cause cushioning, preventing efficient penetration. Wet drilling seems to be responsible for the formation of more fines than dry drilling due to secondary comminution attributed to higher flow resistance of particles in water than in air.

3 - Lubrication

Oil used in rock drills should emulsify with water, but should also resist flushing away by water. Its adhesion to steel should be stronger than its adhesion to water (70, 84).

Lubrication affects the movement of the piston, especially on the return stroke; it will therefore affect rotation and blow rate. While a lack of oil is definitely detrimental, an excess of oil is not serious (24).

4 - Thrust

Thrust is the only external variable that can be controlled by the drill operator and it is therefore the only variable that will affect the performance of the rock drill. This variable has been studied empirically (70, 26, 24, 89) and fundamentally (83, 60) by many researchers.

Empirical studies have shown, that for a given air pressure, penetration rate is definitely related to thrust and the machine is characterized by three operating zones (Fig. 2.13).

(a) At low thrust, the bit-rock and the machine-steel contacts are not maintained for every blow and the machine will "bounce". Under these conditions, the piston will overstroke, causing increased rotation due to rotational inertia, lower blow rate, lower penetration rate and relatively higher rate of dust formation.

(b) In the balanced zone, thrust is sufficient and energy transfer to the rock is at a maximum. This zone extends over a relatively wide range of thrust values. The machine operates at nominal

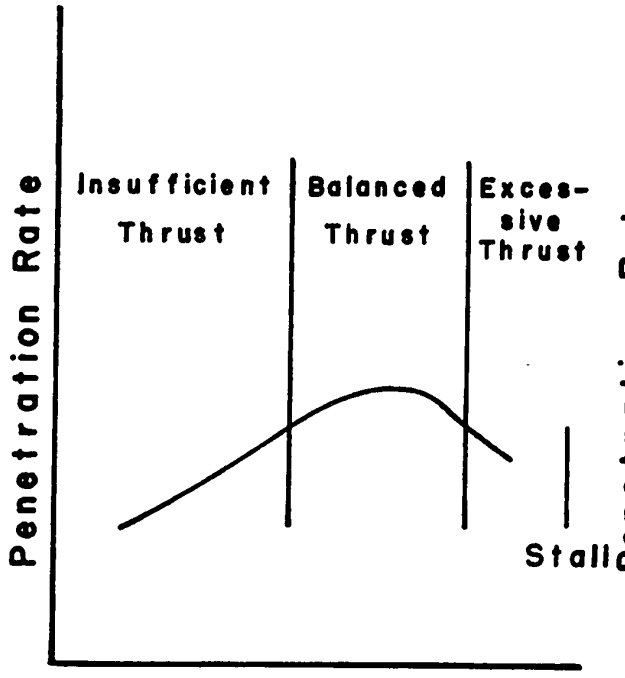

Fig. 2.13

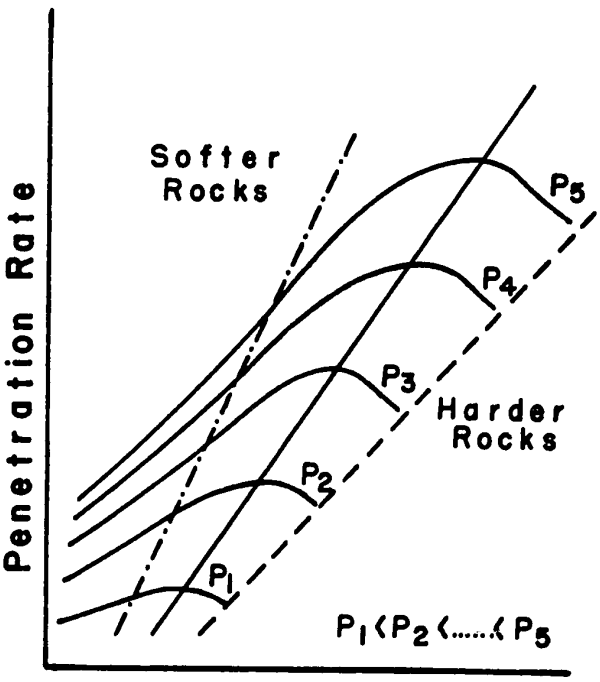

Fig. 2.14

stroke length and inertial rotation is considerably reduced;

(c) When the thrust becomes excessive, the bit will cut a deep groove and the strong torque which develops on the bit due to the resistance of the groove wall will reduce the rotation rate. When the limiting value is reached, rotation of the steel will cease and the machine will stall.

The same series of events will occur at various air pressures; the higher the pressure, the greater the thrust required (Fig. 2.14). This relationship is shown by the line joining the maximum of each thrust-penetration curve. The location of this line varies with the rock, moving to the left for soft rocks and to the right for hard rocks.

5 - Thrust Momentum

Analytical solutions of the thrust requirements have been provided by Simon (83) and Hustrulid (60). Since the former's analysis does not include any rock factor in its final expression, the solution should be accepted with reservation. According to Hustrulid, energy transfer from the piston will occur only if the machine and steel are in contact at the end of the forward stroke of the piston. For equilibrium, the sum of momentum must be zero. When the piston reaches the forward limit of its stroke, three conditions may occur:

(a) The steel and machine do not make contact; the piston will come to zero velocity and its

momentum will cancel the machine momentum, with the result that no thrust will be required to keep the machine static;

(b) The machine and steel are in contact; part of the forward piston momentum will be transferred to the front part of the machine and will cancel an equal amount of machine backward momentum. The other part of the momentum will be transferred to the drill steel and a strain wave will then move towards the bit-rock interface. This will leave the machine unbalanced, and a forward thrust on the machine equal to the backward momentum and the wave momentum available for rock fragmentation will be required to maintain equilibrium.

$$F_T = 2\, a\, B_F \int_0^{\tau} \sigma_i \, dt \qquad (2.8)$$

where F_T = forward thrust;

B_F = blow frequency;

τ = duration of energy transfer from piston to the steel;

(c) The steel may already be energized at time of impact due to a reflected wave whose energy is a fraction ζ of the incident energy, therefore, the total thrust required will have the general form

$$F_T = 2\, a\, B_F \left(1 + \zeta\right) \int_0^{\tau} \sigma_i \, dt \qquad (2.9)$$

Another condition is necessary in order to obtain rock penetration, namely the bit-rock contact must be maintained.

Again, Hustrulid has shown that the minimum thrust is that given by equation (2.8).

The literature reports very little data concerning the relationship between thrust and particle size. Inett (61) reports that the specific surface area increases linearly with the thrust and inversely with the bit diameter. However, he claims that this large specific surface area is due mainly to secondary comminution, a result to be expected from indexing theories.

E - MACHINES

Basically, the rock drill is a free-running piston within a chamber, and its motion is controlled by air pressure, machine thrust and rock properties. The combined action of these three independent variables and machine characteristics will control blow velocity, blow rate, drill steel rotation, blow energy and energy transfer.

1 - Machine Characteristics

It is generally agreed that the penetration rate is directly proportional to the machine power which is a function of air pressure and piston bore. In the operating range, penetration rate becomes a function of blow energy and blow rate, the latter being the more important of the two.

In the first part of this literature review, it was stated that the shape of the stress wave controls the efficiency

of energy transfer from the machine to the drill steel and therefore controls the penetration rate. The stress wave equation was derived by Fairhurst and co-workers at the University of Minnesota (38).

$$\sigma_t = \sigma_0 \, e^{-\frac{Eat}{Mc}} \qquad (2.10)$$

where σ_t = instantaneous stress at time t;

σ_0 = maximum stress amplitude;

M = mass of piston.

The value of the maximum stress σ_0 was also determined by the same group of researchers.

$$\sigma_0 = \frac{VE}{c}\left[\frac{D^2}{D^2 + d^2}\right] \qquad (2.11)$$

where V = piston impact velocity;

D = piston diameter;

d = drill steel diameter.

The following conclusions may be drawn from an analysis of equations 2.10 and 2.11:

(a) Two pistons of the same diameter and with the same impact velocity but of different lengths will produce the same maximum stress amplitude.

(b) Two pistons of different diameters having the same kinetic energy will produce different maximum stresses with the piston having the

larger diameter producing higher maximum stress.

(c) Two pistons of the same diameter and kinetic energy but of different lengths will produce different peaks. In such a case, the shorter piston will have a higher maximum impulse.

The shape of the stress wave is not only characterized by its peak value but also by its decay rate. It was found that the longer pulse duration transfers more energy to the rock. In particular, equation 2.10 shows that, at a given time t after impact, the light piston will produce a shorter duration pulse. It may be concluded that a lighter hammer will have

(i) a faster decay rate;

(ii) a high velocity of impact;

(iii) a low energy transfer coefficient;

(iv) a high rate of fines formation.

In 1946, Hildick noted that a long piston machine minimized the production of dust and improved lubrication and maintenance. This contributed to the present trend towards longer pistons which will produce lower peak stress and longer wave duration.

2 - Machine Operation

The force acting upon the piston is determined by the air pressure while the stroke length, which is the accelerating distance, determines the piston impact velocity. Fairhurst and Kim (36) have shown that the piston energy is transfered to the

drill steel according to a function of

$$\left(1 - e^{-\frac{m}{M}}\right) \qquad (2.12)$$

where m = mass of the drill steel.
M = mass of piston

This expression shows that the energy transfer is closely related to the machine itself and is relatively independent of the piston velocity. Moreover, when the drill steel exceeds a length of four feet, the exponential term of equation 2.12 becomes negligible and it is then believed that 100% of the piston energy will be transmitted to the rod (60, 38).

During the forward stroke of the piston, compressed air acts over the larger face of the piston and all of the energy is used to accelerate the piston towards the drill steel. However, upon the return stroke, the rotation mechanism becomes engaged and the thrust on the machine causes resistance to rotation. Furthermore, the air pressure now acts upon the smaller surface of the piston. These factors will determine the stroke length and, consequently, will also determine the subsequent blow energy, rotation rate and blow frequency. In order to control these variables, rock drill manufacturers have designed piston rifle bars of different pitch lengths. Table 2.2 shows the various possible combinations of controllable parameters and the resultant reactions of the machine. This analytical table permits the conclusion that a short pitch machine offers a preferable design, because it can be adapted to both soft and hard rocks with a minimum of dust production. A short pitch machine usually

BLOW - RATE, ROTATION - RATE RELATIONS							
OPERATING CONDITIONS			MACHINE PERFORMANCE				
ROCK	THRUST	PITCH	BIT IMPRINT	STROKE LENGTH	ROTATION RATE	BLOW RATE	COMMENTS
soft	low	short	fairly deep	nominal	high	fairly high	very efficient
soft	low	long	fairly deep	long nominal	fairly high	high	efficient, more fines
soft	high	short	very deep	short under-stroke	very low	very very high	machine stalls
soft	high	long	very deep	under stroke	very very low	very high	tendency to stall
hard	low	short	shallow	over stroke	very high	very low	bouncing, wear
hard	low	long	shallow	long over stroke	high	low	bouncing, wear, dust
hard	high	short	deep	nominal	fairly high	high	very efficient
hard	high	long	long nominal	high	high	rather low	dusty, efficient

Table 2.2

produces a higher blow rate than a long pitch machine.

The relationship between rotation rate and dust formation is important; at a low RPM the increase in the number of blows per revolution, results in a small index angle and a high degree of comminution. Since blow energy and rotation are interdependent, the formation of dust can be reduced by decreasing both parameters simultaneously. Empirical research has shown that the maximum blow rate occurs at the optimum thrust value and that thrust is therefore the most critical parameter which can be changed during drilling (61).

F - TOOLS

Drilling tools include integral steels, sectional steels, couplings, detachable bits and reamers. The large variety of tools available on the market is evident proof that the proper choice of equipment will influence the penetration rate and the cost of operation. Although numerous studies to date have been focused on the length and size of the drill steel, even greater effort has been devoted to the study of drill bits.

1 - Drill Steels

The main function of the drill steel is to transmit machine energy to the bit. From an examination of Equation 2.12, it may be concluded that a drill steel of large diameter can transmit a larger fraction of the incident energy. However, when the length of the steel exceeds four feet, the exponential

term approaches zero (Equation 2.11). This shows that the cross-sectional area of the steel is barely capable of changing the maximum value of the stress wave; nevertheless the decay rate (Equation 2.7) indicates that the larger steel will have a shorter pulse which would be detrimental to efficient energy transfer. It follows that the length of the steel should always be considered in a stress transmission analysis.

The findings of previous researchers may be summarized as follows:

(a) A drill steel of small diameter will have a tendency to bend. This leads to the concept of the stem rigidity factor δ which was introduced by Irving (62);

$$\delta = \frac{kL^2}{r} \qquad (2.13)$$

where L = length of the drill rod;

r = radius of the drill rod.

The larger the deflection, the greater the amount of energy lost in flexural waves;

(b) Hustrulid (60) has reported that up to 30% of the incident energy in the drill steel is lost due to bending as a result of eccentric loading, bent rods or plastic deformation at the shank end;

(c) Hartman (54) reported that, for a similar bit size and shape, the drill steel of larger crossection will have a lower penetration rate. This is probably due to an increased loss of rotation due

to inertia and to reduced clearance in the hole. Moreover, the resultant rubbing causes secondary comminution and abrasion;

(d) Loss of energy varies with the length of the drill steel. About 1% of the incident energy is lost per foot of drill steel but this loss may reach 10% in the case of sectional steel using couplings;

(e) In the present rock drilling system, bit-rock contact is maintained by the thrust on the machine. According to Hartman, this system favors eccentric loading and reduces the energy transfer to 84% of the value obtained when the steel moves with the piston as in the case of the original piston machine;

(f) The use of small bits may appear to be beneficial due to the smaller volume of rock removed per blow. However, the increase in penetration rate by such bits is heavily counterbalanced by the reduction in rigidity of the drill steel and the consequent loss of energy in bending waves. It is therefore recommended that the use of small diameter rods be limited to short holes (62, 93).

2 - Drill Bits

During the past 20 years, tungsten carbide bits have been used almost exclusively for drilling. The carbide, which is brittle, is usually alloyed with about 10% cobalt to increase its

toughness. Nevertheless, some brittleness remains and this is the limiting factor that controls the cutting angle of the bits.

(a) Bit Size:

Small diameter bits require the removal of less material per unit length of penetration and therefore result in a faster penetration rate. Mondanel (70) shows that the following geometrical relation must hold:

$$\text{Penetration rate} \approx \frac{1}{b^2} \qquad (2.14)$$

where b = bit diameter

However, in the case of small bits, the peripheral distance between blows is comparatively short and fine cuttings are produced. The production of dust by chisel bits is very high because the center of the hole is subject to a severe comminution process.

(b) Bit Angle:

Considerable efforts by a number of researchers have been made to find the optimum included angle of the cutting edge of the bit (62, 54). It is now recognized that a small cutting angle will cause breakage by shearing, while an obtuse angle will cause fracture by crushing due in part to increased frictional forces along the cutting faces. Wider angles will promote more steeply inclined cracks with a minimum of fracture towards the free face of the rock. When the cutting angle exceeds 90^{o}, all fracture takes place by crushing and there is very little difference in particle size distribution when the cutting angle of the bit is increased. However when the cutting angle is less

than 90°, fracture by chipping predominates.

Experimental and theoretical relations were determined by Hartman for included bit angle and depth of penetration, but there appears to be little consistency in his results(54).

$$H \approx \left(\frac{T}{\text{Tan } \theta/2} \right)^N \qquad (2.15)$$

where H = depth of crater;

θ = total bit included angle;

N = exponent varying from 0.5 to 1.0 according to different investigators.

Better agreement exists between crater volume and blow energy and it is accepted that the volume of the crater is proportional to the blow energy, regardless of the shape of the bit.

$$Y \approx B_e \qquad (2.16)$$

The following relation also holds for small included angles:

$$Y \approx \frac{T}{\text{Tan } \theta/2} \qquad (2.17)$$

where Y = volume of crater;

B_e = blow energy.

In practice, drilling in soft ground requires an acute included angle bit and a long pitch rifle bar to prevent machine stalling, while, in harder rocks, the opposite combination of design factors would be more beneficial and would reduce excessive bit wear(62, 37).

(c) Bit Shape:

Chisel bits and cruciform bits are the two main types of bits on the market at present. Practice has shown that the IBULCE (Intensity of blow per unit length of cutting edge) of the chisel bit will be a little more than twice the value for the cruciform bit when the same blow energy is applied to bits of similar diameter. Consequently, a chisel bit subjected to low energy should be used for a relatively soft rock. However, the penetration rate in soft rock can be improved when a cruciform bit is used in a machine with a heavier blow. In hard rocks and in large holes, optimum penetration rates can only be attained with cruciform bits. Fissured ground will also favour the use of the cruciform bit because a low IBULCE is necessary to prevent stalling (62).

Chisel bits and cruciform bits are difficult to compare with respect to their dust generation characteristics. The chisel bit will cut a deep imprint and will turn at a relatively low rate. The relatively small index angle will develop dust by comminution at the center of the hole. The removal of the central section of such a bit has improved penetration rate by as much as a third. With cruciform bits, the penetration per blow is lower and ridges may be left between successive blows on each rotation of the bit. Since dust production is mostly associated with low IBULCE values, it is generally believed that cruciform bits are "dustier" than chisel bits and that their strength lies in their adaptability to both soft and hard rocks.

Other bit shapes have been studied; for instance, at the end of the steel bit era, the French researcher Coeuillet (26) derived several bit designs that would insure even duty on all sections of the cutting edges. Unfortunately, such profiles are impractical because they cannot be adapted to WC usage due to the sharpening difficulties that would be encountered.

Hartman (54) concluded that the most desirable bit shape is the wedge with an angle of less than 90°. However, in all commercial bits the bit angle is about 110°, a value at which the wedge shape loses much of its merits. Research is now directed towards hemispherical indentors or button bits and Fairhurst claims that, in this case, the specific energy is approximately half the value obtained with chisel bits (38).

(d) Bit Wear (62, 24)

Wear is strictly related to rotation. At low penetration rates, the torque resistance to rotation is low and the bit rotates at a faster rate, resulting in considerable abrasion on the cutting edge. When steel bits were still in use, the loss of gauge due to radial wear under such conditions was very severe, especially in wet drilling. Accordingly, it follows that excessive rotation will have the following effects:

(i) reduce bit life;

(ii) reduce blow energy;

(iii) reduce penetration;

(iv) favor dust formation by abrasion.

The above factors can be partially mitigated by increased air

pressure and additional thrust on a longer pitch machine.

G - DRILLING COMMINUTION

Rock drilling is a comminution process because it is an operation in which energy is expended on a cohesive mass of brittle material with the production of an heterodispersed assembly of particles. The peculiar aspect of rock drilling is that energy is applied to a very small area so that a small groove is cut into the solid rock resulting in the formation of a mass of fine particles. Rock properties were discussed partially previously, but additional comments are pertinent.

1 - Rock Strength

Rock strength, drilling strength, drillability, etc. are some of the confusing expressions found in rock drilling literature to describe the resistance of rock to breaking stresses. Protodyakonov (76) who described several rock properties, concluded by basing his strength coefficient upon a comminution test. He expressed the belief that the most important properties in rock drilling are hardness, abrasiviness and plasticity. On the other hand, Mather (69) found so much confusion in the concepts of hardness that he suggested a relationship between drilling, texture and rock structure. Simon (56) observed the lack of symmetry about the longitudinal axis of the wedge and, on this account, confirmed Mather's conclusion. Prior to this, Simon (81) had stated that the grain size of the rock and the crossectional area of the tip of the wedge in contact with it are of the same

order of magnitude, and that, consequently, the rock always behaved as if it were heterogeneous, making it impossible to predict the performance of a given blow. Other researchers built their theories upon tensile and compressive strengths (78) with little success. Drop tests provided compressive strengths which varied considerably from blow to blow and also varied with the rate of loading and bit angle. It is now known that all determinations of rock strength are machine dependent and do not provide absolute values.

2 - Summary of Rock Properties

The above views lead to the following conclusions:

(a) The process of rock fracture is as yet only vaguely understood;

(b) Examination reveals that the planes of rupture tend to follow the boundaries of interlocking crystals, indicating that separation results from tensile stresses;

(c) Griffith's theory of rupture, which is based on surface tension, applies and, in fact, indicates that the use of wetting agents (77) will enhance this form of rupture;

(d) The effect of friction is logically explained as a factor which reduces drillability when bits with large included angle are used;

(e) The variation of energy requirements for indexed fracture is well-known;

(f) The energy requirements for fracture are also

related to environmental factors, a phenomenon well-recognized in deep well drilling.

3 - Particle Size

The work of Ertl & Burgh (34) on the size distribution of the debris from a drill hole must be considered as one of the first efforts to associate the techniques of comminution analysis with rock drilling. Although the authors assumed that the particles were all of the same prismatic shape, they found that the surface area of particles produced per unit of time diminished when the penetration rate increased. A more elaborate research by Hartman (53) supported this hypothesis, since he also found that the factors favorable to efficient drilling contributed to the reduction of dust formation. Inett (61) lists several recommendations of which the two most pertinent are:

(a) Proper drilling equipment must be selected for a given rock; for example, a hard rock requires a heavy machine, cruciform bits, etc.; and

(b) The proper thrust must be maintained on the machine so that it operates in the balanced zone.

Hartman studied the bit cutting angle and recommended the use of a smaller included angle so as to induce failure through shear which would result in large particles. However, the manufacturers still supply bits with included angles of approximately 110^{o} which penetrate the rock mostly by crushing and produce a high percentage of fine particles.

The coarse fractions of particle size histograms are

very erratic. However, the cumulative size distributions usually show a flattening at a certain point which is usually related to average grain size. The writer also found this type of distribution in his research, but his interpretation of the results does not conform with the above.

4 - Shape of Cuttings

In spite of the fact that very few researchers attempted to analyse the shape of the rock particles produced by drilling, it is recognized that the larger fragments, coming mostly from chipping, are flaky. Ertl & Burgh (34) estimated the shape of shale particles to be rectangular parallelepipeds measuring x, 2x, x/4.

Moore (71) agrees that chips are flaky but states that the coarser fraction of the material produced in the inverted cone under the bit is generally irregular in shape and the fine fraction becomes equidimensional. A study conducted by Ong (72) on the shape of rock drilling debris revealed similar findings; namely:

(i) smaller particles are predominently equidimensional;

(ii) larger particles are elongated;

(iii) a particular mineral will have its preferential shape.

III. SYNOPSIS OF COMMINUTION PRINCIPLES

A - INTRODUCTION

The writer conceives comminution as a process in which a mass of cohesive brittle material is reduced to an assembly of particles as a result of work done upon it. The operations of crushing, grinding, blasting and drilling are therefore comminution processes. The techniques of comminution appeared interesting in this environmental study because dust may be seen as the smallest class size of particles produced in any comminution process.

Bond (14) has limited the process of comminution to cases where energy is applied as kinetic energy. Harris (50) had defined comminution as an encounter which might result in fracture, in terms of which simple handling becomes an unsuccessful event.

Modern industry uses the theories of small particles and comminution in the fields of ore dressing, mining, ceramics, abrasives, paints, cereals, etc. However, industrial hygienists are also interested in small particles because dust is responsible for industrial pneumoconioses, the most important group of occupational diseases.

Activities in comminution research may be divided in three groups:

1 - Descriptive Comminution

Interest is centered on the prediction of machine performance by means of mathematical models or experimental charts. It is a statistical approach based upon observation of experimental results.

2 - Analysis of Particle Size Distribution

Researchers in this field of activities endeavour to describe the distribution curve either by mathematical curve fitting or by the development of a theory of fracture of brittle materials.

3 - Analysis of Energy-Size Relations

Workers in this group endeavour to develop models that would permit the prediction of the characteristics of a given assembly of particles based upon machine specifications and power consumption. Valuable time has been lost in academic discussions in this particular field of endeavour.

In this thesis, the sole interest in comminution is to arrive at a better understanding of rock drilling. The analytical aspects of size distribution and energy relations will be discussed briefly and included in this review of descriptive comminution.

B - DESCRIPTIVE COMMINUTION

Comminution operations bring rock and machine together to produce an heterodispersed assembly of particles. The final

distribution obtained depends upon the interdependency of these two elements. The literature review of the subject may then be divided as follows:

(i) elements primarily related to the nature of rocks;

(ii) elements primarily related to machine characteristics.

Comminution has been a favoured subject of research for the last forty years, but only a few papers have made significant contributions to major advances in the semi-empirical science. Only the most important papers will be mentioned in this discussion; for a more complete bibliography, the reader should consult the publications of the D.S.I.R. (32), Harris (50) and Orr (74).

1 - Rock Factors

The product of a given comminution event will be controlled to some extent by some properties of the rock, the mechanism of fracture, the energy consumption, the environmental factors and the limits of comminution.

(a) Nature of Rocks

Gaudin (43) divides rocks into homogeneous and heterogeneous types. Rocks which have the same properties in all directions and are free of cracks or banding are classed as homogeneous. Theoretically, such rocks do not exist: all rocks have been submitted to geological events that have left in them some historical marks. However, Gaudin considers that sedimentary and metamorphic rocks are heterogeneous while the majority of igneous

rocks have homogeneous properties.

A block of rock contains weakness planes which are due to inclusions, intergranular boundaries, cleavage planes and chemical impurities. The smaller the specimen, the lower is the probability of the presence of weaknesses and the higher is its resistance to fracture. This is supported by the glass thread experiment performed by Griffith (46), the thin metal cutting tests by Walker and Shaw (92), and numerous grindability data.

Theoretically, the cohesive forces between molecules should equal the total heat of vaporisation of a material (47). However, crystals are not perfect; they show dislocations (28) and even the bonds between atoms are different. It follows that the actual breaking strength of a rock is much lower than the theoretical value due to dislocations, flaws and cracks.

Mineral properties, as well as history factors, affect the resistance of rock to fragmentation. Rocks are made up of minerals, most of which are anisotropic. Petrological factors control the grain size and general texture of the rock, while geological events leave evident structural features within the mass. The initial effect in the fragmentation process, either by drilling or blasting, is to complete the actual separation or severance of already existing weaknesses, reduce binding strength of others, and initiate new cracks so that further crushing and grinding will produce a size distribution affected by past history (19). This history concept was presented as a law by Bennett and Brown (7): "When work is done on a brittle material,

the energy appears in part as new surface of fragmented products, and in part as the creation of fresh inner weaknesses".

(b) The Process of Fracture

Fracture may be accompanied by plastic deformation in a manner similar to that which occurs in the case of fatigue. It is claimed that planes of low interatomic bonds slide against each other (46, 28) maintaining the original distance that existed between atoms, but leaving traction-free cracks at the ends of the plane and causing attrition in interstices. Griffith claims that in fatigue, molecules will take a preferred orientation leaving faces of lower binding energy from which fractures will progress. Furthermore, on thermodynamic considerations, Poncelet (75) shows that a crack which has developed as a result of strain energy exceeding the strength of cohesion between atoms is irreversible, from which it follows that fatigue failure is cumulative. These theories are not incompatible for brittle materials, such as rocks, which are rich in weakness planes arising from multiple causes.

Brittle materials will break with little or no plastic deformation. Due to the presence of flaws, Griffith has shown that a stress concentration builds up at the tip of cracks and fracture occurs when stress reaches a maximum value.

$$\Psi = 2N\sqrt{\frac{\lambda}{\nu}} \qquad (3.1)$$

where Ψ = breaking stress;

N = tensile stress normal to the plane of the crack;

λ = thickness of the crack;

ν = radius at the tip of the crack.

If the stress is maintained on the specimen, fracture will progress to complete separation, since fracture across a specimen is progressive (75).

A large discrepancy is observed between calculated values from equation 3.1 (14) and actual breaking stresses of specimens. The cracks cause stress concentrations at their tip due to reduced effective area; as a result, theoretical breaking stress is considerably lower than the theoretical value. However, Griffith (46) supported the theory by tests on hollow glass cylinders.

Rocks are much stronger in compression than in tension. Griffith has established a mathematical relationship between compressive and tensile strength of fracture, but such a function is generally not supported by experience. Gaudin (43) has claimed that tension fractures are intergranular while this is not necessarily the case in compression. However, Poncelet (75) has shown that even in compression, atoms are displaced and fracture finally occurs by tension. The weakness of rock in tension is used to advantage in blasting; explosives generate a compressive wave which reflects at a free face as a tension wave, breaking off rock into slabs (86).

The phenomenon of fracture in uniaxial compression is not so easily explained. Fracture is usually explained as a two-step process, namely:

(i) energy is first used to build up strain to a critical value;

(ii) the addition of a small amount of stress will cause separation. Taplin (87), Bond and Wang(12) and Schuhmann (80) have established theories fitting this general pattern. Schuhmann adds that cracking is initiated at a weak point followed by crack multiplication decreasing in length according to a geometric progression in a pattern similar to tree branching; this corollary is useful in explaining size distributions.

(c) Energy Consumption

Comminution energy usually acts by compression or shear. Paradoxically, the energy required to create new surfaces is considerably greater than that theoretically necessary to produce fracture of cohesive bonds. The study of energy balance has been a popular subject for research, especially among Rittinger's supporters. Elaborate analyses of the subject are presented by Orr (74), Bergstrom (9), Harris (50), Charles and de Bruyn (21).

Currently, comminution workers conclude that approximately 1% of the fracture energy is used to create new surfaces. Chemical changes and lattice rearrangement (74) account also for 1% to 2%. Orr (74) assumes that 20% to 50% of the energy is used for elastic and plastic deformation.

An important aspect of energy consumption is kinetic

energy of impacting equipment and impacted material. Bergstrom (9) shows in an intriguing experiment that kinetic energy of large fragments represents 45% of energy consumption which is used partially in secondary fracture. The balance of energy is believed to be dissipated as friction losses, vibrations, sound, electrical effects, etc., all of which finally end as heat losses. However, there is enough knowledge on the means of energy consumption to reject Bond's thesis (14) that, in comminution, kinetic energy is transformed into heat, although heat becomes the final degradation step in energy transformation.

(d) Environmental Factors

Several factors have been investigated to assess their possible contributions in rock fragmentation and it was natural to concentrate early efforts on heat. Bond and Djingheuzian (30) believed that heat was used as useful energy because they found an increase in particle specific surface area corresponding to an increase in heat. A similar finding was reported earlier by Andrews (3). A fundamental study of thermal stress is presented by Marovelli (67) but, unfortunately, he does not comment on the mechanical efficiency of the process. Fuerstenau (27) attempted to fracture rocks with a laser beam, but the procedure proved costly and inefficient.

A more practical approach to the study of the effects of heat is devoted to the study of intercrystalline fracture. Gaudin and Brown (18) observed that the various minerals of heterogeneous rocks have different coefficients of expansion, in

which case heating should cause fracture. These early experiments did not confirm their belief but, as in the case of Andrews, they obtained finer grinding and less size dispersion at higher temperature. Critics of their work claimed that better results would have been produced by rapid cooling. Later work (41) confirmed that heat treatment causes intergranular fracture, due either to differential expansion, anisotropic expansion or crystallographic changes; quartz, for example. It is safe to conclude that heat contributes to finer grinding.

Hardness was another property of rock believed to be a great energy consumer; Fahrenwald (35) and Piret (5) showed an increase in energy consumption with hardness, but we know that for finer particles, a stronger cohesion limits the importance of this finding. According to Griffith's theory, the use of any media that will wet a particle should change strength. This was confirmed by Rehbinder (77); he improved drilling rate by as much as 50% in exceptional conditions by using wetting agents, but in general, drilling rate improvement was of the order of 15%. Other advantages of wetting were a more efficient flushing action and a better dust abatement.

Wet and dry grinding operations produce different results. Fuerstenau (39) has found that wet grinding gives parallel size distribution plots while dry grinding gave a set of curves becoming flatter as the size modulus decreased.

Other factors investigated, such as calcining and atmospheric conditions, were not of significant importance.

(e) Size of Fragments

Martin (68) expressed the law of constancy governing the fracture of brittle materials: "No matter whether the particles are large or small, they break down in the same manner all down the scale". As a corollary we may believe that the pattern of fracture is a function of the rock alone but Gaudin (43) has indicated that the machine will change the distribution. Epstein (33), Broadbent and Callcott (16) must be credited for the confirmation that the size distribution and shape of fragments are controlled by the combination of machine and rock properties.

Comminution is best understood by the analysis of the products. It is customary now to use the cumulative form to represent the size distribution of an assembly of particles (Fig. 3.1). Most size distribution plots are curved at the top as shown by the "actual" curve on Fig. 3.1 but they become almost linear at the lower end; when this straight section is extended across the graph, it becomes the Gaudin-Schuhmann model which is expressed mathematically by equation 3.2 below:

$$Y = 100\left(\frac{x}{k}\right)^{\alpha} \qquad (3.2)$$

where Y = % in weight of particles smaller than size ;

x = particle size, microns;

k = size modulus;

α = size distribution factor of the Gaudin-Schuhmann distribution.

The straight line is the theoretical Gaudin-Schuhmann distribution. The curved line is a typical actual size distribution obtained in a comminution process. This empirical model is completely defined by two parameters: the size modulus k and the distribution constant α . Although the Gaudin-Schuhmann equation is definitely a poor model, it is easy to apply and is adequate for a qualitative discussion of comminution.

The actual description of an assembly of particles produced in the process of comminution has been a difficult task

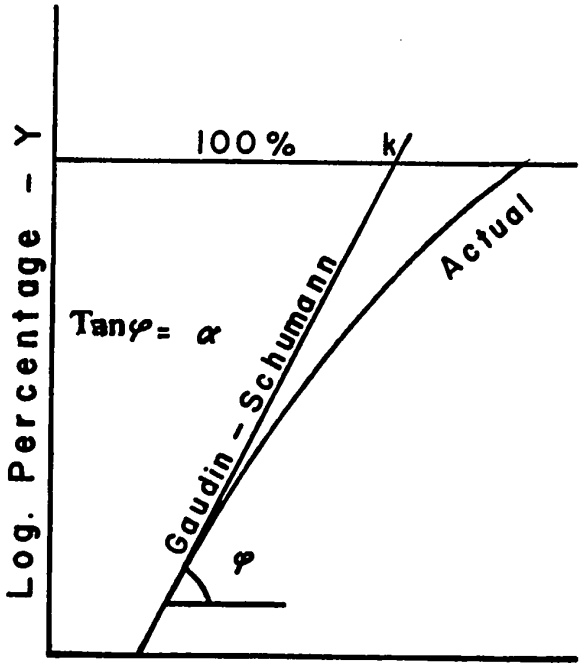

Typical Cumulative Size Distribution

Fig. 3.1

throughout the years, because there were no sizing methods available to cover the complete range of particle sizes encountered in these processes; for practical reasons, the use of sieves became widespread and the majority of models are based upon their use.

Early in the present century, research was oriented towards the definition of particle size but, as particles were generally irregular in shape, several proposals were suggested in order to define the average or equivalent diameter based upon a given physical property (57, 2, 73). At the present time, the A.S.T.M. accepts several definitions of particle diameter and the engineer must select the method that fits his needs.

Size distributions, using particle diameters as the independent variable, were used in comminution until 1940 and are still used today by industrial hygienists and air pollution workers. They are convenient when dealing with classified particles, either by a natural or an artificial technique, so that the mixture may be considered as monodispersed.

Today, in comminution studies, the cumulative weight distribution is used almost exclusively. Researchers have attempted to devise models that would fit the actual size distribution, as shown on Fig. 3.1, and efforts have been made especially to associate their equations with a theory of fracture of brittle, homogeneous materials. Generally, the theories were developed for a single blow on a single particle, and the results extended for multi-events on a large number of particles.

The models most often quoted are the Rosin-Rammler equation and its variations (79, 8, 6, 66) and the Gaudin-Meloy equation with its modifications (42, 10). More complicated equations were developed (44, 52, 64) but they require the determination of several parameters, not associated with any specific physical properties of rocks, as well as the necessary use of computers for their calculation; they are less attractive to the field engineer.

A major evolution was brought about by the findings of Epstein: he recognized that rock was characterized mainly by its primary breakage function while the machine, due to its selective properties, controlled the final size distribution. The primary breakage function is described by Reid et al. (63) as the size distribution of material broken out of an initial single screen interval, when no further fracture of the broken material occurs. Broadbent & Callcott (16) introduced the use of matrices to apply Epstein's finding mathematically.

Recently, Reid et al. (63) developed a technique to determine the primary breakage function, the rate of change of size distribution in a given grinding unit with time and from this data the size distribution of a product in a given unit can be predicted after a certain time of operation. The use of mathematical equations to describe a size distribution is avoided and the results obtained are representative of the existing conditions when this technique is used. The writer has used a similar approach in his research.

(f) Limits of Comminution

Providing comminution equipment is capable of reducing rock to any size, what is the smallest particle size that can be produced?

Theoretically, we should be able to reduce any material to the unit size crystal by physical means (6); however, the finer we crush the material the harder it is to break, indicating that the unit size of a particle may be larger than the smallest possible crystal. Bond and Maxson went so far as to suggest that the smallest particles encountered are not the result of direct fracture, but that they are simply unlocked in the process of comminution.

A traditional approach to discuss the grinding limit rests upon the observation that the specific surface area of crushed material tends towards a limit as grinding is increased. Gaudin's "Textbook of Mineral Dressing" presented the figure 0.001μ as the smallest particle; Bennett (6) believed the limit nearer to one micron for coal, Bond (15) set the value at 0.69 micron based upon crystallographic theories and finally, Harris (51) came back to the original idea of the unit crystal to set the grinding limit at a few thousandths of a micron.

The only practical consideration that may be drawn from the true knowledge of the grinding limit is the determination of the true slope at the fine end of the size distribution curve. However, in the field of industrial hygiene, this aspect is interesting because respirable dust particles are smaller than

five microns and we still ignore the physiological action of the smallest particles. In air pollution, very small particulates are believed to act as condensation nuclei and, if SO_2 is present in the air, the metal content of the particle will act as a catalyst to cause the formation of a droplet of H_2SO_4, a much stronger irritant and corrosive agent than SO_2 alone.

2 - Machine Factors

The machine controls the mechanisms of rock fracture and the final size distribution obtained from the comminution of a rock in a given piece of equipment will be associated with the special characteristics of the machine. Moreover, the machine type and size will determine the amount of energy available for rock size-reduction as well as the rate of application of this energy.

(a) Mechanism of Fracture

Gaudin (43) recognized impact and shear as two different mechanisms in comminution processes, both acting simultaneously to varying degrees. In 1964, Kinasevich et al. (29) identified three types of comminution processes, namely, impact, chipping and abrasion, each type producing its own characteristic size distribution curve (Fig. 3.2).

Like Gaudin, Kinasevich's group believed that the final particle size distribution from a crushing or grinding unit is the result of a composite of the three comminution mechanisms. This concept will be discussed in detail later in this thesis

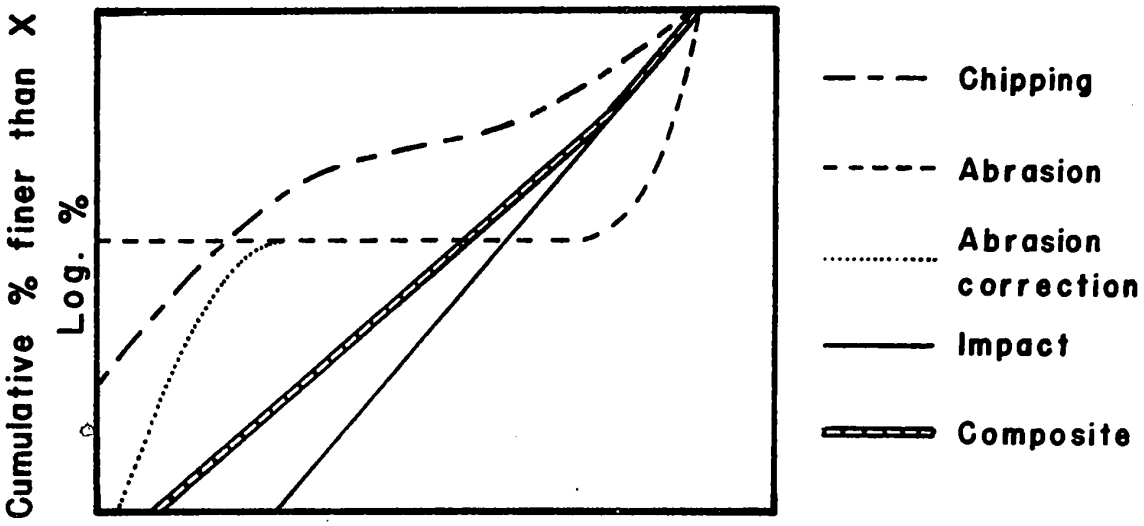

Types of fracture mechanisms - Kinasevich, 1964

Fig. 3.2

since the bulk of this research work is based upon it.

In studying Fig. 3.2, it will be noted that the impact size distribution plot is linear, but the composite distribution line is curved. If the size fractions were small, we would observe several humps in the composite plot (44). Explanations for the curvature and the presence of humps are usually attributed to natural grain size (43), repeated fracture (44, 42), hindering (20) or heterogeneity (5). In this drilling research, humps were observed in every test and it will be shown that they are related to repeated fracture and that humps are primarily machine dependent.

(b) Characteristics of Comminution Equipment

Most rock properties, such as hardness, grindability or drillability are machine dependent; similarly, we know that different types of grinding units will deliver products of different size distributions. Machines are always biased towards coarser particles which absorb the greater part of the supplied energy. Somasundaran (85) has demonstrated that the fraction of energy consumed in a ball mill is proportional to the particle volume; that is, that particle size is the controlling factor of energy distribution.

The interdependency of rock properties and machines can be explained only by the selective characteristics of the type of comminution equipment. According to Epstein (33), the final distribution of a product is a function of the probability of fracture of a particle and the pattern of breakage of a single particle.

Broadbent and Callcott (16) used matrix analysis to apply Epstein's theory and an Australian group of researchers headed by Lynch (66) made proficient use of the combined principles for a multitude of ore dressing and chemical engineering operations.

The fundamental operation of a machine using or producing an assembly of particles is described by the general relation

$$D = B\,S + (I - S) \qquad (3.3)$$

where D = a matrix describing the machine operation;

B = breakage matrix or a matrix representing the specific action of a machine on an assembly of particles;

I = unit matrix representing the total assembly of particles submitted to the machine action;

S = a selection matrix representing the fraction of each size which is degraded by the machine or is altered by its action.

The final product of the machine is given by the relation:

$$P = D \cdot f \qquad (3.4)$$

where P = product size distribution;

f = feed size distribution.

This approach is extremely versatile and is used in mineral processing and chemical engineering.

The selective properties of grinding equipment were studied, particularly for the development of grinding kinetic theories, either for a batch or a continuous process. It was observed that, when a sized material is placed into a comminution unit, the performance of the machine changes continuously as a function of time. At the beginning of the process, there is a rapid depletion of feed particles and a constant rate of formation of fines; further grinding shows a variation in both the rate of depletion of feed material and in the rate of formation of larger particles, but the rate of formation of fines remains

constant. This is illustrated particularly well in Fig. 3.3.

The fact that the rate of change in concentration of a given size of material is constant for a certain time in the fine sizes led the researchers to consider grinding as a first order rate process. Reid (63) developed practical equations for batch and continuous grinding equipment where such a constant rate is observed. An important corollary to this condition is that the cumulative size distribution plot is linear in the region where the rate of formation is constant.

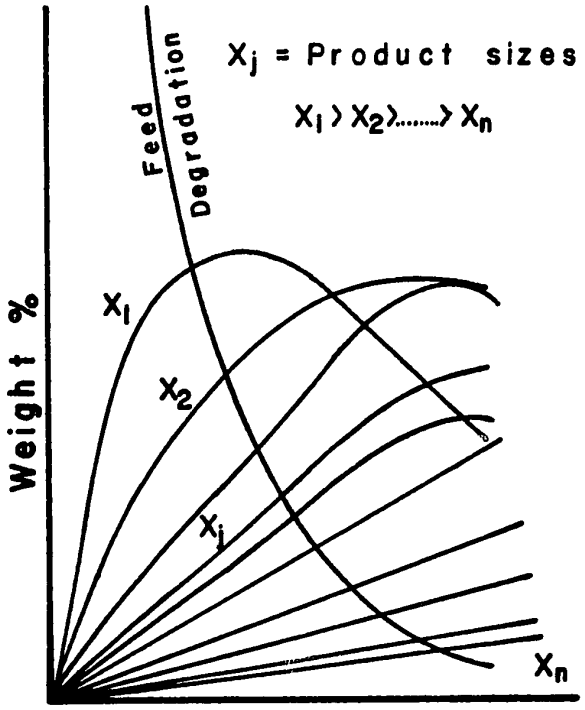

From Arbiter & Bhrany (133)

Fig. 3.3

It must be emphasized that grinding may be considered as a first order rate process only for a certain time, especially for the smaller sizes; for this reason, it is theoretically incorrect to consider time as an equivalent measure of energy. It is observed that, as grinding time increases, the size distribution has a tendency to become flatter and the size modulus decreases, tending towards a limit.

There is a definite difference in specific energy of fracture between large and small particles; as the feed size decreases, the grindability becomes nearly constant: this is related to the selective characteristic of the grinding apparatus (85).

C - ENERGY-SIZE RELATIONS

The topic of energy-size relations has been a choice field of research in the last fifty years and this survey of comminution literature would be incomplete without a discussion on the subject. Publications on energy aspects of comminution are very numerous and interesting critical analyses are available (32, 50, 1, 59). However, the specific energy of fracture in percussive drilling is a function of the index angle; we cannot therefore expect any energy law to hold and we must recognize that the energy-size relations are primarily machine dependent.

1 - Rittinger's Law

The first law of comminution is known as Rittinger's

law and dates back to 1867. It is purely empirical and is based upon the observation that, in comminution, the work done in particle size reduction is proportional to the new surface area produced. In fact, it was found that the energy-surface area plot gave a straight line (49, 5); this linearity was the main argument used to support the law. Assuming that all comminution energy is used to break interatomic bonds, calculations show that the mechanical efficiency of comminution equipment is in the order of 1% to 3% (43, 5); consequently, interatomic binding energy cannot be the controlling factor in comminution. Additionnally, Rittinger's hypothesis assumes homogeneity in binding energy, but there are cracks, weakness planes, inclusions, cleavage planes, etc. in rocks which are responsible for a variety of binding energy levels. In conclusion, the law will apply only for a small range of particle sizes and does not enjoy universal application.

2 - Kick's Law

Kick's Law was derived in 1885 from sound principles of resistance of materials, assuming rock was perfectly homogeneous and that fracture occurred when a critical strain was exceeded. Kick stated that for any unit weight of ore particles, the energy required to produce any desired reduction in the volume of all particles in the mass is constant, regardless of the original size of the particles. This law is not supported by experience; it overestimates the energy requirements for the fracture of coarse particles and underestimates the demand for the breaking of fines (92, 59).

3 - The Third Theory of Comminution

Rittinger stated that the energy used in comminution is a function of the surface area of the particles, while Kick derived a relation showing that the energy of fracture is proportional to the volume of the particle. In fact, neither statement agrees with exprerience, and Bond simply proposed in the "Third Theory of Comminution" that the true energy relation lies between the two, the valid relations being

$$E \approx x^{2.5} \qquad (3.5)$$

where x = particle diameter;

E = energy.

After defining the Work Index, W_i, as the work required to reduce a material from infinite size to a product size of which 80% is passing 100 microns, Bond arrived at the practical relation

$$\text{Work} = W_i \left(\frac{1}{\sqrt{P_s}} - \frac{1}{\sqrt{F_s}} \right) \qquad (3.6)$$

where P_s = size in microns of the square opening through which 80% by weight of the crushed product particles will pass;

F_s = the screen size in microns passing 80% of the Feed particles;

W_i = Work Index, determined by experiments.

Bond's Third Theory has been an efficient tool in mineral dressing and chemical engineering (31), but is cannot be considered as a physical law because the Work Index is machine

dependent; the Work Index varies with particle size and it is necessary to apply several correction factors in order to meet specific conditions. As in Rittinger's and Kick's laws, Bond's Third Theory fits well for a certain range of particle size.

4 - Charles' Law

A general energy-size relation was published by Gilliland (91)

$$dE = -C\,x^{-n}dx \qquad (3.7)$$

where C and n are constants

This relation is interesting because it includes the three previous laws (Table 3.1) and it was used for the derivation of Charles' Law.

Value of n	Law
1	Kick's
2	Rittinger's
1.5	Bond's

Table 3.1

Charles' Law (23) is primarily a mathematical model; it is a combination of the Gaudin-Schuhmann size distribution equation and Gilliland's energy statement. The new energy relation was written as follows:

$$E = A\,k^{1-n} \qquad (3.8)$$

where A and n are constants;

k = size modulus as in equation 3.2.

Further research provided the other relation:

$$a - n + 1 = 0 \qquad (3.9)$$

so that the final form of Charles' relation is

$$E = Ak^{-a} \qquad (3.10)$$

where a = size distribution factor in equation 3.2.

The actual cumulative particle size distribution curve produced in a comminution process is generally not linear; this is strongly supported by the active research of a large group of mathematically minded scientists, who attempted to find a representative model of the size distribution, namely: Gaudin-Meloy, Gilvarry-Bergstrom, Klimpel-Austin, et al. The energy-size relation, as written in equation 3.10, was supported by Arbiter and Bhrany, and it was to be expected because their rate equation is based upon the linearity of a part of the Gaudin-Schuhman plot. However, it is now recognized that the linearity does not generally exist in a size distribution plot and therefore the value "a" cannot be properly defined. Consequently, Charles' Law should be written:

$$E = Ak^{-\beta_c} \qquad (3.11)$$

where $\beta_c \neq a$

Tartaron (88) revised Charles' derivation and

discovered that the relation 3.9 is a mathematical impossibility; more interestingly, Tartaron also found that Charles' Law is primarily similar to Kick's Law, and is also associated with Rittinger's and Bond's Laws.

5 - General Statement

Agar and Brown (1) believed that none of the energy relations presented so far apply to all comminution conditions. Holmes (58) derived a law from a combination of Kick's Law and Bond's Work Index and arrived at an energy relation which has the same form as Charles' Law. Consequently, Agar and Brown are definitely conservative by writing the energy relation as follows:

$$\left(\begin{matrix}\text{Comminution}\\ \text{Energy}\end{matrix}\right) = \left(\text{Constant}\right)\left(\begin{matrix}\text{Product}\\ \text{Size}\end{matrix}\right)^{(\text{Exponent})} \qquad (3.12)$$

The value of the constant is often related to grindability and is machine dependent; the exponent is not essentially a rock property, since its value is also modified by the equipment.

6 - Rate of Loading

There is a lack of agreement between workers on the actual effects of dynamic factors. There is proof that the nature of the process determines the size distribution (21, 22), high velocity blows producing a finer distribution, but less dispersion. It is believed that the range of rates of loading used in comminution is too small to be considered an important element (65), although Bond (13) had previously rejected static

tests in favor of dynamic tests because the products of the latter are more comparable to those from commercial equipment.

The most important studies on rate of loading are those of Charles and de Bruyn (21, 22). As in percussive rock drilling, these workers found that, unless the striking mass is light, a single impact will always result in at least two distinct blows, and sometimes repeated blows, a condition responsible for a high rate of dust formation. Our present knowledge leads to the conclusion that impacting masses should be of light weight in order to avoid repeated fracture and that low impact velocity is responsible for less plastic deformation and a larger size dispersion. Fracture under static conditions definitely differs from fracture under dynamic conditions, the former being preferable from an environmental point of view.

D - SHAPE OF PARTICLES

Most size distribution models, energy-size relations or surface area calculation theories are based upon the assumption of a definite particle shape, but very little serious work has been devoted to shape studies. There are a number of techniques available for measuring shape factors (57, 2), but the quantitative results obtained are meaningless unless a qualitative term is used to describe the particles and the method used for their determination.

Particle shape is extremely important, even more so than size, since it is responsible for the particle behavior in

relation to inhalation properties; moreover, shape controls rate of dispersal, packing interaction, agglomeration, resistance to crushing, settling rate, etc.

Until about 1940, the average shape of crushed particles was assumed to be the same for both large and small particles (48). We realize today that the proportion of equidimensional, elongated or flaky material varies with size (50).

The equipment used influences the shape of fragments: rolls, rod mills, and jaw crushers produce the same types of particles, but ball and pebble mills will cause roundness of the coarser particles (43); high-velocity impacts produce equidimensional particles (22), while low-velocity impacts result in a greater proportion of thin and elongated particles. Environmental factors, such as heat (18) may promote intergranular fracture and the shape of fragments will depend upon the rock itself: Finally, equipment is a limiting factor in particle size formation and the production of fines is balanced by the grouping of agglomerates held together by weak attraction forces or a relatively strong solid bridging caused by fusion and friction; this last property is put to use in the relatively new process of spheronizing.

E - DUST FORMATION IN COMMINUTION

The United States Public Health Service suggests the following concept for dust (90):

"Dusts are formed from solid organic or inorganic

materials by reducing their size through some mechanical process, such as crushing, drilling or grinding. Particles thus created vary in size from visible to the submicroscopic, but with their composition being the same as the material from which they were formed".

The writer will assume in this thesis that any factor responsible for the formation of fines is a favourable dust generating mechanism. From the foregoing analysis presented in this survey of literature on comminution, we may list the dust-forming factors as follows:

(i) a large reduction in size by primary breakage;

(ii) prolonged batch processing;

(iii) overloading, which can cause hindering and thus prevent free crushing;

(iv) dynamic loading, which produces more dust than static loading;

(v) for equivalent kinetic energy, a high-velocity low-mass system is preferable to a low-velocity high-mass system, because the latter predominantly results in double impact;

(vi) dry operations produce more fines than wet operations and the use of wetting agents in wet processes further reduces the production of fines;

(vii) higher temperature favours the formation of fines;

(viii) the ideal grinding unit will have absolute selectivity for a specific size, will operate with single blows and in free crushing conditions.

Summing up, the most evident and most important element involved in dust formation is repeated fracture. The pattern of fracture is controlled mainly by the rock, but the machine influences this pattern by its selective characteristics. In single fracture, the coarser material is eliminated with only a single generation of fines; in the case of repeated fracture, the elimination of an additional amount of coarse material is replaced by a significant increase of dust.

IV - DESIGN OF EXPERIMENTS

A - OBJECTIVES

Percussive rock drilling is an operation responsible for the formation of large quantities of dust which may be detrimental to the health of workers, especially when dealing with rocks rich in free silica, asbestos, or other hazardous minerals. The ultimate objective of this research project is to arrive at a basic understanding of the dust-forming mechanisms in rock drilling, so that machine design can be modified to achieve a relatively dust-free operation.

Hartman, Cheatham and Inett (53, 24, 61) expressed the belief that dust formation varies inversely as the penetration rate, but this is not fully supported by experimental data. Accordingly, it was planned to study rock drilling by consecutive single blows, so that the comminution studies could be related to the more familiar rock drilling studies based upon penetration rates. This approach would permit an evaluation of existing knowledge in percussive rock drilling and make a further contribution to the science of comminution.

Kinasevich et al. (29) have shown that, in a comminution operation, there are three types of fracture processes, described as (i) impact crushing, (ii) chipping and (iii) abrasion. The same three processes are recognized in rock drilling, but they are associated with specific variables. Abrasion is mostly related to rotation, chipping to indexing and impact crushing to

both axial loading and bit design. The author attempted to design comminution tests simulating each type of rock fracture in percussive rock drilling. Hopefully, these comminution tests would have permitted the establishment of the size distribution equations for each type of fracture and, at the same time, the identification of the type of fracture most responsible for dust formation. The author expected to calculate the fraction of rock broken by each mechanism of fracture for any given set of fixed drilling variables, thereby finding the most efficient and most sanitary drilling conditions.

These objectives were maintained but such an approach was partly rejected when it became progressively evident that the size distribution approach would add but little further enlightenment concerning the process of dust formation itself. However it is of interest to record that the Gaudin-Meloy equation fitted the rock drilling operations and that, in most of the experiments, the exponent varied between 8 and 12.

B - ASSUMPTION

The end product of a crushing or grinding operation is an assembly of particles which may vary from several inches in diameter down to submicron sizes. In the previous chapter on comminution, dust is very vaguely defined; hygienists are interested only in respirable dust, that is particles below five microns for silica dust, but up to fifty microns in length in the case of minerallic fibres. Due to lack of precision, both in

sizing instruments and in the terms of definition, the author has therefore classified all particles passing through the 325 mesh sieve, that is, 44 micron apertures, as dust.

Bhrany and Brown (11) published the results of some interesting research on particle sizing and their work confirms that

(i) no sizing instruments are capable of measuring accurately the complete range of particle sizes produced in comminution operations;

(ii) different types of sizing instruments will give size distribution plots sensibly parallel but never superimposed;

(iii) size distribution plots are almost linear in the fine size range.

Consequently, it is assumed in this thesis, that any factor responsible for an increased number of particles smaller than 44 microns will also be responsible for an increased production of respirable dust.

C - COMMINUTION HYPOTHESES

The process of fracture in rock drilling was described previously as an alternate series of impact crushing and chipping events (Fig. 2.1). In axial loading, Bergstrom et al. (9) have shown that the crushing of spherical particles resulted in a mass of very fine particles due to crushing and a few large fragments due to chipping. Bergstrom claimed that these fragments carried

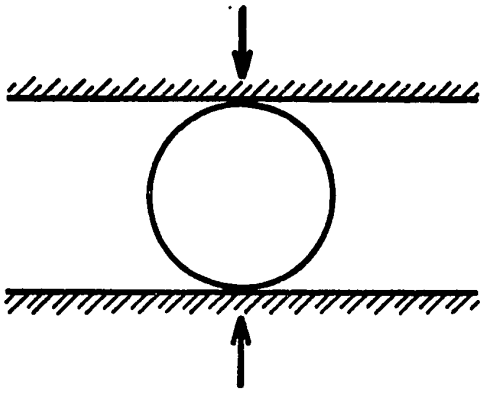

Loading Stage

Fig. 4.1

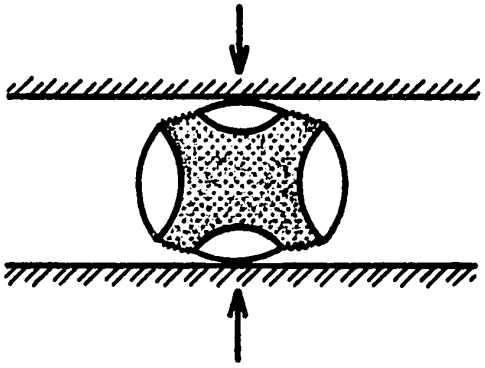

Formation of Particles

Fig. 4.2

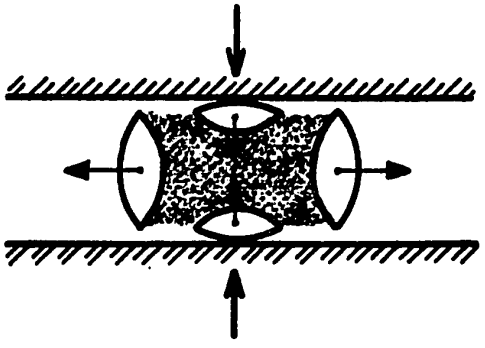

Separation of Particles

Fracture of Spherical Particles by Axial Loading

Fig. 4.3

From Bergstrom et al.(9)

with them 45% of the input energy as kinetic energy; the series of diagrams (Fig. 4.1 to Fig. 4.3 inclusive) illustrates the sequence of events suggested to explain the fracture mechanism.

The author deduced from these observations, that even in free crushing (20) as described above, the fine rock particles generated between the large fragments (Fig. 4.2) are due to confinement. A similar condition would exist in rock drilling, where the material under the bit is crushed and a quasi-hydrostatic pressure under the bit causes the chipping of large fragments along the cutting edge of the bit.

The author planned his comminution studies to verify the following hypotheses

(1) That the final size distribution of particles of a rock drill is the summation of several crushing and chipping micro-events. (Fig. 2.1).

(2) That the fracture micro-event in rock drilling is simulated by the fracture of a loose particle in free crushing.

(3) That the formation of large chips in rock drilling, due to indexed fracture, is related to the previous fragmentation history of the rock. (An infinite number of experiments would be needed to define the size distribution of these large fragments).

(4) That rock is not a solid continuum; adhesive bonds between faces of crystals and grains vary from point to point due to dislocations, crystallographic systems, rock texture and geological structure.

(5) That weakness planes divide the rock into an assembly of particles represented by the primary breakage function. This concept leads to the consideration that drilling is a rate process where time is replaced by a number of micro-events.

(6) That a single micro-event in rock drilling will break a total mass of material approaching zero gram with an energy corresponding to a certain number of blows on a loose particle of a given size.

D - COMMINUTION TESTS

The comminution approach in studying the drillability of a rock was suggested by Protodyakonov in 1962 (76). In late 1970, Brook and Misra (17) suggested a standard procedure to determine the Protodyakonov Number, and concluded that the stamp mill method for determining drillability would be the most rewarding in further research.

This approach was particularly attractive to study dust formation. Impact tests were run on particles of three different sizes, however, the author retained only the tests made on feed material passing through an 8 mesh sieve but retained on a 16 mesh screen. This size range is comparable to the width of the bit in contact with the rock at the time of drilling.

A manual diamond drill core breaker, size BX, was used by the author for the comminution tests (Fig. 4.4). The arrangement consisted of a steel plate, measuring one square foot on which was placed an open chassis. The slot measured

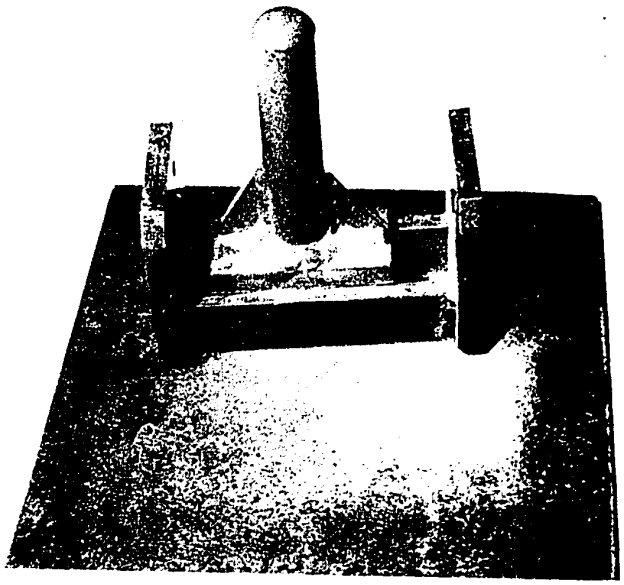

FIG. 4.4

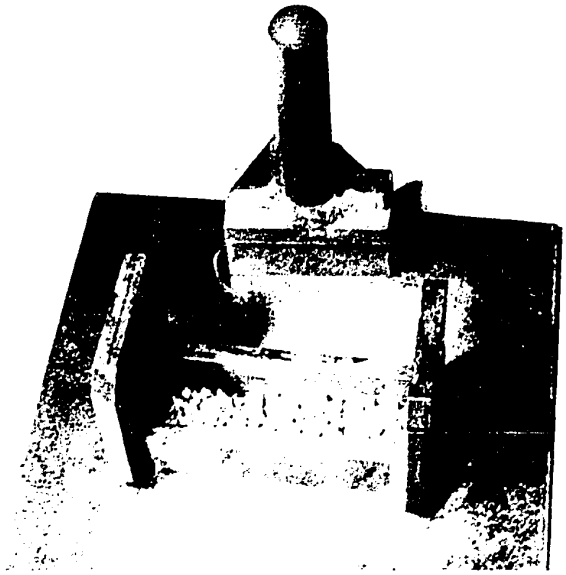

FIG. 4.5

INSTRUMENTS USED FOR THE COMMINUTION TESTS

$1\frac{3}{4}$" X 6" and the guide was 1" high. The hammer is $4\frac{1}{2}$" long and slides loosely into the slot. The feed material was spread evenly (Fig. 4.5) in the bottom of the slot and the hammer, weighing about six pounds, was used to crush the material by impact blows.

The blow energy was not measured; the height of fall of the hammer was, at the most, equal to the height of the guide slot and for such a short accelerating distance - provided the blow frequency was maintained - the blow energy was satisfactorily constant. It is estimated that the blow energy varied between one foot-pound and half a foot-pound. The hammer was shorter than the length of the slot, so that, during the tests, blows were applied at random along the slot. These two testing conditions were believed to be in agreement with actual rock drilling, where the blow energy varies from blow to blow, as well as the index angle.

This instrument was selected as a possible tool to simulate rock drilling in the light of the hypotheses and objectives previously mentioned.

Tests were run on samples weighing from five to one hundred grams and the total energy ranged from 25 to 400 blows. The size analysis of the product is described later in this chapter.

The ultimate objective of the comminution tests was to extrapolate the fraction of a product of a given size for a

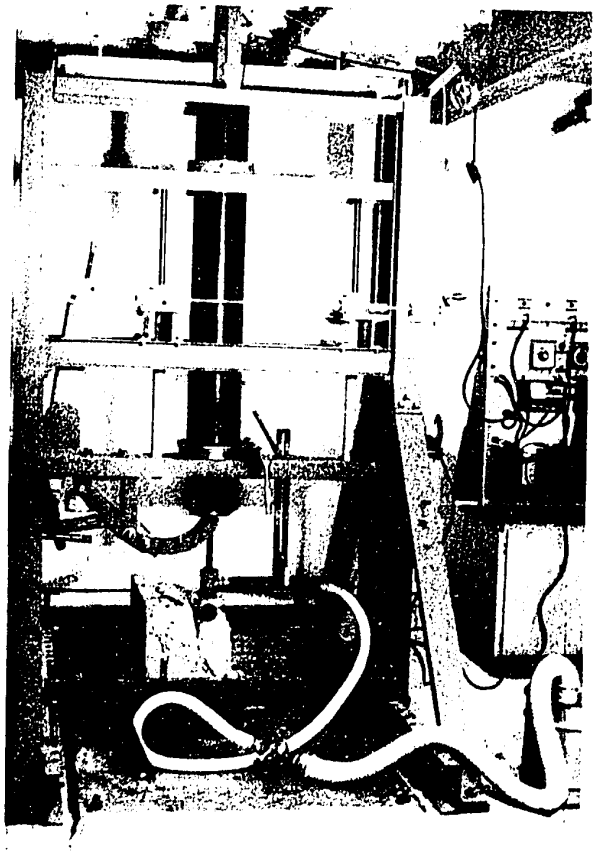

FIG. 4.6 — GENERAL ARRANGEMENT -- SINGLE-BLOW ROCK-DRILL

sample approaching zero gram for any number of blows, which was the hypothetical condition of the micro-events of fracturing in rock drilling.

E - SINGLE-BLOW ROCK-DRILL

A drop-hammer drill was designed to study percussive drilling variables (Fig. 4.6). Objections to this type of system are numerous (60, 72) if absolute results are wanted, but qualitative results were considered adequate for this research.

Basically, the drill is a 6" cylindrical weight falling from different heights inside a piece of metal tubing. Holes were drilled in the guide tube to eliminate air resistance and for the measurement of the fall distance (Fig.4.7). The weight was moved inside the tube by means of a magnet; it was brought up to the desired height by means of a manual hoist and was allowed to fall by de-energizing the magnet. Weights varied from approximately 25 lbs to approximately 100 lbs and the maximum height of fall was slightly in excess of four feet. A machine tappet was imbedded into the weight in order to prevent its deformation and also to allow energy transfer to the drill steel with minimum loss.

The drill steel was held in place on the rock before impact. Contact of the steel with the rock, representing a thrust of about 45 lbs, was ensured by means of four split cylinders bolted around the collar of the drill steel (Fig.4.8). The drill steel head protruded through the collar weights so that the drop-weight contacted only the drill steel at the time of impact.

Two slots were cut on the side of the drill steel collar weight (Fig. 4.8) in order to keep the steel in a set position inside the lower end of the tube. A set of guides bolted inside the tube engaged into these slots. Drill steel rotation was performed manually by means of a ratchet wrench, gear and worm arrangement (Fig. 4.7). There were 120 teeth on the gear, so that angles as small as $1\frac{1}{2}^{o}$ could be accurately

Fig. 4.7 - Rotation mechanism and height of fall measurement.

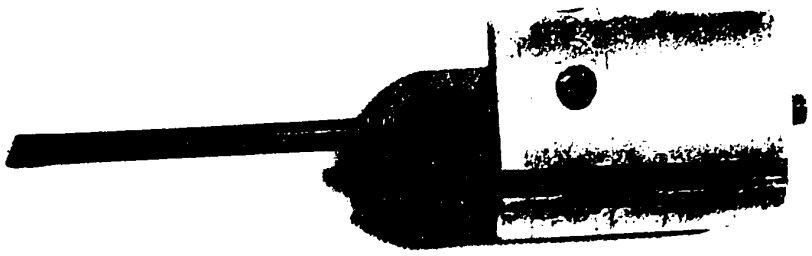

Fig. 4.8 - Drill steel thrust and guide arrangement

measured.

A mechanical arrangement was incorporated into the machine to capture the hammer after its initial rebound from the rock, so as to prevent secondary fracture of the fragments. The system was capable of gripping up the drill after its rebound although it could not prevent the first reflected wave from reaching the rock. While it may theoretically be incorrect to describe the apparatus positively as a single-blow rock-drill, it can be stated that the drill steel does not make any contact with the rock again after it is separated from it.

The drill steel pick-up system is illustrated in Fig. 4.9. It has three elements:

(i) a lever system;

(ii) a spring inside a piston, which forces the lever to move counterclockwise; the characteristic deformation of the spring is 75 lbs to the inch;

(iii) a 400 lb capacity magnet holding the lever, thereby preventing its rotation.

When the power is cut off from the magnet holding the drop weight, a timer (with an accuracy of 0.01 sec.) is simultaneously set in motion. The weight begins its fall, the timer de-energizes the lever magnet, the weight impacts the drill steel, the drill steel rebounds, and the lever picks it up during its upward movement. Proper timing is guaranteed by keeping a constant gap between the end of the lever and the drill steel collar weights. Final height and timing adjustments were controlled by

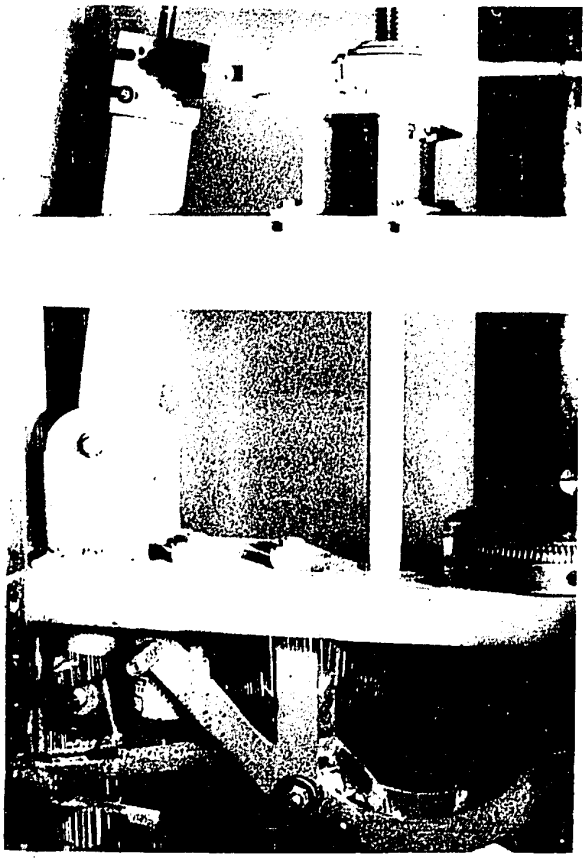

Fig. 4.9 - Drill steel pick-up mechanism

Fig. 4.10 - Rock sample mounting arrangement

lifting the whole tube assembly by means of two screw jacks (Fig. 4.6).

The floor design of the apparatus was critical; it was desired to provide continuity between the sample on which drilling was to be performed and the base, in order to provide a condition comparable to a massive rock face in mining. In order to meet this objective, the apparatus was mounted on a 12" thick reinforced concrete base. A 1" thick base plate, machined on the top face, was grouted and bolted to the foundation. The sample was wedged into a heavy tray, with a 1" bottom plate machined on both faces (Fig. 4.10). The rock sample was cut and polished to fit solidly in the tray and was tightly wedged to prevent any movement. A standard Pallet truck was used to move the rock. A system of cross bars and pins kept the tray in place on the floor so as to maintain the drill hole centered correctly.

F - COLLECTION OF PARTICLES

All tests were carried out in dry drilling conditions and the system of particle collection can be seen on Fig. 4.6. A small shop vacuum cleaner was used for suction.

A four inch diameter membrane filter with a pore size of eight microns, was used for all tests. The filter was supported by a photo-etched stainless steel screen, with an additional heavy wire screen for extra rigidity. The filter was placed in the circuit by means of two 4" dessicator covers (Fig. 4.11, 4.12), which were kept together by a stainless steel preformed

wire. Flexible tubing, PVC pipe fittings, and plastic foam were used to make a tight enclosure and exhaust system from the collar of the drill hole to the filter.

Impact blows were applied with the suction on the filter; airborne dust particles were sucked towards it. However, the suction was too low to lift and carry larger particles to the filter. The large particles in the bottom of the hole were recovered by increasing the suction through the use of a smaller tube (Fig. 4.13).

Usually, a sample was made from the particles after

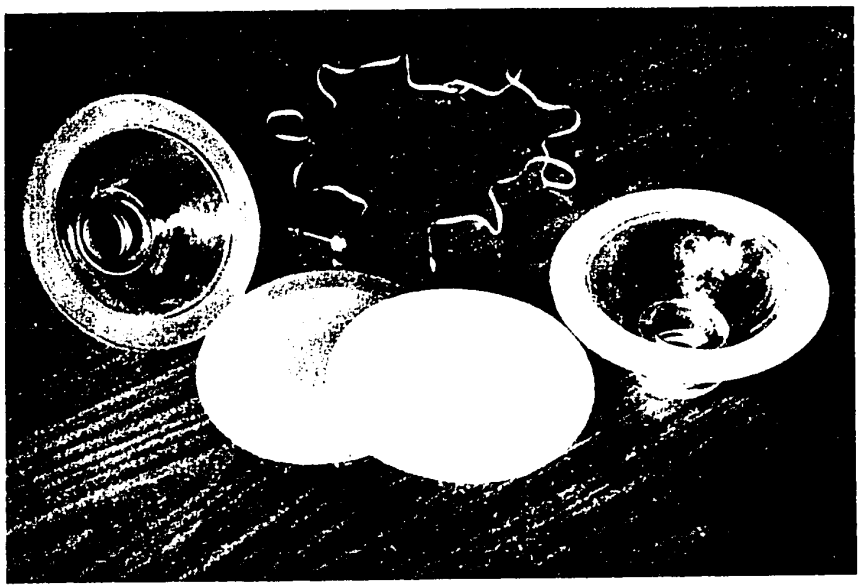

Fig. 4.11 - Parts of particles collecting system

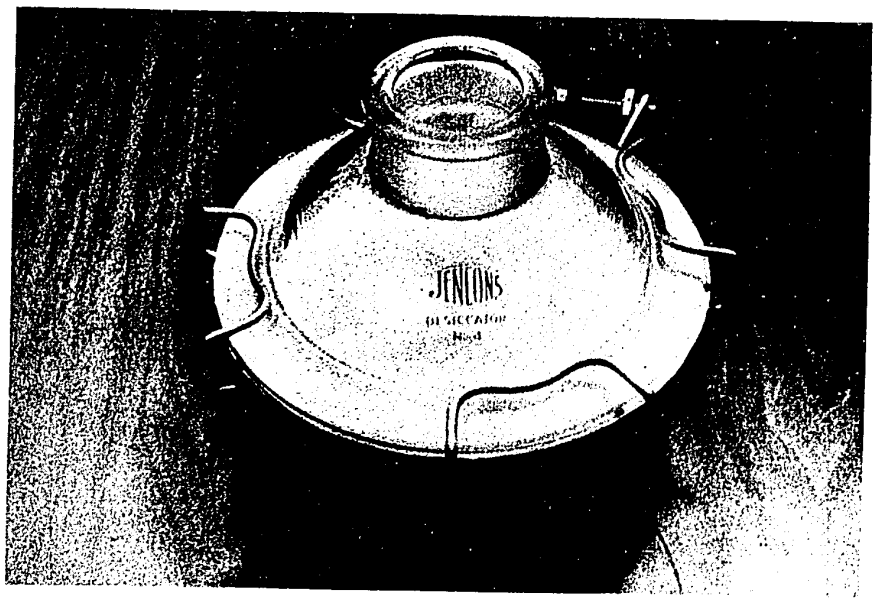

Fig. 4.12 - Assembled particles collecting system

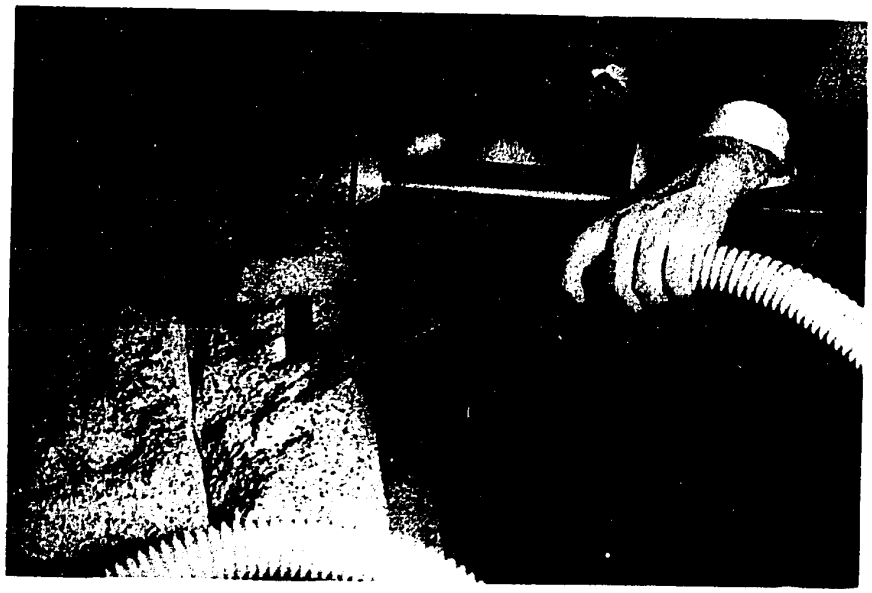

Fig. 4.13 - Collecting particles from bottom of hole

a complete or half a revolution of the bit. The flexible tube and pipes were cleaned by shaking and the filter was cleaned with a small camel hair brush. The same filter was used for several tests.

G - SIZING OF PARTICLES

Several hundred samples were collected and sized rapidly and accurately by a method capable of measuring all of the particles in a given product. The author selected sieves because most comminution studies are based upon their use and they were expected to give satisfactory results. The sieves selected and used were $^{1}/2"$, 3, 4, 6, 8, 16, 20, 30, 50, 70, 100, 140, 200, 325, and 400 mesh. Shaking was carried out on a standard Ro-Tap Machine. The screening times were always sufficiently long to be well within the limits at which particles pass through the sieve at a relatively constant rate (2).

All screening was done in the dry state so as to avoid the extra time required for the wet screening. However, a series of tests were run for both wet and dry particles in order to compare results. According to these tests, there were no corrections necessary for material retained on the 100 mesh sieve or for larger openings. The following correction factors were determined for the other sieves:

Sieve Number	Corrected Weight
140 mesh	0.93 X (observed weight)
200 mesh	0.95 X (observed weight)
325 mesh	1.10 X (observed weight)

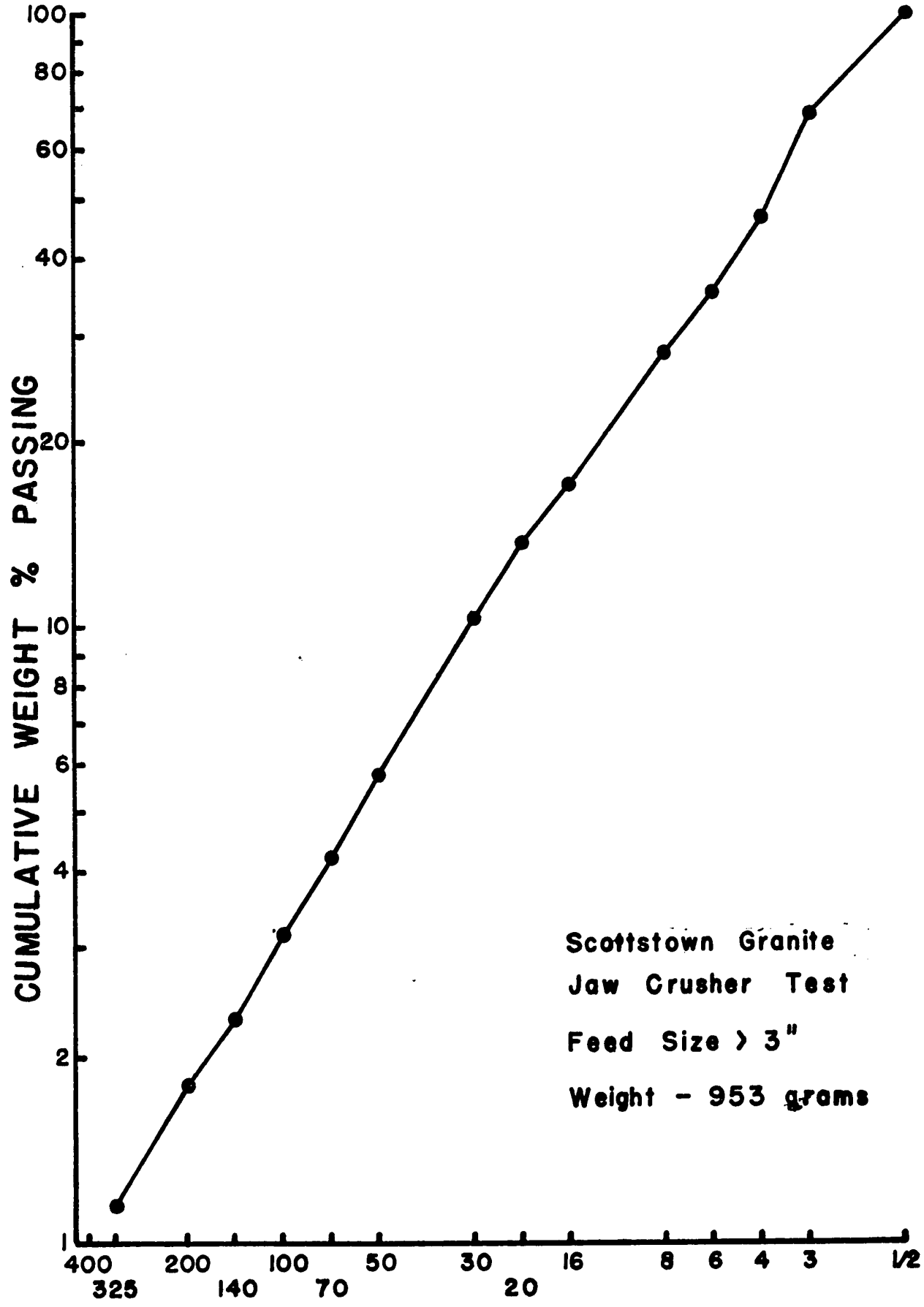
CUMULATIVE WEIGHT % PASSING
100
80
60
40
20
10
8
6
4
2
1
400
325
200
140
100
70
50
30
20
16
8
6
4
3
1/2
SCREEN SIZE (MESH)
Scottstown Granite
Jaw Crusher Test
Feed Size > 3"
Weight - 953 grams

Fig. 4.14

Sieve Number	Corrected Weight
400 mesh	1.18 X (observed weight)
-400 mesh	Adjust by difference

All the results presented in this thesis were corrected according to these factors but the resulting changes were not significant.

H - CHOICE OF ROCK

Traditionally, drill tests have been performed on monominerallic rocks such as quartz, limestone and marble. Occasionally granite was also used. The author chose to work on a multiminerallic rock so as to approximate working condition in a mine, rather than a monominerallic rock which is often anisotropic. Granite was selected since it is rich in free silica and is therefore suited for an environmental study of rock drilling.

Seven different types of granite were available in the Montreal area as rock specimens. A series of comminution tests, as described previously, were made on each of them as well as crushing tests in a laboratory crusher. Scottstown granite from the Eastern Township was chosen. It is a medium coarse grained grey granite recognized by the tradesmen of the region as a rock that can be cut equally well in all directions. The size distributions obtained from the different comminution tests, as well as from crushing, indicate that the rock is relatively free of bias (Fig. 4.14).

V - DRILLING COMMINUTION

A - SIZE DISTRIBUTION OF PERCUSSIVE DRILLING DEBRIS

Twenty-two series of percussive drilling experiments were conducted with the single-blow rock-drill in order to study some aspects of drilling comminution, and three series of tests were performed with a conventional rock drill. The primary goal of these tests was to determine the particle size distribution in a steady regime associated with a given drilling condition. As a rule, samples from the first four or five complete revolutions of the drill steel had to be rejected because they contained an excessive amount of coarse fragments due to chipping from the collar of the hole.and did not represent penetration conditions at a constant rate.

A typical size distribution of rock drilling debris is plotted in Fig. 5.1 and the results of all tests appear in Appendix A. The plots are characterized by a sag in the vicinity of the 140 mesh size and an absence of linearity even in the fine sizes. This shape of curve suggests multiple fracture and possibly, a strong deviation from a first order rate process. Since the sag near the 140 mesh is not apparent on the hammer test results as seen in Fig. 5.3 to 5.9 inclusive, it was considered not to be due to faulty sieves.

The author viewed percussive drilling as a rate process where the number of micro-events per blow replaces the variable "time". Fig. 2.1 illustrates this process and illustrates

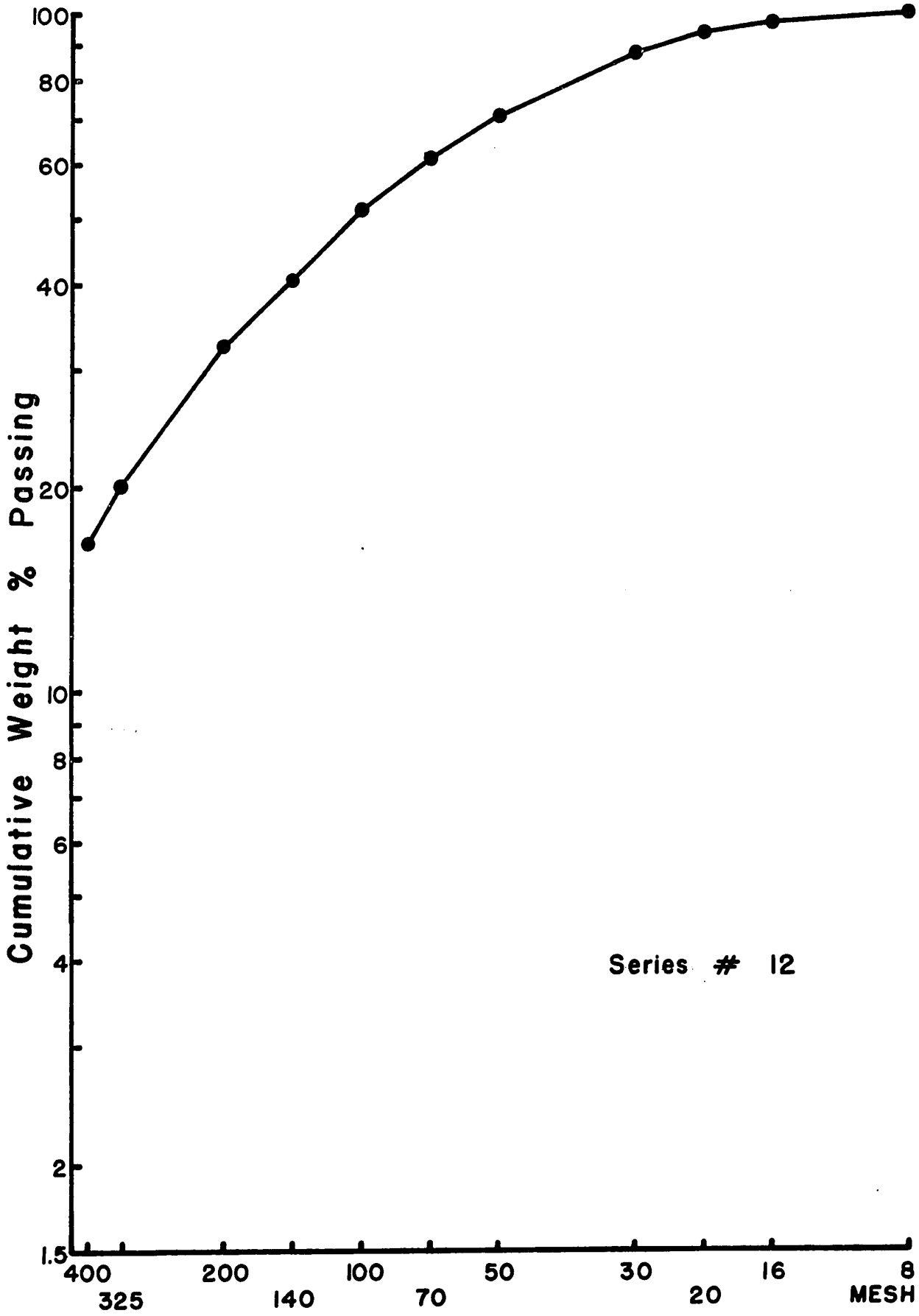

Fig. 5.1 Typical Size Distribution – Drilling

clearly that the rate of penetration is not constant, in fact it decreases with energy. Consequently, rock drilling cannot be considered as a first order reaction.

The comparison of hammer test results and drilling data allowed the writer to present a new approach to the understanding of drilling comminution.

B - GROUNDS FOR COMMINUTION TESTS

It will be recalled that Kinasevich et al. (29) identified three different processes in comminution operations and associated each with a particular type of size distribution. On accepting this theory, it was decided to plan some experiments which would lead to an understanding of the drilling comminution process. It was expected that the hammer tests would provide the size distribution model for axial impact loading and the single-blow rock-drill would allow the determination of the size distribution equation for chipping. Efforts proved fruitless, because impact tests, as well as drilling tests, fitted the Gaudin-Meloy equation with an equal degree of confidence, above 90% when using the Chi-Square tests. However, this work confirmed the previous hypothesis that the impact hammer test procedure simulates breakage in percussive drilling.

The breakage of a particle assembly has been viewed as a combination of two processes by Epstein (33) and followers. In the first process, the comminution equipment is said to "select" a proportion of the particles for breakage. In the second process,

the "selected particles" are broken in a regular manner; the proportions of particles of each size formed by these means are described by the breakage function (Fig. 5.2). Rock drilling is not a comminution operation which fits perfectly into the above description. In this particular case, the Gaudin-Meloy equation could have been used for the breakage function; however, as the size distribution for very different drilling conditions were rather similar, the value of the selection function was questioned. It is doubtful also whether this method of analysis of the size-distribution curves would have provided an explanation for the point of inflexion present around the 140 mesh size in every test.

The author then considered drilling as a batch process where a single blow is an event comprising a number of micro-events (Fig. 2.1). This assumption is logical because, in a usual grinding process such as rod milling, the total number of fracture events is proportional to the duration of the operation. Reid et al. (63) proposed a working formula to estimate the size distribution in a grinding unit after a known period of operating time. Their work was based both on the existence of a primary breakage function free from secondary fracture and independent of feed size, and on the observation that, in some grinding machines, the rate of change in weight of a given size material is constant. Experimental evidence supports Epstein's theory that the breakage function can be independent of initial size; it follows that it may be expressed on a relative scale (Fig. 5.2). The interesting feature of Reid's method to estimate the size-distribution at a

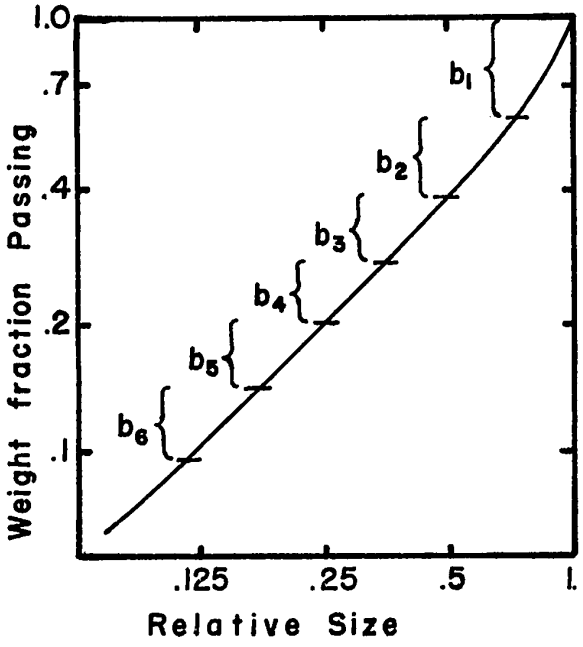

Fig. 5.2 Typical breakage function (From Reid et al)

given time lies in the use of the observed values for the breakage function and the observed rate function instead of idealized mathematical models. This philosophy was finally selected as the most valuable for this study of drilling comminution.

Difficulties arose when attempting to use Reid's method of calculation. It was observed that the rate of variation in weight of material of a given size with the number of blows was not constant (Fig. 5.10, 5.11, 5.12), that is, the hammer test procedure is not a first order rate process. Consequently, if the previous hypothesis is correct that rock breakage in the hammer test simulates rock breakage in percussive drilling, it

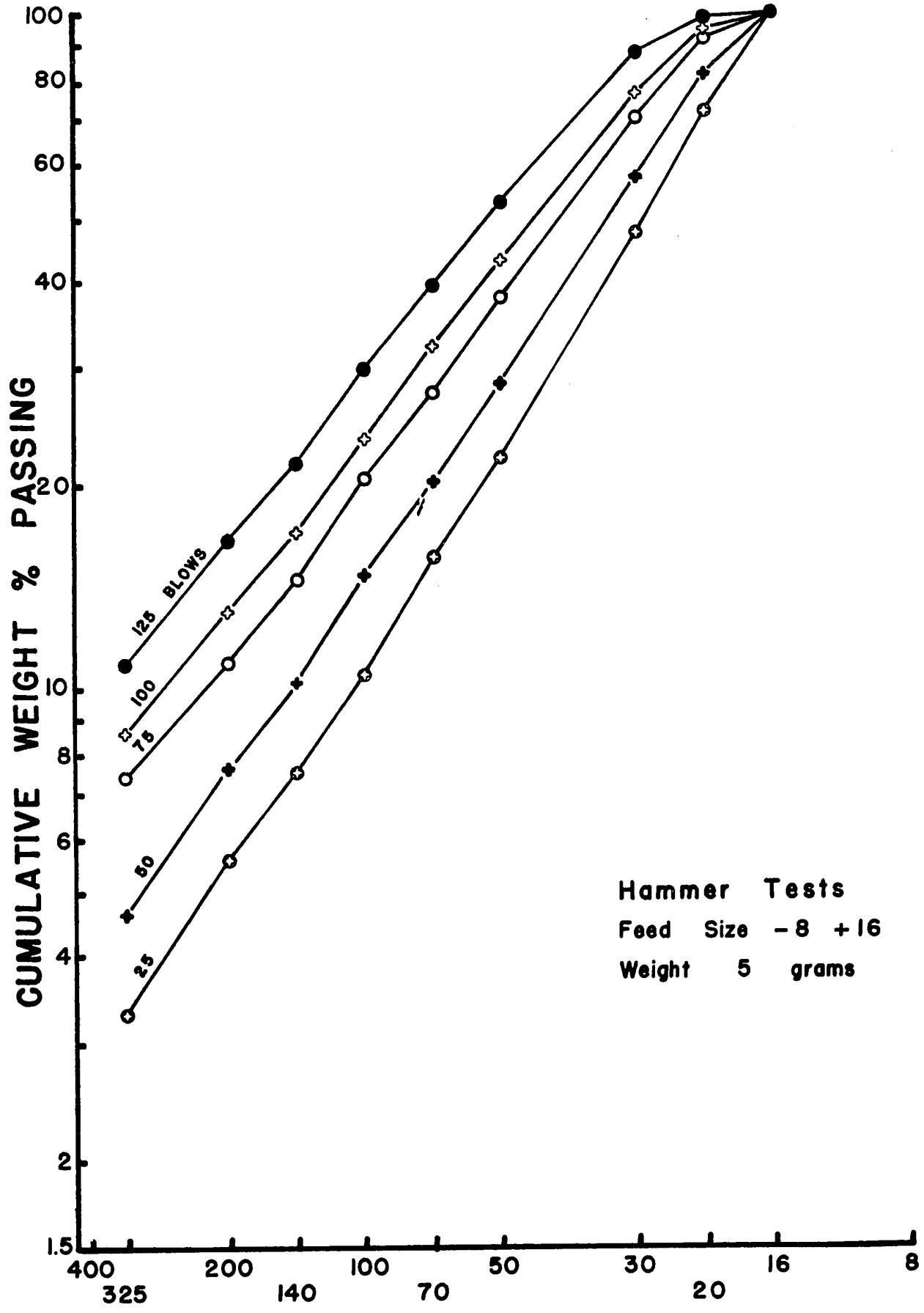
CUMULATIVE WEIGHT % PASSING
100
80
60
40
20
10
8
6
4
2
1.5
125 BLOWS
100
75
50
25
Hammer Tests
Feed Size -8 +16
Weight 5 grams
400
325
200
140
100
70
50
30
20
16
8
SCREEN SIZE (MESH)

Fig. 5.3

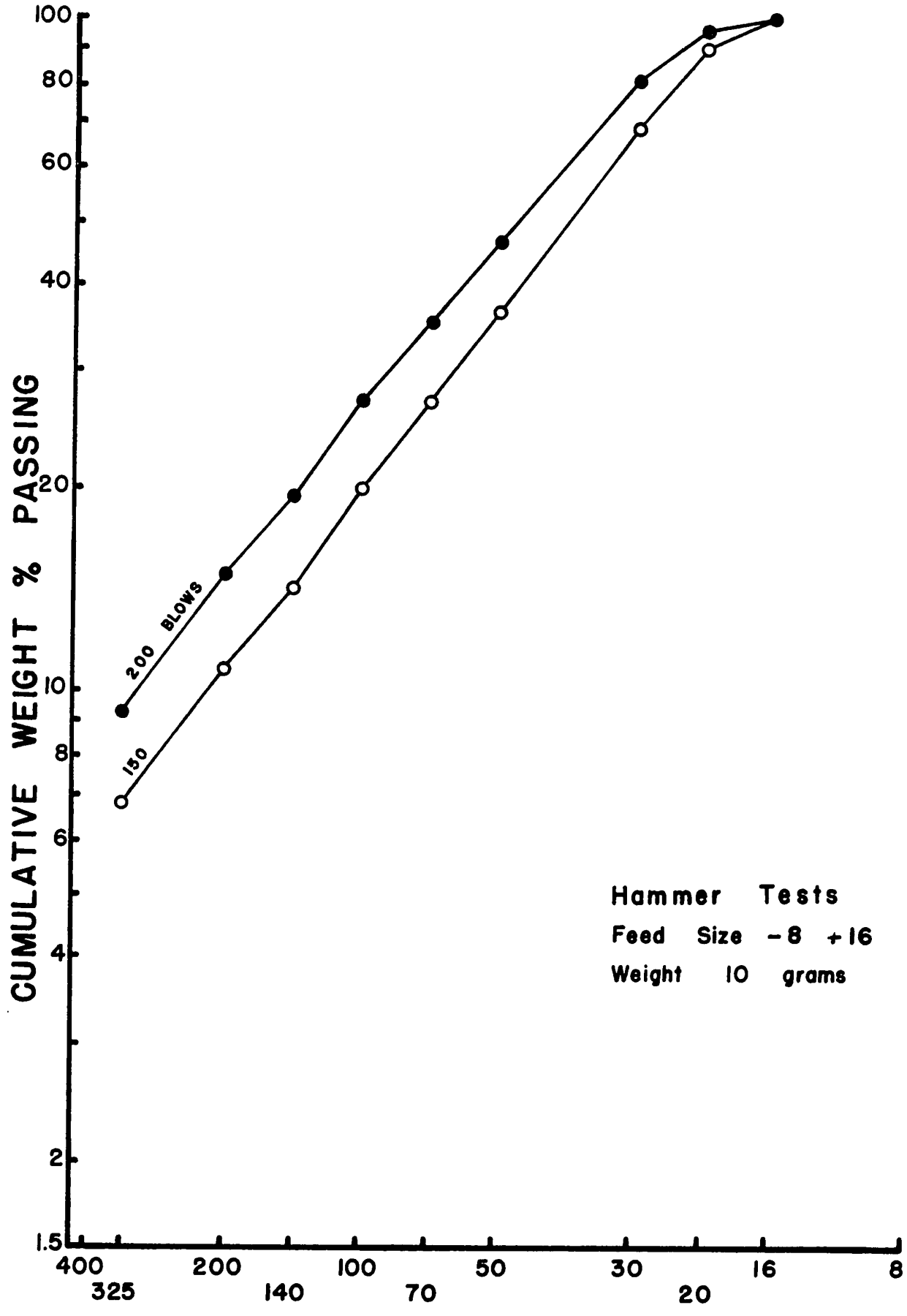
CUMULATIVE WEIGHT % PASSING
100
80
60
40
20
10
8
6
4
2
1.5
200 BLOWS
150
Hammer Tests
Feed Size -8 +16
Weight 10 grams
400
325
200
140
100
70
50
30
20
16
8
SCREEN SIZE (MESH)

Fig. 5.4

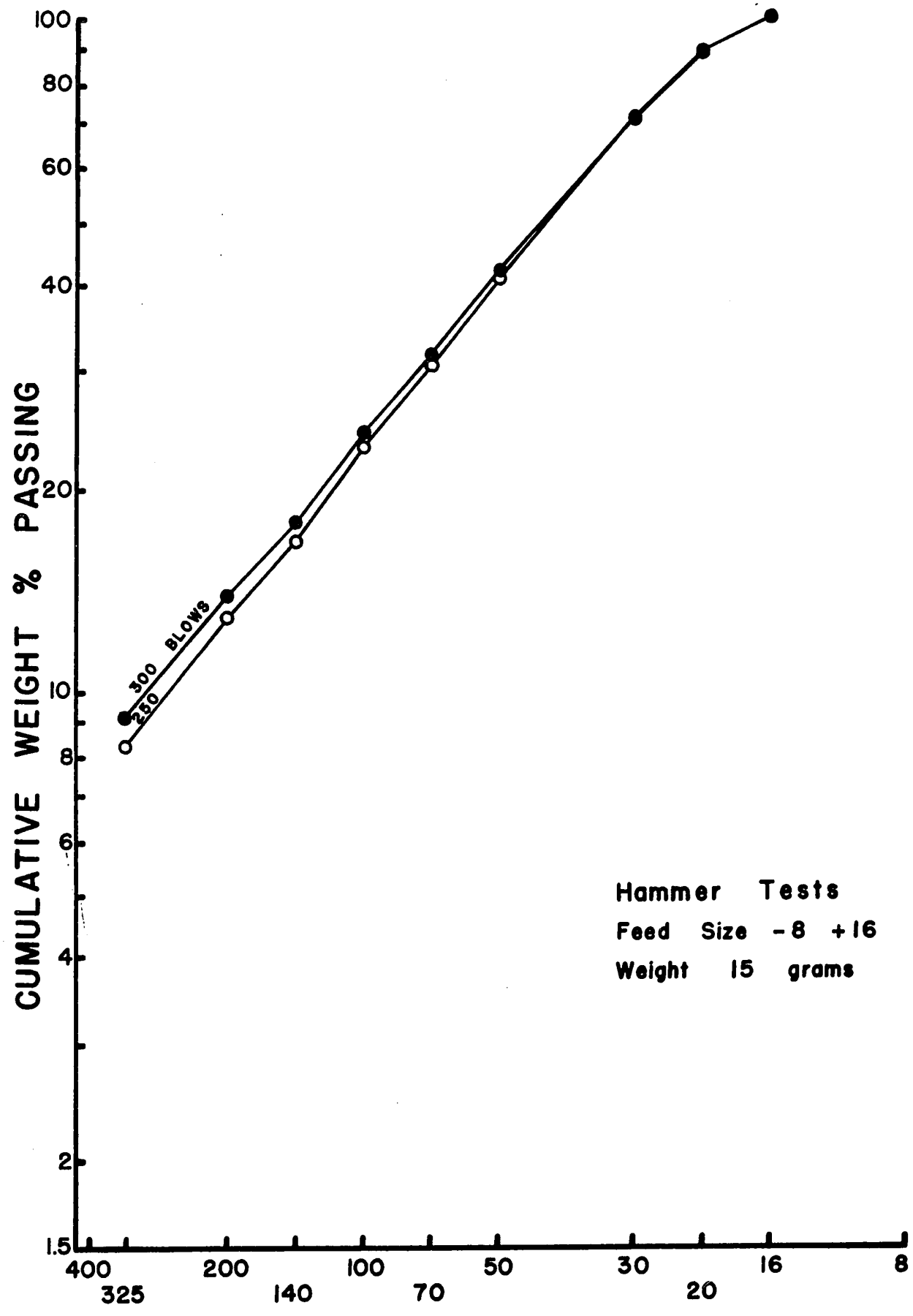
CUMULATIVE WEIGHT % PASSING
100
80
60
40
20
10
8
6
4
2
1.5
300 BLOWS
250
Hammer Tests
Feed Size -8 +16
Weight 15 grams
400
325
200
140
100
70
50
30
20
16
8
SCREEN SIZE (MESH)

Fig. 5.5

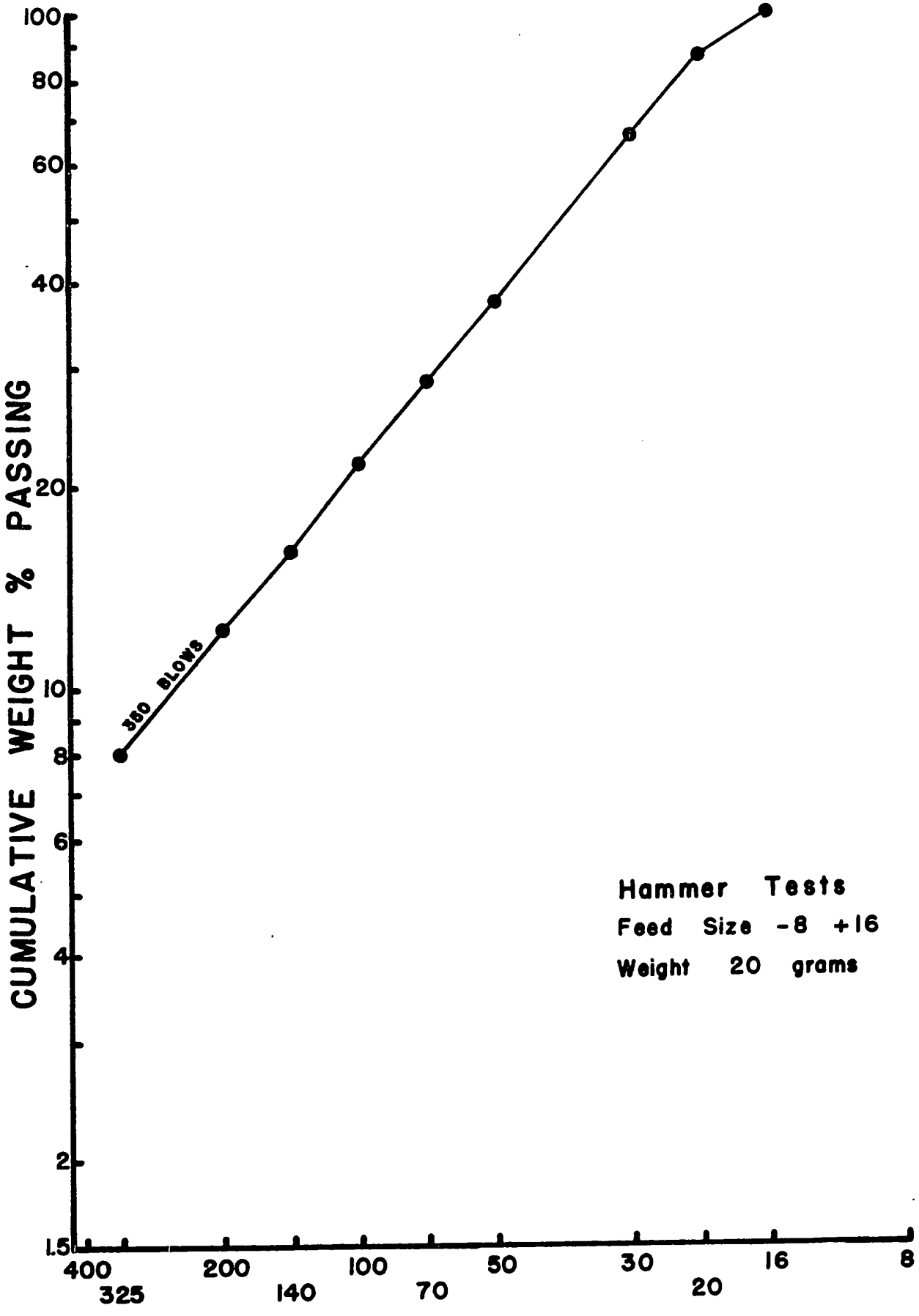
CUMULATIVE WEIGHT % PASSING
100
80
60
40
20
10
8
6
4
2
1.5
380 BLOWS
Hammer Tests
Feed Size -8 +16
Weight 20 grams
400
325
200
140
100
70
50
30
20
16
8
SCREEN SIZE (MESH)

Fig. 5.6

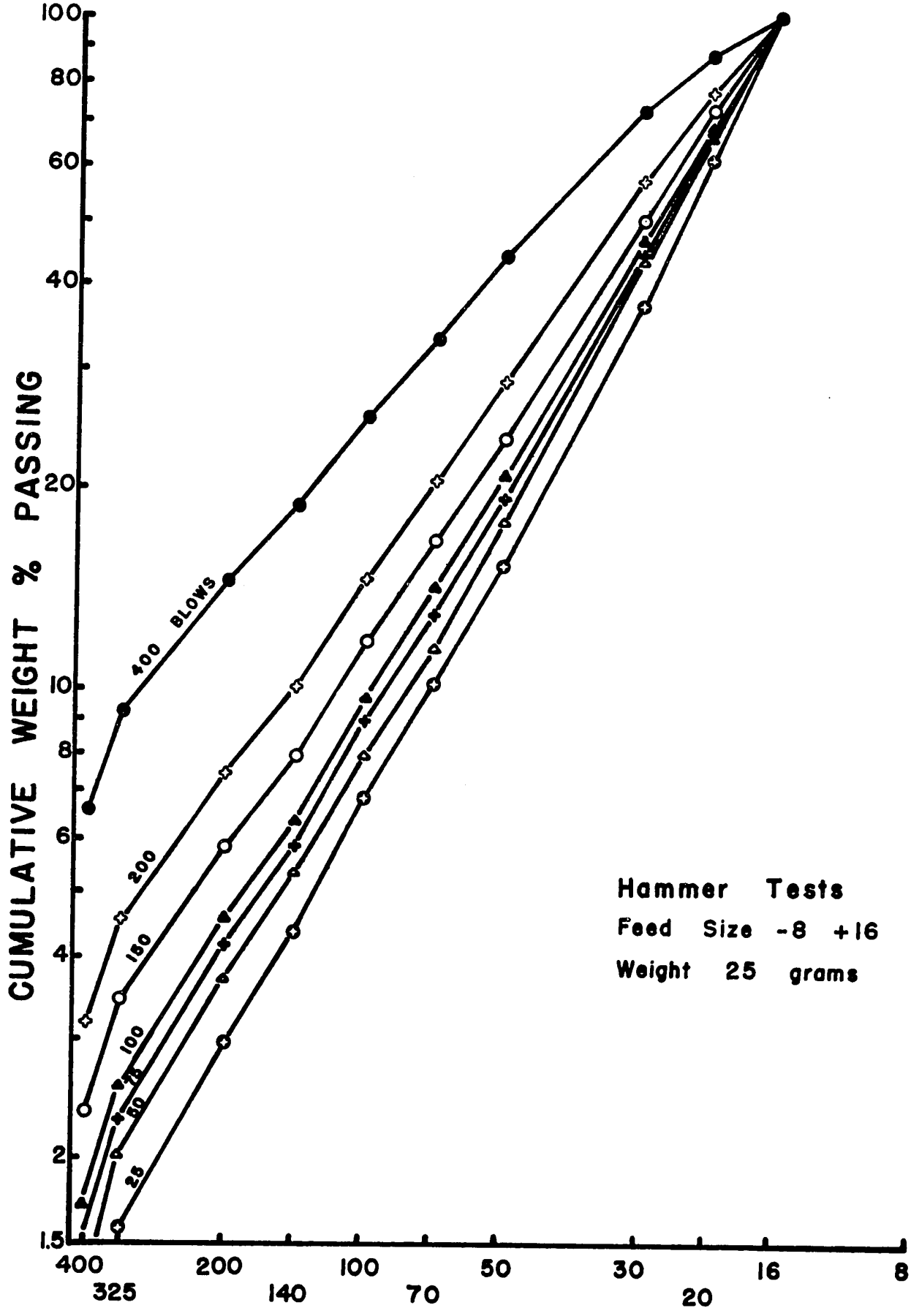
CUMULATIVE WEIGHT % PASSING
100
80
60
40
20
10
8
6
4
2
1.5
400 BLOWS
200
150
100
75
50
25
Hammer Tests
Feed Size -8 +16
Weight 25 grams
400
325
200
140
100
70
50
30
20
16
8
SCREEN SIZE (MESH)

Fig. 5.7

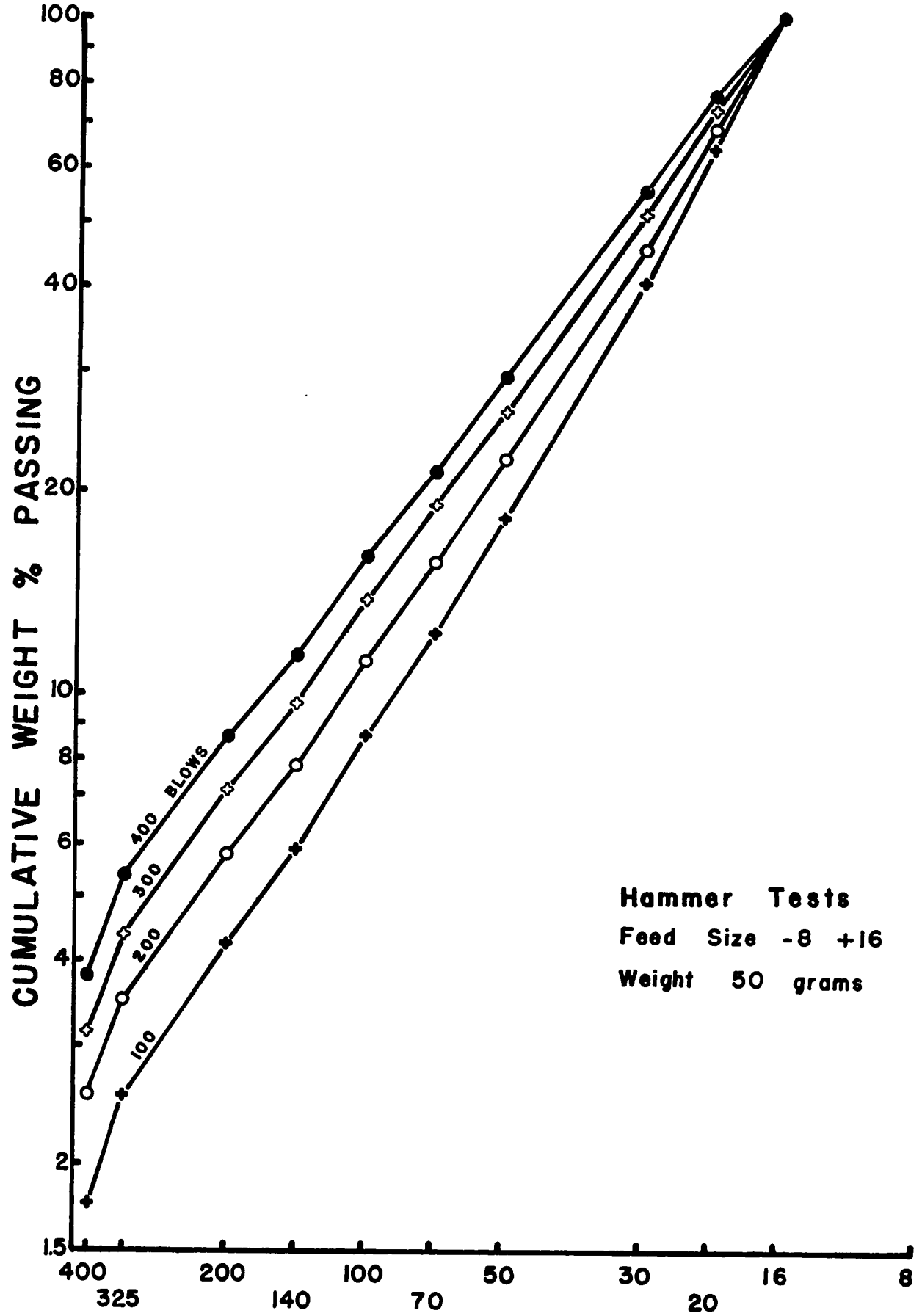
CUMULATIVE WEIGHT % PASSING
100
80
60
40
20
10
8
6
4
2
1.5
400 BLOWS
300
200
100
Hammer Tests
Feed Size -8 +16
Weight 50 grams
400
325
200
140
100
70
50
30
20
16
8
SCREEN SIZE (MESH)

Fig. 5.8

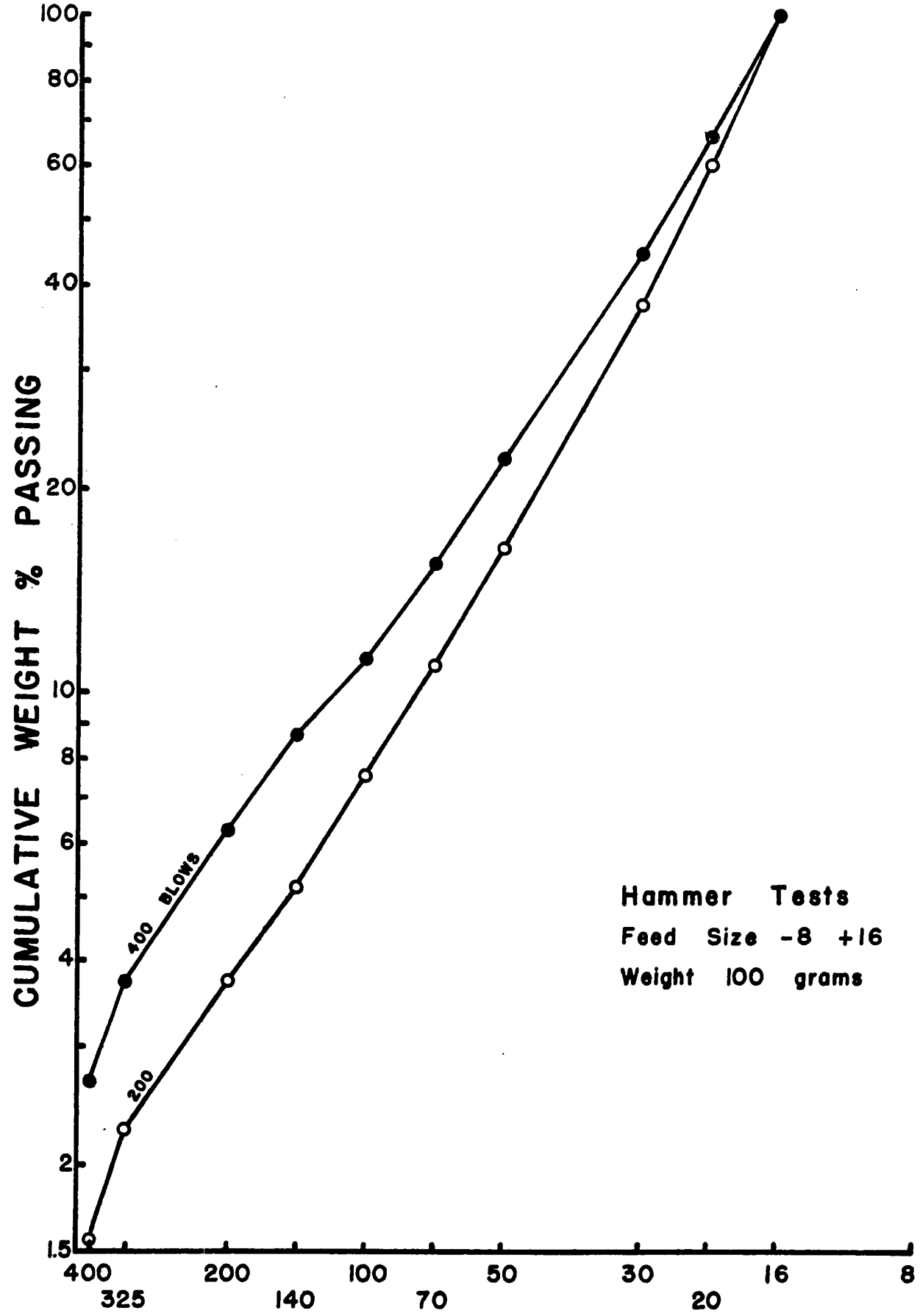
CUMULATIVE WEIGHT % PASSING
100
80
60
40
20
10
8
6
4
2
1.5
400 BLOWS
200
Hammer Tests
Feed Size -8 +16
Weight 100 grams
400
325
200
140
100
70
50
30
20
16
8
SCREEN SIZE (MESH)

Fig. 5.9

can be concluded that rock drilling is not a first order rate process.

C - GRAPHICAL SOLUTION

The amount of material broken in a single blow by a rock drill is a fraction of a gram and the blow energy is proportional to the total number of micro-events in that blow. The detailed graphical analysis of drilling comminution was conducted as follows:

Step (1): Hammer tests were made on samples weighing from 5 grams to 100 grams at energy levels of 25 blows to 400 blows. The particle size distribution for each category of tests is plotted in Fig. 5.3 to Fig. 5.9 and the results are tabulated in Appendix B. From these experiments, the author planned to extrapolate graphically the size distribution for a sample of negligible mass for any energy level, that is, the micro-event distribution. The smallest samples tested weighed five grams because it was felt that smaller samples would yield inconsistent results due to heterogeneity of rock. The results reported for the five gram samples are the mean of ten individual tests.

Step (2): The second step of the procedure consisted in plotting on a grid the weight fraction passing through a given sieve for every combination of sample weights and number of hammer blows. This is illustrated in Fig. 5.10; from this plot plan, contours of iso-percentages were traced, as shown, and prolonged to intersect the system of axes. However, since the contour method is considered insufficiently accurate to be used alone, profiles

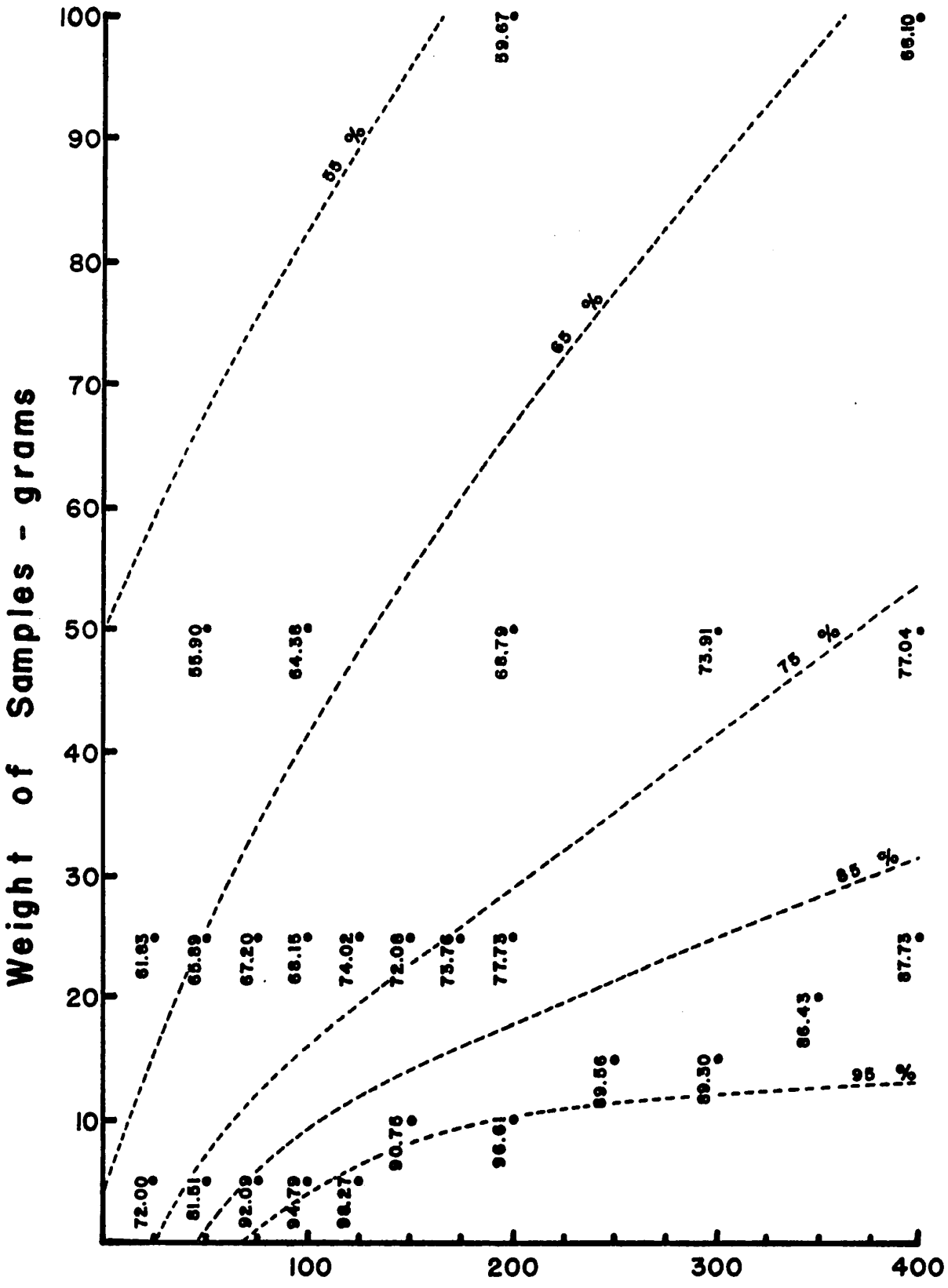

Fig. 5.10

CUMULATIVE % WEIGHT (-20 MESH)

were also made in directions parallel to each axis, as in Fig. 5.11 and Fig. 5.12. The 'zero gram' extrapolation values are found for every energy level by profiles drawn parallel to the weight axis as in Fig. 5.10. An example of the graphical extrapolation is shown in Fig. 5.11 and the results are plotted in Fig. 5.12.

The 'zero gram' line in Fig. 5.12 represents the fraction of material finer than 20 mesh produced by a given number of hammer blows or drilling micro-events. Although the 'zero blow' line in Fig. 5.11 has no physical meaning, it helps to determine, by extrapolation, the fraction of material broken in a single micro-event. The value at the origin of Fig. 5.10 is an approximation of the virtual size distribution of unbroken rock, that is, the primary breakage function of the rock. This procedure was repeated for every size fraction and the plots appear in Appendix C.

Step (3): The third step of the procedure consists in plotting the primary breakage factors for every particle size so as to obtain the primary breakage function. In order to do this, the percentage value for 'zero-blow zero-gram' is plotted for each size fraction. (vide Fig. 5.13). In this figure, it is seen that the curve is slightly concave, with a slope nearing unity. This is in agreement with the general shape of primary breakage functions usually reported in the literature (vide Fig. 5.2). In this particular case, although the function is of no use for future calculations, the shape of the curve indicates that the procedure followed in the graphical solution leads to acceptable results. However, the primary breakage function is far from being

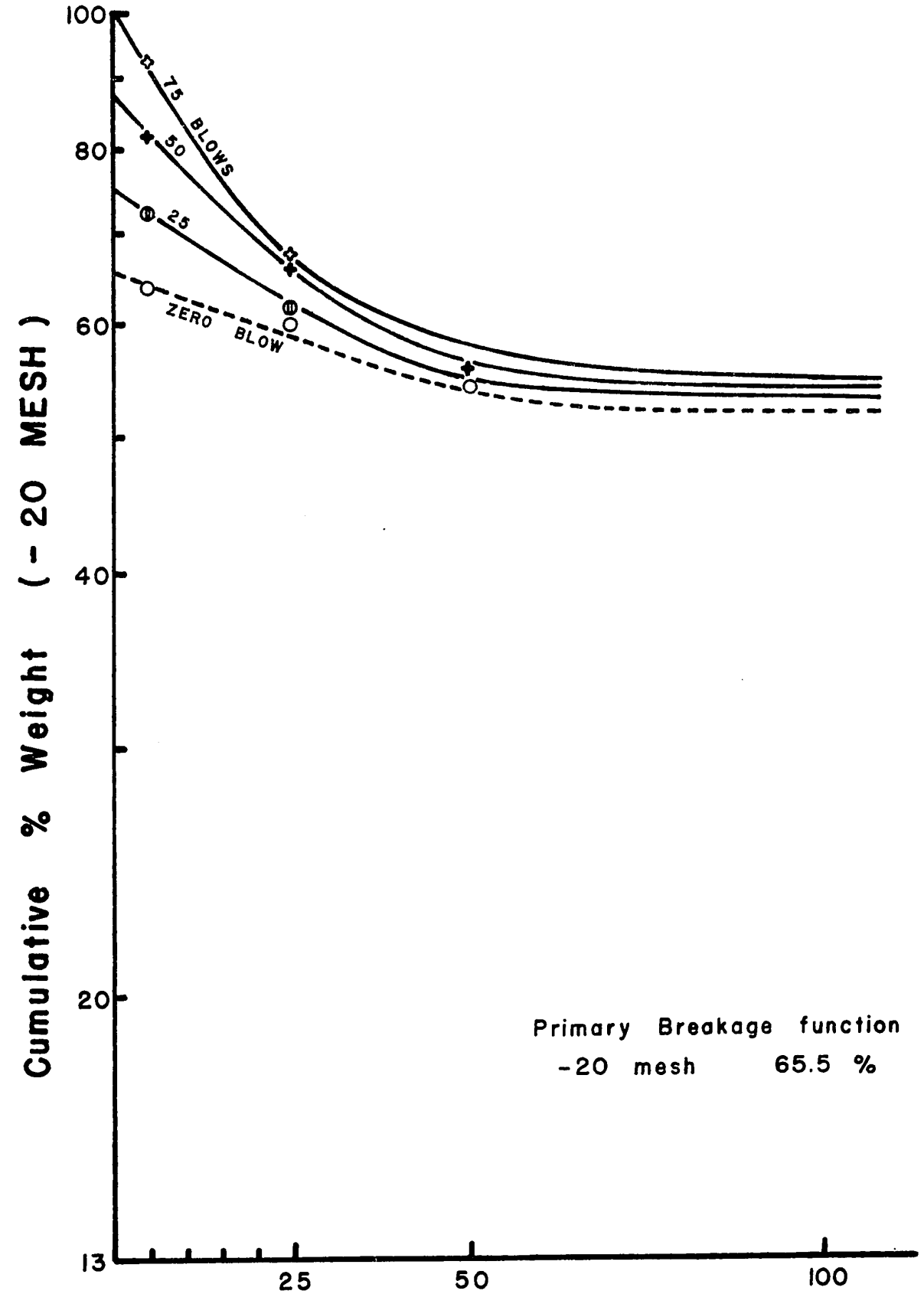

Fig. 5.11 EXTRAPOLATION TO ZERO GRAM

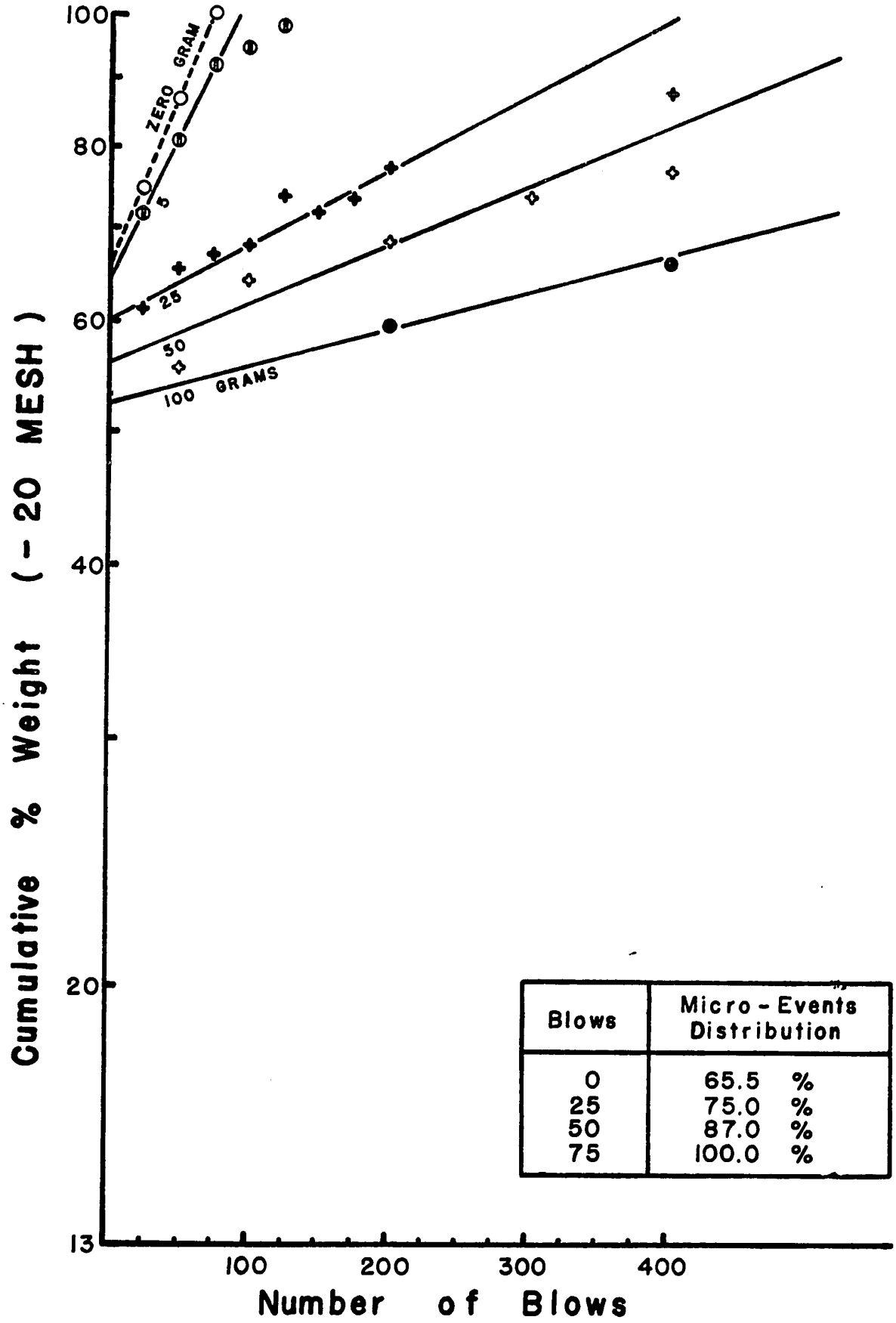

Blows	Micro - Events Distribution
0	65.5 %
25	75.0 %
50	87.0 %
75	100.0 %

Fig. 5.12 EXTRAPOLATION TO ZERO BLOW

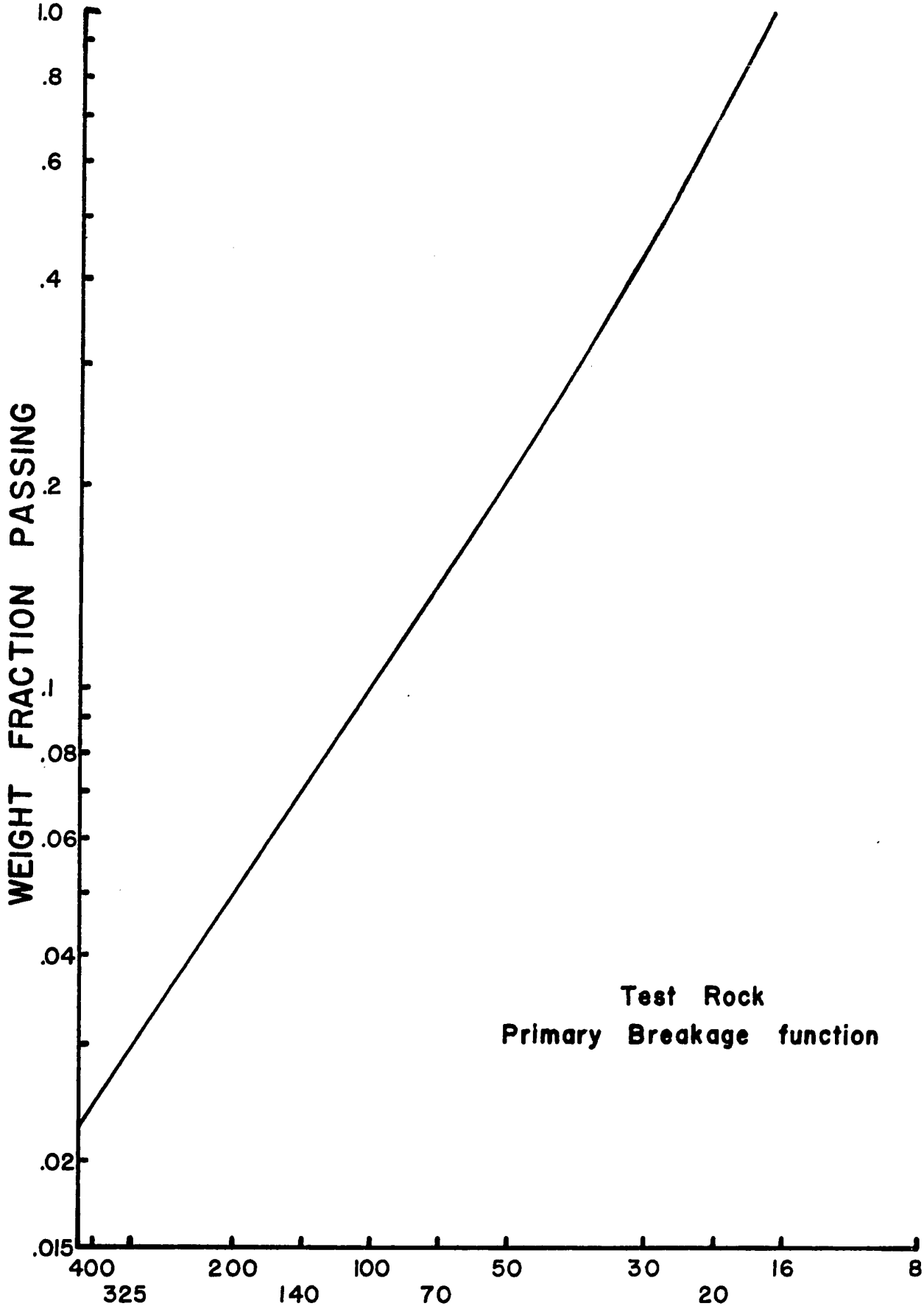
1.0
.8
.6
.4
.2
.1
.08
.06
.04
.02
.015
WEIGHT FRACTION PASSING
Test Rock
Primary Breakage function
400
325
200
140
100
70
50
30
20
16
8
SCREEN SIZE (MESH)

Fig. 5.13

meaningless; it shows that a minimum of 2% dust will be produced even in the single fracture of "-8 mesh+16 mesh" particles of Scottstown granite. This dust production must be compared with the "-400 mesh" curve values for the case of multiple fracture.

Step (4): A summary of the 'zero gram' curves for each sieve size is prepared as a next step in the technique (Fig. 5.14). From this graph, the size distribution produced by a given number of hammer blows on a sample mass nearing zero gram can be read. For example, the size distribution for 100 blows is tabulated on the graph. In accordance with the hypotheses mentioned previously, Fig. 5.14 becomes a chart from which the cumulative size distribution for a particular energy, corresponding to a certain number of hammer blows or drilling micro-events, can be read. The linearity and parallelism of these individual lines were not "fitted"; the set of curves is the direct result of the tests.

Step (5): The examination of drilling results and hammer test results so as to perceive similarity or dissimilarity must be made by comparing the frequency distributions of the various class sizes. In order to be consistent, there must be a constant ratio between the largest and the smallest particle in each class size; consequently, the limits of the class sizes were selected as follows:

- 16 mesh	+	30 mesh
- 30 mesh	+	50 mesh
- 50 mesh	+	100 mesh
-100 mesh	+	200 mesh
-200 mesh	+	400 mesh
-400 mesh		

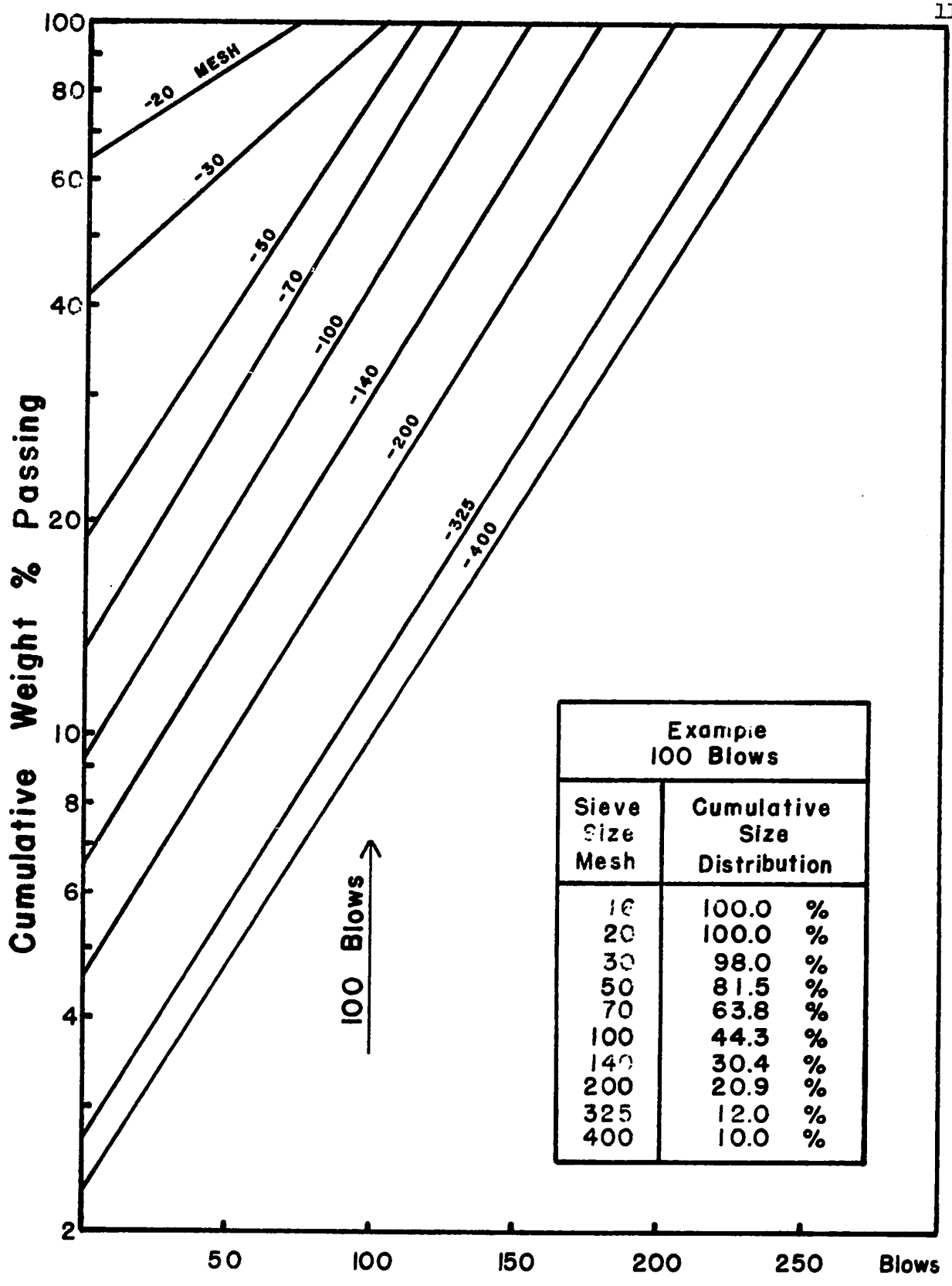

Example 100 Blows	
Sieve Size Mesh	Cumulative Size Distribution
16	100.0 %
20	100.0 %
30	98.0 %
50	81.5 %
70	63.8 %
100	44.3 %
140	30.4 %
200	20.9 %
325	12.0 %
400	10.0 %

Fig. 5.14 : CUMULATIVE SIZE DISTRIBUTION FOR A NUMBER OF MICRO-EVENTS

The 'zero gram' frequency distribution for each class size is easily found from Fig. 5.14 by simple subtraction. The use of Fig. 5.14 is simple; for instance, if it is desired to find the fraction of 'zero gram' of the class size '-50 mesh+100 mesh' produced after 90 hammer blows,

Read Fig. 5.14, curve -50 mesh:	70.3%
Read Fig. 5.14, curve -100 mesh:	37.7%
Difference:	32.6%

The resulting differences were calculated as illustrated above for all values of each class size and are plotted in Fig. 5.15. While this graph is similar to that of Arbiter and Bhrany, (Fig. 3.3), it must be observed that there is no linearity in any section, that is, it confirms that the hammer test is definitely not a first order rate process. Consequently, instead of using the breakage function and the rate function to calculate the instanteneous size frequency distribution after a certain number of hammer blows, it is necessary to read off the values on a graph, such as Fig. 5.15. In this way, rock drilling comminution can be adequately studied.

Step (6): A histogram is prepared for the drilling test under study. The results from test series No. 12 are presented in Fig. 5.16. It was observed that all drilling tests, whether performed on the single-blow rock-drill or with an actual rock drill, gave the same general type of histogram. While it is not intended in this chapter to study the individual effects of specific drilling variables, it is desired instead to understand drilling as a comminution process.

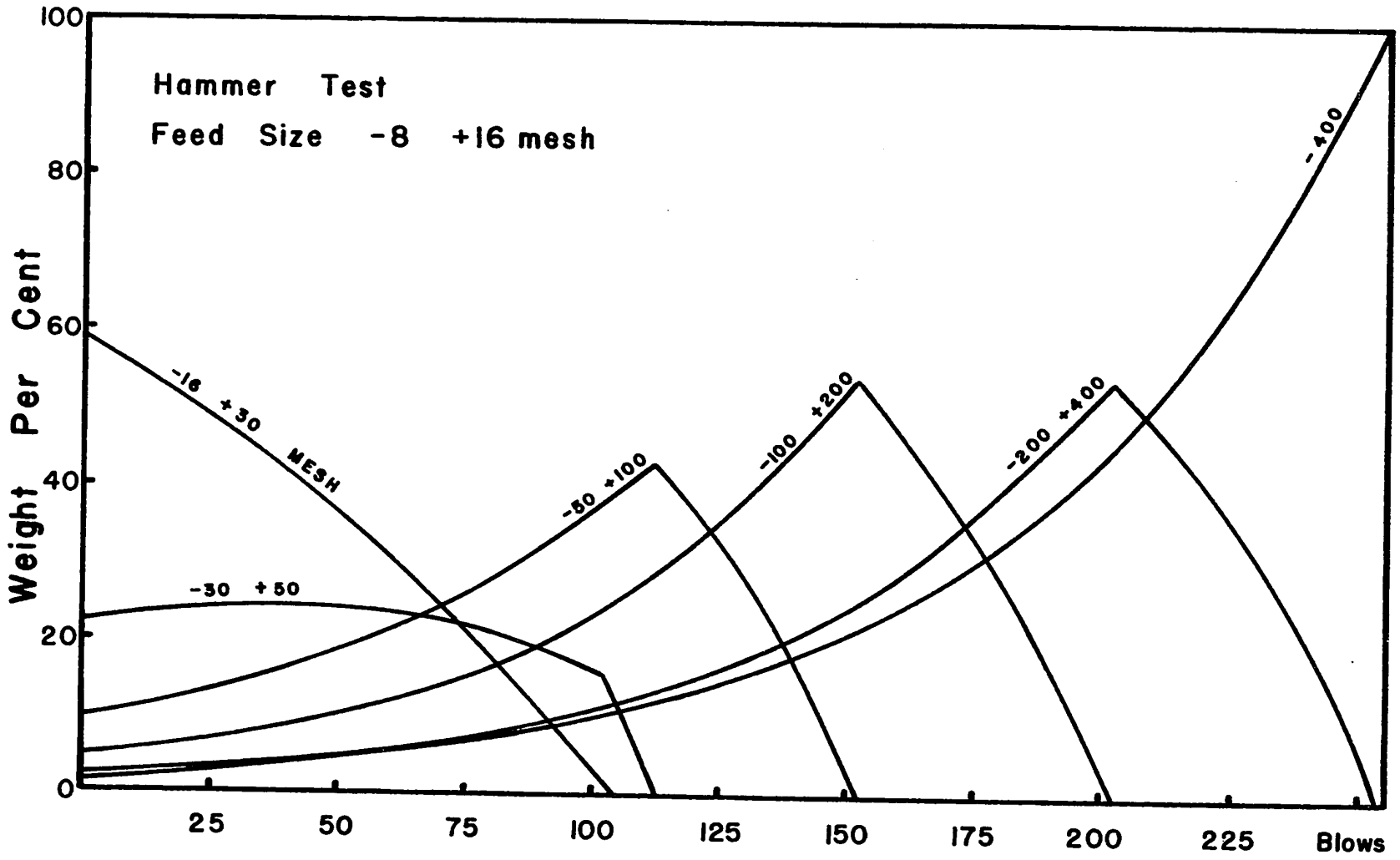

Fig. 5.15 : RATES OF FORMATION OF PARTICLES OF INDIVIDUAL CLASS SIZES

Step (7): Particles produced in the class size -8 mesh +16 mesh (Fig. 5.16) are considered to be due to pure chipping. These large fragments are few in number, but they cannot be disregarded as they are directly related to the index angle. The small number of these particles does not permit statistical interpretation by means of a mathematical model.

Step (8): Assuming that the frequency distribution of the drill test particles is the summation of a number of micro-events of the same nature as for the hammer test, the number of micro-events corresponding to the drill test frequency distribution may be found as follows by the method illustrated in the following example:

(a) In Fig. 5.16, read 9.8% for the size fraction -16 +30 mesh.

(b) In Fig. 5.15, read on curve -16 + 30 that 9.8% corresponds to less than 91 blows.

(c) Repeat procedure a and b above for every class size of particles of the drill test. It will be noted that for sizes -50 +100, -100 +200, -200 + 400 mesh in Fig. 5.15, the sections to the left of the apex represent the formation of material while the sections to the right represent depletion of material.

(d) Summarize all results graphically, as in Fig. 5.17.

Step (9): Theoretically, if drilling is exactly the same type of comminution as impact hammer crushing, it should be possible to find, from Fig. 5.17, a number of micro-events per drill blow common to all size classes. However, from Fig. 5.2, there are at

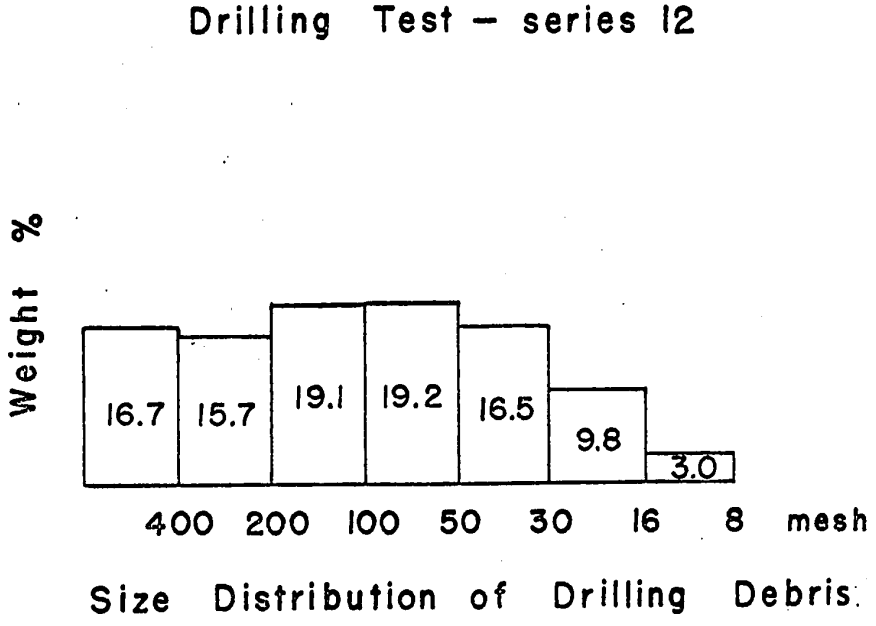

Fig. 5.16 – Typical Histogram – Drilling

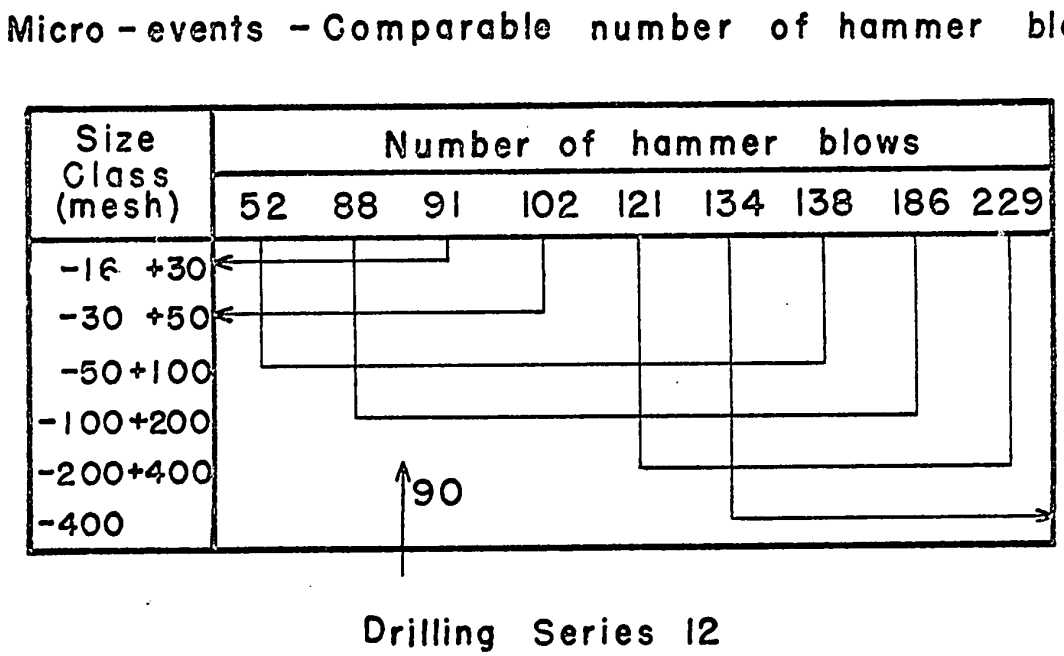

Fig. 5.17 – Determination of the number of micro-events per blow

least two zones in the drilling tests, as is indicated by the sag around the 140 mesh size. A corresponding zoning is recognized in Fig. 5.17; the four largest size classes overlap in the range of 88 to 91 hammer blows. (The value of 90 blows was selected as the model of the rock drilling situation investigated and its histogram can be seen in Fig. 5.18.)

Step (10): Impact crushing is responsible only for a fraction of the total amount of rock broken in drilling. That fraction is the factor by which the "90 blows" frequency distribution of the hammer test (Fig. 5.18) must be multiplied so that it fits completely within the drilling distribution (Fig. 5.19). This factor was found by calculating the ratio of drilling frequency % (Fig. 5.16) to the "90 blows" frequency % (Fig. 5.18) for every size class and selecting the lowest value (Fig. 5.19).

Step (11): The total area of the histogram in Fig. 5.19 represents the total amount of material broken in a single blow of the rock drill and is divided into three different distributions respectively identified as areas A, B, and C.

Step (12): Area A (Fig. 5.19) covers 59.6% of the histogram, that is, 59.6% of the material was broken by impact crushing as in the hammer test, corresponding to 90 micro-events per drill blow.

Step (13): Areas B and C were redrawn on a common base line (Fig. 5.20); the weight percentage of each size fraction was found by simple subtraction from data in Fig. 5.19.

Step (14): Area B in Fig. 5.20 represents coarse particles. This distribution was very erratic from test to test, and the author has concluded that this fraction of material was produced by chipping due to index fracture. In the particular example,

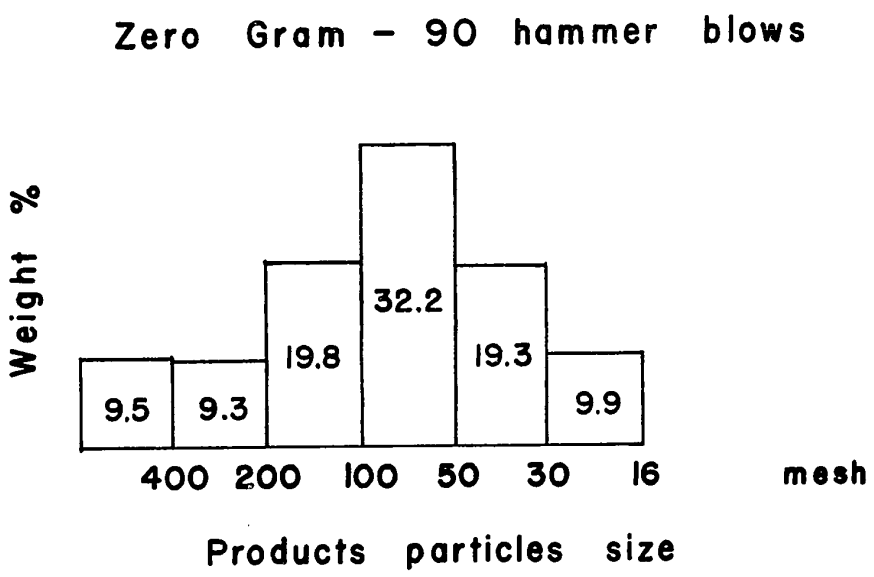

Fig. 5.18 — Typical histogram of hammer tests

$$\text{Reduction ratio} = \frac{19.2}{32.2} = 0.596$$

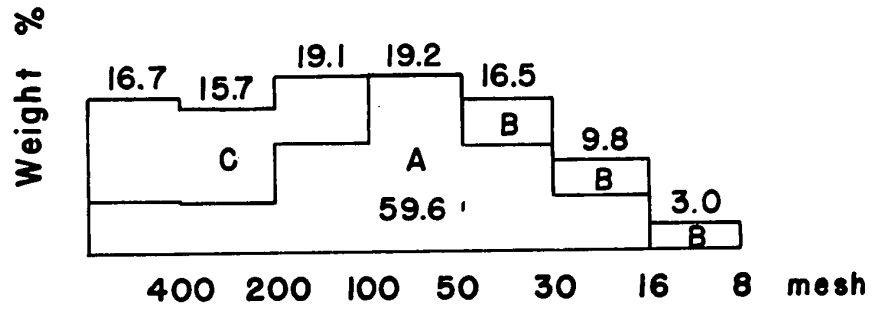

Fig. 5.19 — Fitting histogram of hammer tests for 90 blows (Fig. 5.18) into Drilling test histogram (Fig. 5.16)

Drilling Test Analysis (series # 12)

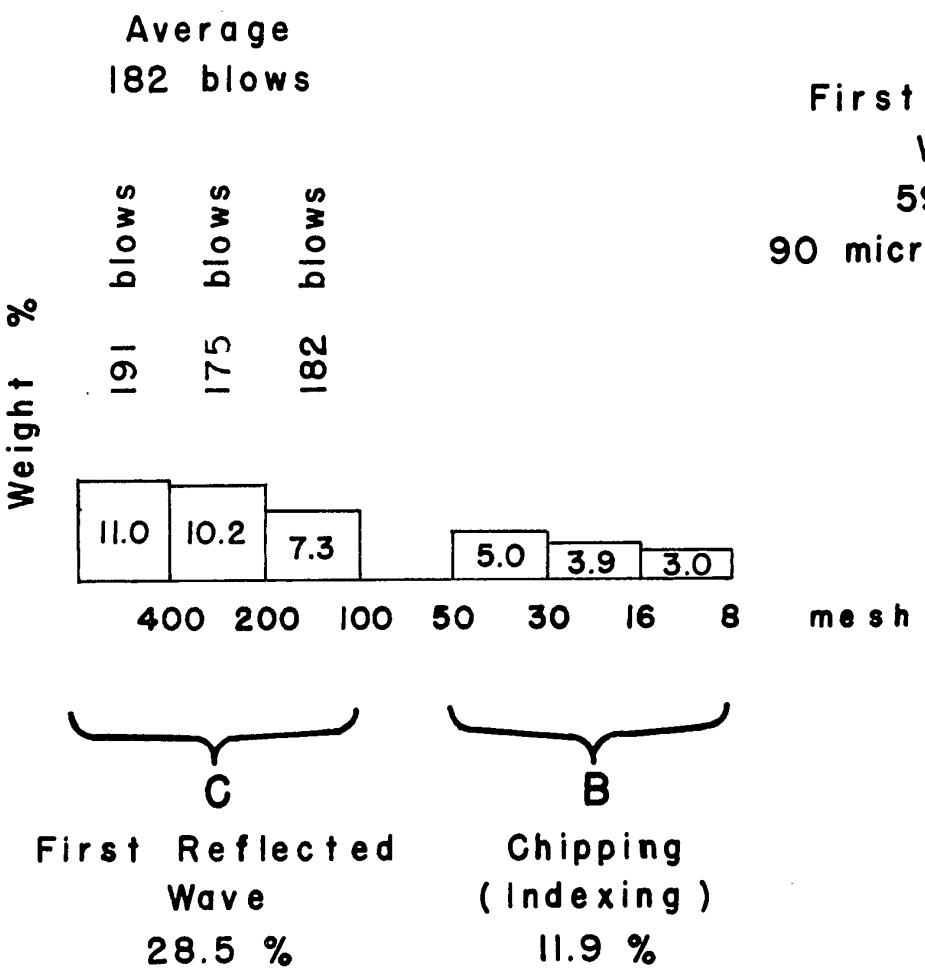

Average number of micro-events per impact

$$\text{micro events} = \frac{(191 + 175 + 182 + 90)}{7} = 91$$

Fig. 5.20 - Types of fracture in percussive Drilling

11.9% of the rock was broken by chipping.

Step (15): Distribution C, Fig. 5.20, was analyzed with the aid of Fig. 5.15, believing it may have been due to a different type of impact crushing. The following results were found:

Size -100 + 200 mesh	182 blows
Size -200 + 400 mesh	175 blows
Size -400 mesh	191 blows
Average number of blows	182

It was fascinating to observe that the number of micro-events for distribution C was exactly double that for distribution A. This was observed for all drill tests, including those with the commercial rock drill. This distribution represents the material which sustains the impact of the first incident wave as well as the action of the reflected wave. In this particular case, 28.5% of the total material is subjected to repeated fracture (Fig. 5.20). This material does not represent additional penetration but pulverisation of already broken material.

Step (16): All other drilling test results are tabulated in the Appendix A.

D - THE PROCESS OF BIT PENETRATION

This drilling comminution study leads to further analysis of the bit penetration mechanism illustrated in Fig. 2.1. The sequence of penetration events in drilling is now seen as follows:

1 - The bit edge comes in contact with the rock and

as the energy is concentrated over a very small fraction of the length of the cutting edge, surface irregularities are crushed until the energy is distributed over a larger fraction of the length of the bit edge.

2 - A crack propagates directly under the longitudinal axis of the drill rod due to concentrated loading under the cutting edge.

3 - With increased penetration, the area of the bit in contact with the rock increases and crushing takes place under the bit.

4 - Due to rock porosity, the bit penetrates into the rock and builds up a quasi-hydrostatic pressure in the rock under the total area of the bit in contact with it. This zone is bounded by two converging cracks that develop from the contour of the bit surface in contact with the rock.

5 - The walls retaining the crushed material fail due to triaxial pressure at the points of minimum energy requirement, that is, on the free face of the rock. The coarse fragments formed are due to tension fracture. This is the chipping phase. The presence of radial cracks shows fracture but incomplete separation. An excellent photo-micrograph supporting this description is presented by Gnirk (45).

6 - Once the chips are removed, a part of the crushed material under the bit is liberated and the bit penetrates suddenly into the rock. In Fig. 2.1, these first six steps are illustrated by the first positive slope segment and the first negative slope segment.

7 - Upon the second loading of the rock by the bit, energy is no longer transmitted directly to the rock, but continuity is broken by the cushion of crushed material. Due to this lack of continuum, efficiency of energy transfer is reduced and it can be seen in Fig. 2.1 that as the number of penetration steps increases, the positive slope segments become steeper. Similarly, the negative slope segments are also steeper and shorter, indicating a much less efficient process of penetration. This is a phase of pulverization and dust formation.

E - CONCLUSIONS

The following conclusions became evident from the drilling comminution studies:

(1) The fragments produced in the chipping phase are usually not subjected to multiple fracture in single-blow drilling. However, in conventional drilling, the larger fragments may be subjected to secondary fracture due to particle kinetic energy (9), rotation of the bit at the bottom of the hole, and mainly to abrasion or crushing along the drill steel during the flushing process of the hole.

(2) Drilling comminution is definitely not a first order rate reaction and the hammer test is an adequate representation of the type of fracture that takes place in the rock under the area in contact with the bit.

(3) The choice of an average slope 'K' by Hustrulid as in Fig. 2.1, in order to predict the force-penetration relation, may indicate that there is always an advantage in increasing the

force on the bit. On the contrary, the actual jagged shape of the force-penetration diagram as well as the drilling comminution experiments indicate that theoretically, an efficient rock drill will have a high blow rate, a relatively low blow energy and the indexing will be such that it will favor the maximum amount of chipping.

(4) Rock drilling is characterized by multiple fracture; it follows that reduction in dust formation is possible only by reducing the number of micro-events per blow; this is theoretically possible in two ways, mainly a reduction of the blow energy and, mostly, by finding a means to prevent the formation of the reflected wave.

(5) Efficient rock penetration is produced during the first incident wave only, while the reflected wave action is used almost exclusively to pulverize material already broken. Fig. 5.21 drawn from Hustrulid's thesis is evidence that the reflected wave does not perform useful work.

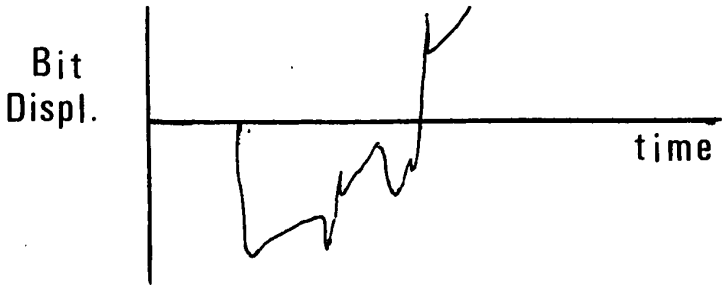

Fig. 5.21 - Displacement-time Record (after Hustrulid (60)).

(6) The shape of the reflected wave is the same as that of the first incident wave but of different maximum stress value. This was previously shown by Equation 2.6.

7 - Tests done with the commercial rock drill and the single-blow rock-drill showed that in both cases, the number of micro-events per blow was the same. The only parameters equal in both cases were the drill rods and bits. Consequently, the decay rate is not modified seriously by the shape or the mass of the piston and the drill rod is the dominant factor responsible for efficient energy transfer to the rock; this is also partly indicated by Equation 2.7.

8 - The reflected wave is the most important factor responsible for dust formation.

9 - Referring to Fig. 5.20, if repeated fracture was avoided, it can be seen from Area C that the fraction 11% of dust would not have been formed, a reduction in the order of 60%, based on the amount of dust shown in Fig. 5.19.

VI - INFLUENCE OF SPECIFIC VARIABLES

A - INTRODUCTION

Our knowledge of percussive rock drilling indicates that the penetration rate depends primarily upon the blow energy, blow rate, rotation rate, thrust and bit design. The experiments in this research program were planned to further our understanding of rock breakage phenomena in percussive drilling, to link size distribution data with penetration rate results, and to determine the operating conditions leading to the formation of the least amount of dust. The interdependency of rock drilling variables complicates the study of the drilling process and the author was led into a descriptive analysis of indexing mechanism in order to interpret the results of his findings.

B - THE CONCEPT OF HISTORY

Bennett, Brown and Crone (19, 8, 7) supported the theory that energy of fracture for brittle materials is used partly in the creation of particles and partly in the formation of cracks. From this, it follows that a cohesive piece of rock previously submitted to severe stresses would normally require less energy for granulation than another piece of similar rock previously exposed to lower levels of stresses.

Thin sections were cut through the walls and bottom of a drill hole in order to ascertain the extent and nature of damage around it. Fig. 6.1 is an assembly of photomicrographs

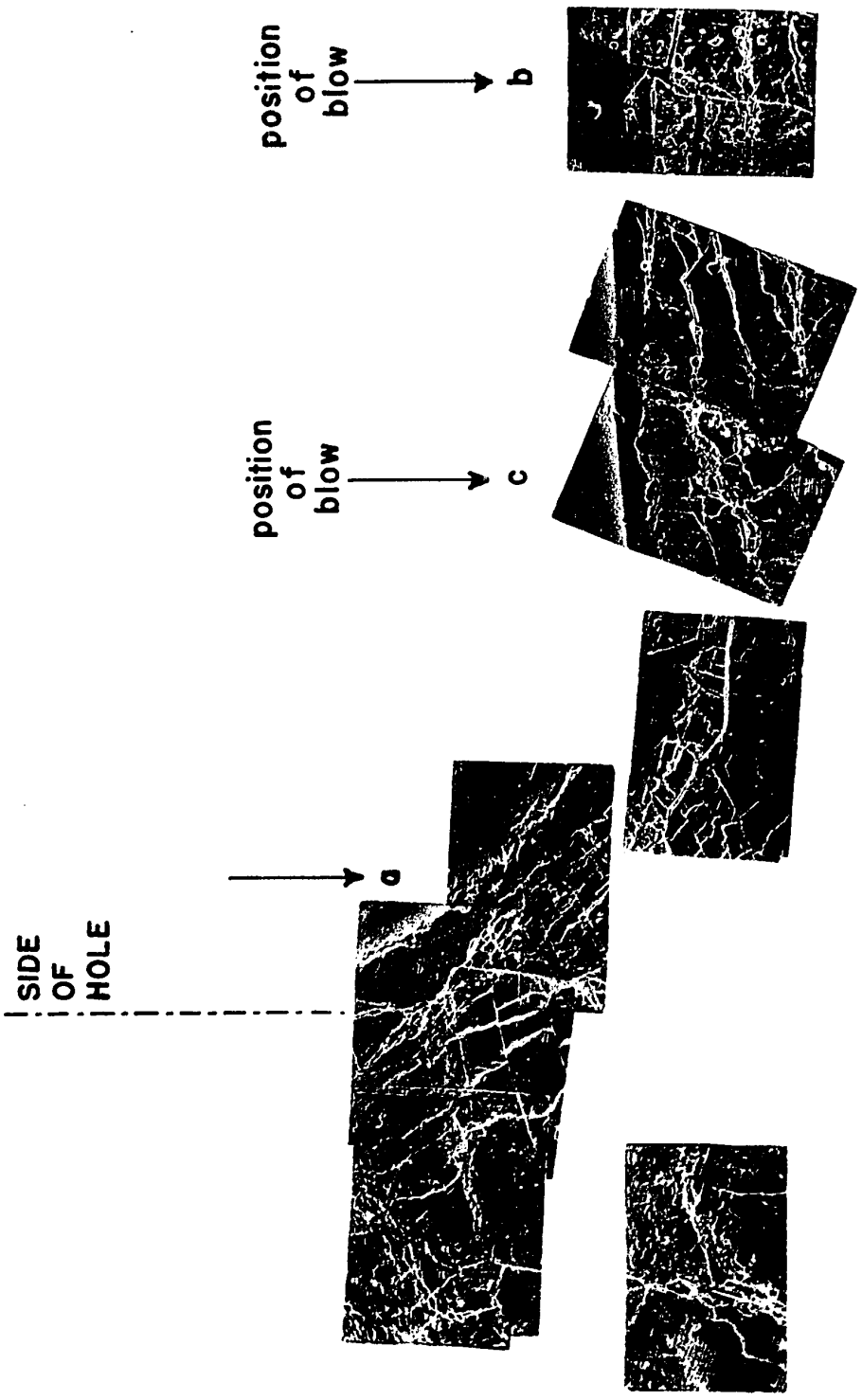

Fig. 6.1 : Thin section through wall and bottom of a drill hole

Fig. 6.2 : Cracks remote from wall of drill hole

Fig. 6.3 : Cleavage and boundary fractures

Fig. 6.4 : Cracks on wall of drill hole

from one of the thin sections where cracks are clearly observed. The hole had been cleaned by light vacuum aspiration to prevent the removal of particles loosely held in place. There is no doubt that unbroken rock along the walls as well as at the bottom of the hole is severely fractured, yet, the individual particles formed thereby are securely locked together. An observation (Fig. 6.2) made at a location remote from the wall of the hole shows very thin cracks while near the walls (Fig. 6.4), wide open cracks are evident. Other photographs (Fig. 6.3) show that grain boundaries and cleavage planes are important controlling factors in the process of rock fragmentation.

Reverting to Fig. 6.1, it would appear that fracture by impact crushing near point 'a' would produce fine particles due to the previous history of the rocks, while a chisel blow around points b' and 'c' could produce larger chips, especially when a free face is available to permit indexing.

C - INDEXED FRACTURE

The upper part of the force-penetration diagram (Fig. 2.1) is steeper at higher energy levels because the coefficient of energy transfer decreases due to the relative movement of particles and the lack of rock continuity in the inverted cone of crushed material under the bit. When blows are struck in old grooves upon consecutive turns, the possibility of efficient indexing is reduced considerably for the above reason. Accordingly, test conditions were chosen to avoid these siting circumstances.

1 - Choice of Rotation Angles

In order to prevent the striking of blows at the same place on consecutive passage of the cutting edge, the angles of rotation selected had to include a number which was not a primary number of 360. As the first primary number excluded from 360 is 7 and the gear of the rotation mechanism of the single-blow rock-drill turns 3^{o} per tooth, the rotation angles selected were multiples of 21^{o}. Tests were carried out with angles of $10\frac{1}{2}^{o}$, 21^{o}, 42^{o}, 63^{o} and 84^{o}. In this manner, a chisel bit was striking into an old groove every seventh passage of the cutting edge or every $3\frac{1}{2}$ complete revolutions.

2 - Twofold Indexing

The total rotation of the drill steel is ω (Fig. 6.5a) and on a given turn, imprints are left along lines 1-1. When the rotation angle satisfies the condition mentioned in the previous paragraph, the drill steel will strike along line 2-2 on the next passage of the cutting edge, so that

$$\omega = \alpha + \beta$$

Cracks left in the rock by previous impacts along the set of lines 1-1 will alter the crater volume removed by the blow along line 2-2 because indexing can and will occur on each side. In rotation, therefore, indexing is a twofold variable and its study must be done in systems, that is, the angle α is kept constant and the angle β is the variable.

3 - Discrete Character of Index Angles Systems

In percussive drilling, since the bit strikes the

bottom of the hole a given number of times per revolution, the angle β is not a continuous variable but rather takes discrete values (Fig. 6.5b).

A chisel bit rotates an angle β between strikes; after 'n' strikes, the blow will be applied between two existing grooves so that

$$n\omega = 180 + \alpha$$

It follows that, for different values of n, a discrete set of values for α and β can be established.

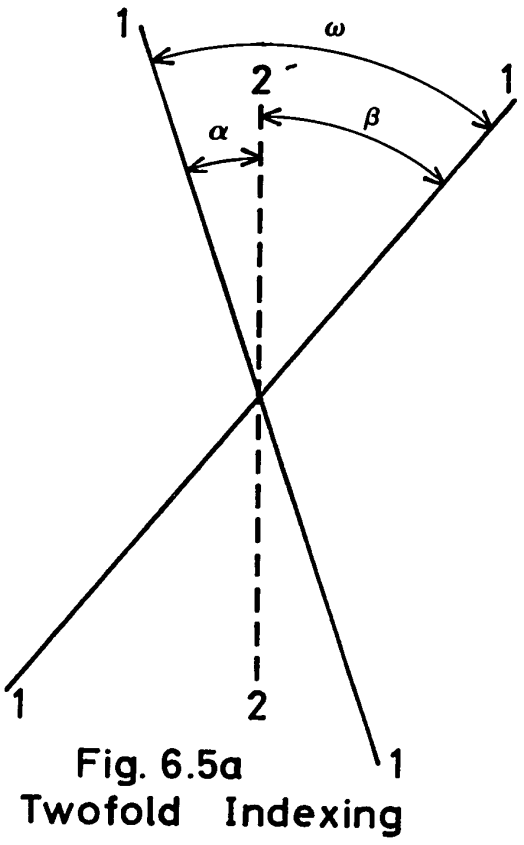

Fig. 6.5a
Twofold Indexing

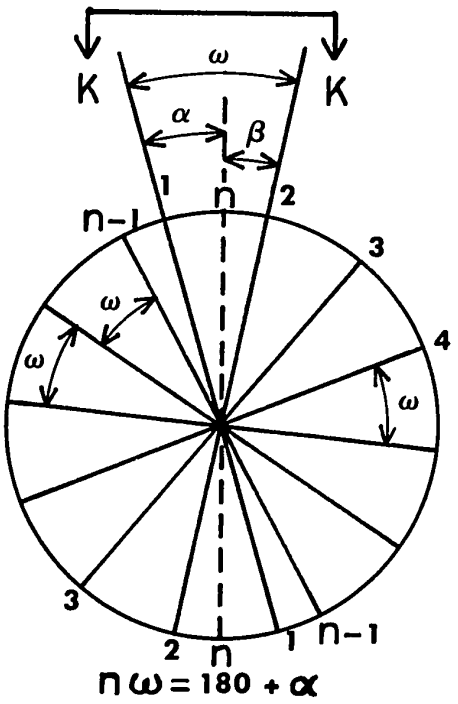

Fig. 6.5b
Discrete values of ω

Fig. 6.5 : Characteristics of twofold indexing.

$$\omega = \frac{180 + \alpha}{n}$$

where α = Constant

$\beta = \omega - \alpha$

Most of the tests of this project were conducted for an α system of 9^{o} and a few values of 12^{o}.

4 - Rock Breakage in Twofold Indexing

The type of fracture and size of crater in twofold indexing is controlled by the blow energy, the distance from the closest imprint on either side of the impact line and history of the rock. When studying the periphery of a hole in the direction 'KK', Fig. 6.5b, the following situation is observed: (Fig. 6.6)

Imprints under lines '1' (Fig. 6.6), have left a crater indicated by the shaded area 'a' and a zone of crushed

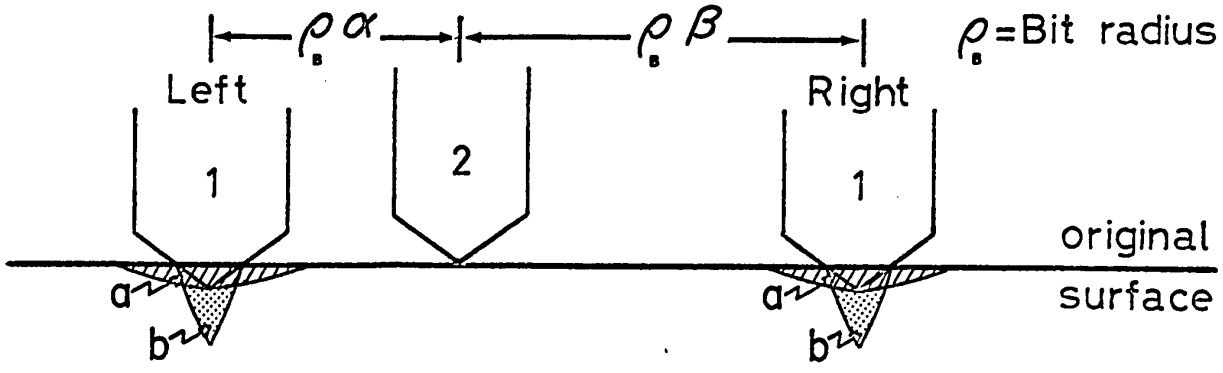

Fig. 6.6 : View 'KK' from Fig. 6.5b.

material 'b' left in situ under the bit. When the bit impacts along line '2', the volume of rock removed will vary with the energy applied. The following possibilities, based upon the equality of blow energy along lines '1' and '2', may be listed as below:

(a) At very low energy, the end result is a series of small craters, equal in size, and independent.

(b) An increase in energy will permit the breaking of the crater under line '2' to break into the nearest crater under line '1', on the left side in Fig. 6.6.

(c) Further increase in energy causes breakage into both adjacent craters but fracture does not progress beyond the crushed zones under the previous impact lines '1'.

(d) Additional increase in energy will be inefficient because the fractured rock contained in the inverted cones 'b' prevents energy transfer. Microscopic and macroscopic examination of particles found in the crater of line '2' show compaction of fines in the forms of tablets.

(e) Experiments have shown that the crushed material in the inverted cones under existing craters act as a barrier for energy transfer and arrest the process of indexing.

D - ENERGY SERIES

The force-penetration curve (Fig. 2.1) is a jagged

line and, whenever a straight line is used to represent the average force-penetration function, it is implied that penetration is proportional to the applied force. However, experimental work reported previously shows that the crater volume is a linear function of the blow energy but, as the crater volume is a function of the square of the bit penetration, we can write (54)

$$\text{Energy} \approx (\text{Penetration})^2$$

The author carried out five groups of tests with a weight of 28.7 lbs at a total rotation of $10\frac{1}{2}^{o}$ to test the energy relationships. The results of the tests are shown in Fig. 6.7. It is observed that penetration increases to a maximum as energy increases but, above a certain level of energy, the penetration decreases. These findings are far removed from the straight line assumption.

This decrease in penetration at high energy level was most informative. The examination of the particles showed a large amount of caking and a large amount of dust adhered to the coarse particles. Above all, these results confirm that the presence of inverted cones of crushed material prevents energy transfer beyond them and limits the efficiency of indexing. The upper part of Fig. 6.7 shows also that, at high energy, there is an increase in the production of fine particles as well as a considerable increase of multiple fracture. This curve shows that the least amount of multiple fracture occurs at the point of maximum penetration, that is, when the energy is just sufficient to produce complete indexing on each side of the

center line of the bit. This will occur when the angles α and β are different but almost equal.

It is also possible to conclude here that it is beneficial to operate a machine at a high rotation angle; this allows the operator to apply a higher blow energy and if angles α and β are large, increased fractures are possible, resulting in relatively low dust formation and high penetration rate.

1 - Specific Energy

Usually in drilling, the specific energy is the amount of energy required to break a unit volume of rock. However, it was impossible in these experiments to measure the amount of energy actually used in breaking, since only the available energy was measurable. In order to avoid direct comparison of these results with classical studies, the specific energy was calculated in grams per unit of energy. (The Specific gravity of rock is 2.73, so, a simple division would give the specific energy per unit volume).

The specific energy curve so calculated should have the same shape as that obtained with energy actually consumed because the decay factor (Equation 2.7) varies only with the geometry of the hammer, while the slope 'K' varies with the used energy (Fig. 2.1). According to Simon (Fig. 2.9), the fraction of energy transferred from the steel to the rock is the ratio of the decay factor to 'K'. We may therefore conclude that the specific energy curve as presented in this work will have the

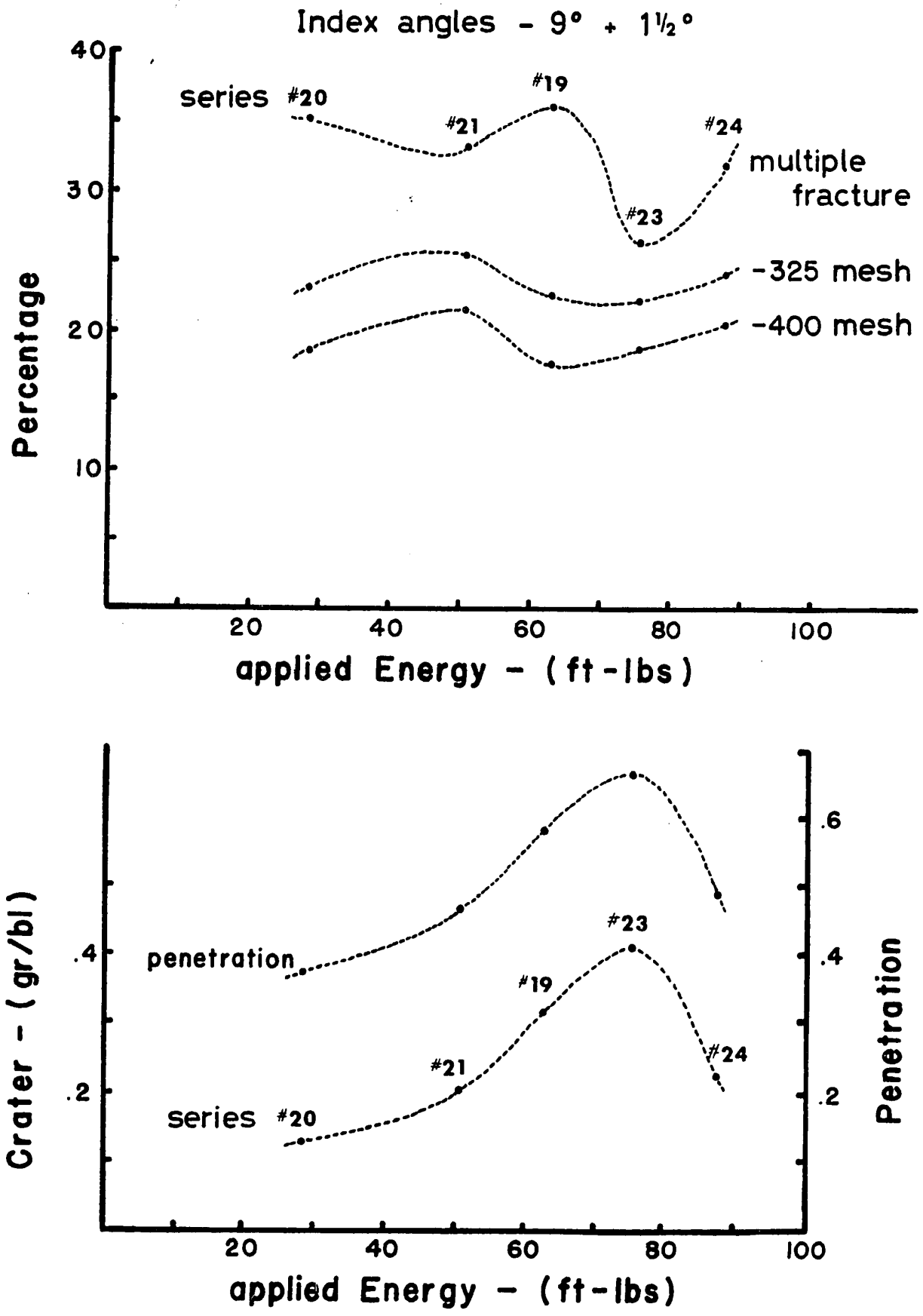

Fig. 6.7 ENERGY SERIES - CONSTANT IMPACT WEIGHT

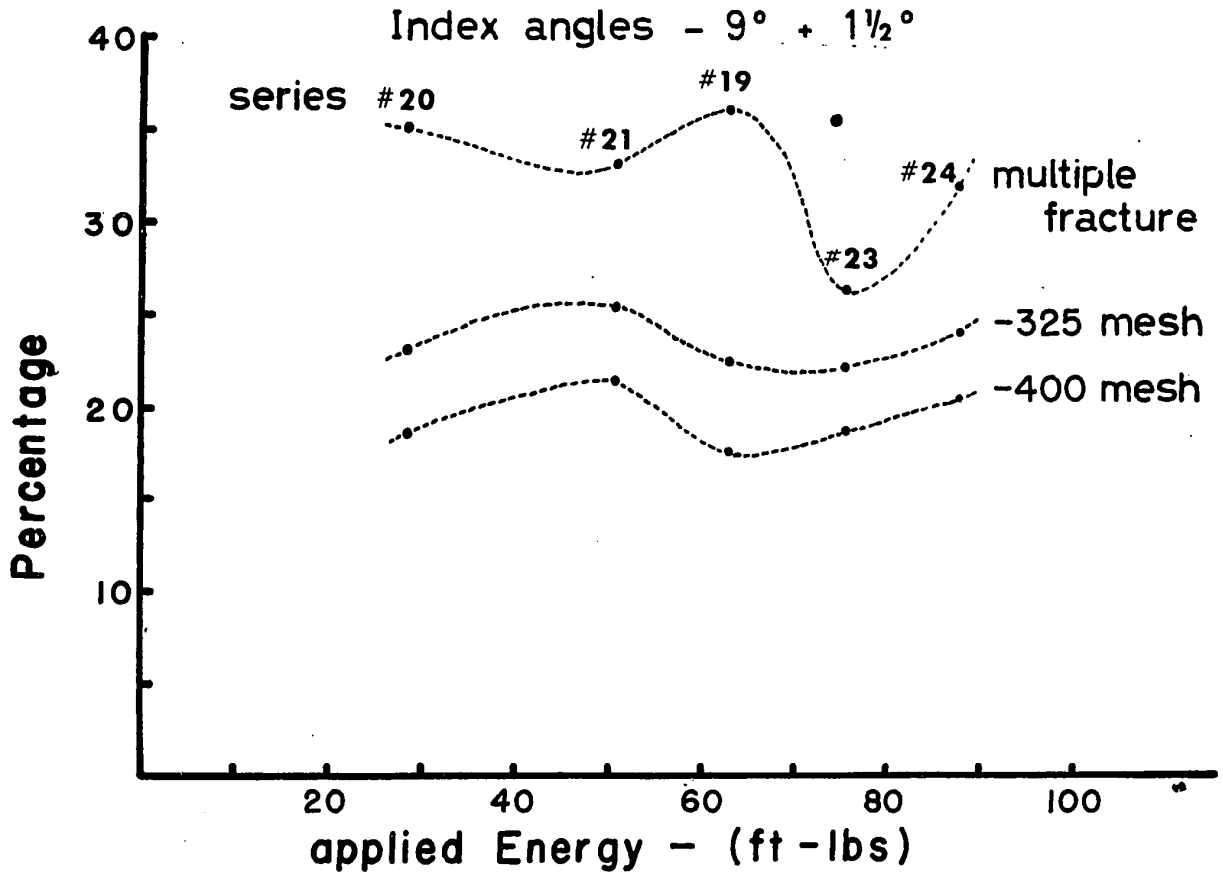

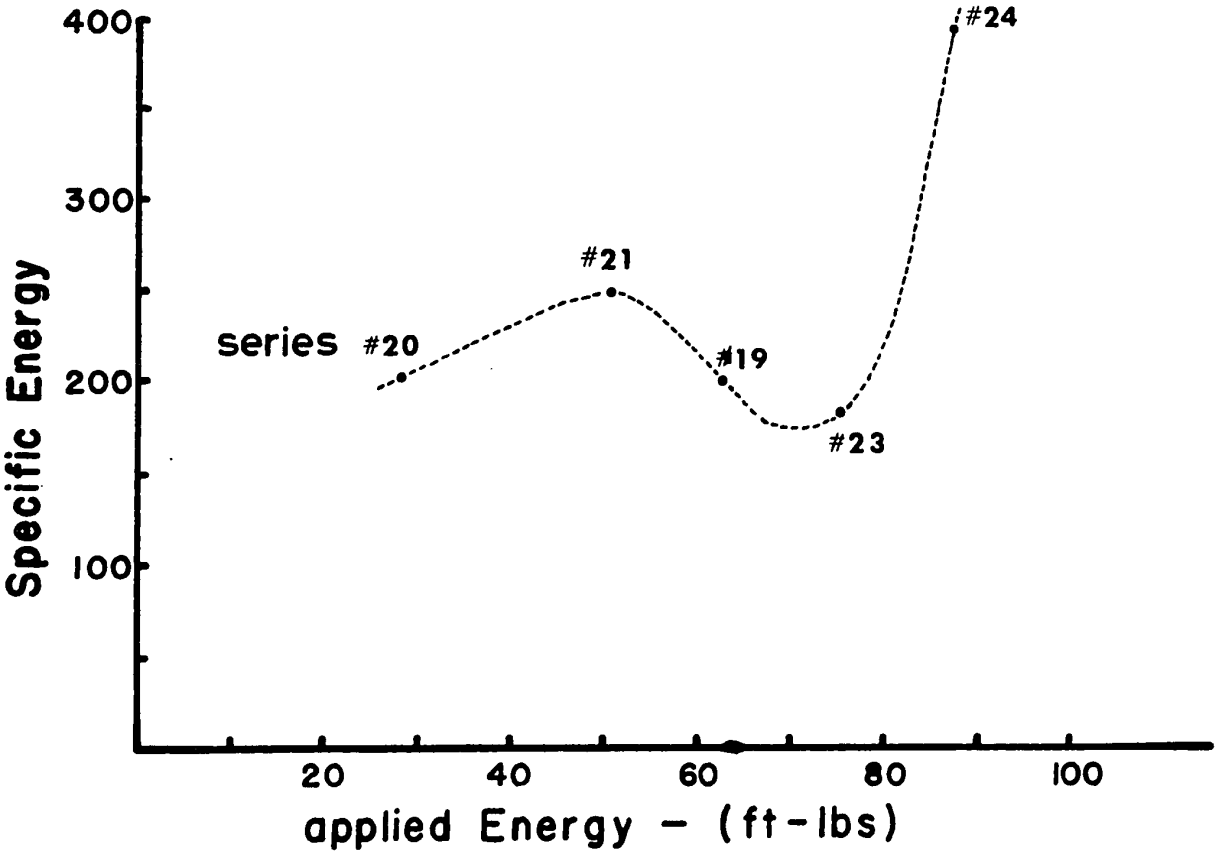

Fig. 6.8 ENERGY SERIES - CONSTANT IMPACT WEIGHT

same shape as the true specific energy curve, but the maxima and minima may not necessarily show the proper relative amplitudes, However, this was deemed sufficient to meet the objectives of this research, that is, determine the dust forming conditions.

The experimental specific energy curve is plotted in the lower part of Fig. 6.8 and its shape is now easily explained with the help of Fig. 6.9 and the concepts of twofold indexing and history. The drawing of Fig. 6.9 is a development view of the periphery of a drill hole:
a, b, and c are the imprints of the cutting edge along the wall of the drill hole on a first turn;
d and e are the imprints left by the cutting edge on the next passage.

It will be observed that the conventional rock drill produces less dust than the experimental drill; this may be explained by the fact that even in percussive drilling, some breakage takes place in the bottom of the hole due to shear caused by

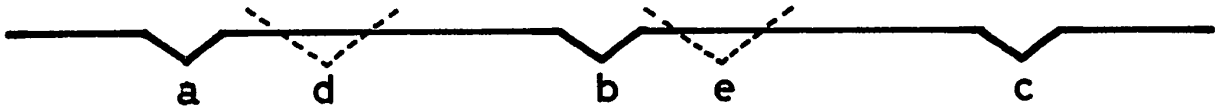

a,b,c - First passage of the cutting edge.

d,e - Next passage of cutting edge.

Fig. 6.9 : Development view of the periphery of a drill hole.

friction of the bit during rotation. This is why in test series 33 to 35 inclusive, the amount of multiple fracture is considerably lower than with the single-blow rock-drill. It is seen that friction of the bit at the bottom of the hole during rotation is beneficial; although it may cause dust by abrasion, it separates already broken material from the solid mass of rock and prevents multiple fracture, a much more serious factor of dust formation.

The experimental results are now readily explained (Fig. 6.8):

Series 20 - Energy is sufficient to remove completely the rock between points b and c.

Series 21 - Energy is sufficient to remove completely the rock between b and c but insufficient to break the barrier created by the broken rock under b and c. The specific energy curve reaches a maximum.

Series 19 - Energy is sufficient to remove completely the rock between b and c as well as part of the rock between b and d.

Series 23 - The specific energy curve goes through a minimum because all of the rock between c and d is removed.

Series 24 - Tremendous amounts of energy would be required to break the energy barrier created by the craters below c and d; consequently, the specific energy increases almost asymptotically.

This series of experiments confirms the previous hypotheses on indexing and energy relationships.

2 - Graphical Experiments on Specific Energy

Although the explanations on the mechanism of indexing presented above appear acceptable, the author felt the need for additional support. Cheatham (25) calculated the shape of a crater produced by a single blow on a homogeneous rock by a sharp or dull tooth assuming different degrees of internal friction and a variety of bit included angle. Combining Cheatham's and Hartman's data, the author selected the shape of crater shown in Fig. 6.10 as an acceptable actual crater shape.

The graphical experiments were carried out as follows:

(a) As in the case of Fig. 6.9, the study was made from the development view of a drill hole upon its periphery.

(b) Fig. 6.11a shows the crater and crushed sections produced by consecutive blows along the perimeter at the bottom of the drill hole.

(c) Fig. 6.11b shows the amount of rock removed by a

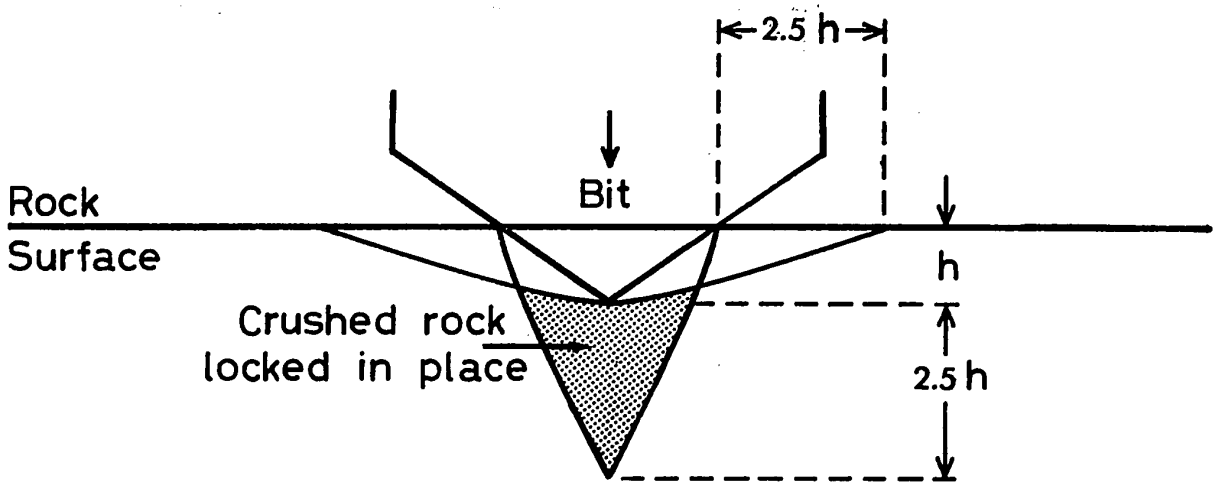

Fig. 6.10 : Selected shape of crater.

blow striking between two previous blows. The amount of rock removed by this blow is controlled by the blow energy and fracture does not progress beyond the existing inverted cones of crushed material.

(d) As the bit included angle is near 90^{o}, it can be assumed that

$$\text{Energy} \approx (\text{Penetration})^{2}$$

(e) The volume of rock removed in a single blow is proportional to the cross-sectional area of the crater and this was measured by means of a planimeter.

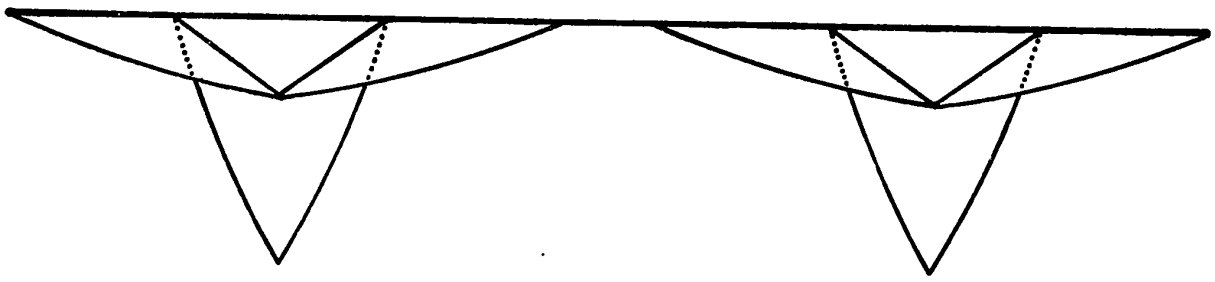

Fig. 6.11a : Craters formed by two consecutive initial blows.

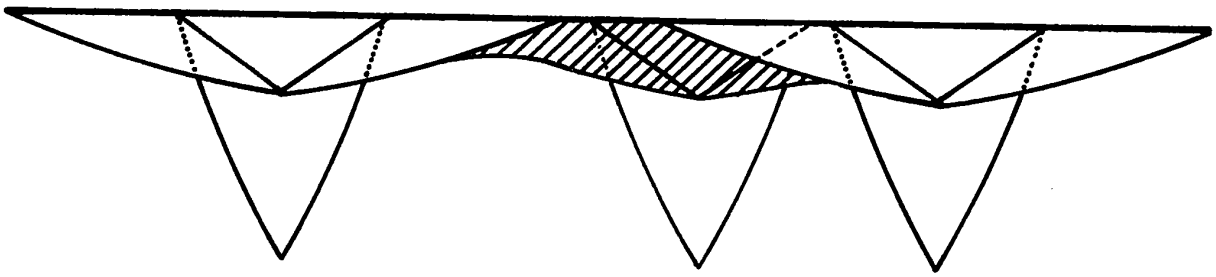

Fig. 6.11b : Material removed by a blow striking between two existing craters.

(f) The specific energy was then calculated as follows:

$$\text{Specific energy} \approx \frac{(\text{Penetration})^2}{\text{Cross-section area of crater}}$$

(g) A complete set of specific energy values was calculated for a 9° system at six different energy levels and results are tabulated in Table 6.1. The arrows in each column indicate that the specific energy remains constant once the rotation between blows exceeds a certain value.

The comparison of physical experiments and graphical tests can be made from Fig. 6.12 and good agreement is observed. Consequently, there is sufficient evidence to support the mechanism of indexing previously presented and corresponding energy relationships.

3 - Energy - Dust Relations

The particle size distributions obtained with the single-blow rock-drill at different energy levels are plotted in Fig. 6.13. From the preceding analysis on penetration and specific energy, it became apparent that series #23 was run in conditions approximating top efficiency, that is, conditions where complete twofold indexing was taking place. Similarly, series #23 shows the largest dispersion (Fig. 6.13) of particle sizes and the concentration of -325 mesh is the lowest of all tests performed (top part of Fig. 6.12).

It is very interesting to note that the lowest amount of multiple fracture was also found in series #23 (Top part of

TABLE 6.1

Values for the Complete Set of Data

9^o System								
Graphical Experiments - Specific Energy Tests								
n	ω	β	Specific Energy $= h^2/v$					
			h=½	h=1	h=2	h=3	h=4	h=5
1	189	180						
2	94.5	85.5						
3	63	54						
4	47.25	38.25						
5	37.8	28.8						17.1
6	31.5	22.5						
7	27	18					14.8	17.6
8	23.62	14.62						
9	21	12				13.3	15.8	20.4
10	18.9	9.9						
11	17.18	8.18			11.6	15.1	22.1	25.7
12	15.75	6.75						
13	14.53	5.53						
14	13.5	4.5		12.8	14.3	22.4	21.0	20.8
15	12.6	3.6						
16	11.81	2.81	8.9	14.3	18.2	15.3	22.8	18.9
17	11.11	2.11						
18	10.5	1.5	9.3	17.2	12.9	15.2	19.3	23.2
19	9.94	.94						
20	9.45	.45						
21	9.00	0	13.9	14.3	16.1	15.1	23.2	23.4

n = Number of blows per half turn

ω = Total rotation between blows

β = Variable index angle

α = Fixed index angle of 9^o

h = Energy level

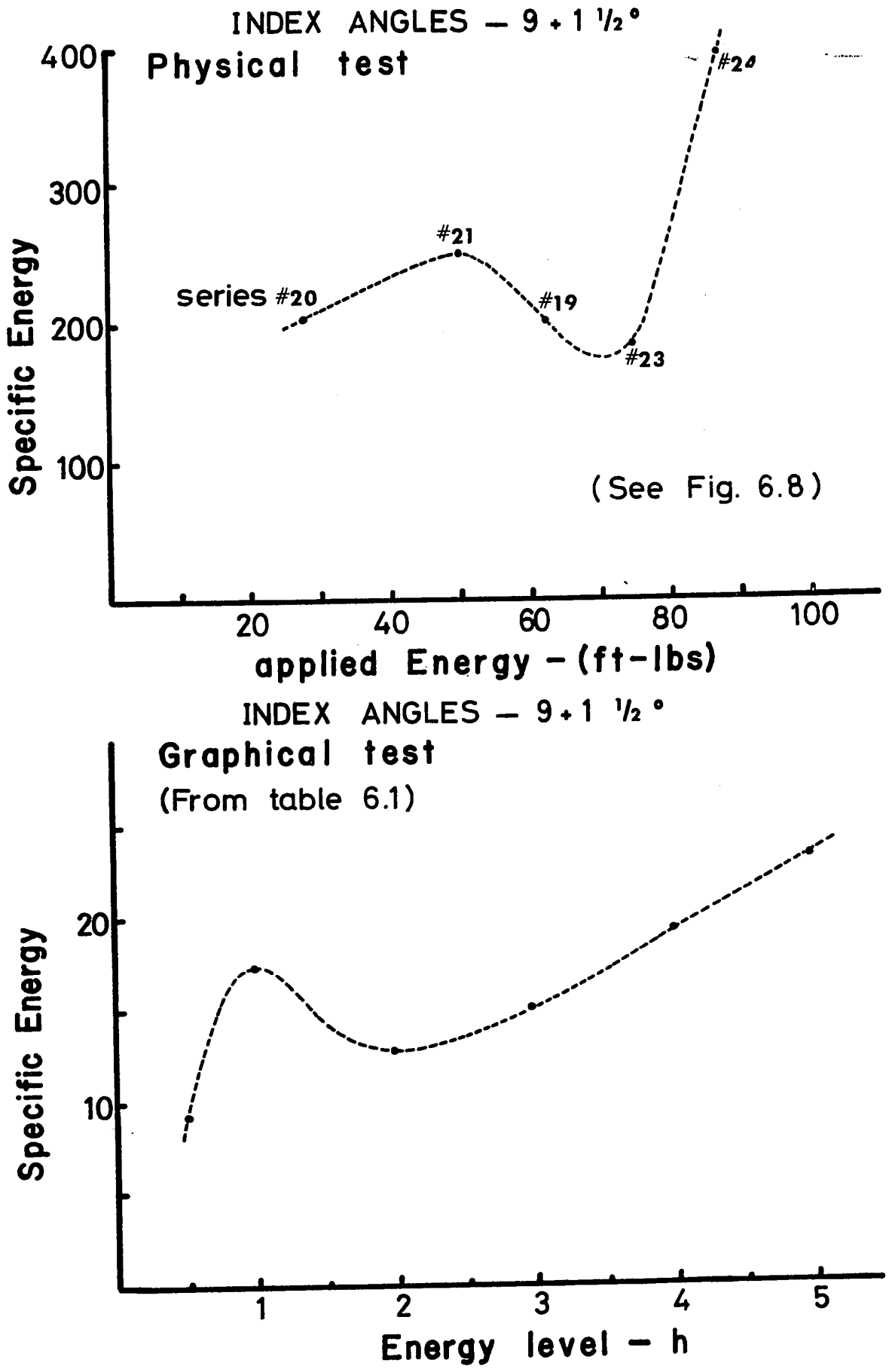

Fig. 6.12 : Comparison of physical and graphical

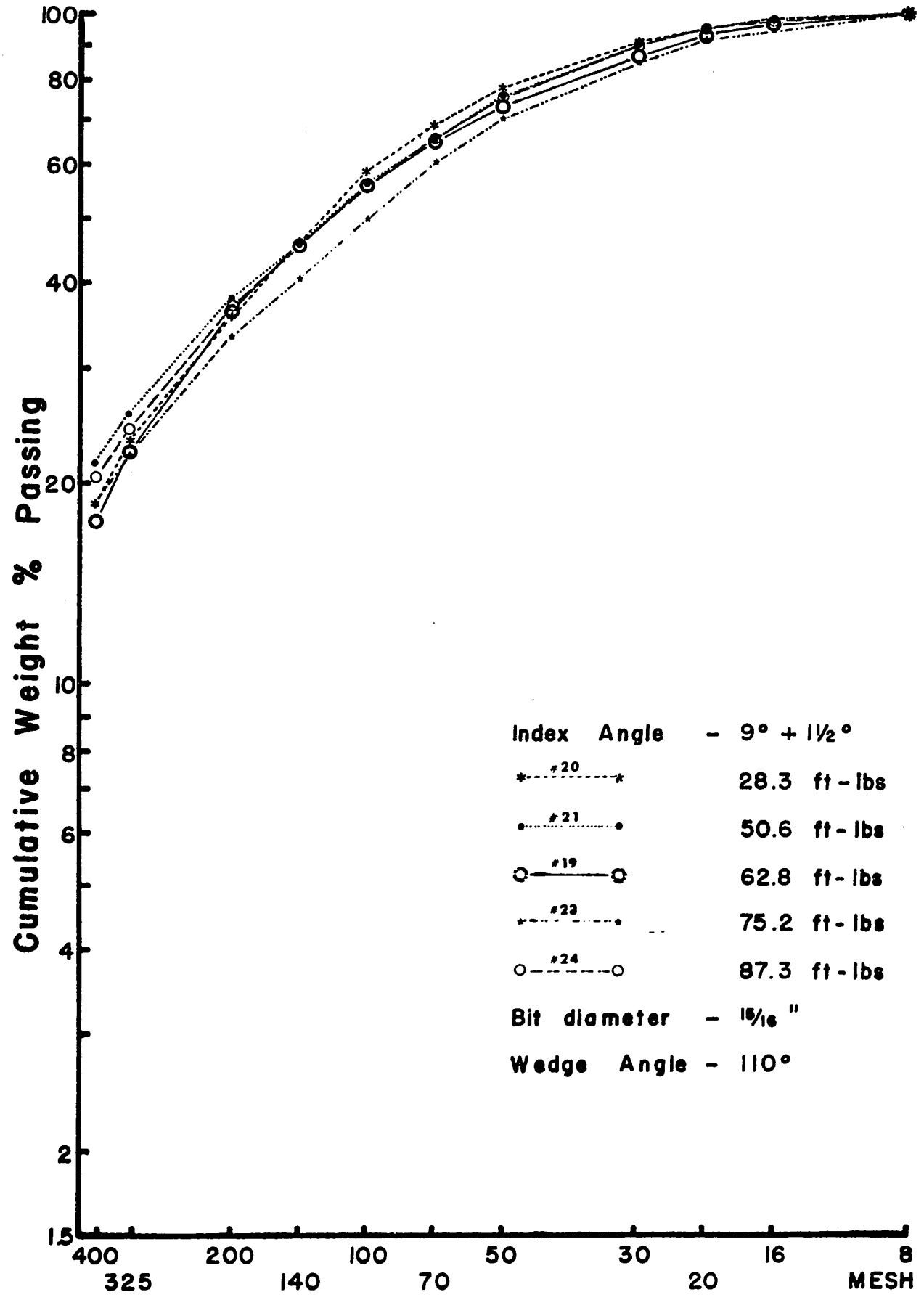

Fig. 6.13 ENERGY SERIES - CONSTANT IMPACT WEIGHT

Fig. 6.12). As a result, it can be concluded without doubt that the optimum operating conditions in percussive drilling coincide with the optimum conditions from the environmental point of view.

4 - Effect of Blow Velocity

The literature points out that there is a difference in penetration between static and dynamic values but once the velocity of impact exceeds a certain value, there is no difference in penetration rate. The author carried out a series of tests to study this variable, since Charles and de Bruyn supported the theory that higher velocities favoured the formation of fines. The size distributions obtained in four groups of tests are plotted in Fig. 6.14. In these tests the blow energy was constant at 87.3 ft.-lbs., while the impact weights and heights of fall varied. It is evident that the range of values that could be tested with the apparatus could not reject or support any particular theory with certainty, but it appears that blow velocity is not an important element in dust formation for the range of velocities encountered in the existing rock drills. This result was expected from the discussion presented by Hustrulid in his thesis (60).

5 - Conclusions from Energy Series

These experimental results and corresponding analyses permit the conclusions that:

(i) the damaged rock under a bit imprint prevents lateral energy transfer and prevents efficient indexing;

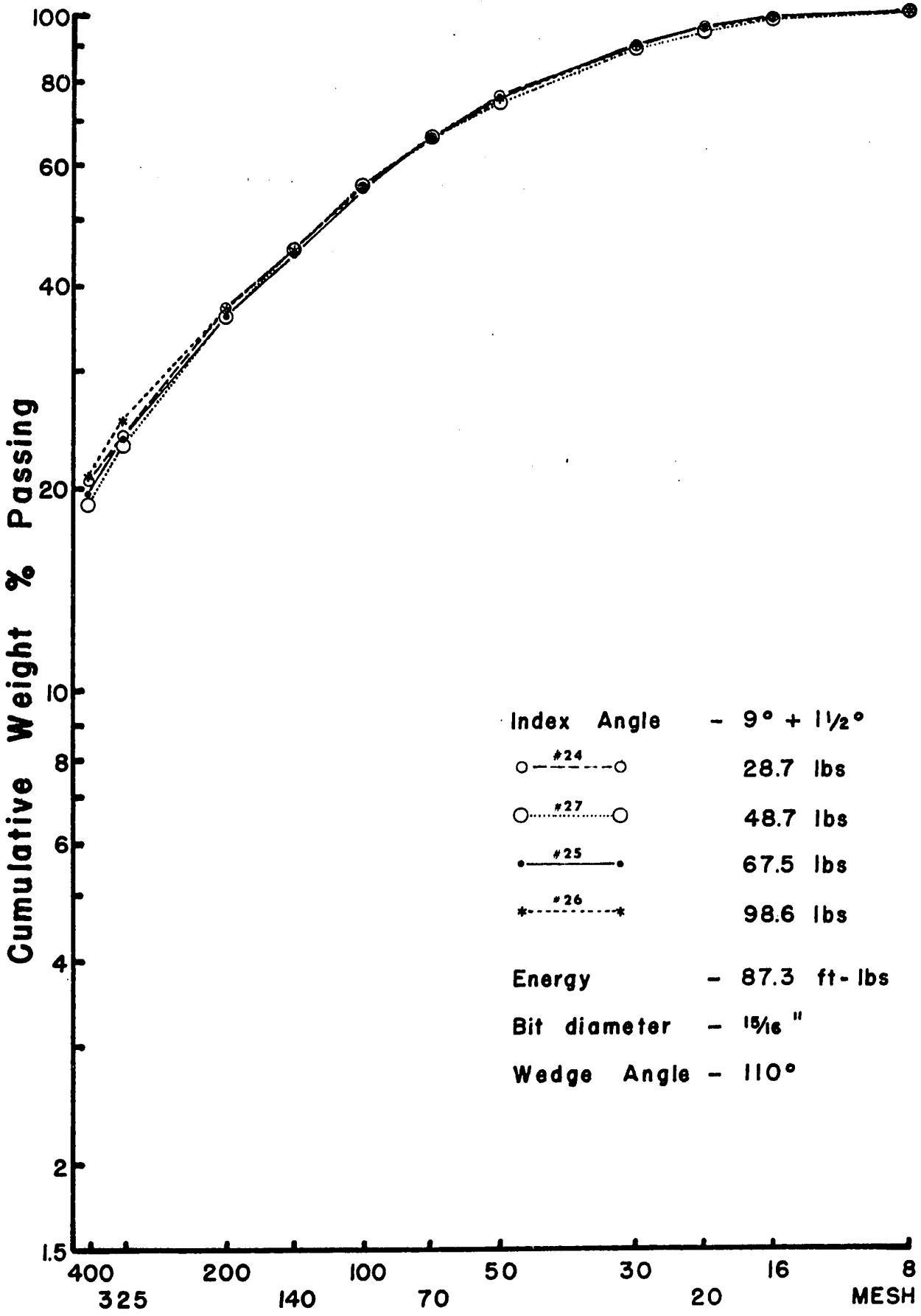

Fig. 6.14 BLOW VELOCITY SERIES

(ii) any increase in blow energy above the minimum required for indexing on both sides of the line of impact is useless and even detrimental;

(iii) rotation in a rock drill should be such as to prevent the striking of blows at the same place on consecutive turns. This is possible only if the drill has an independent rotation;

(iv) an increase in blow energy must be accompanied by an increase in rotation rate in order to permit efficient indexing on both sides of the line of strike;

(v) in order to reduce the possibilities of blows striking more than once along a given line per complete revolution, the bit design should be modified in order to eliminate symmetry. An offset bit, if it could be manufactured to be sharpened easily, should therefore be very desirable;

(vi) considering the work of Charles and de Bruyn (21, 22), as well as that of Hustrulid, we must conclude that the machine piston must be as light as possible in an effort to break the steel-piston contact immediately after the first impact; in this way, the first reflected wave from the bit-rock contact will separate the bit from the rock and prevent multiple fractures. This should be the goal of future research in percussive drilling, that is, the elimination of the first steel-piston reflected wave which is useless and

detrimental;

(vii) it seems apparent that the most efficient machine should have independent rotation, high blow-rate and low blow-energy;

(viii) the optimum use of the energy appears to occur when angles α and β are about equal and when the energy is sufficient to produce complete twofold indexing. In the case of a 9^{o} system, this occurs when the total rotation exceeds 17.18^{o} (See table 6.1, $n = 11$).

E - INDEX ANGLE SERIES

The second most important variable in percussive drilling is rotation. The study of this variable was made at fixed levels of energy for systems of 9^{o} and 12^{o}. The results for the 9^{o} system are discussed below and compared with the graphical tests while the data for the 12^{o} system appear in Appendix D.

Variation of the rotation between blows proved to be the only factor which influenced significantly the size distribution (Fig. 6.15) of the fragments. The tests also showed that provided rotation exceeds a certain value, the penetration, specific energy and size distribution remained unchanged (Fig. 6.16 and 6.17). These curves have the same shape as those of Fig. 2.6. It is therefore apparent that, while insufficient rotation is undesirable, excessive rotation will be relatively harmless if excessive wear due to rotation can be avoided.

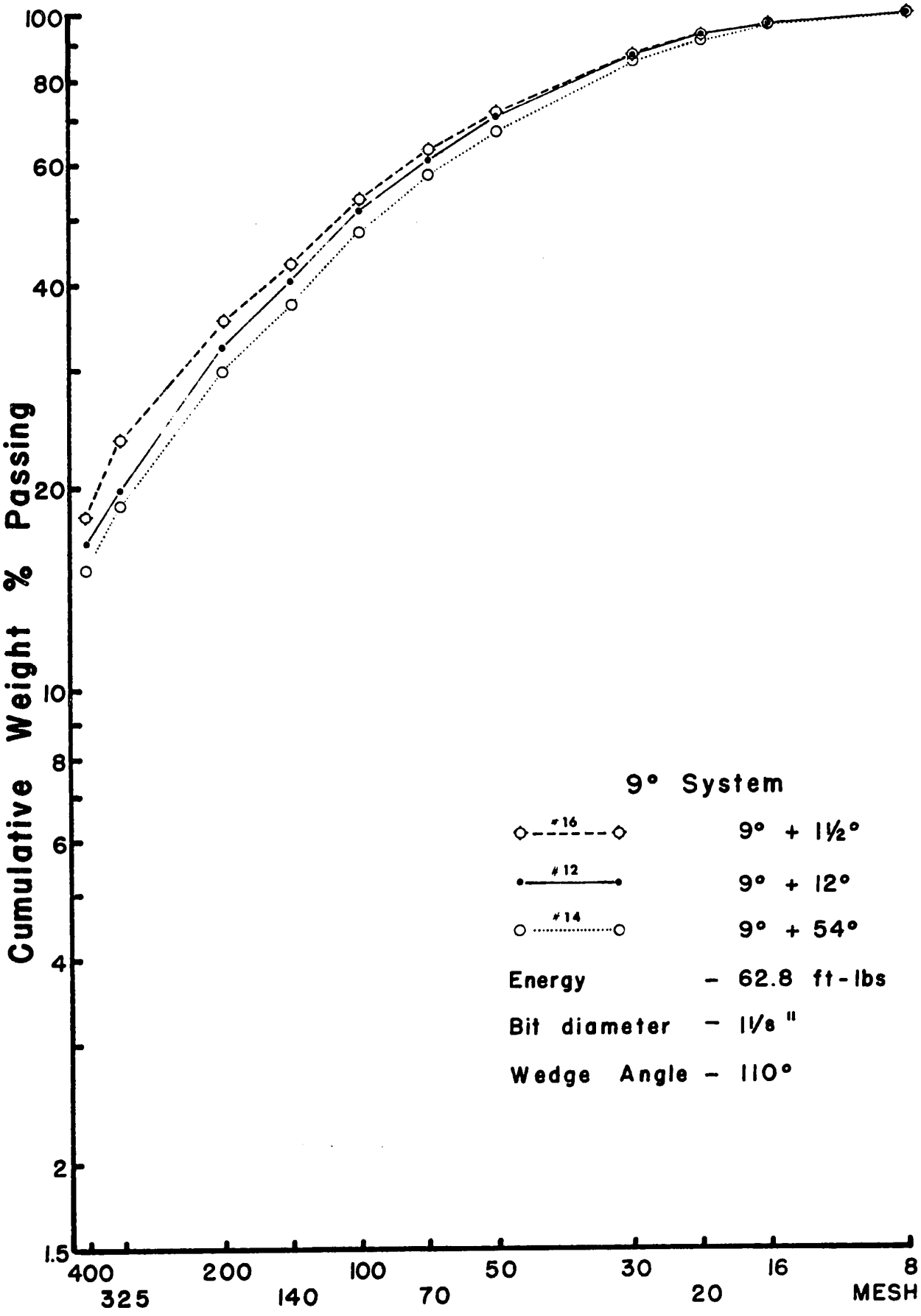

Fig. 6.15 INDEX ANGLE SERIES

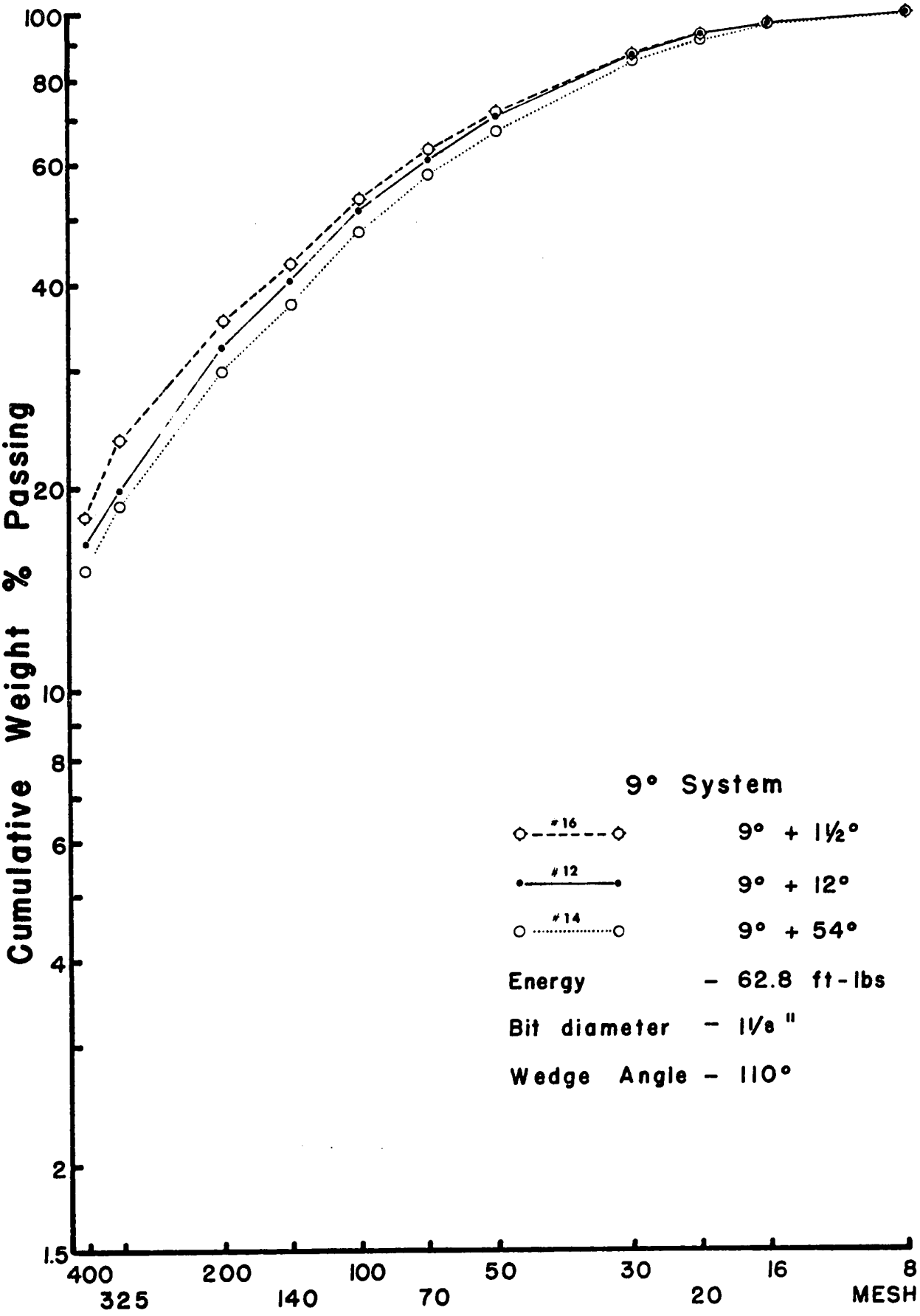

Fig. 6.15 INDEX ANGLE SERIES

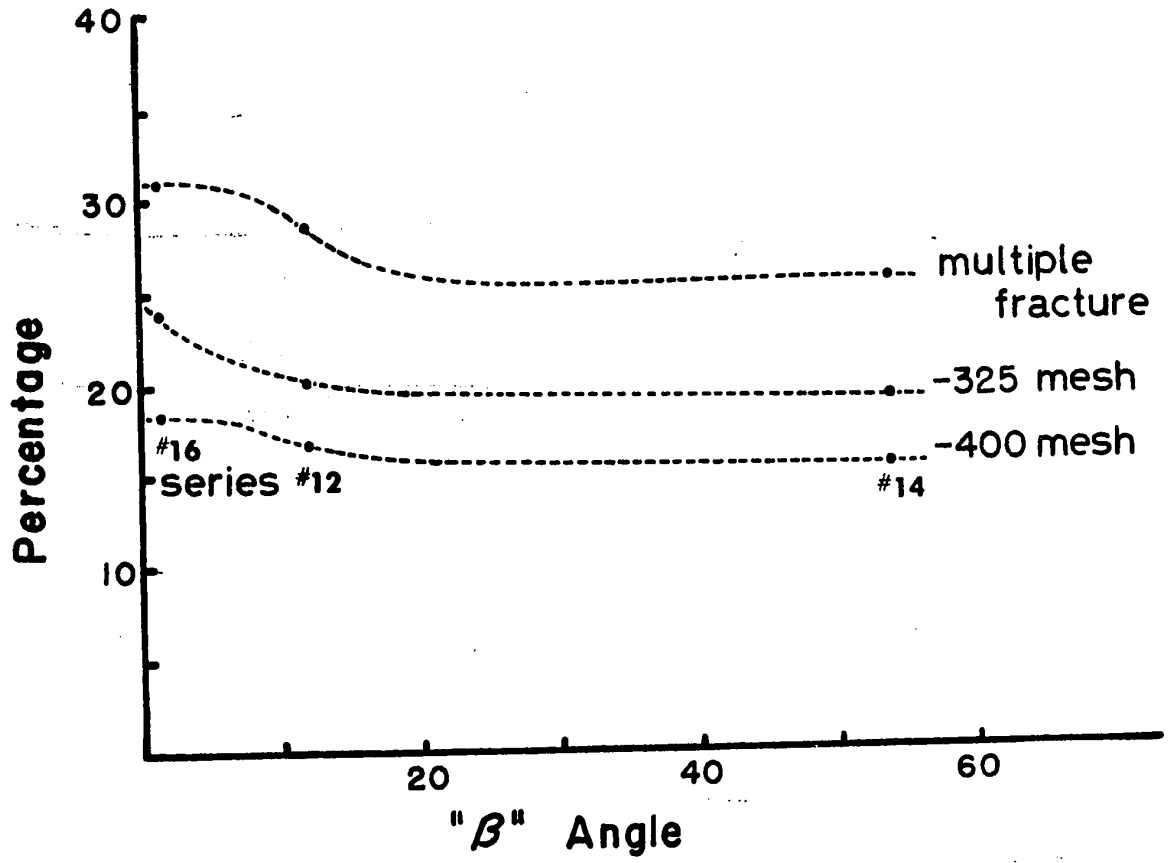

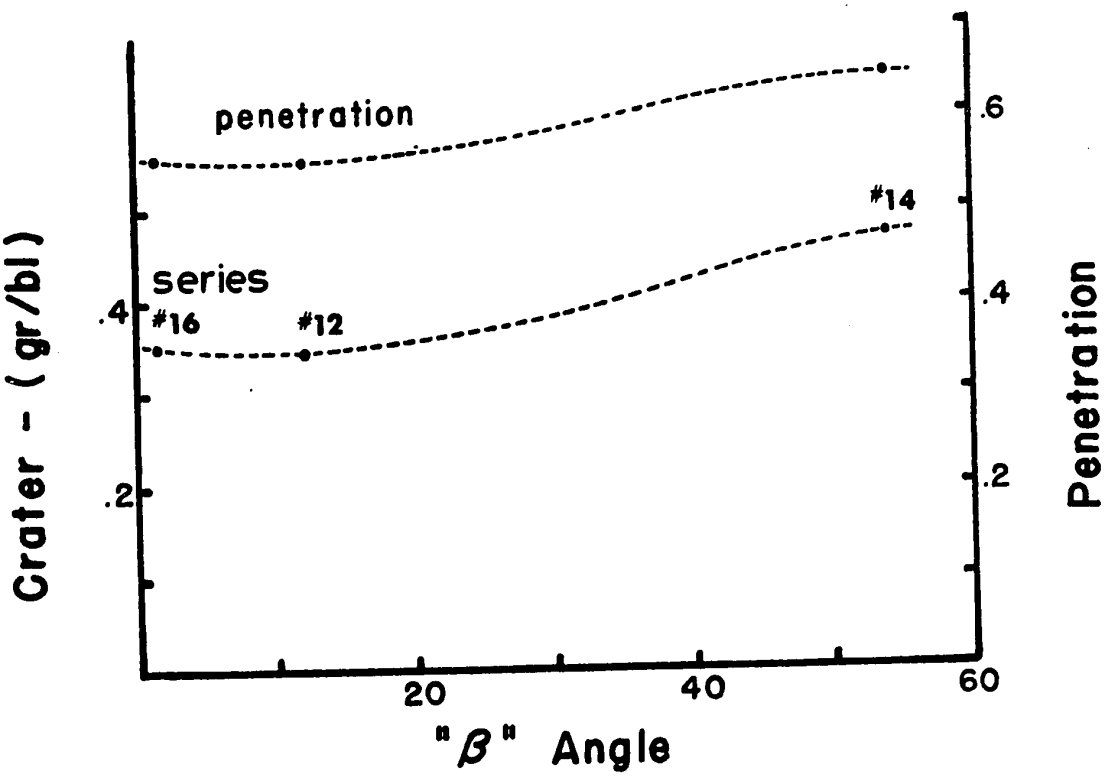

Fig. 6.17 INDEX ANGLE SERIES - 9° SYSTEM

Interesting conclusions may be drawn from the comparison of the physical specific energy tests with the graphical specific energy experiments (Fig. 6.18). It is observed that the lowest specific energy for any index angle is not a constant as reported by Hartman (55) but rather, the specific energy requirements in the zone of twofold indexing appear to increase with the blow energy. This conclusion is in contradiction with Equation 2.2 and Fig. 2.7, nevertheless, this is a logical conclusion since the slope of the force-penetration diagram (Fig. 2.1) increases with force. From the point of view of mechanical efficiency, it again appears desirable to design low blow energy machines.

The index angle is the only variable that is capable of changing somewhat the rate of dust formation. The drilling condition responsible for the least amount of dust is also the condition of optimum penetration rate as seen in Fig. 6.17.

F - BIT INCLUDED ANGLES

Hartman has shown that the bit angle is important only if it is less than 90^{o}. The author's tests included angles of 86^{o}, 95^{o} and 110^{o} and, from these, he agrees with Hartman (28). There is no difference in the size distribution (Fig. 6.19) for the three cases studied and the amount of dust formed (-325 mesh) is constant in all three cases. There is a small decrease in specific energy for the bit angle of 86^{o} (Fig. 6.20) and this, too, is in agreement with Hartman. It must therefore be concluded

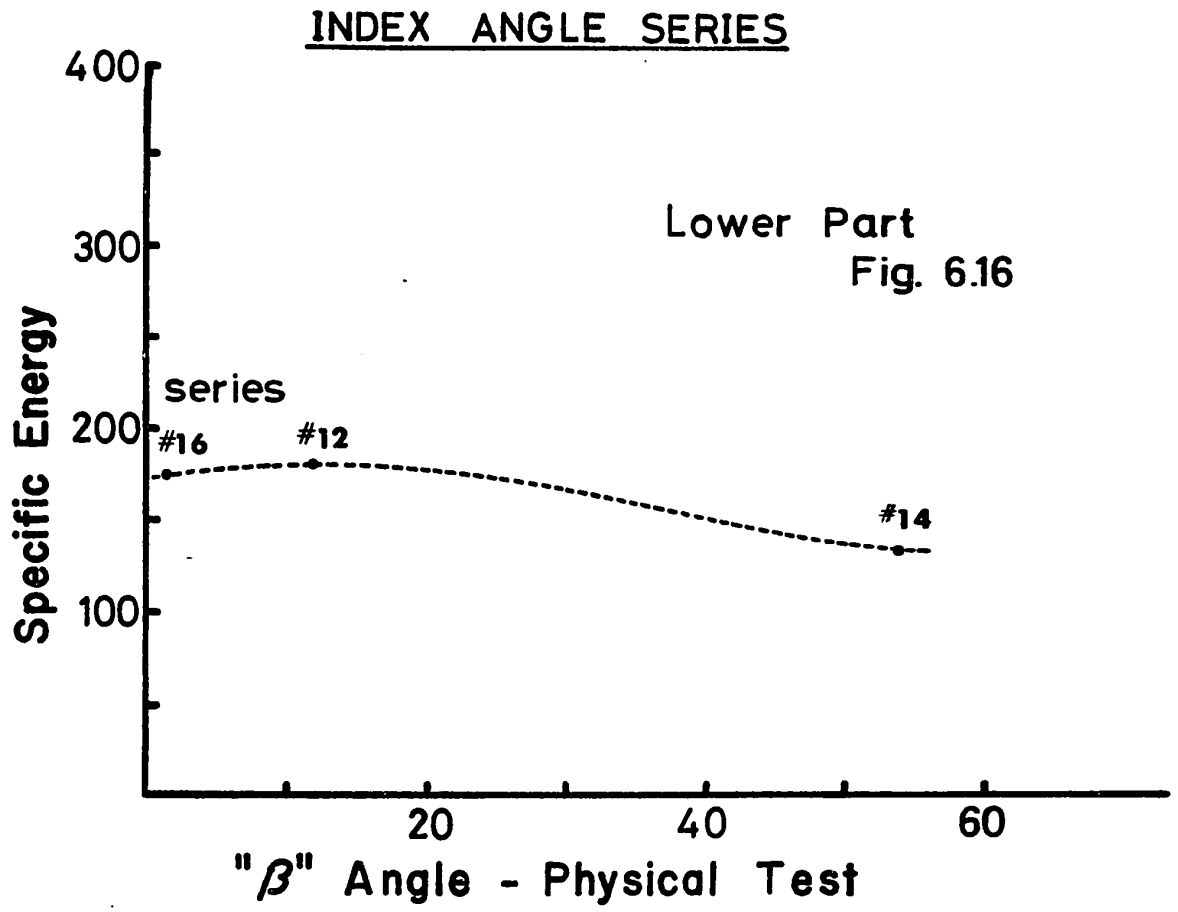

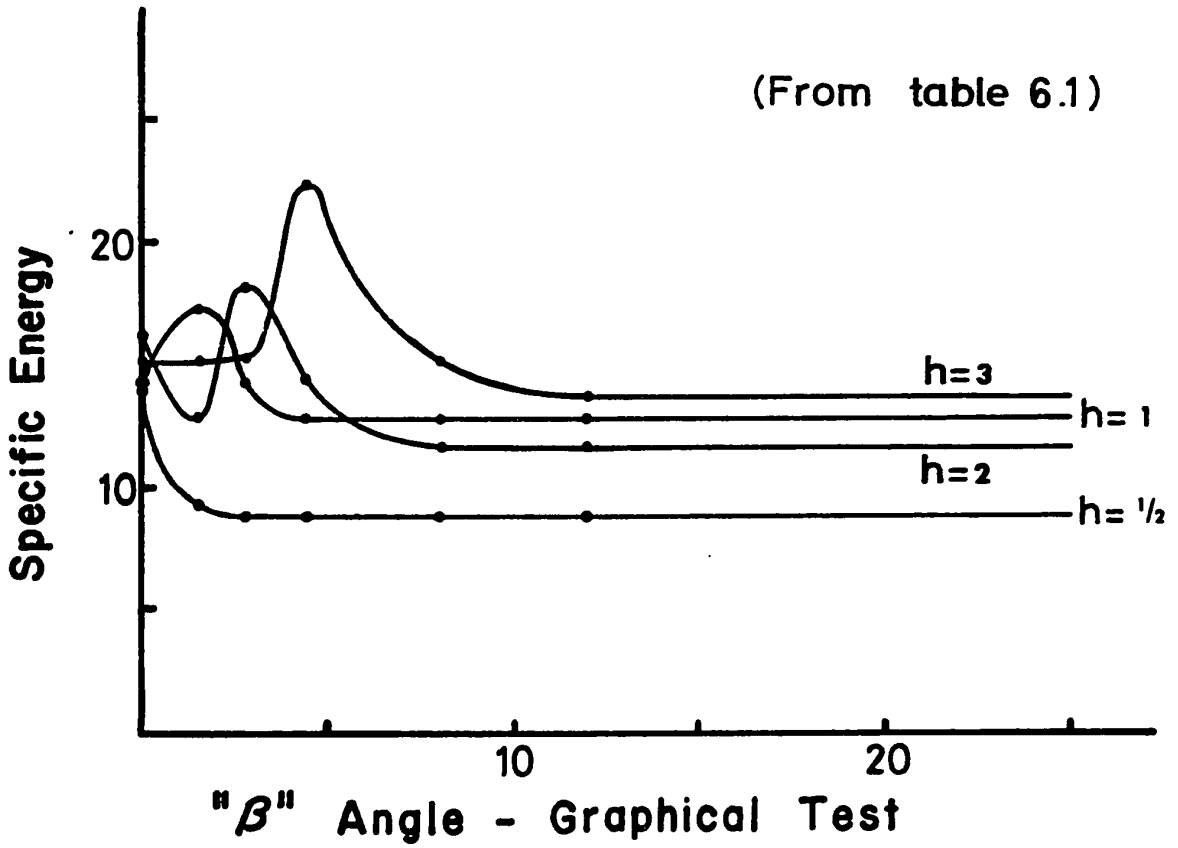

Fig. 6.18 : Comparison of physical and graphical Tests

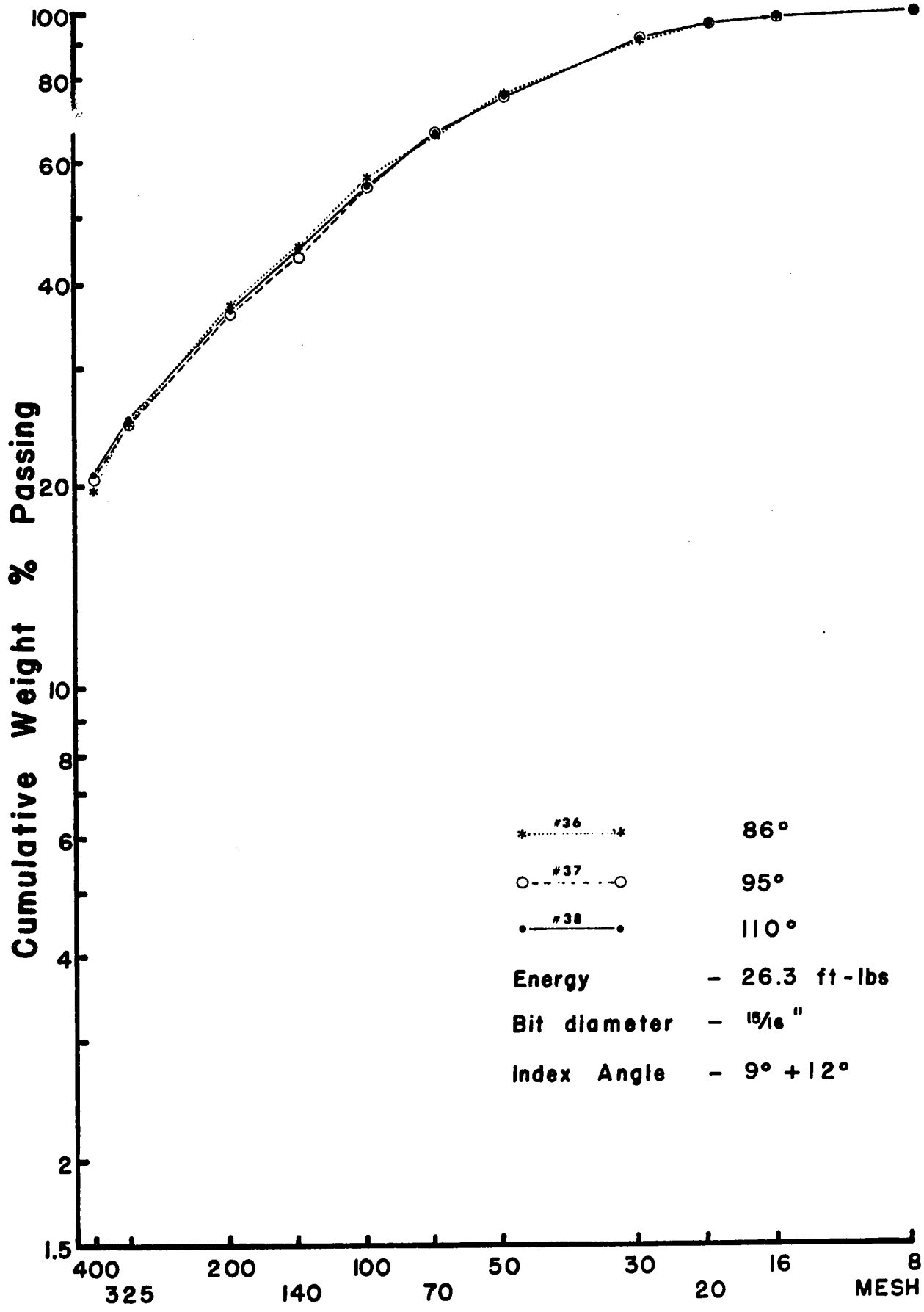

Fig. 6.19 BIT INCLUDED ANGLE SERIES

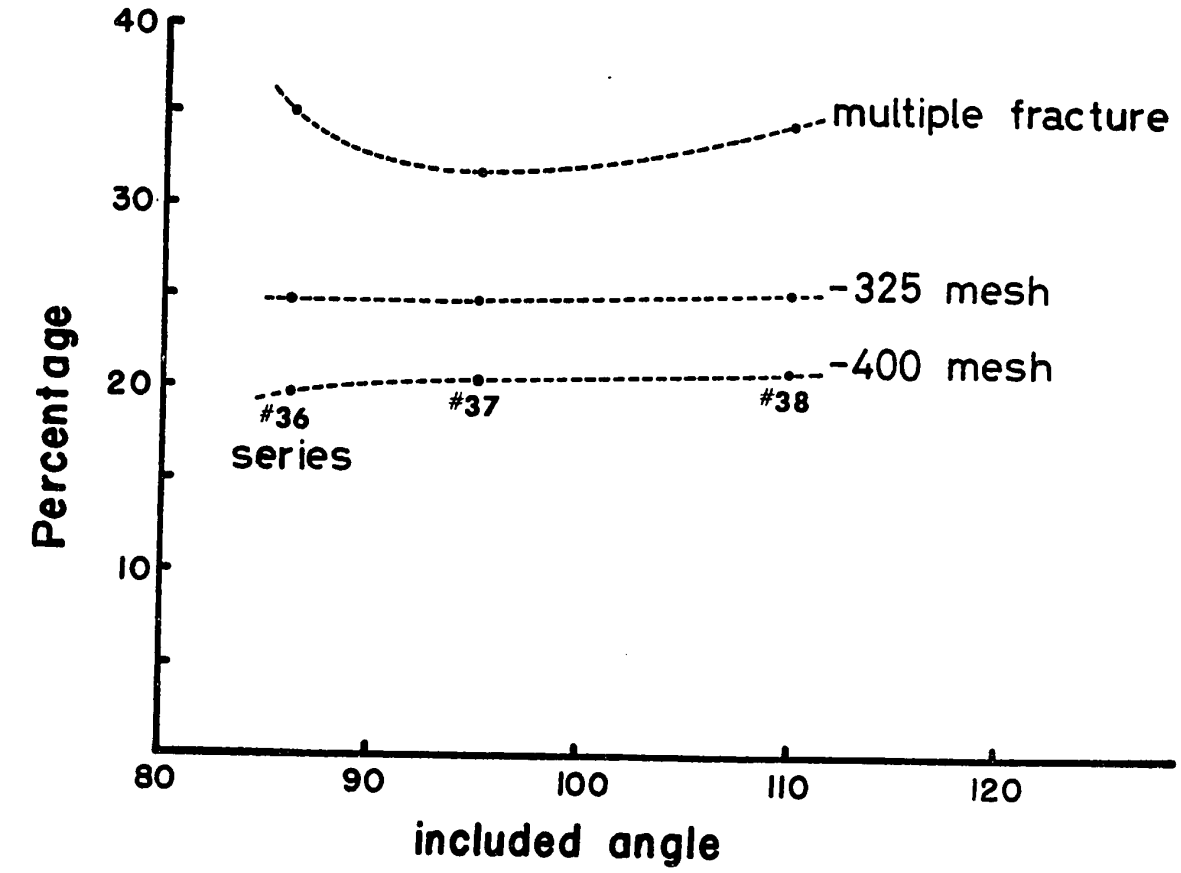

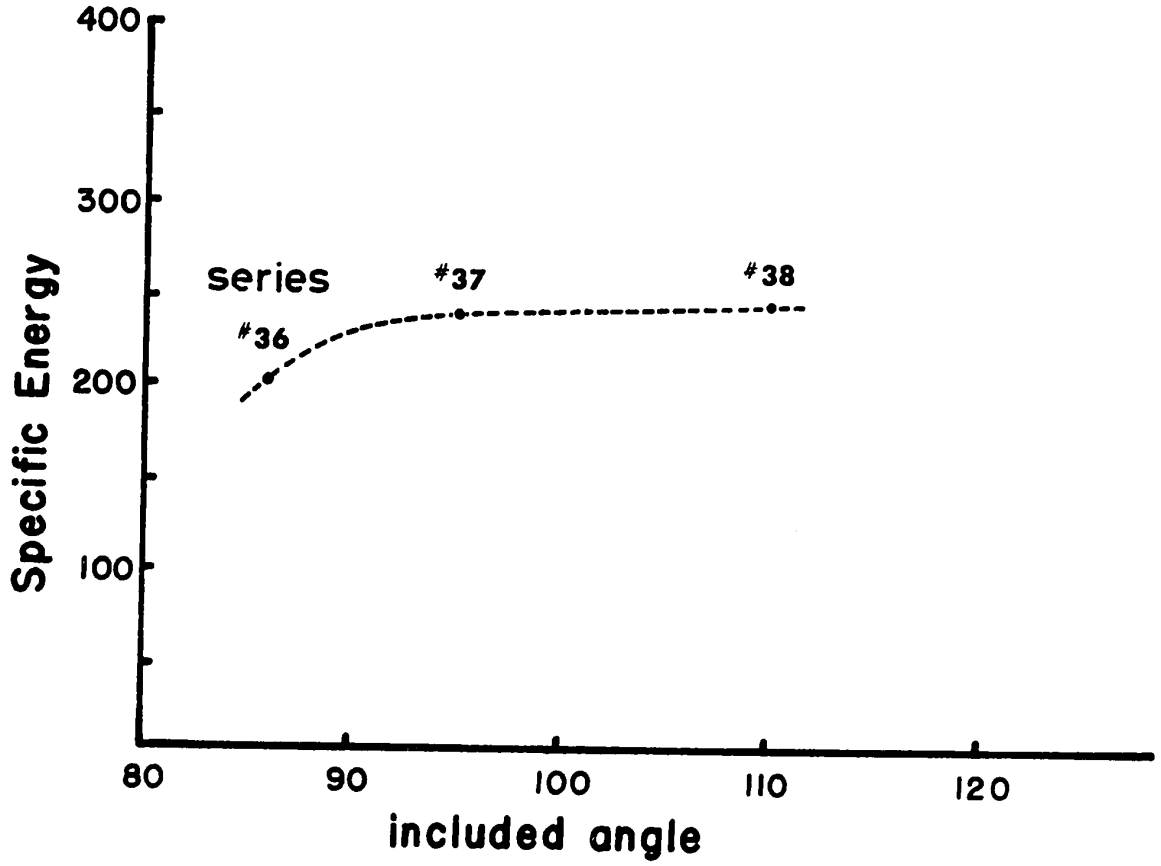

Fig. 6.20 BIT INCLUDED ANGLE SERIES

that modifications of bit design for improvement of drilling practices should not be based upon a choice of a new cutting angle. As mentioned earlier, there is scope for research into the design of new types of bits, such as the button bit or any type of non-symmetric designs. Since fracture in the bottom of a hole takes place mainly by axial impact crushing, and since bit wear is primarily due to rotation, new bits should be designed accordingly.

Experiments carried out do not permit verification of equations 2.15 to 2.17 inclusive because the number of included angles tested is too small and because the same energy was used in all tests. Tests were primarily designed to understand dust formation with conventional chisel bits and it has been shown that dust formation cannot be controlled significantly by varying the included angle of the cutting edge of a bit.

G - INFLUENCE OF BIT SIZE

Three bit diameter sizes were studied mainly to understand their respective influence upon dust formation. It was known that the penetration rate varied inversely with the bit diameter, because more material must be removed per unit length of axial distance; however, it seemed logical to expect a different size distribution for different bit sizes. It can be seen in Fig. 6.21 that the amount of material coarser than 100 mesh is larger for the 1 3/8" bit than for the 15/16", but finally the amount of material finer than 325 mesh is about the same for the

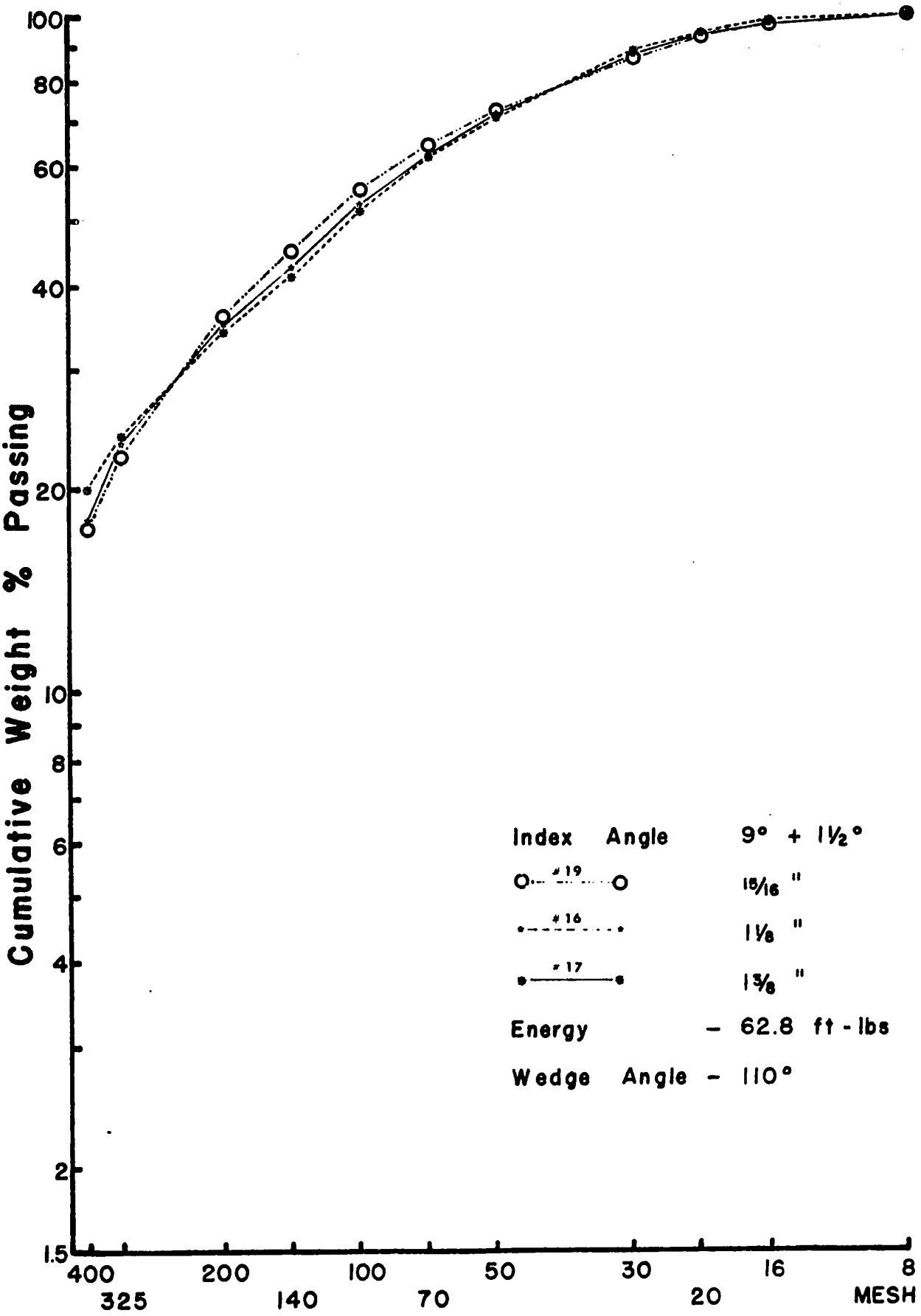

Fig. 6.21 BIT SIZE SERIES

three bit sizes tested.

A somewhat puzzling curve is seen in the top part of Fig. 6.22; it is difficult to understand the high percentage of multiple fracture for the small diameter bit, series #19 and yet, to see hardly any difference in the amount of fines. In all other cases, an increase in the amount of fines corresponds to an increase of multiple fractures. A partial explanation to this phenomenon can be found by plotting the intensity of Blow per Unit length of Cutting Edge (IBULCE) in the lower part of Fig. 6.22. Since both curves have the same shape, several conclusions may be derived:

(i) the shorter the cutting edge on a bit, the lower must be the blow intensity if dust is to be avoided;

(ii) the present tests do not permit the comparison of mechanical efficiency of different bit diameters because such comparison is possible only if the IBULCE is equal for all bits. However, the specific energy curve (Fig. 6.22) indicates that the smaller bits are less efficient;

(iii) if the IBULCE had been constant for all bit sizes, there should have been much less dust with the larger bits, since the peripheral distance between points of impacts along the hole wall increases with the bit diameter and favours indexed fractures.

Summarizing, it may be stated that a small diameter

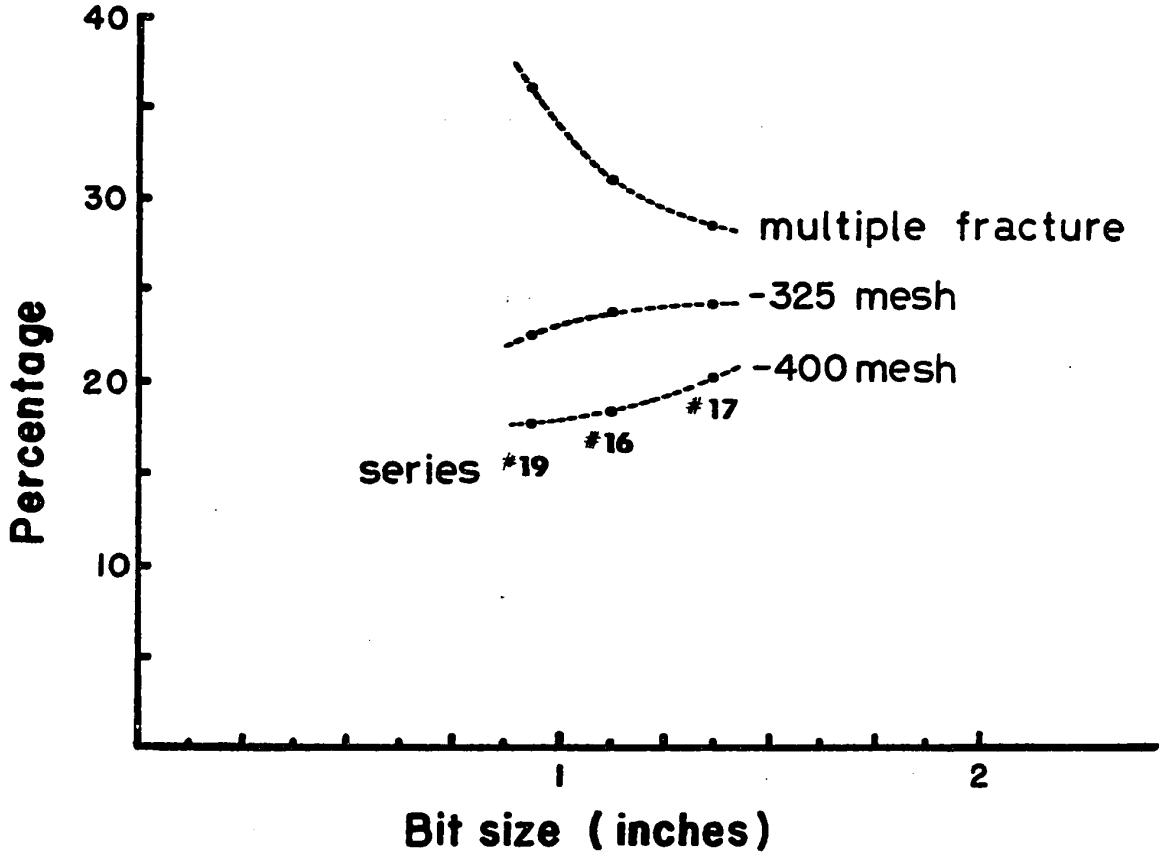

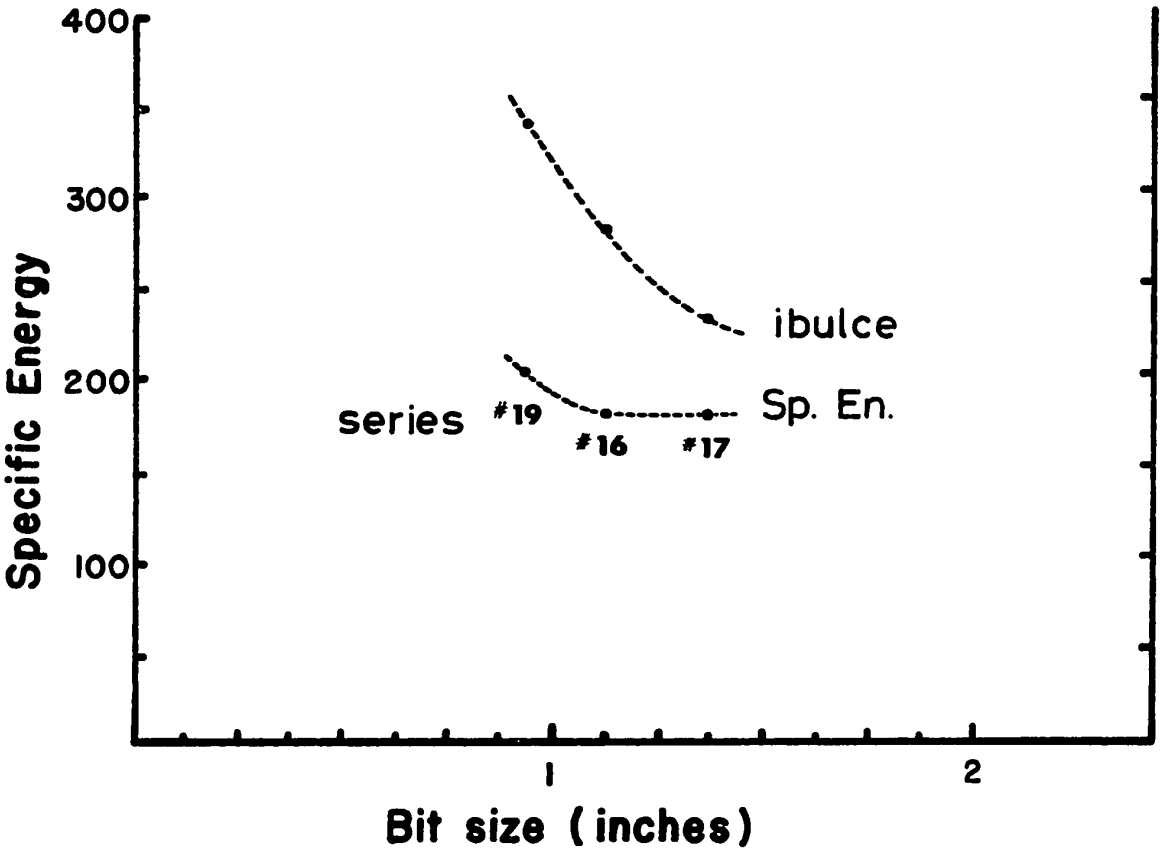

Fig. 6.22 BIT SIZE SERIES

chisel bit will cause a high degree of pulverization in the center of the hole and only a small fraction of material will break by chipping; this is an explanation compatible with the shape of the multiple fracture curve in Fig. 6.22; however, a large diameter chisel bit drilling with the same total energy as the small diameter chisel bit will have a much lower IBULCE value. As a result, (Fig. 6.22-1), the crater volume will remain constant for a given total blow energy, but the amount of dust will be somewhat smaller. If tests had been carried out with still larger bit diameters, it is expected that the amount of dust formed would increase rather than remain on a plateau as expected from the specific energy curve in Fig. 6.22.

H - FLUSHING

The influence of flushing was studied by varying the number of blows between cleaning operations. These tests could also be considered as the comparison between the drilling of uppers and flat holes; in the former case, it may be concluded that flushing is always efficient while flushing is not so efficient when drilling flat or down holes. Since drilling tests were carried out in dry conditions, the amount of fine particles formed was less than when drilling is performed under wet conditions. It was observed (Fig. 6.23) that, unless particles are removed from the bottom of the hole after a single impact blow, the size distribution of fragments remains constant.

A comparative analysis of flushing was carried out with a small portable rock drill using the same drill rod and the

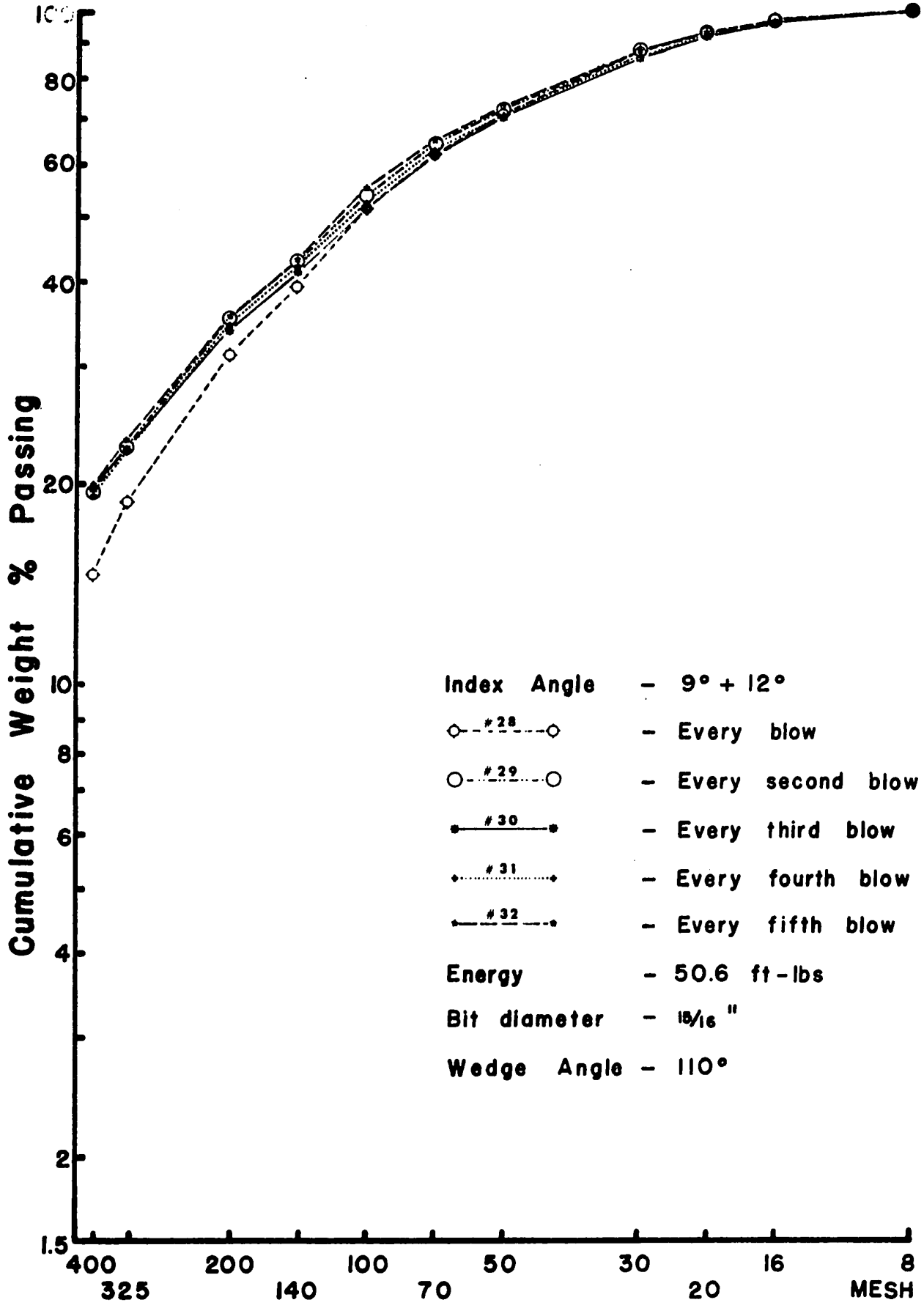

Fig. 6.23 FLUSHING SERIES

same type of cutting edge. Results of these tests appear in Fig. 6.24. Drilling conditions are not precisely defined because the objective of these tests was to compare the results obtained with the single-blow rock-drill and a standard rock drill. The size distributions for both the experimental drill and the commercial drill are compatible. It appears from the rock drill tests that good flushing eliminates the formation of a large amount of dust due to a reduction in secondary fracture.

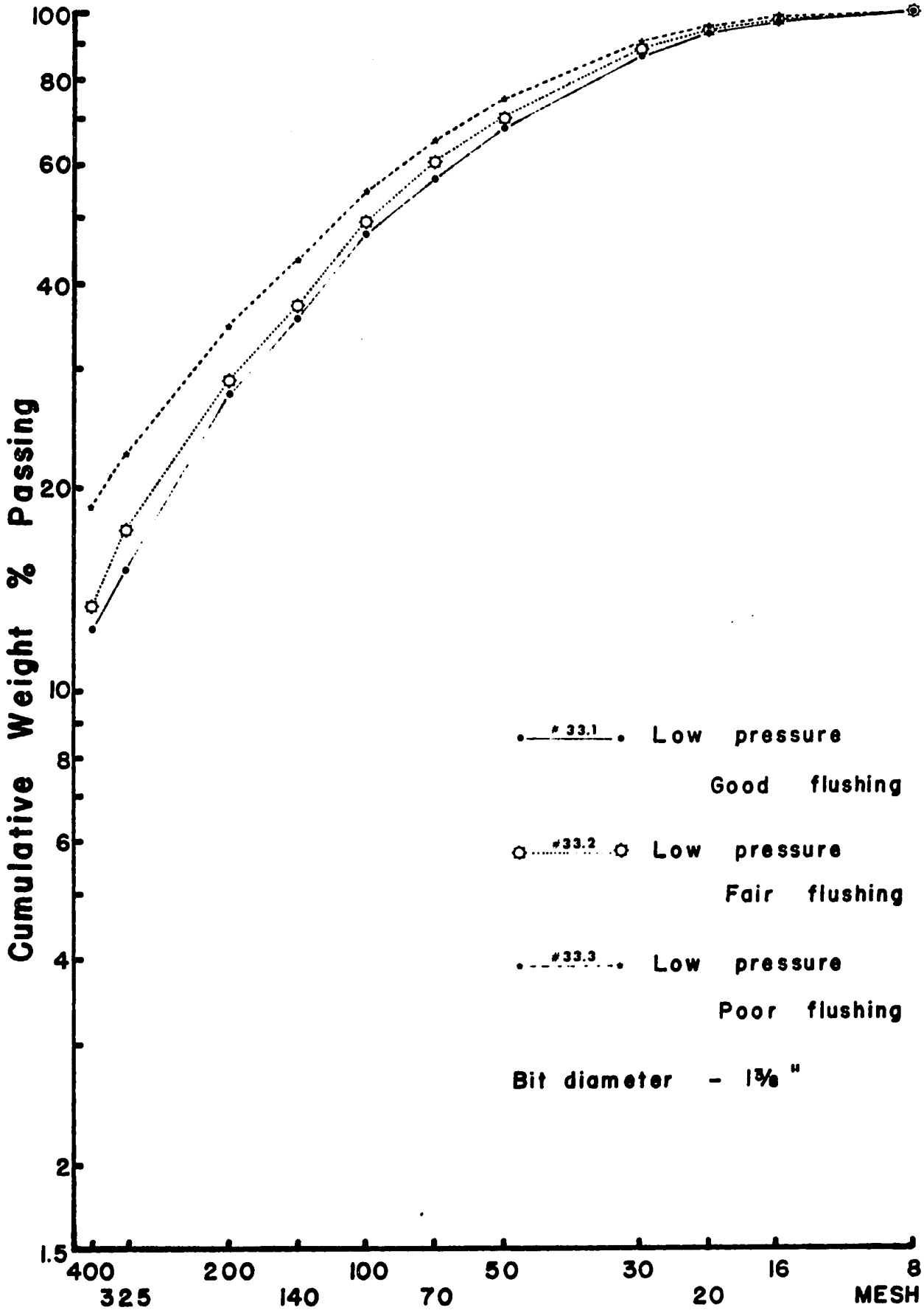

Fig. 6.24 ACTUAL DRILLING TESTS

VII - CONCLUSIONS

The principal findings of this thesis may be summarized as follows:

1 - Rock breakage in percussive drilling may be seen as a rate process but it is not a first order reaction.

2 - A percussive rock drill using a chisel bit breaks rock in the same manner as a hammer crushes a rock particle resting on a plate.

3 - An impact blow of a drill bit onto the rock will result in a series of breakage events which, in this thesis, have been called micro-events.

4 - The drill bit penetration into rock is represented by the force-penetration diagram which is a broken line (as shown by Simon and Hustrulid); each change of direction in this line corresponds to a micro-event in the process.

5 - The number of micro-events per single drill blow is a strict function of the drill steel geometry; the geometry of the hammer itself does not appear important. This is an agreement with Hustrulid's fundamental model of percussive drilling (Equation 2.6).

6 - A comminution test comparable to the Protodyakonow procedure was designed and found satisfactory as a means of determining the number of fracture micro-events in a single blow of a rock drill.

7 - The new comminution test procedure permits the calculation of the amount of rock broken by chipping as well as the amount of rock crushed by the passage of the first incident stress wave and the amount which sustains repeated fracture due to the passage of the first reflected stress wave.

8 - The size distribution of particles formed in rock drilling fits the Gaudin-Meloy distribution but the use of this model would not have shown the effect of the first reflected stress wave in the drill steel upon the particles formed by the first incident stress wave.

9 - Energy transfer from the hammer to the rock proceeds in two events: the first incident stress wave and the first reflected stress wave. It was found that the first incident wave breaks rock by chipping and crushing, but the first reflected wave does not do any useful work; it pulverizes material previously crushed by the passage of the first incident wave.

10 - The amount of dust formed in drilling could be reduced by as much as 60% if the bit-rock contact is broken immediately after the passage of the first incident stress wave and there would be no loss in penetration rate.

11 - Fracture in the bottom of a drill hole is controlled by conditions left in the rock by previous blows.

12 - The damaged rock left in place under a given bit imprint prevents lateral energy transfer in the bottom of the hole and therefore limits the process of indexing.

13 - Since indexing will occur on both sides of the line of impact, it is seen as a twofold process.

14 - The rotation of the drill steel must be independently controlled and must increase with the intensity of the blow energy in order to profit completely from the twofold indexing possibilities.

15 - The bit designs should be modified in order to reduce the possibilities of blows striking more than once along a given line per complete revolution.

16 - The experiments indicate that from the viewpoint of mineral dust production, an efficient rock drill should have a high blow rate, a low blow energy and an independently controlled rotation.

17 - No single variable in the present percussive drill can modify significantly the amount of dust formed in drilling operations except rotation, which must vary inversely with the blow energy.

18 - Future research programs are indicated on the following subjects:

a) non-symmetric drill bits;
b) reduction of the hammer-drill steel contact time;
c) determination of the factors responsible for the number of micro-events per single drill blow; theoretically, a low number of micro-events per blow will produce a flat-force penetration rate.

BIBLIOGRAPHY

1 - Agar, G.E., Brown, J.H., "Energy Requirements in Size Reduction", Trans. C.I.M.M., 57, 147, 1964.

2 - Allen, T., "Particle Size Measurement", Chapman & Hall, London 1968.

3 - Andrews, L., "Classified Grinding Research", Trans. I.M.M., 48, 141, 1939.

4 - Antonides, L.E., "New Ideas and Techniques in Drilling and Blasting", Eight Annual Drilling and Blasting Symposium, University of Minnesota, 1958.

5 - Axelson, Adams, Johnson, Kwong, Piret, "Basic Laboratory Studies in the Unit Operation of Crushing", Trans. A.I.M.E., 190, 1061, 1951.

6 - Bennett, J.G., Brown, R.L., Crone, H.G., "The Relation Between Size Distribution and Breakage Process", J. Inst. Fuel 14, 111, 1941.

7 - Bennett, J.G., Brown, R.L., "Broken Coal; The Mechanics of Partial Degradation", J. Inst. Fuel, 40, 135, 1941.

8 - Bennett, J.G., "Broken Coal; J. Inst. Fuel, 10, 22, 1936.

9 - Bergstrom, B.H., Sollenberger, C.L., "Kinetic Energy Effect in Single Particle Crushing", Trans. A.I.M.E., 220, 373, 1961.

10 - Bergstrom, B.H., "Empirical Modification of the Gaudin-Meloy Equation", Trans. A.I.M.E., 235, 45, 1966.

11 - Bhrany, U.N., Brown, J.H., "Particle Size Measurement and Control", Trans. A.I.M.E., 223, 248, 1962.

12 - Bond, F.C., Wang, J.T., "A New Theory of Comminution", Trans. A.I.M.E., 187, 871, 1950.

13 - Bond, F.C., "Crushing Tests by Pressure and Impact", Trans. A.I.M.E., 169, 58, 1946.

14 - Bond, F.C., "The Third Theory of Comminution", Trans. A.I.M. E., 193, 484, 1952.

15 - Bond, F.C., "Comminution Exposure Constant by the Third Theory", Trans. A.I.M.E., 208, 1372, 1958.

16 - Broadbent, S.R., Callcott, T.G., "A Matrix Analysis of Processes Involving Particle Assemblies", Phil. Trans. Roy. Soc. London, 249A, 99, 1956.

17 - Brook, N., Misra, B., "A Critical Analysis of the Stamp Mill Method of Determining Protodyakonov Rock Strength and Development of a Method Determining a Rock Impact Hardness Number", Twelth Symposium on Rock Mechanics, University of Missouri, (Ed. Clark, G.B.), 1970.

18 - Brown, J.H., Gaudin, A.M., Loeb, C.M., "Intergranular Comminution by Heating", Trans. A.I.M.E., 211, 490, 1958.

19 - Brown, R.L., "The Measurement of Coal Strength", Fuel, 27, 82, 1948.

20 - Carey, W.F., Stairmand, C.J., "A Method of Assessing the Grinding Efficiency of Industrial Equipment", Recent Development in Mineral Dressing, London, 117, 1953.

21 - Charles, R.J., deBruyn, "Energy Transfer by Impact", Trans. A.I.M.E., 205, 47, 1956.

22 - Charles, R.J., "High Velocity Impact in Comminution", Trans. A.I.M.E., 205, 1028, 1956.

23 - Charles, R.J., "Energy-Size Reduction Relationships in Comminution", Trans. A.I.M.E., 208, 80, 1957.

24 - Cheatham, J.B., Inett, E.W., "Factors Affecting the Performance of Percussive Drills", Trans. I.M.M., 63, 45, 1953.

25 - Cheatham, J.B., "An Analytical Study of Rock Penetration by a Single Bit Tooth", Publication No. 187, Shell Development Company, Houston, Texas, 1958.

26 - Coeuillet, M., "Etude cyclique de la Foration Percutante", Revue de l'Industrie Minière, 32, 235, 1951.

27 - Cohn, Fuerstenau, "Fracture of Nonmetallic Solids by Laser Irradiation", Trans. A.I.M.E., 238, 90, 1967.

28 - Cottrell, A.H., "The Mechanical Properties of Matter", New York, London; Wiley 1964.

29 - Crabtree, Meloy, Fuerstenau, Kinasevich, Mular, "Mechanisms of Size Reduction in Comminution Systems", Trans. A.I.M.E., 229, 207, 1964.

30 - Djingheuzian, L.E., "Development of the Science of Grinding", Trans. C.I.M.M., 55, 374, 1952.

31 - Djingheuzian, L.E., "A Study of Operating Data from Ball Mills Operating in Quebec, Ontario, Manitoba and British Columbia", Trans. C.I.M.M., 60, 290, 1957.

32 - D.S.I.R., "Crushing and Grinding", (Bibliography) Her Majesty's Stationery Office, London, 1958.

33 - Epstein, B., "Logarithmic-Normal Distribution in Breakage of Solids", Ind. Eng. Chem., 40, 2289, 1948.

34 - Ertl, Burgh, "Observations of the Relation of Drilling Speed to the Size of Cuttings", Mining Technology, Vol. 12, No. 4, TP. 2409.

35 - Fahrenwald, A.W., "Some Fine Grinding Fundamentals", Trans. A.I.M.E., 112, 88, 1934.

36 - Fairhurst, C., Kim, D.K., "Energy Transfer in Percussive Drilling", Proceedings of the Eight Annual Drilling and Blasting Symposium, University of Minnesota, 1958.

37 - Fairhurst, C., Lacabanne, W.D., "Some Principles and Developments in Hard Rock Drilling Techniques" Proceedings of the Sixth Drilling and Blasting Symposium, University of Minnesota, 1956.

38 - Fairhurst, C., "Recent Drilling Research at the University of Minnesota", Proceedings of the Twenty-seventh Annual Mining Symposium and Thirty-Eight Annual Meeting at the Minnesota Section, 1966.

39 - Fuerstenau, D.W., Sullivan, D.A., "Size Distribution in Wet and Dry Grinding". Trans. A.I.M.E., 220, 397, 1961.

40 - Garner, N.E., Gatlin, C., "Experimental Study of Crater Formation in Plastically deforming rocks", Preprint 498. Society of Petroleum Engineers, 1963.

41 - Gaudin, A.M., Brown, "Mechanism of Intergranular Comminution by Heating", Trans. A.I.M.E., 217, 423, 1960.

42 - Gaudin, A.M., Meloy, T.P., "Model and a Comminution Distribution Equation for Single Fracture", Trans. A.I.M.E., 223, 40, 1962.

43 - Gaudin, A.M., "An Investigation of Crushing Phenomena" Trans. A.I.M.E., 73, 253, 1926.

44 - Gilvarry, J.J., Bergstrom, B.H., "Fracture and Comminution of Brittle Solids", Trans. A.I.M.E., 220, 380, 1961.

45 - Gnirk, D.F., Cheatham, J.B., "An Experimental Study of Single Bit-tooth Penetration into Dry Rock at Confining Pressures of 0 to 5000 psi", Second Conference on Drilling and Rock Mechanics, University of Texas, January 1965.

46 - Griffith, A.A., "The Phenomena of Rupture and Flow in Solids", Philosophical Transactions of the Royal Society (London), 221A, 163, 1921.

47 - Griffith, A.A., "Theory of Rupture", Proceedings of the First International Congress for Applied Mechanics, Delft, 1924.

48 - Gross, J., Zimmerly, "Crushing and Grinding", Trans. A.I. M.E., 87, 7, 1930.

49 - Gross, J., "Summary of Investigation on Work in Crushing" Trans. A.I.M.E., 112, 116, 1934.

50 - Harris, C.C., "On the Role of Energy in Comminution: A Review of Physical and Mathematical Principles", Trans. I.M.M., Sect. C, 75, C 37, 1966.

51 - Harris, C.C., "On the Limit of Comminution", Trans. A.I. M.E., 238, 17, 1967.

52 - Harris, C.C., "The Application of Size Distribution Equations to Multi-Event Comminution Processes". Trans. A.I.M.E., 241, 343, 1968.

53 - Hartman, H.L., Pfeider, E.P., "Exhaust Control in Dry Percussive Drilling", Tech. Pub. A.I.M.E., 4005 A, 1955.

54 - Hartman, H.L., "Basic Studies of Percussion Drilling", Trans. A.I.M.E., 214, 68, 1959.

55 - Hartman, H.L., "The Simulation of Percussion Drilling in the Laboratory by Indexed-Blow Studies". Proceedings of First Conference on Drilling and Rock Mechanics, University of Texas, 1964.

56 - Heins, R.W., Street, N., "Hardness Reduction through Wetting" Trans. A.I.M.E., 229, 223, 1964.

57 - Herdan, G., "Small Particle Statistics", Second Edition, Butterworth & Co. (Publishers) Ltd., 88, Kingsway, London, 1960.

58 - Holmes, J.A., "A Contribution to the Study of Comminution in a Modified form of Kick's Law", Trans. Inst. Chem. Engrs. (London), 35, 125, 1957.

59 - Hukki, R.T., "Proposal for a Solomonic Settlement Between the Theories of Von Rittinger, Kick and Bond", Trans. A.I.M.E., 220, 403, 1961.

60 - Hustrulid, W., "Theoretical and Experimental Study of Percussive Drilling of Rock", University of Minnesota, Ph.D., 1968. (Engineering, Mining).

61 - Inett, E.W., "Some Further Factors Affecting Percussive Drilling Performance and their influence on the Size Distribution of the Cuttings". Trans. I.M.M., 68, 37, 1959.

62 - Irving, C.D., "Some Aspects of Rock Drilling Practice (The Witwatersrand Goldfield)", Trans. I.M.M., 55, 97, 1946.

63 - Kelsall, D.F., Reid, K.J., Stewart, P.S.B., "The Study of Grinding Processes by Dynamic Modelling" Electrical Engineering Transactions of the Institution of Engineers, Australia, Vol. EE5, No 1, P. 173, March 1969.

64 - Klimpel, R.R., Austin, L.G., "The Statistical Theory of Primary Breakage Distribution for Brittle Materials", Trans. A.I.M.E., 232, 88, 1965.

65 - Koster, J., "Deformation of Solids", U.S.B.M., R.I. 3223, 1934,

66 - Lynch, A.J., "A Mathematical Model of a Multi-Stage Comminution System", Preprint 10D, 58th Annual Meeting of the American Institute of Chemical Engineers, 1965.

67 - Marovelli, Chen, Veith., "Thermal Fragmentation of Rock", Trans. A.I.M.E., 235, 1, 1966.

68 - Martin, G., Blyth, G.E., Tongue, H., "Researches on the Theory of Fine Grinding", Trans. Ceram. Soc. (Engl.), 23, 61, 1923.

69 - Mather, W.B., "Rock Hardness as a Factor in Drilling Problems", Trans. A.I.M.E., 190, 173, 1951.

70 - Mondanel, M., "La Foration Percutante dans le Creusement des Bowettes", Rev. Indus. Min., St. Etienne, 31, 294, 1950.

71 - Moore, Gault, Lugn, "Experimental Impact Craters in Basalt" Trans. A.I.M.E., 226, 258, 1963.

72 - Ong, C.G., "A Study of Penetration by Percussive Drills", McGill University, M.Eng., 1970 (Engineering, Mining).

73 - Orr, C., Jr., Dalla Valle, J.M., "Fine Particle Measurement" The Macmillan Company, New York, 1959.

74 - Orr, C., Jr., "Particulate Technology" The Macmillan Company, New York, 1966.

75 - Poncelet, F., "The Mechanism of Fracture Propagation", Trans. A.I.M.E., 229, 161, 1964.

76 - Protodyakonov, M.V., "Mechanical Properties and Drillability of Rocks", 5th Symposium, University of Minnesota, (Ed. C. Fairhurst), 1963.

77 - Rehbinder, P.A., Schreiner, L.A. Zhigach, K.F., "Hardness Reducers in Drilling", Translation from the Russian (1944) C.S.I.R., Melbourne, Australia.

78 - Reichmuth, D.R., "Correlation of Force-Displacement Data with Physical Rock Properties for Percussive Drilling System",
Proceedings of the Fifth Symposium on Rock Mechanics, University of Minnesota, 1962.

79 - Rosin, P., Rammler, E., "The Laws Governing the Fineness of Powdered Coal", J. Inst. Fuel, 7, 29, 1933.

80 - Schuhmann, R. Jr., "Energy Input and Size Distribution in Comminution" Trans. A.I.M.E., 217, 22, 1960.

81 - Simon, R., "Theory of Rock Drilling" Proc. 6th Annual Drilling and Blasting Symposium, University of Minnesota, 1956.

82 - Simon, R., "Energy Balance in Rock Drilling", Batelle Memorial Institute, Columbus Ohio, Proceedings of First Conference on Drilling and Rock Mechanics, University of Texas, 1964.

83 - Simon, R., "Transfer of the Stress Wave Energy in the Drill Steel of a Percussive Drill to the Rock". Int. J. Rock Mech. Mining Sci., 1, 397, 1964.

84 - Simpson, D.N., Parry, V.S., "Percussive Drilling in Hard Rock" Iron and Coal Review, 163, 173, 1951.

85 - Somasundaran, Fuerstenau, D.W., "Preferential Energy Consumption in Tumbling Mills", Trans. A.I.M.E., 226, 132, 1963.

86 - Starfield, A.M., "Dynamic Stresses and Wave Propagation, an Introduction", Eight Symposium on Rock Mechanics, University of Minnesota, September 1966.

87 - Taplin, T.J., "Practical Crushing Efficiency", Min. Mag., 50, 18, 1934.

88 - Tartaron, F.X., "Comminution Theory" Trans., A.I.M.E., 222, 183, 1963.

89 - U.S.B.M., "Drillability Studies - Laboratory Percussive Drilling", R.I. 7300, 1969.

90 - U.S. Department H.E.W., "The Industrial Environment - Its Evaluation and Control", Publication No. 614, 1965.

91 - Walker, W.H., Lewis, W.K., McAdams, W.H., Gilliland, K.K., "Principles of Chemical Engineering" Ch. 9: Crushing and Grinding; McGraw Hill Company, New York, 1937.

92 - Walker, D.R., Shaw, M.G., "A Physical Explanation of the Empirical Laws of Comminution", Trans. A.I.M.E., 199, 313, 1954.

93 - Wells, E.S., "Percussion Rock Drilling with Tungsten Carbide Tipped Bits"., Chem. Engng. Min. Rev., 41, 135, 1949.

APPENDIX A

DRILLING TEST RESULTS

Definitions

$$\text{Crater Volume} \approx \frac{\text{Weight of Rock Removed}}{\text{Total Number of Blows}}$$

$$\text{IBULCE} \approx \frac{\text{Total Energy}}{\text{Bit Size}}$$

$$\text{Sp. Energy} \approx \frac{\text{Total Energy}}{\text{Crater}}$$

$$\text{Penetration} \approx \sqrt{\frac{\text{Crater}}{\text{Bit Size}}}$$

Remarks

1 - All values listed are taken from samples obtained in steady regime, that is, at a depth beyond the collaring effect.

2 - Types of fracture and number of micro-events are calculated by the method presented in the thesis.

Series	12	
Hammer	28.7	lbs.
Height	2.188	ft.
Angle	21	deg.
Bit	1 1/8	in.
Blows	224	
Rotation	4683	deg.
Flushing	1	
Broken	77.96	gr.

Corrected Cumulative Size Distribution

Mesh	Micron	% Passing
8	2380	100
16	1190	97.0
20	841	93.6
30	595	87.2
50	297	70.7
70	210	61.2
100	149	51.5
140	105	40.6
200	74	32.4
325	44	20.1
400	37	16.7
-400	-37	0

Crater	0.3480
IBULCE	55.8186
Sp. Energy	180.4484
Penetration	0.5561
Total Energy	62.8
Indexing	$9^{o}+12^{o}$ $12^{o}+9^{o}$
Chipping	11.9%
Single Fracture	59.6%
Double Fracture	28.5%
Fracture Events	91

Series	13	
Hammer	28.7	lbs.
Height	2.188	ft.
Angle	42	deg.
Bit	1 1/8	in.
Blows	129	
Rotation	5418	deg.
Flushing	1	
Broken	64.76	gr.

Corrected Cumulative Size Distribution

Mesh	Micron	% Passing
8	2380	100
16	1190	96.2
20	841	91.9
30	595	84.8
50	297	67.5
70	210	57.6
100	149	47.5
140	105	37.3
200	74	29.8
325	44	19.5
400	37	15.9
-400	-37	0

Crater	0.5020
IBULCE	55.8186
Sp. Energy	125.0918
Penetration	0.6680
Total Energy	62.8
Indexing	$12^{o}+30^{o}$
Chipping	15.9%
Single Fracture	60.6%
Double Fracture	23.5%
Fracture Events	93

Crater: gr/bl; IBULCE: ft-lbs/in; Sp.Energy: ft-lbs/gr/bl;
Penetration: in/bl; Total Energy: ft-lbs.

Series	14	
Hammer	28.7	lbs.
Height	2.188	ft.
Angle	63	deg.
Bit	1 1/8	in.
Blows	103	
Rotation	6489	deg.
Flushing	1	
Broken	48.46	gr.

Corrected Cumulative Size Distribution

Mesh	Micron	% Passing
8	2380	100
16	1190	96.5
20	841	91.8
30	595	85.0
50	297	67.3
70	210	58.3
100	149	48.0
140	105	37.8
200	74	30.0
325	44	19.0
400	37	15.3
-400	-37	

Crater	0.4705
IBULCE	55.8186
Sp. Energy	133.4665
Penetration	0.6467
Total Energy	62.8
Indexing	$9^{o}+54^{o}$
Chipping	11.7%
Single Fracture	62.9%
Double Fracture	25.4%
Fracture Events	90

Series	15	
Hammer	28.7	lbs.
Height	2.188	ft.
Angle	84	deg.
Bit	1 1/8	in.
Blows	59	
Rotation	4956	deg.
Flushing	1	
Broken	29.79	gr.

Corrected Cumulative Size Distribution

Mesh	Micron	% Passing
8	2380	100
16	1190	96.8
20	841	93.1
30	595	87.0
50	297	71.0
70	210	60.0
100	149	50.5
140	105	40.3
200	74	31.0
325	44	17.9
400	37	13.0
-400	-37	

Crater	0.5049
IBULCE	55.8186
Sp. Energy	124.3715
Penetration	0.6693
Total Energy	62.8
Indexing	$12^{o}+72^{o}$
Chipping	8.2%
Single Fracture	64.5%
Double Fracture	27.3%
Fracture Events	92

Crater: gr/bl; IBULCE: ft-lbs/in; Sp.Energy: ft-lbs/gr/bl;
Penetration: in/bl; Total Energy: ft-lbs.

Series	16	
Hammer	28.7	lbs.
Height	2.188	ft.
Angle	10 1/2	deg.
Bit	1 1/8	in.
Blows	206	
Rotation	2369	deg.
Flushing	1	
Broken	72.63	gr.

Corrected Cumulative Size Distribution

Mesh	Micron	% Passing
8	2380	100
16	1190	97.1
20	841	93.6
30	595	87.5
50	297	71.7
70	210	62.8
100	149	53.0
140	105	42.8
200	74	35.2
325	44	23.6
400	37	18.2
-400	-37	

Crater	0.3526
IBULCE	55.8186
Sp. Energy	178.0921
Penetration	0.5598
Total Energy	62.8
Indexing	$9^{o} + 1\frac{1}{2}^{o}$
Chipping	8.9%
Single Fracture	60.2%
Double Fracture	30.9%
Fracture Events	92

Series	17	
Hammer	28.7	lbs.
Height	2.188	ft.
Angle	10 1/2	deg.
Bit	1 3/8	in.
Blows	171	
Rotation	1795.5	deg.
Flushing	1	
Broken	60.37	gr.

Corrected Cumulative Size Distribution

Mesh	Micron	% Passing
8	2380	100
16	1190	98.1
20	841	94.5
30	595	87.8
50	297	71.0
70	210	62.0
100	149	51.5
140	105	41.3
200	74	34.2
325	44	24.1
400	37	20.0
-400	-37	

Crater	0.3530
IBULCE	45.6703
Sp. Energy	177.8912
Penetration	0.5066
Total Energy	62.8
Indexing	$9^{o} + 1\frac{1}{2}^{o}$
Chipping	12.8%
Single Fracture	58.8%
Double Fracture	28.4%
Fracture Events	94

Crater: gr/bl; IBULCE: ft-lbs/in; Sp.Energy: ft-lbs/gr/bl;
Penetration: in/bl; Total Energy: ft-lbs.

Series	19	
Hammer	28.7	lbs.
Height	2.188	ft.
Angle	10 1/2	deg.
Bit	15/16	in.
Blows	171	
Rotation	1795.5	deg.
Flushing	1	
Broken	53.80	gr.

Corrected Cumulative Size Distribution

Mesh	Micron	% Passing
8	2380	100
16	1190	96.6
20	841	92.8
30	595	86.5
50	297	72.7
70	210	64.5
100	149	55.5
140	105	45.3
200	74	36.2
325	44	22.4
400	37	17.6
-400	-37	

Crater	0.3146
IBULCE	66.9829
Sp. Energy	199.6056
Penetration	0.5792
Total Energy	62.8
Indexing	$9^{o} + 1\frac{1}{2}^{o}$
Chipping	10.2%
Single Fracture	53.8%
Double Fracture	36.0%
Fracture Events	91

Series	20	
Hammer	28.7	lbs.
Height	0.917	ft.
Angle	10 1/2	deg.
Bit	15/16	in.
Blows	103	
Rotation	1081.5	deg.
Flushing	1	
Broken	13.40	gr.

Corrected Cumulative Size Distribution

Mesh	Micron	% Passing
8	2380	100
16	1190	98.2
20	841	95.3
30	595	90.9
50	297	77.7
70	210	68.5
100	149	58.2
140	105	45.9
200	74	36.4
325	44	23.2
400	37	18.6
-400	-37	.0

Crater	0.1301
IBULCE	28.0715
Sp. Energy	202.2891
Penetration	0.3726
Total Energy	28.3
Indexing	$9^{o} + 1\frac{1}{2}^{o}$
Chipping	12.5%
Single Fracture	52.2%
Double Fracture	35.3%
Fracture Events	93

Crater: gr/bl; IBULCE: ft-lbs/in; Sp.Energy: ft-lbs/gr/bl;
Penetration: in/bl; Total Energy: ft-lbs.

Series	21	
Hammer	28.7	lbs.
Height	1.764	ft.
Angle	10 1/2	deg.
Bit	15/16	in.
Blows	206	
Rotation	2163	deg.
Flushing	1	
Broken	42.09	gr.

Series	23	
Hammer	28.7	lbs.
Height	2.619	ft.
Angle	10 1/2	deg.
Bit	15/16	in.
Blows	120	
Rotation	1260	deg.
Flushing	1	
Broken	49.2	gr.

Corrected Cumulative Size Distribution

Mesh	Micron	% Passing
8	2380	100
16	1190	98.4
20	841	95.5
30	595	89.7
50	297	75.3
70	210	65.0
100	149	56.0
140	105	45.8
200	74	37.9
325	44	25.4
400	37	21.5
-400	-37	

Corrected Cumulative Size Distribution

Mesh	Micron	% Passing
8	2380	100
16	1190	94.8
20	841	91.0
30	595	84.5
50	297	69.7
70	210	60.0
100	149	49.5
140	105	40.2
200	74	33.1
325	44	22.1
400	37	18.7
-400	-37	0

Crater	0.2043
IBULCE	54.0019
Sp. Energy	247.8073
Penetration	0.4668
Total Energy	50.6
Indexing	$9^{o} + 1\frac{1}{2}^{o}$
Chipping	8.8%
Single Fracture	58.1%
Double Fracture	33.1%
Fracture Events	92

Crater	0.4100
IBULCE	80.1763
Sp. Energy	183.3299
Penetration	0.6613
Total Energy	75.2
Indexing	$9^{o} + 1\frac{1}{2}^{o}$
Chipping	8.0%
Single Fracture	65.7%
Double Fracture	26.3%
Fracture Events	92

Crater: gr/bl; IBULCE: ft-lbs/in; Sp.Energy: ft-lbs/gr/bl;
Penetration: in/bl; Total Energy: ft-lbs.

Series	24	
Hammer	28.7	lbs.
Height	3.042	ft.
Angle	10 1/2	deg.
Bit	15/16	in.
Blows	154	
Rotation	1617	deg.
Flushing	1	
Broken	34.34	gr.

Corrected Cumulative Size Distribution

Mesh	Micron	% Passing
8	2380	100
16	1190	98.3
20	841	95.2
30	595	89.5
50	297	75.3
70	210	65.3
100	149	55.5
140	105	45.3
200	74	36.9
325	44	24.0
400	37	20.5
-400	-37	0

Crater	0.2230
IBULCE	93.1258
Sp. Energy	391.5053
Penetration	0.4877
Total Energy	87.3
Indexing	$9^{o} + 1\frac{1}{2}^{o}$
Chipping	6.4%
Single Fracture	61.6%
Double Fracture	32.0%
Fracture Events	93

Series	25	
Hammer	67.5	lbs.
Height	1.293	ft.
Angle	10 1/2	deg.
Bit	15/16	in.
Blows	137	
Rotation	1438.7	deg.
Flushing	1	
Broken	29.07	gr.

Corrected Cumulative Size Distribution

Mesh	Micron	% Passing
8	2380	100
16	1190	98.3
20	841	95.4
30	595	90.2
50	297	75.1
70	210	65.7
100	149	55.0
140	105	44.1
200	74	35.9
325	44	23.6
400	37	19.5
-400	-37	

Crater	0.2122
IBULCE	93.096
Sp. Energy	411.2983
Penetration	0.4757
Total Energy	87.3
Indexing	$9^{o} + 1\frac{1}{2}^{o}$
Chipping	8.3%
Single Fracture	60.5%
Double Fracture	31.2%
Fracture Events	93

Crater: gr/bl; IBULCE: ft-lbs/in; Sp.Energy: ft-lbs/gr/bl;
Penetration: in/bl; Total Energy: ft-lbs.

Series	26	
Hammer	98.6	lbs.
Height	0.885	ft.
Angle	10 1/2	deg.
Bit	15/16	in.
Blows	86	
Rotation	1795.5	deg.
Flushing	1	
Broken	28.08	gr.

Corrected Cumulative Size Distribution

Mesh	Micron	% Passing
8	2380	100
16	1190	97.8
20	841	94.7
30	595	89.3
50	297	74.5
70	210	65.6
100	149	55.5
140	105	44.8
200	74	36.8
325	44	25.1
400	37	20.8
-400	-37	0

Crater	0.3265
IBULCE	93.0784
Sp. Energy	267.2619
Penetration	0.5902
Total Energy	87.2610
Indexing	9° + 1½°
Chipping	9.7%
Single Fracture	57.3%
Double Fracture	33.0%
Fracture Events	94

Series	27	
Hammer	48.7	lbs.
Height	1.792	ft.
Angle	10 1/2	deg.
Bit	15/16	in.
Blows	44	
Rotation	462	deg.
Flushing	1	
Broken	14.90	gr.

Corrected Cumulative Size Distribution

Mesh	Micron	% Passing
8	2380	100
16	1190	97.5
20	841	94.0
30	595	88.5
50	297	73.8
70	210	65.8
100	149	55.8
140	105	45.0
200	74	35.7
325	44	23.0
400	37	18.9
-400	-37	0

Crater	0.3386
IBULCE	93.0884
Sp. Energy	257.7389
Penetration	0.6010
Total Energy	87.2704
Indexing	9° + 1½°
Chipping	11.3%
Single Fracture	51.6%
Double Fracture	37.1%
Fracture Events	91

Crater: gr/bl; IBULCE: ft-lbs/in; Sp.Energy: ft-lbs/gr/bl;
Penetration: in/bl; Total Energy: ft-lbs.

Series	28	
Hammer	28.7	lbs.
Height	1.764	ft.
Angle	21	deg.
Bit	15/16	in.
Blows	34	
Rotation	714	deg.
Flushing	1	
Broken	7.75	gr.

Corrected Cumulative Size Distribution

Mesh	Micron	% Passing
8	2380	100
16	1190	97.3
20	841	93.3
30	595	87.4
50	297	70.8
70	210	61.9
100	149	51.2
140	105	39.4
200	74	31.2
325	44	18.9
400	37	15.8
-400	-37	

Crater	0.2279
IBULCE	54.0019
Sp. Energy	222.1448
Penetration	0.4931
Total Energy	50.6268
Indexing	$9^{o}+12^{o}$, $12^{o}+9^{o}$
Chipping	13%
Single Fracture	59%
Double Fracture	28%
Fracture Events	90

Series	29	
Hammer	28.7	lbs.
Height	1.764	ft.
Angle	21	deg.
Bit	15/16	in.
Blows	50	
Rotation	1092	deg.
Flushing	2	
Broken	12.18	gr.

Corrected Cumulative Size Distribution

Mesh	Micron	% Passing
8	2380	100
16	1190	97.1
20	841	93.5
30	595	87.8
50	297	72.4
70	210	64.2
100	149	53.7
140	105	43.0
200	74	35.3
325	44	22.8
400	37	19.6
-400	-37	

Crater	0.2436
IBULCE	54.0019
Sp. Energy	207.8276
Penetration	0.5097
Total Energy	50.6268
Indexing	$9^{o}+12^{o}$
Chipping	12.1%
Single Fracture	56.3%
Double Fracture	31.6%
Fracture Events	92

Crater: gr/bl; IBULCE: ft-lbs/in; Sp.Energy: ft-lbs/gr/bl;
Penetration: in/bl; Total Energy: ft-lbs.

Series 30

Hammer	28.7	lbs.
Height	1.764	ft.
Angle	21	deg.
Bit	15/16	in.
Blows	51	
Rotation	1071	deg.
Flushing	3	
Broken	12.68	gr.

Corrected Cumulative Size Distribution

Mesh	Micron	% Passing
8	2380	100
16	1190	96.1
20	841	92.1
30	595	85.9
50	297	70.1
70	210	61.7
100	149	51.3
140	105	41.4
200	74	33.9
325	44	22.6
400	37	19.8
-400	-37	

Crater	0.2473
IBULCE	54.0019
Sp. Energy	204.7182
Penetration	0.5136
Total Energy	50.6268
Indexing	$9^{o}+12^{o}$ $12^{o}+9^{o}$
Chipping	14.3%
Single Fracture	57.0%
Double Fracture	28.7%
Fracture Events	93

Series 31

Hammer	28.7	lbs.
Height	1.764	ft.
Angle	21	deg.
Bit	15/16	in.
Blows	16	
Rotation	33.6	deg.
Flushing	4	
Broken	4.21	gr.

Corrected Cumulative Size Distribution

Mesh	Micron	% Passing
8	2380	100
16	1190	96.0
20	841	91.7
30	595	86.0
50	297	70.6
70	210	62.7
100	149	52.3
140	105	42.1
200	74	34.5
325	44	22.4
400	37	19.3
-400	-37	

Crater	0.2631
IBULCE	54.0019
Sp. Energy	192.4242
Penetration	0.5297
Total Energy	50.6268
Indexing	$9^{o}+12^{o}$ $12^{o}+9^{o}$
Chipping	15.4%
Single Fracture	54.0%
Double Fracture	30.6%
Fracture Events	93

Crater: gr/bl; IBULCE: ft-lbs/in; Sp.Energy: ft-lbs/gr/bl;
Penetration: in/bl; Total Energy: ft-lbs.

Series	32	
Hammer	28.7	lbs.
Height	1.764	ft.
Angle	21	deg.
Bit	15/16	in.
Blows	20	
Rotation	420	deg.
Flushing	5	
Broken	4.67	gr.

Corrected Cumulative Size Distribution

Mesh	Micron	% Passing
8	2380	100
16	1190	96.4
20	841	93.4
30	595	88.0
50	297	72.6
70	210	64.9
100	149	55.0
140	105	43.2
200	74	35.6
325	44	23.4
400	37	20.1
-400	-37	

Crater	0.2335
IBULCE	54.0019
Sp. Energy	216.8171
Penetration	0.4991
Total Energy	50.6268
Indexing	$9^{o}+12^{o}$ $12^{o}+9^{o}$
Chipping	11.2%
Single Fracture	57.1%
Double Fracture	31.7%
Fracture Events	92

Series	33-1	
Hammer	P_1	lbs.
Height	-	ft.
Angle	-	deg.
Bit	1 3/8	in.
Blows	-	
Rotation	-	deg.
Flushing	T_1	
Broken	13.72	gr.

Corrected Cumulative Size Distribution

Mesh	Micron	% Passing
8	2380	100
16	1190	97
20	841	93.1
30	595	86.4
50	297	67.9
70	210	57.1
100	149	47.1
140	105	35.6
200	74	27.5
325	44	15.1
400	37	12.4
-400	-37	

Crater	-
IBULCE	-
Sp. Energy	-
Penetration	-
Total Energy	-
Indexing	-
Chipping	14.9%
Single Fracture	62.6%
Double Fracture	22.5%
Fracture Events	90

Crater: gr/bl; IBULCE: ft-lbs/in; Sp.Energy: ft-lbs/gr/bl;
Penetration: in/bl; Total Energy: ft-lbs.

Series	33-2	
Hammer	P_1	lbs.
Height	-	ft.
Angle	-	deg.
Bit	1 3/8	in.
Blows	-	
Rotation	-	deg.
Flushing	T_2	
Broken	16.33	gr.

Corrected Cumulative Size Distribution

Mesh	Micron	% Passing
8	2380	100
16	1190	97.7
20	841	94.3
30	595	88.1
50	297	69.9
70	210	60.3
100	149	49.1
140	105	37.2
200	74	28.7
325	44	17.3
400	37	13.4
-400	-37	

Crater	-
IBULCE	-
Sp. Energy	-
Penetration	-
Total Energy	-
Indexing	-
Chipping	12.9%
Single Fracture	62.6%
Double Fracture	24.5%
Fracture Events	89

Series	33-3	
Hammer	P_1	lbs.
Height	-	ft.
Angle	-	deg.
Bit	1 3/8	in.
Blows	-	
Rotation	-	deg.
Flushing	T_3	
Broken	17.01	gr.

Corrected Cumulative Size Distribution

Mesh	Micron	% Passing
8	2380	100
16	1190	98.6
20	841	95.6
30	595	90.3
50	297	74.4
70	210	64.5
100	149	54.3
140	105	43.0
200	74	34.5
325	44	22.4
400	37	17.7
-400	-37	

Crater	-
IBULCE	-
Sp. Energy	-
Penetration	-
Total Energy	-
Indexing	-
Chipping	9.0%
Single Fracture	60.5%
Double Fracture	30.5%
Fracture Events	91

Crater: gr/bl; IBULCE: ft-lbs/in; Sp.Energy: ft-lbs/gr/bl; Penetration: in/bl; Total Energy: ft-lbs.

Series	34-1	
Hammer	P_2	lbs.
Height	-	ft.
Angle	-	deg.
Bit	1 3/8	in.
Blows	-	
Rotation	-	deg.
Flushing	T_1	
Broken	14.76	gr.

Corrected Cumulative Size Distribution

Mesh	Micron	% Passing
8	2380	100
16	1190	96.5
20	841	92.5
30	595	85.3
50	297	67.5
70	210	57.1
100	149	47.1
140	105	36.8
200	74	29.4
325	44	19.2
400	37	15.5
-400	-37	

Crater	-
IBULCE	-
Sp. Energy	-
Penetration	-
Total Energy	-
Indexing	-
Chipping	15.6%
Single Fracture	61.4%
Double Fracture	23.0%
Fracture Events	90

Series	34-2	
Hammer	P_2	lbs.
Height	-	ft.
Angle	-	deg.
Bit	1 3/8	in.
Blows	-	
Rotation	-	deg.
Flushing	T_2	
Broken	17.17	gr.

Corrected Cumulative Size Distribution

Mesh	Micron	% Passing
8	2380	100
16	1190	97.7
20	841	93.9
30	595	87.2
50	297	69.6
70	210	60.2
100	149	49.2
140	105	38.1
200	74	31.1
325	44	20.1
400	37	17.3
-400	-37	

Crater	-
IBULCE	-
Sp. Energy	-
Penetration	-
Total Energy	-
Indexing	-
Chipping	13.5%
Single Fracture	61.4%
Double Fracture	25.1%
Fracture Events	93

Crater: gr/bl; IBULCE: ft-lbs/in; Sp.Energy: ft-lbs/gr/bl;
Penetration: in/bl; Total Energy: ft-lbs.

Series	34-3	
Hammer	P_2	lbs.
Height	-	ft.
Angle	-	deg.
Bit	1 3/8	in.
Blows	-	
Rotation	-	deg.
Flushing	T_3	
Broken	-	gr.

Corrected Cumulative Size Distribution

Mesh	Micron	% Passing
8	2380	100
16	1190	97.6
20	841	94.2
30	595	88.2
50	297	71.6
70	210	62.7
100	149	52.0
140	105	40.6
200	74	32.2
325	44	19.8
400	37	16.8
-400	-37	

Crater	-
IBULCE	-
Sp. Energy	-
Penetration	-
Total Energy	-
Indexing	-
Chipping	12.2%
Single Fracture	59.2%
Double Fracture	28.6%
Fracture Events	91

Series	35-1	
Hammer	P_3	lbs.
Height	-	ft.
Angle	-	deg.
Bit	1 3/8	in.
Blows		
Rotation		deg.
Flushing	T_1	
Broken	18.92	gr.

Corrected Cumulative Size Distribution

Mesh	Micron	% Passing
8	2380	100
16	1190	97.1
20	841	92.9
30	595	85.9
50	297	68.6
70	210	59.8
100	149	48.9
140	105	38.8
200	74	31.7
325	44	21.1
400	37	18.2
-400	-37	

Crater	-
IBULCE	-
Sp. Energy	-
Penetration	-
Total Energy	-
Indexing	-
Chipping	15.1%
Single Fracture	59.3%
Double Fracture	25.6%
Fracture Events	93

Crater: gr/bl; IBULCE: ft-lbs/in; Sp.Energy: ft-lbs/gr/bl;
Penetration: in/bl; Total Energy: ft-lbs.

Series 35 - 2

Hammer	P_3	lbs.
Height	-	ft.
Angle	-	deg.
Bit	1 3/8	in.
Blows	-	
Rotation	-	deg.
Flushing	T_2	
Broken	43.45	gr.

Corrected Cumulative Size Distribution

Mesh	Micron	% Passing
8	2380	100
16	1190	97.1
20	841	92.6
30	595	84.6
50	297	66.1
70	210	56.2
100	149	46.1
140	105	35.9
200	74	28.5
325	44	18.0
400	37	14.6
-400	-37	

Crater	-
IBULCE	-
Sp. Energy	-
Penetration	-
Total Energy	-
Indexing	-
Chipping	17.4%
Single Fracture	60.2%
Double Fracture	22.4%
Fracture Events	92

Series 35 - 3

Hammer	P_3	lbs.
Height	-	ft.
Angle	-	deg.
Bit	1 3/8	in.
Blows	-	
Rotation	-	deg.
Flushing	T_3	
Broken	67.67	gr.

Corrected Cumulative Size Distribution

Mesh	Micron	% Passing
8	2380	100
16	1190	96.7
20	841	92.7
30	595	85.9
50	297	69.7
70	210	60.4
100	149	50.5
140	105	40.2
200	74	32.5
325	44	21.3
400	37	17.6
-400	-37	

(Losses were very high)

Crater	-
IBULCE	-
Sp. Energy	-
Penetration	-
Total Energy	-
Indexing	-
Chipping	13.4%
Single Fracture	58.9%
Double Fracture	27.7%
Fracture Events	92

Crater: gr/bl; IBULCE: ft-lbs/in; Sp.Energy: ft-lbs/gr/bl;
Penetration: in/bl; Total Energy: ft-lbs.

Series 36

Hammer	28.7	lbs.
Height	0.917	ft.
Angle	21	deg.
Bit	15/16 - 86°	in.
Blows	103	
Rotation	2163	deg.
Flushing	1	
Broken	13.55	gr.

Corrected Cumulative Size Distribution

Mesh	Micron	% Passing
8	2380	100
16	1190	98.7
20	841	96.5
30	595	91.0
50	297	76.1
70	210	65.7
100	149	57.3
140	105	45.3
200	74	37.0
325	44	24.8
400	37	19.7
-400	-37	

Crater	0.1315
IBULCE	28.0715
Sp. Energy	200.1
Penetration	0.376
Total Energy	26.3179
Indexing	9°+12° - 12°+9°
Chipping	8.3%
Single Fracture	56.8%
Double Fracture	34.9%
Fracture Events	92

Series 37

Hammer	28.7	lbs.
Height	0.917	ft.
Angle	21	deg.
Bit	15/16 - 95°	in.
Blows	103	
Rotation	1163	deg.
Flushing	1	
Broken	11.51	gr.

Corrected Cumulative Size Distribution

Mesh	Micron	% Passing
8	2380	100
16	1190	98.6
20	841	96.6
30	595	91.7
50	297	75.1
70	210	65.4
100	149	55.2
140	105	43.7
200	74	35.9
325	44	24.8
400	37	20.5
-400	-37	

Crater	0.1118
IBULCE	28.0715
Sp. Energy	235.9
Penetration	0.346
Total Energy	26.3179
Indexing	9°+12° - 12°+9°
Chipping	8.4%
Single Fracture	60.0%
Double Fracture	31.6%
Fracture Events	92

Crater: gr/bl; IBULCE: ft-lbs/in; Sp.Energy: ft-lbs/gr/bl;
Penetration: in/bl; Total Energy: ft-lbs.

Series 38

Hammer	28.7	lbs.
Height	0.917	ft.
Angle	21	deg.
Bit	15/16 - 110°	in.
Blows	138	
Rotation	3058	deg.
Flushing	1	
Broken	15.07	gr.

Corrected Cumulative Size Distribution

Mesh	Micron	% Passing
8	2380	100
16	1190	98.7
20	841	96.6
30	595	91.5
50	297	75.2
70	210	66.5
100	149	56.4
140	105	44.8
200	74	36.4
325	44	25.1
400	37	20.9
-400	-37	

Crater	0.1092	gr/bl
IBULCE	28.0715	ft-lbs/in
Sp. Energy	241.0	ft-lbs/gr/bl
Penetration	0.343	in/bl
Total Energy	26.3179	ft-lbs
Indexing	9° + 12° - 12° + 9°	
Chipping	9.3%	
Single fracture	56.3%	
Double fracture	34.4%	
Fracture events	91	

APPENDIX B

Tabulated Results of

HAMMER TESTS

Impact Crushing Tests

Series: 7 - 1 Rock: Scottstown Granite Sheet 1 of 7

Description: Feed Size: -8 + 16 mesh; Cumulative, Corrected Wet Frequency Size Distribution

Test N°		641	642	644	643	645					
Weight gr.		5	5	5	5	5					
Blows		25	50	75	100	125					
Unbroken gr.		2.23	0.65	0.16	0.14	0.07					
Broken gr.		7.60	9.09	9.32	9.44	9.71					
1/2	12700										
3	6730										
4	4760										
6	3360										
8	2380										
16	1190	100	100	100	100	100					
20	841	72.00	81.51	92.09	94.79	98.27					
30	595	47.66	57.20	70.36	76.31	87.84					
50	297	22.13	28.49	38.08	43.12	53.08					
70	210	15.81	20.24	27.74	32.37	39.99					
100	149	11.20	14.85	20.78	23.91	30.07					
140	105	7.65	10.35	14.70	17.21	21.90					
200	74	5.65	7.72	11.09	13.24	16.85					
325	44	3.33	4.69	7.49	8.76	11.00					
-400	37										
-400	-37										

Impact Crushing Tests

Series: 7 - 2 Rock: Scottstown Granite Sheet 2 of 7

Description: Feed Size: -8 + 16 mesh; Cumulative, Corrected Wet Frequency Size Distribution

Test N°		662	663								
Weight gr.		10	10								
Blows		150	200								
Unbroken gr.		0.19	0.06								
Broken gr.		9.64	9.66								
1/2	12700										
3	6730										
4	4760										
6	3360										
8	2380										
16	1190	100	100								
20	841	90.75	96.61								
30	595	69.29	81.28								
50	297	37.04	46.92								
70	210	27.17	35.71								
100	149	20.15	27.27								
140	105	14.37	19.62								
200	74	10.89	15.02								
-325	44	6.86	9.37								
400	37										
-400	-37										

Impact Crushing Tests

Series: 7 - 3 Rock: Scottstown Granite Sheet 3 of 7

Description: Feed Size: -8+16 mesh - Corrected Wet Frequency Size Distribution (Cumulative).

Test N°		664	665								
Weight gr.		15	15								
Blows		250	300								
Unbroken gr.		0.37	0.35								
Broken gr.		14.00	13.87								
1/2	12700										
3	6730										
4	4760										
6	3360										
8	2380										
16	1190	100	100								
20	841	89.56	89.30								
30	595	71.75	71.72								
50	297	41.27	42.40								
70	210	30.76	31.99								
100	149	23.24	24.47								
140	105	16.96	18.13								
200	74	13.06	14.05								
325	44	8.40	9.25								
-400	37										
-400	-37										

Impact Crushing Tests

Series: 7 - 4 Rock: Scottstown Granite Sheet 4 of 7

Description: Feed Size: -8 + 16 mesh; Cumulative, Corrected Wet Frequency Size Distribution

Test N°		666									
Weight gr.		20									
Blows		350									
Unbroken gr.		0.94									
Broken gr.		17.71									
1/2	12700										
3	6730										
4	4760										
6	3360										
8	2380										
16	1190	100									
20	841	86.43									
30	595	66.22									
50	297	37.86									
70	210	28.74									
100	149	21.72									
140	105	16.08									
200	74	12.41									
325	44	8.11									
-400	37										
-400	-37										

Impact Crushing Tests

Series: 7 - 5 Rock: Scottstown Granite Sheet 5 of 7

Description: Feed Size: -8 + 16 mesh; Cumulative, Corrected Wet Frequency Size Distribution

Test N°		67	68	69	70	71	72	73	74	75	
Weight gr.		25	25	25	25	25	25	25	25	25	
Blows		25	50	75	100	125	150	175	200	400	
Unbroken gr.		13.15	10.99	9.68	9.79	6.93	7.25	5.94	4.43	1.98	
Broken gr.		11.76	11.84	15.21	15.04	17.90	17.47	18.97	20.30	22.67	
1/2	12700										
3	6730										
4	4760										
6	3360										
8	2380										
16	1190	100	100	100	100	100	100	100	100	100	
20	841	61.83	65.89	67.20	68.15	74.02	72.08	73.76	77.73	87.73	
30	595	37.43	43.06	44.58	44.61	51.06	49.98	51.99	57.14	72.16	
50	297	15.24	17.70	19.27	20.08	24.08	23.76	24.68	28.91	44.11	
70	210	10.22	11.49	12.96	14.10	16.82	16.72	16.88	20.54	33.30	
100	149	6.90	7.95	9.02	9.71	11.90	11.80	11.92	14.58	25.40	
140	105	4.37	5.33	5.86	6.37	8.00	7.96	8.09	10.13	18.89	
200	74	2.99	3.69	4.17	4.54	5.76	5.84	5.89	7.51	14.53	
325	44	1.58	2.02	2.29	2.56	3.46	3.44	3.40	4.53	9.28	
400	37	0.98	1.34	1.51	1.70	2.31	2.35	2.28	3.20	6.62	
-400	-37										

Impact Crushing Tests

Series: 7 - 6 Rock: Scottstown Granite Sheet 6 of 7

Description: Feed Size: -8 + 16 mesh; Cumulative, Corrected Wet Frequency Size Distribution

Test N°		76	77	78	79						
Weight gr.		50	50	50	50						
Blows		100	200	300	400						
Unbroken gr.		19.38	16.18	11.14	8.47						
Broken gr.		30.35	33.59	38.53	41.24						
1/2	12700										
3	6730										
4	4760										
6	3360										
8	2380										
16	1190	100	100	100	100						
20	841	64.38	68.79	73.91	77.04						
30	595	40.92	45.87	51.56	55.58						
50	297	18.35	22.23	26.26	29.51						
70	210	12.42	15.68	19.02	21.41						
100	149	8.70	11.33	13.80	16.00						
140	105	5.91	7.84	9.70	11.49						
200	74	4.29	5.80	7.21	8.68						
325	44	2.55	3.54	4.41	5.40						
400	37	1.77	2.56	3.18	3.83						
-400	-37										

Impact Crushing Tests

Series: 7 - 7 Rock: Scottstown Granite Sheet 7 of 7

Description: Feed Size: -8 + 16 mesh; Cumulative,Corrected Wet Frequency Size Distribution

Test N°		80	81								
Weight gr.		100	100								
Blows		200	400								
Unbroken gr.		50.98	39.54								
Broken gr.		48.78	59.91								
1/2	12700										
3	6730										
4	4760										
6	3360										
8	2380										
16	1190	100	100								
20	841	59.7	66.1								
30	595	37.6	44.6								
50	297	16.4	22.3								
70	210	11.0	15.5								
100	149	7.60	11.30								
140	105	5.18	8,07								
200	74	3.76	6.03								
325	44	2.27	3.75								
400	37	1.60	2.67								
-400	-37										

APPENDIX C

Extrapolation to "Zero Gram" and

"Zero blow" for all Particle Sizes.

HAMMER TESTS

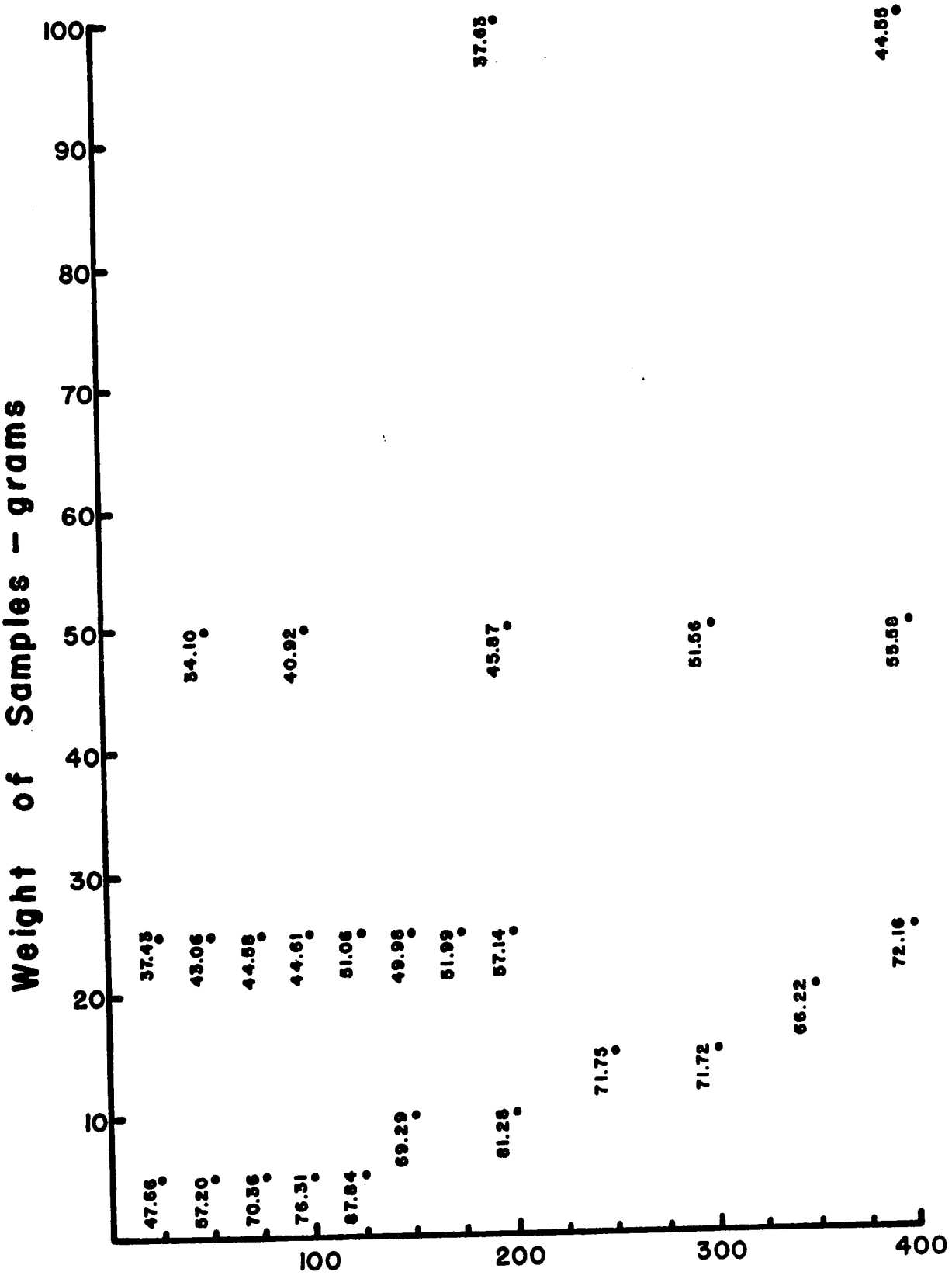

Fig.5.10-1 CUMULATIVE % WEIGHT (-30 MESH)

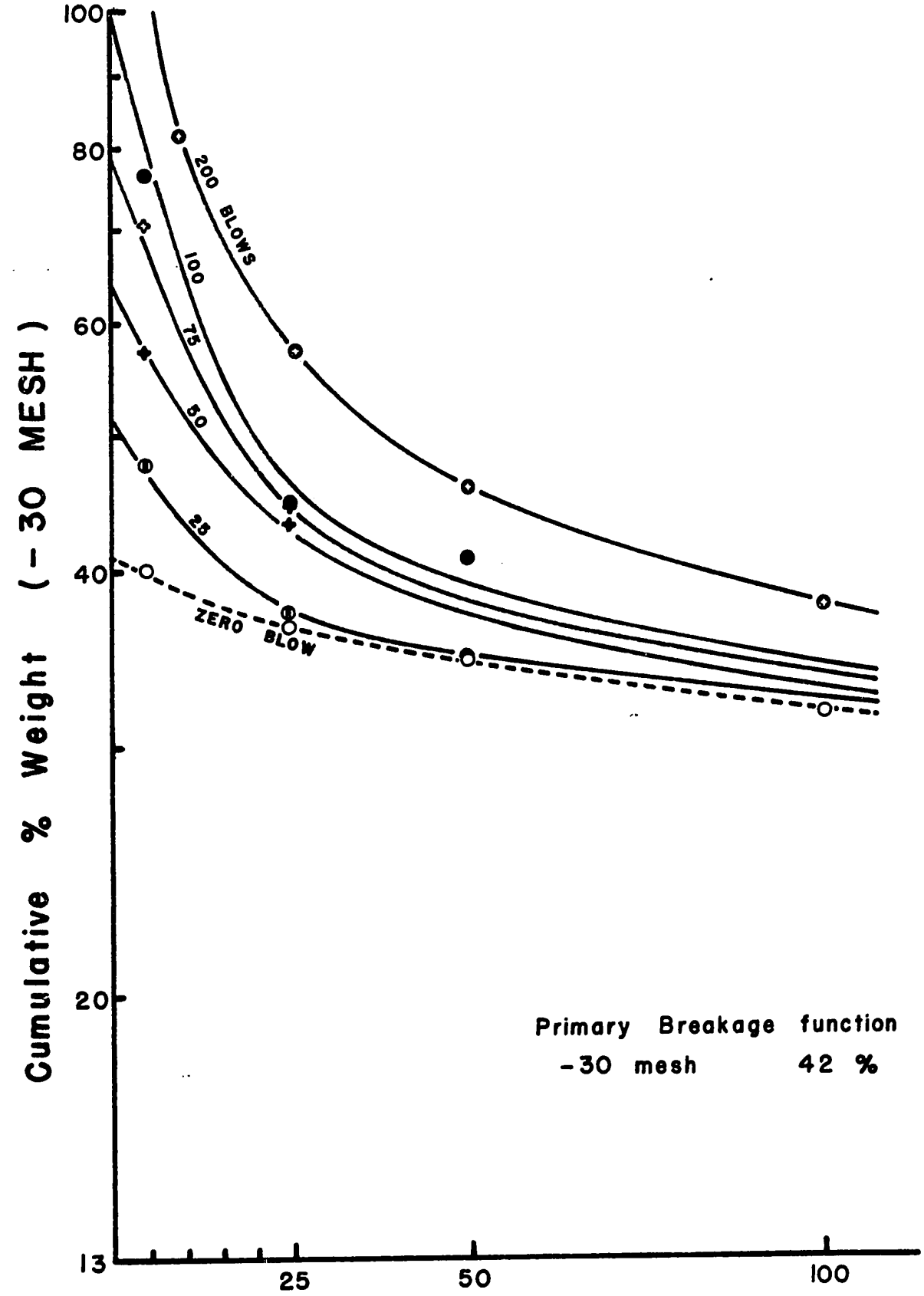

Fig.5.11-1 EXTRAPOLATION TO ZERO GRAM

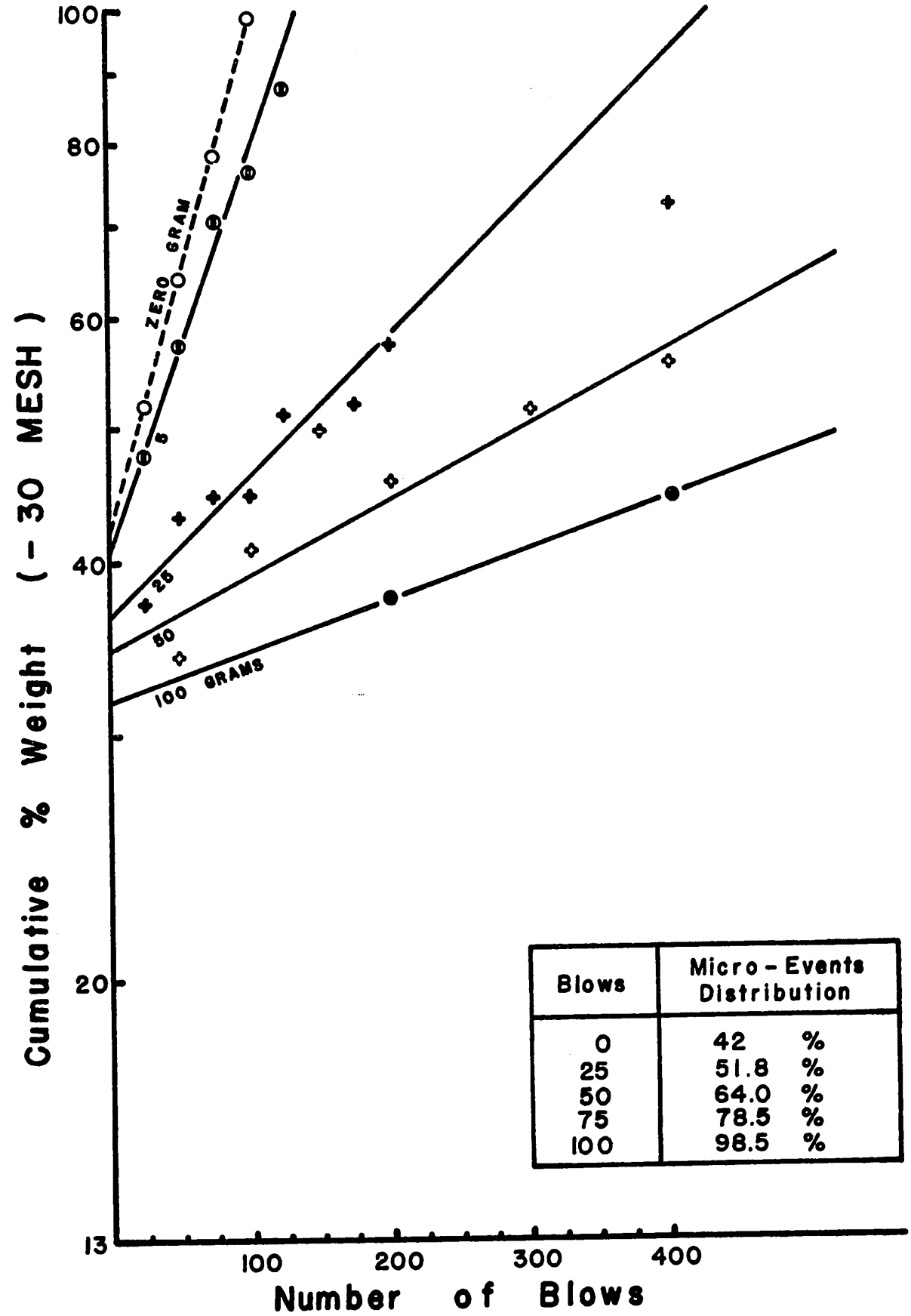

Blows	Micro - Events Distribution
0	42 %
25	51.8 %
50	64.0 %
75	78.5 %
100	98.5 %

Fig.5.12-1 EXTRAPOLATION TO ZERO BLOW

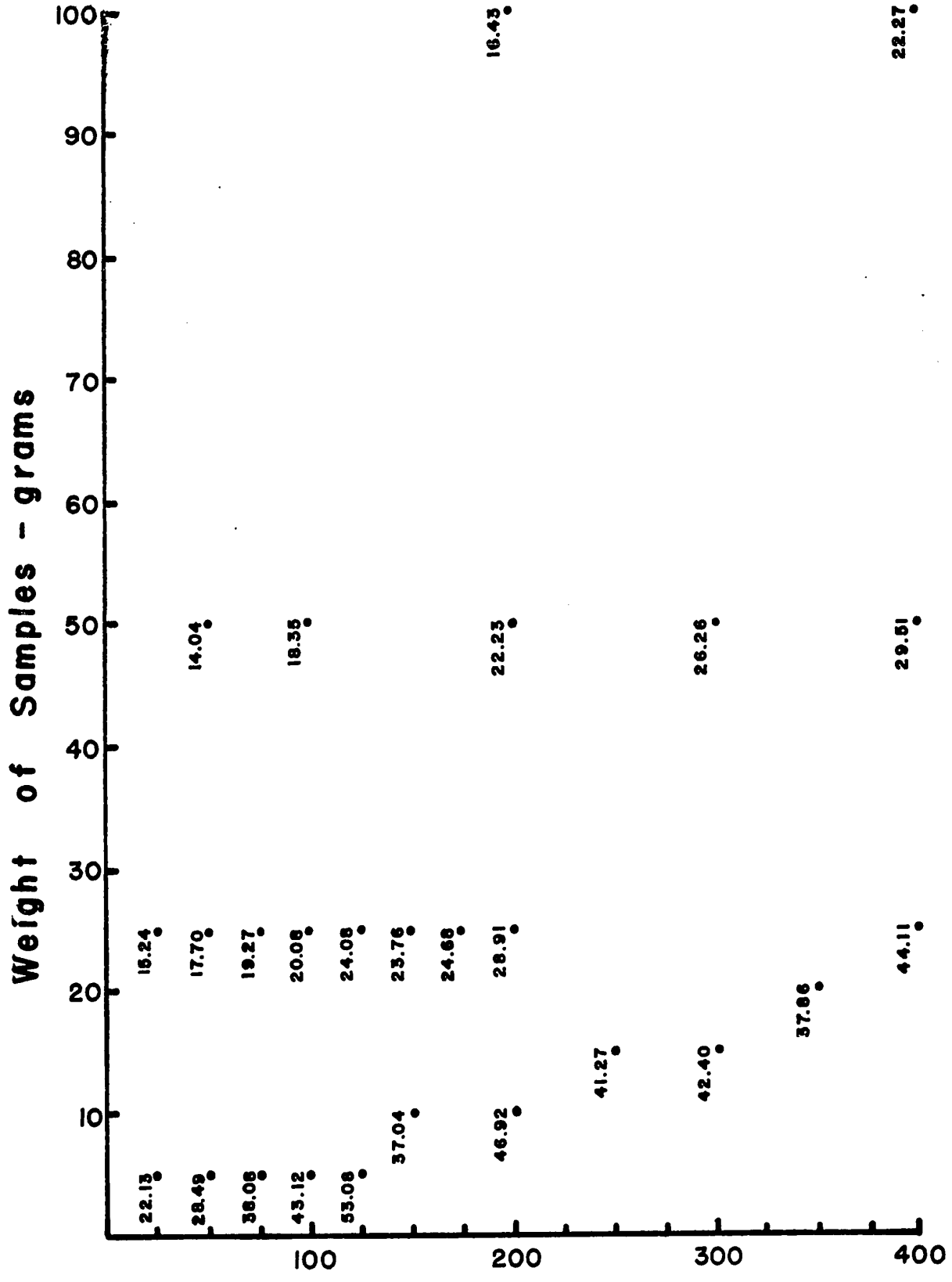

Fig.5.10-2 CUMULATIVE % WEIGHT (-50 MESH)

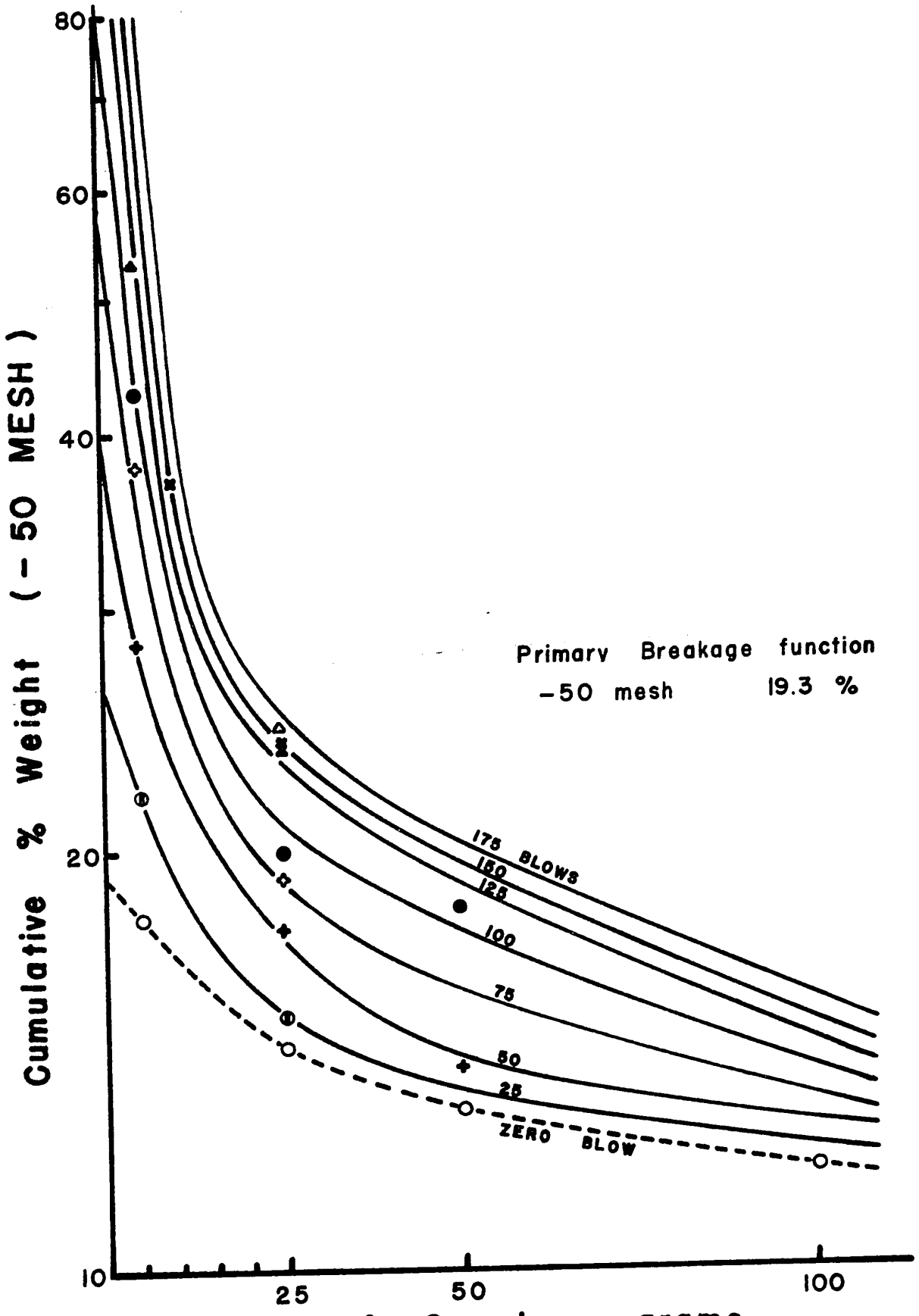

Fig.5.11-2 EXTRAPOLATION TO ZERO GRAM

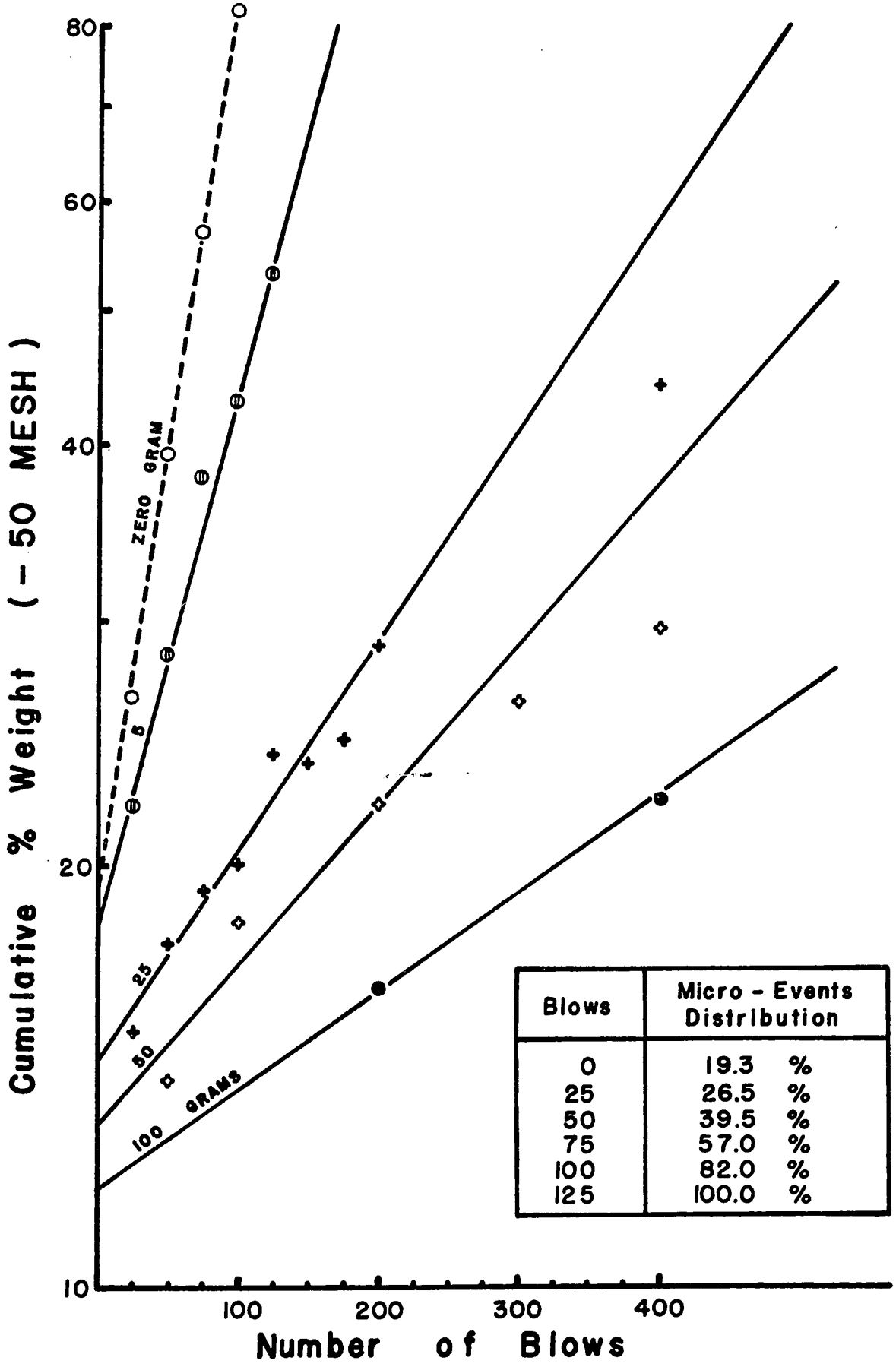

Blows	Micro - Events Distribution
0	19.3 %
25	26.5 %
50	39.5 %
75	57.0 %
100	82.0 %
125	100.0 %

Fig.5.12-2 EXTRAPOLATION TO ZERO BLOW

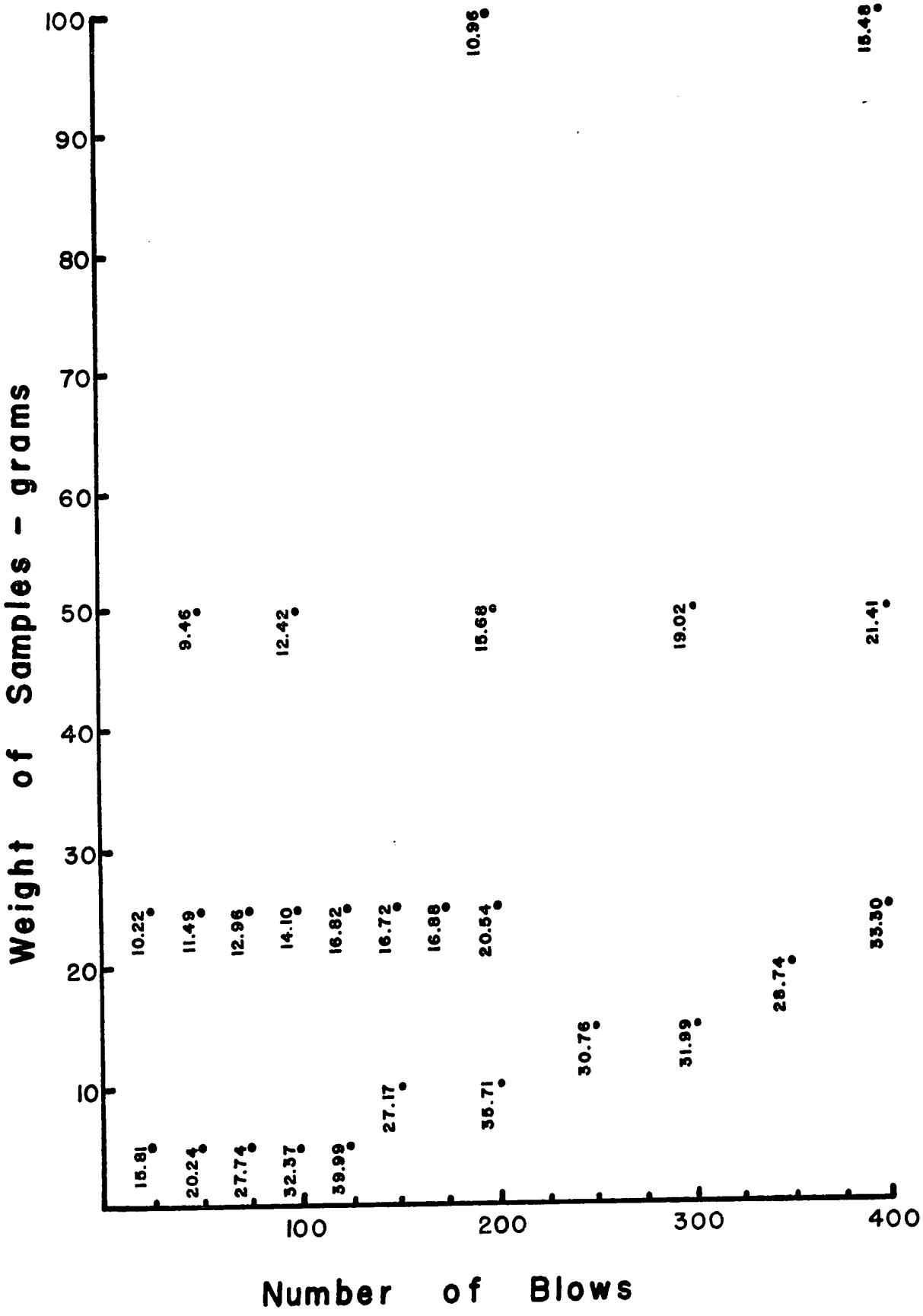

Fig. 5.10-3, CUMULATIVE % WEIGHT (-70 MESH)

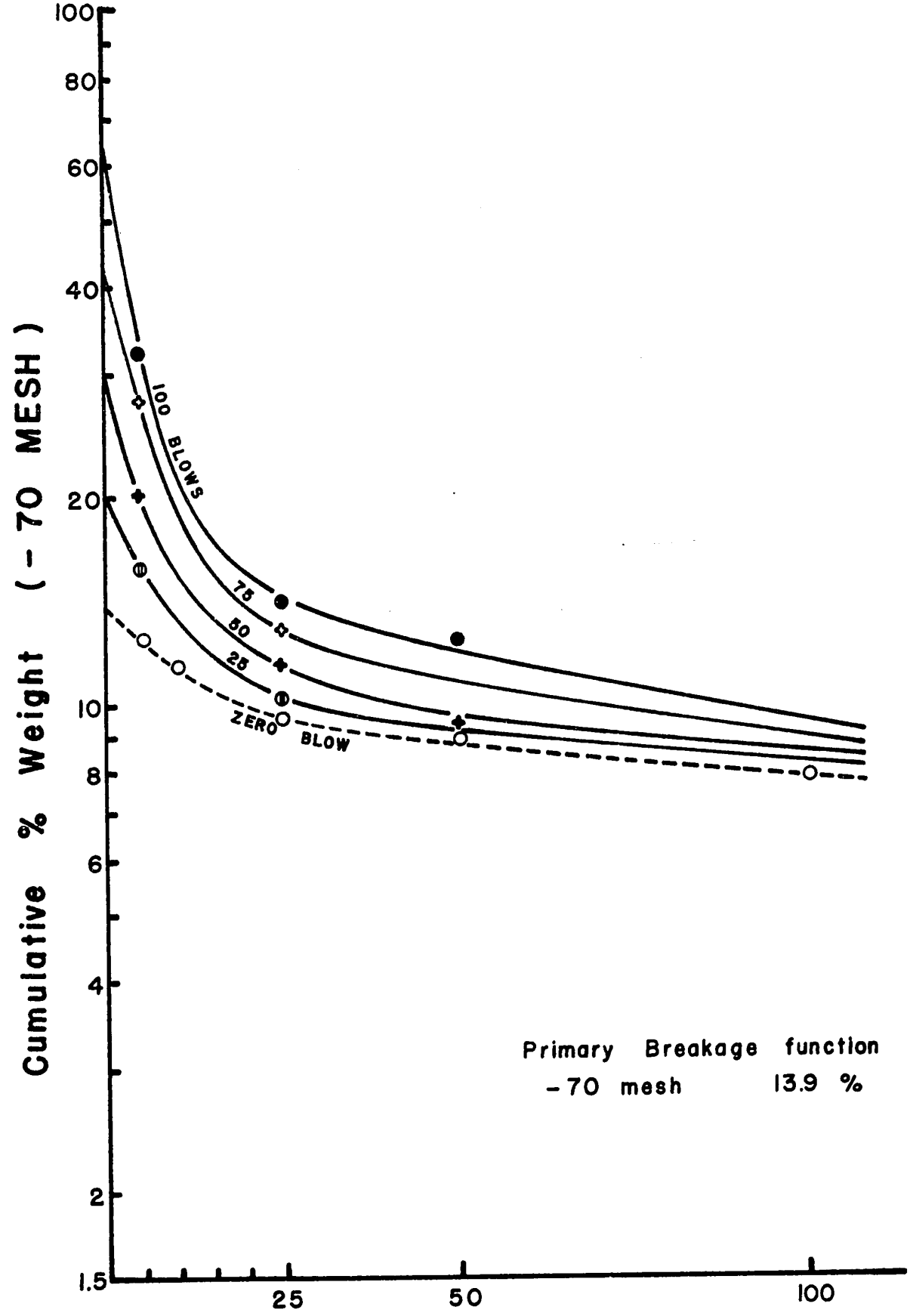

Fig.5.11-3 EXTRAPOLATION TO ZERO GRAM

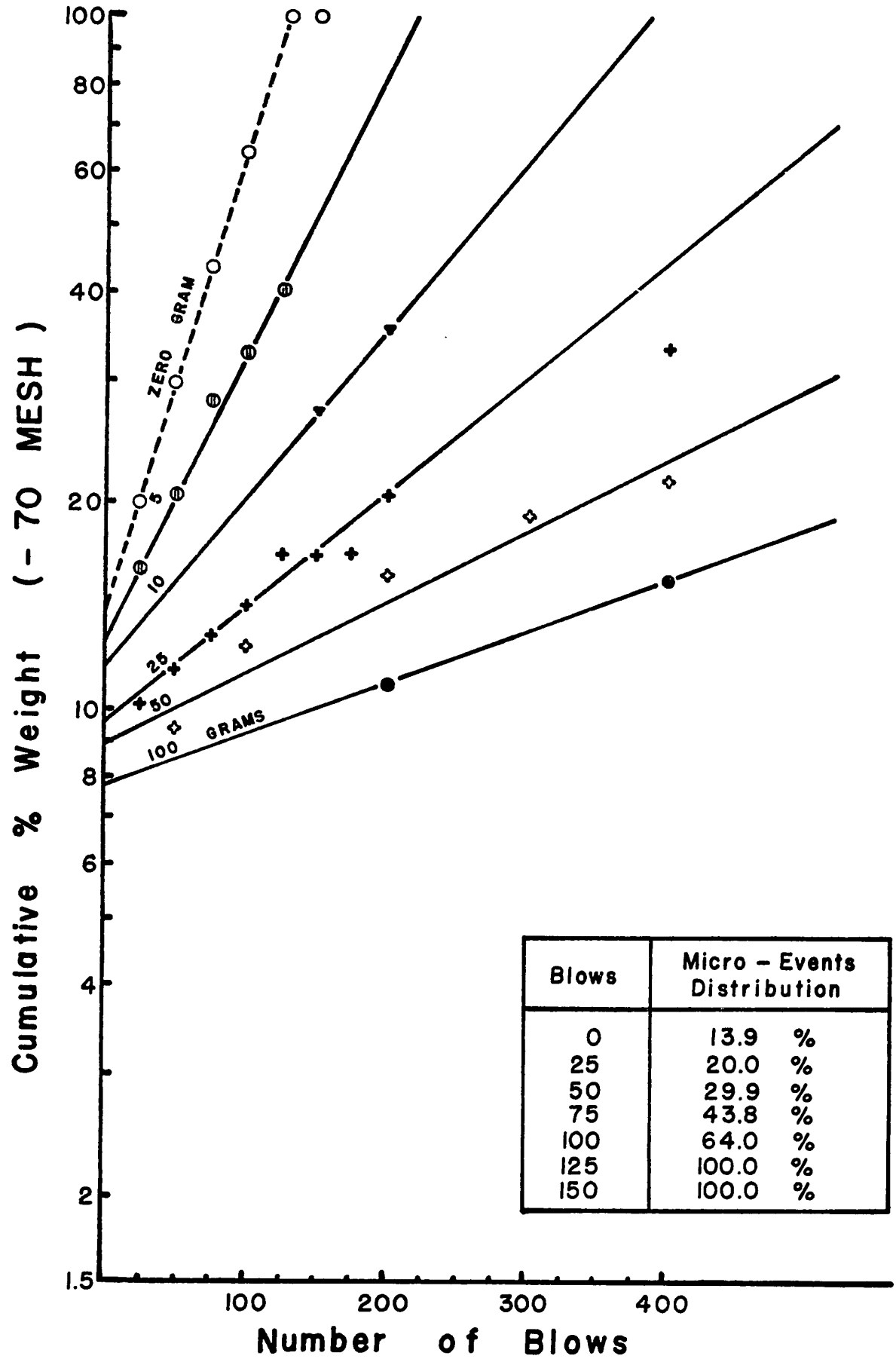

Blows	Micro – Events Distribution
0	13.9 %
25	20.0 %
50	29.9 %
75	43.8 %
100	64.0 %
125	100.0 %
150	100.0 %

Fig.5.12-3 EXTRAPOLATION TO ZERO BLOW

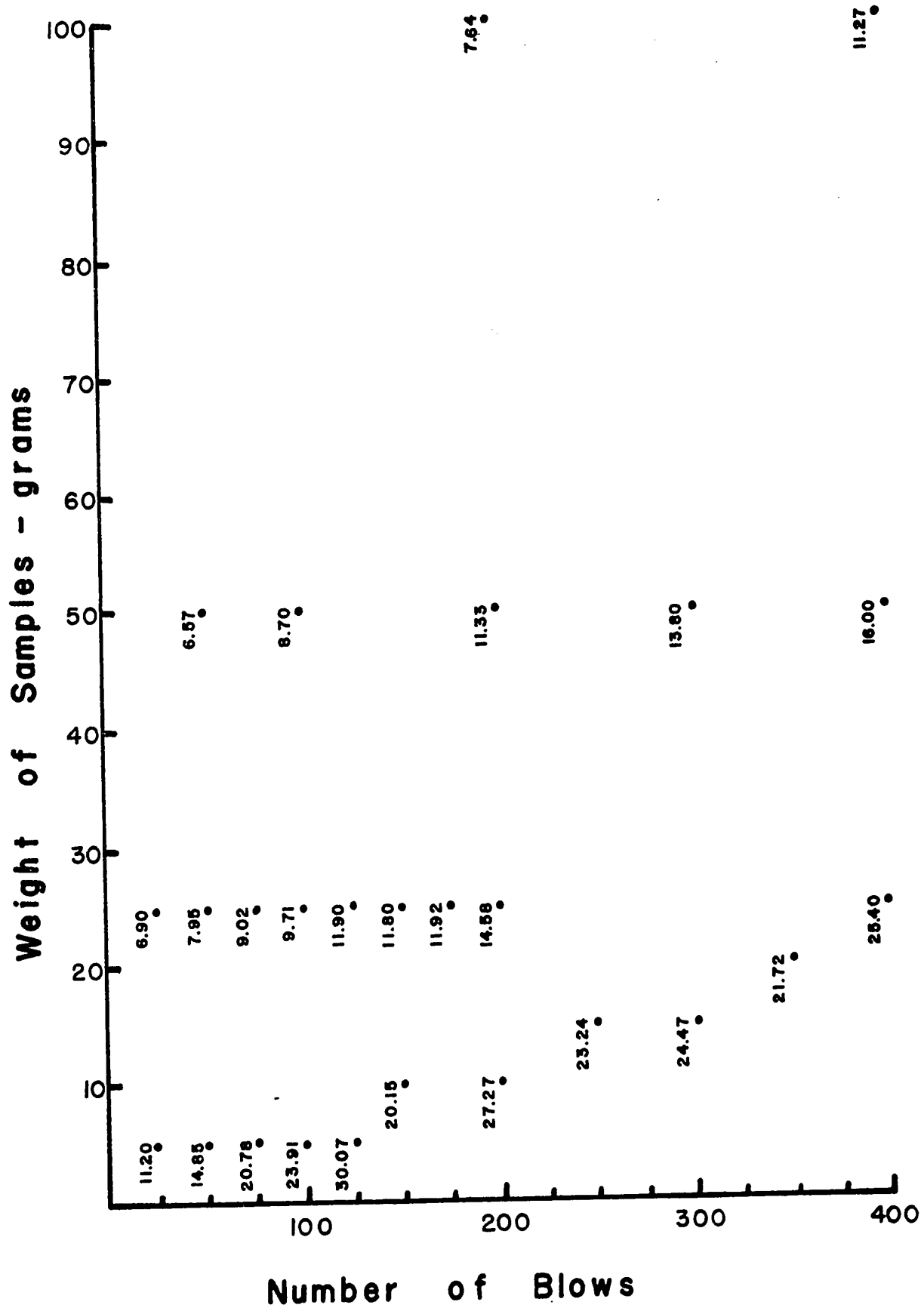

Fig.5.10-4, CUMULATIVE % WEIGHT (-100 MESH)

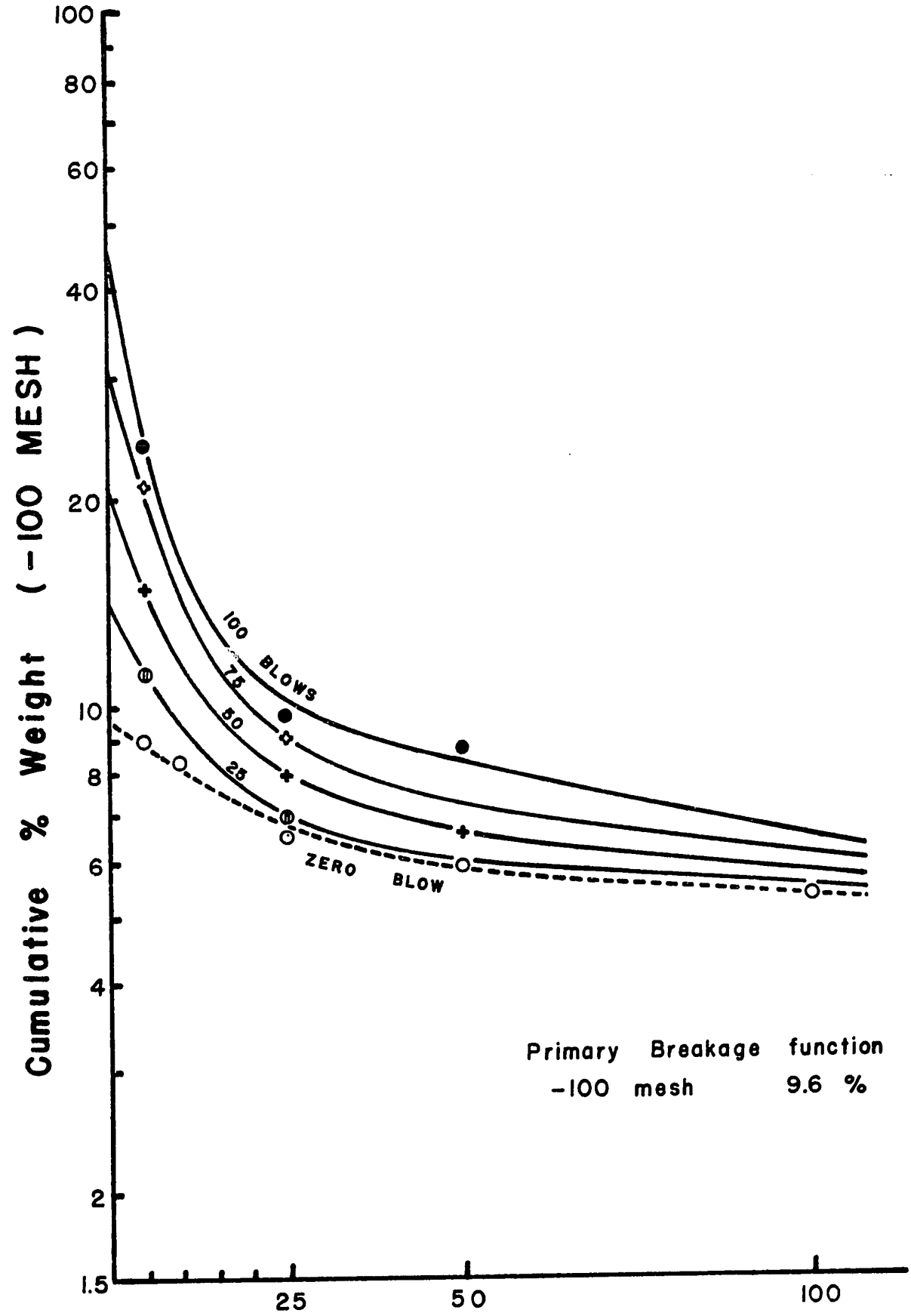

Fig.5.11-4 EXTRAPOLATION TO ZERO GRAM

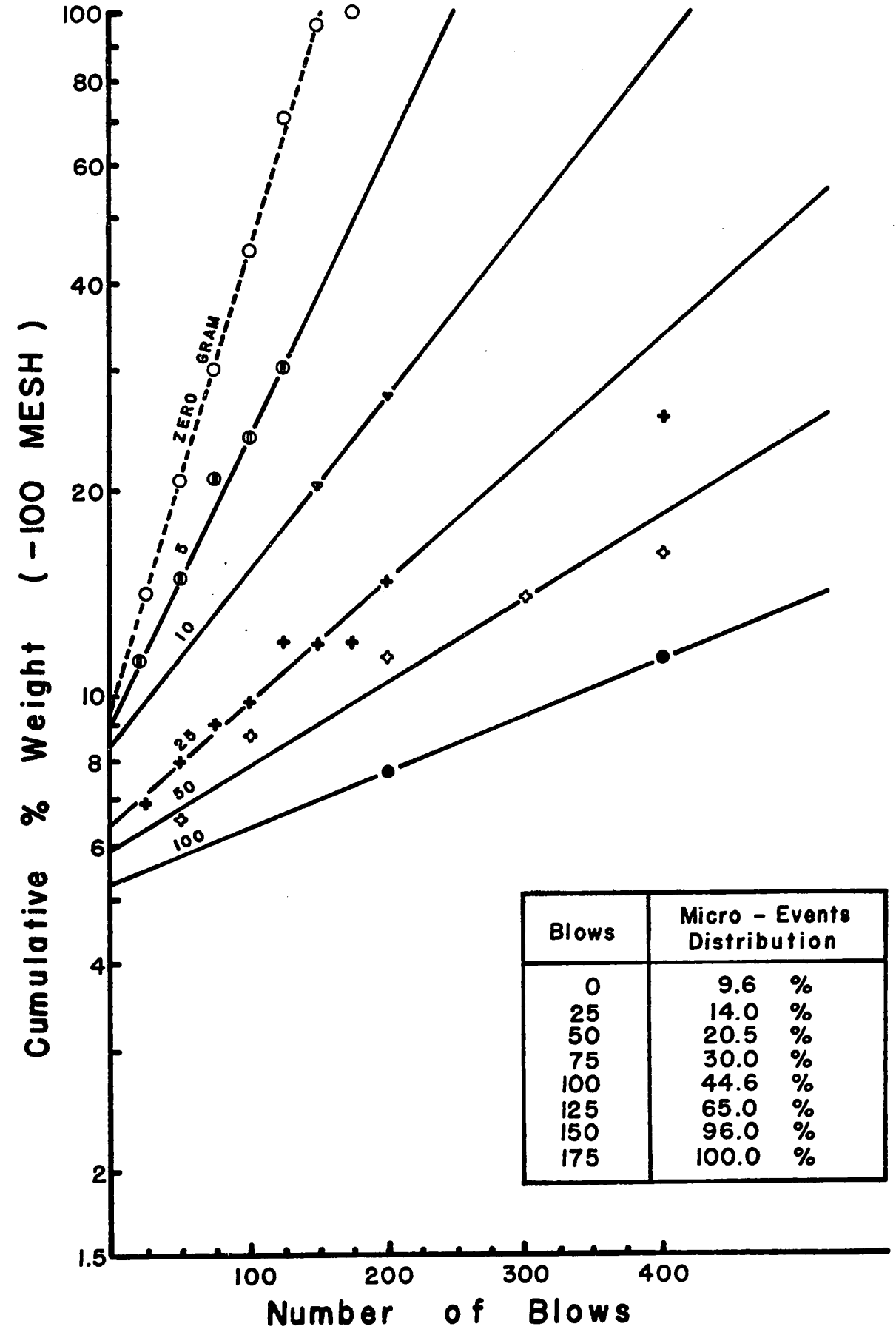

Blows	Micro - Events Distribution
0	9.6 %
25	14.0 %
50	20.5 %
75	30.0 %
100	44.6 %
125	65.0 %
150	96.0 %
175	100.0 %

Fig. 5.12-4 EXTRAPOLATION TO ZERO BLOW

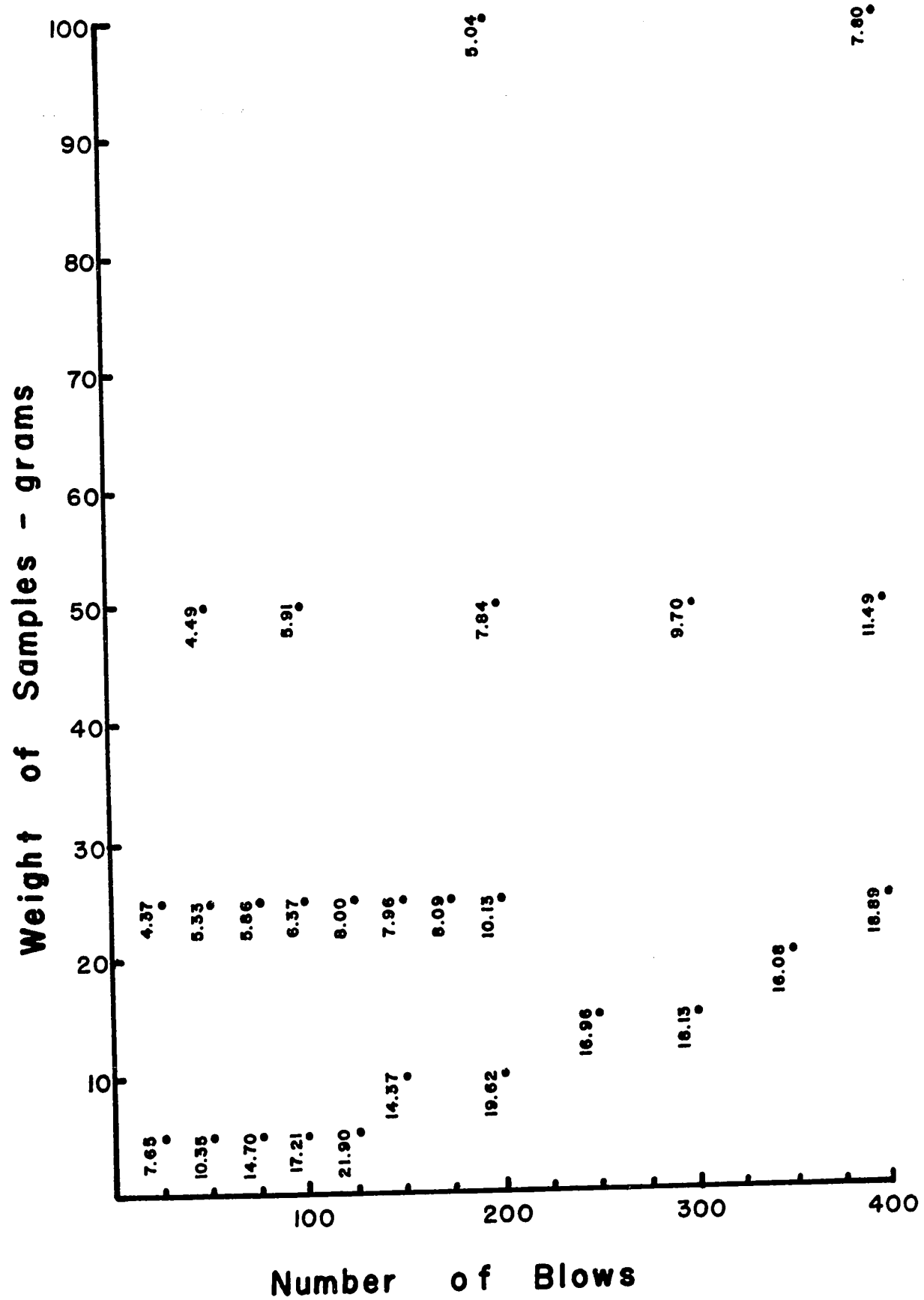

Fig.5.10-5, CUMULATIVE % WEIGHT (-140 MESH)

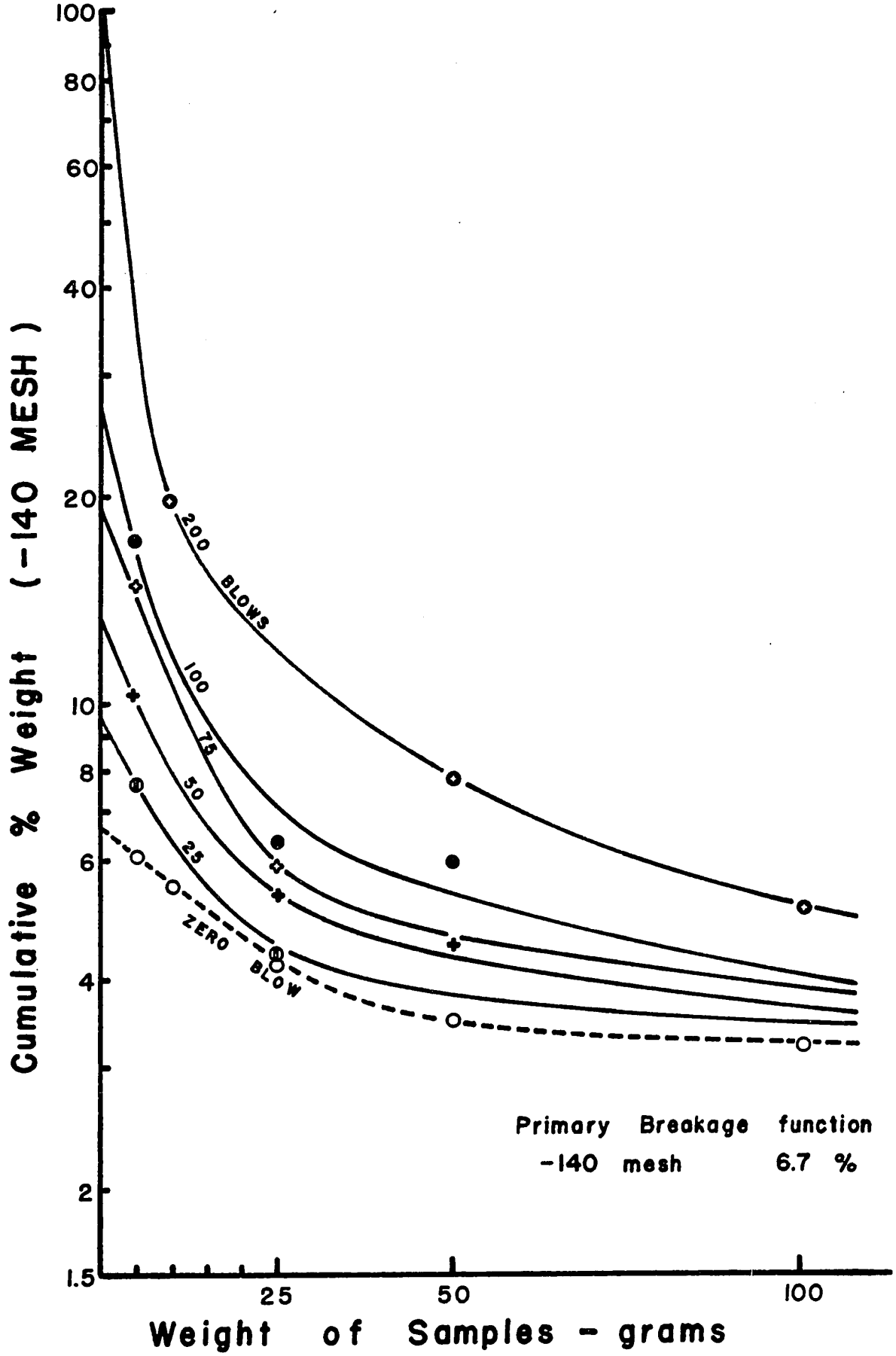

Fig.5.11-5 EXTRAPOLATION TO ZERO GRAM

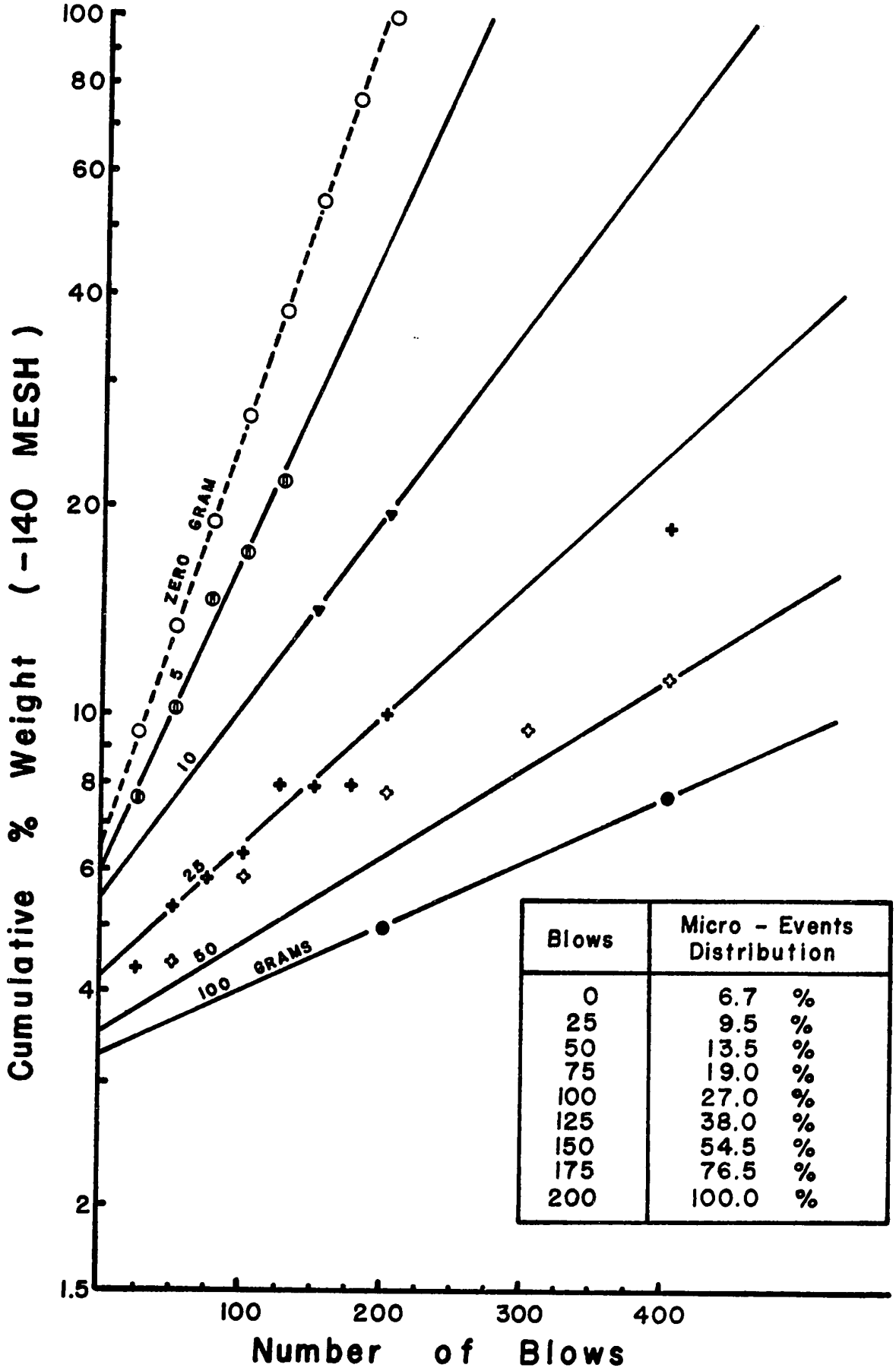

Blows	Micro - Events Distribution
0	6.7 %
25	9.5 %
50	13.5 %
75	19.0 %
100	27.0 %
125	38.0 %
150	54.5 %
175	76.5 %
200	100.0 %

Fig.5.12-5 EXTRAPOLATION TO ZERO BLOW

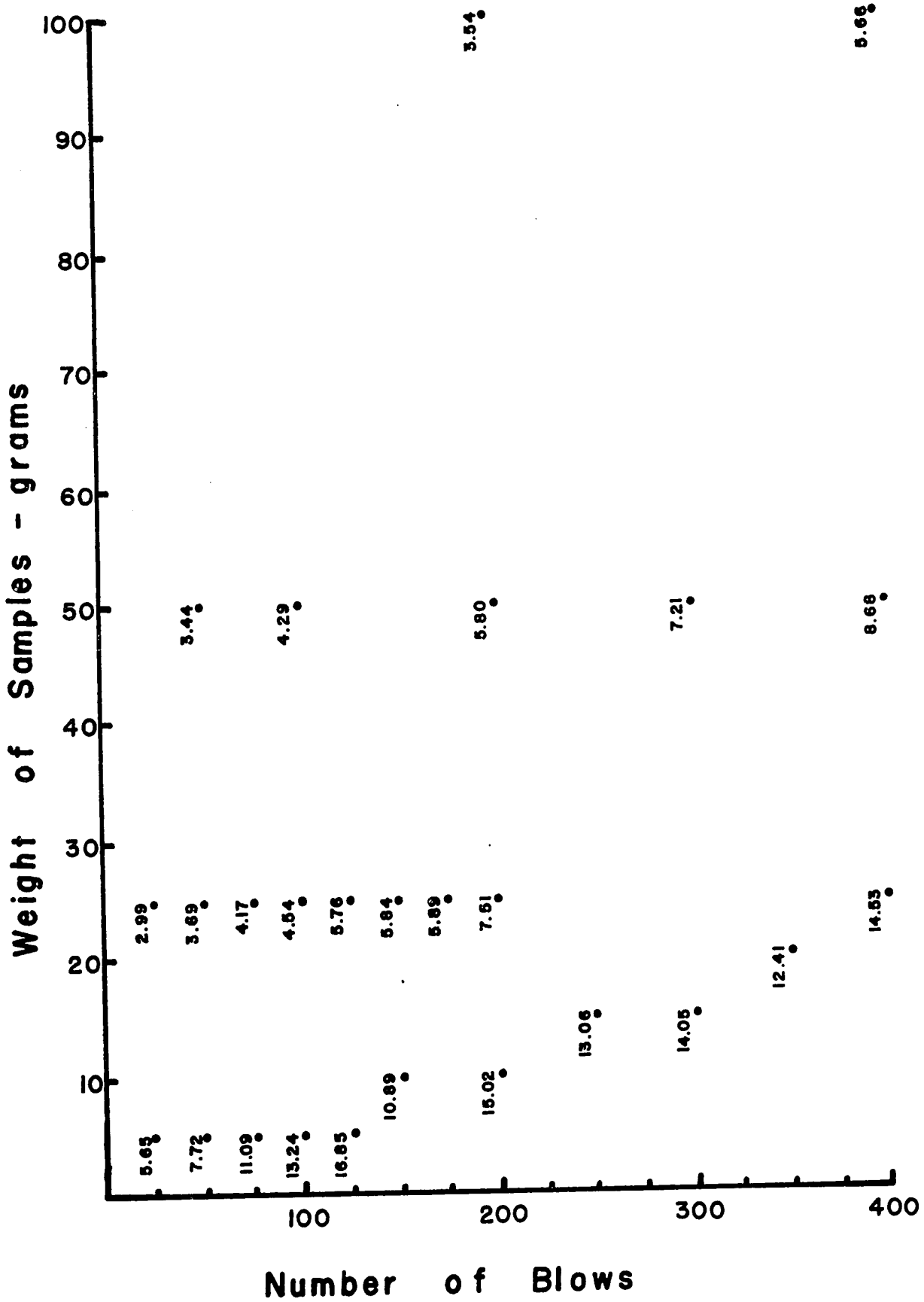

Fig.510-6, CUMULATIVE % WEIGHT (-200 MESH)

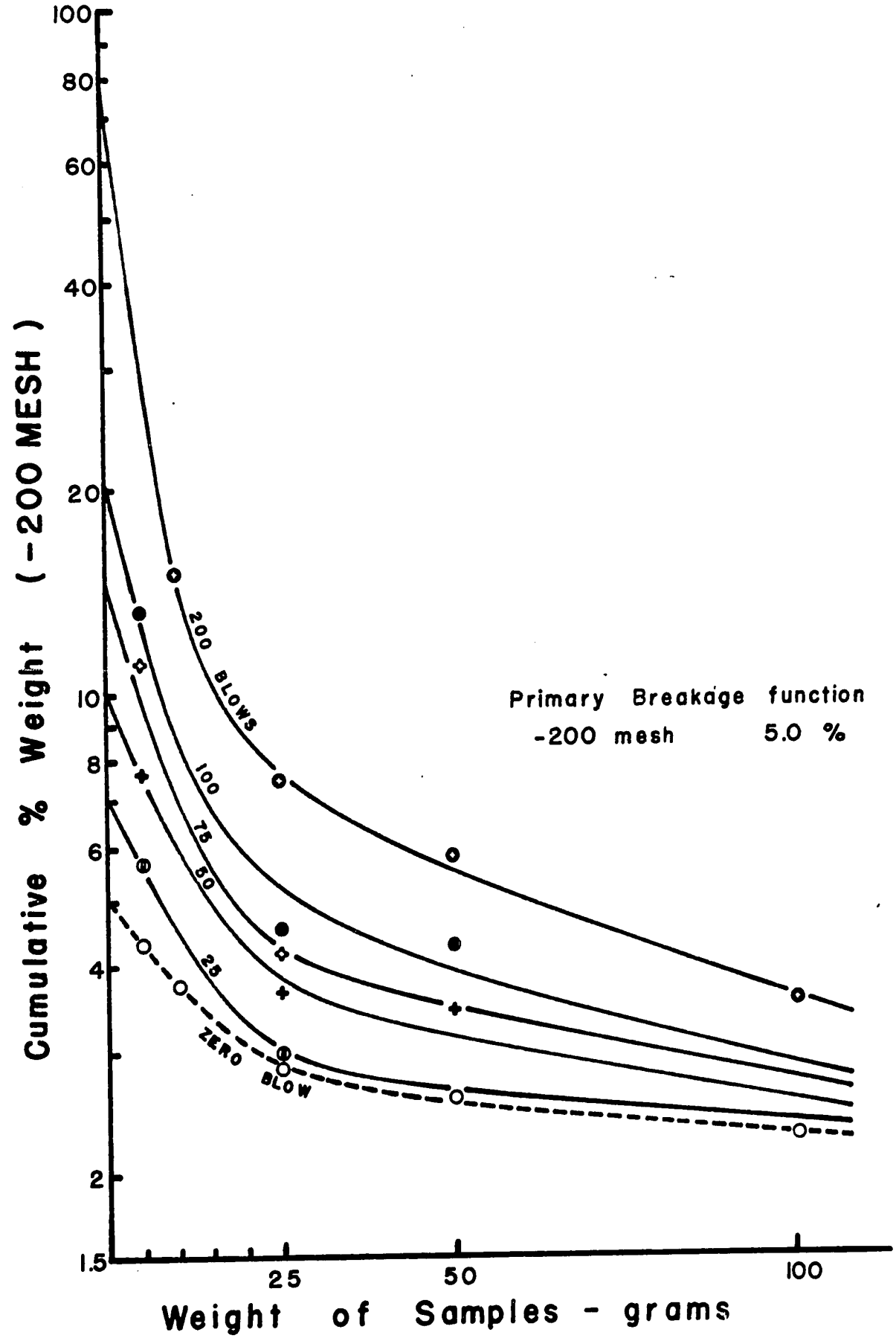

Fig.5.11-6 EXTRAPOLATION TO ZERO GRAM

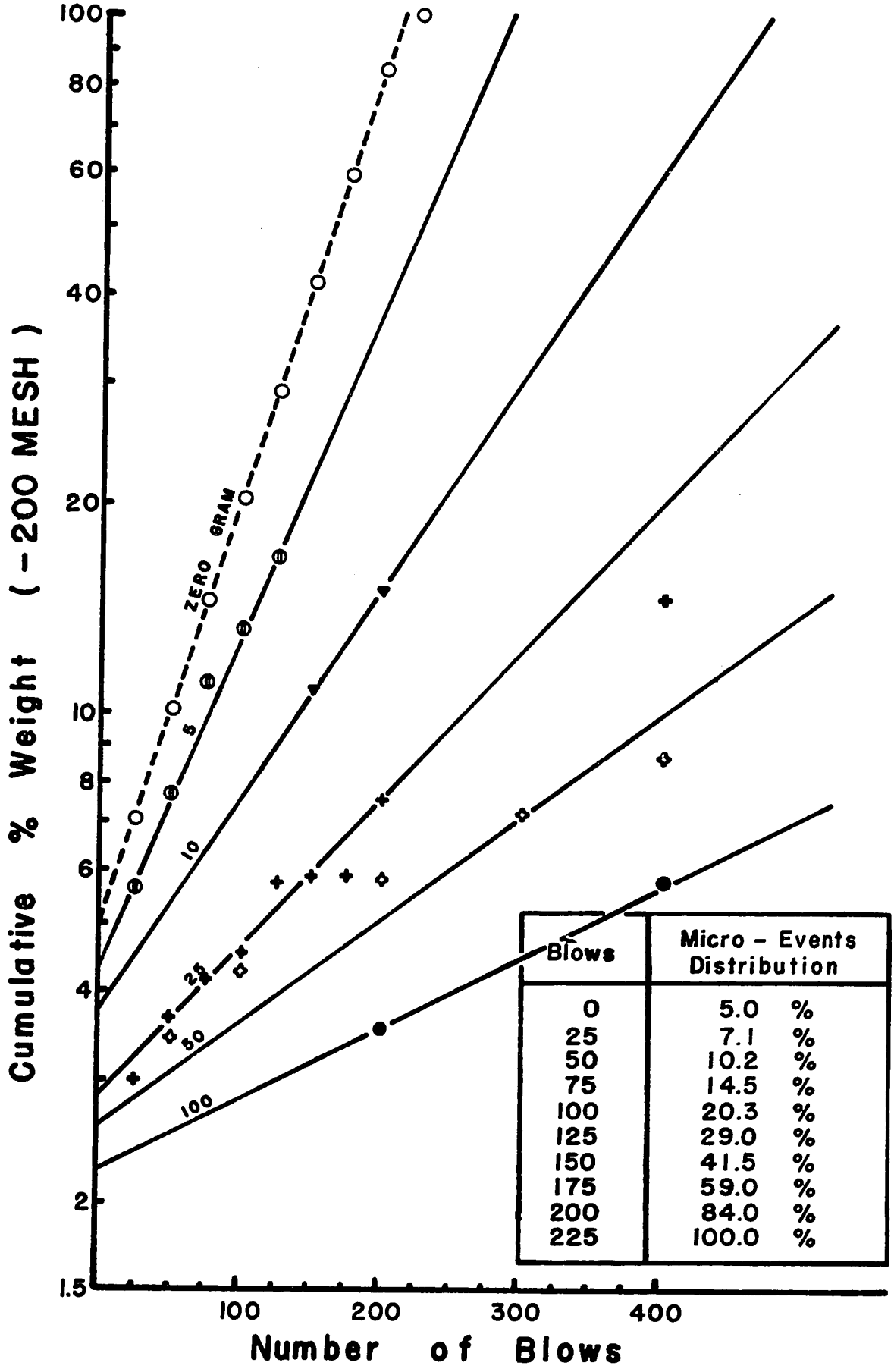

Fig.5.12-6 EXTRAPOLATION TO ZERO BLOW

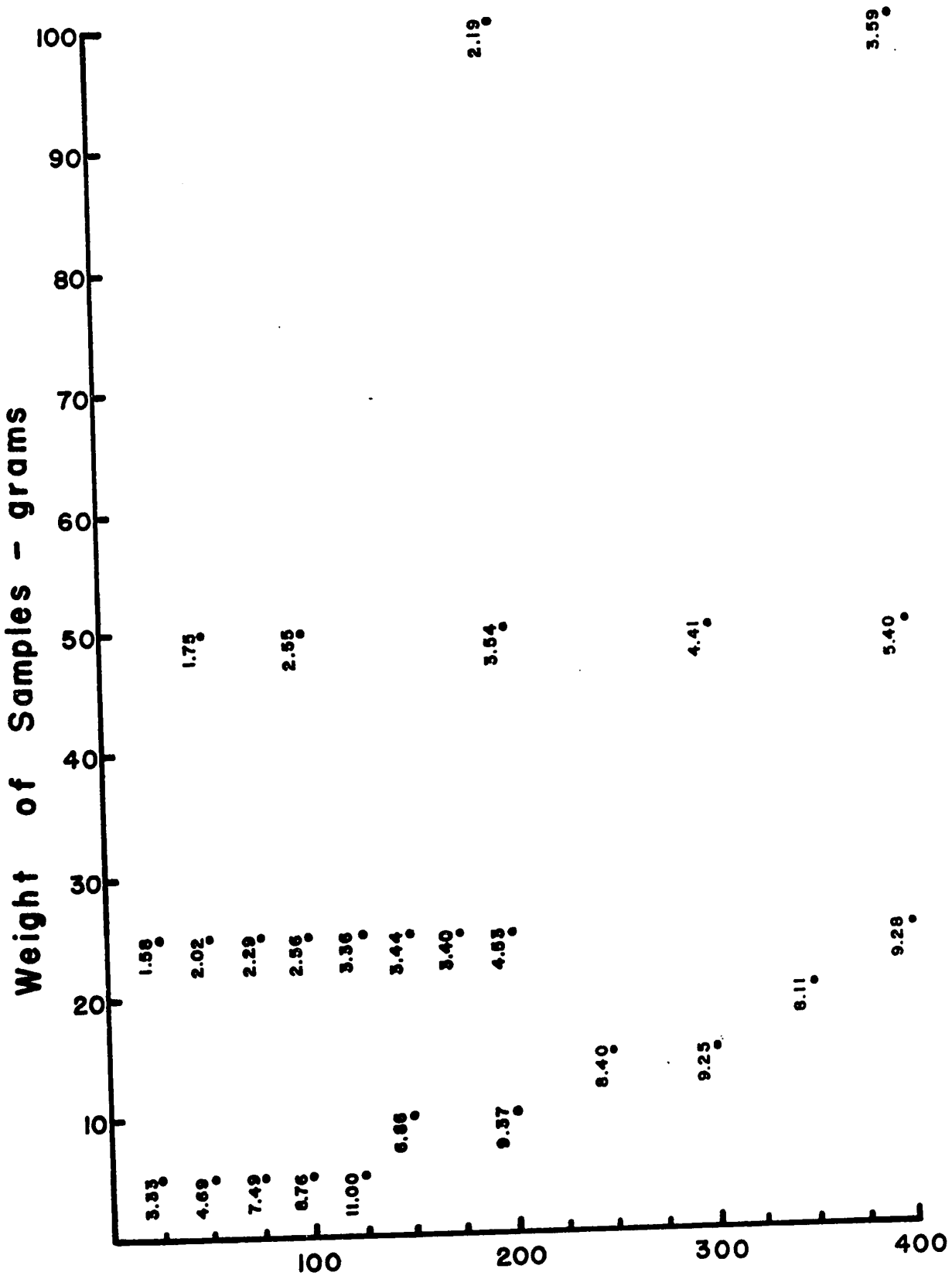

Fig. 5.10-7, CUMULATIVE % WEIGHT (-325 MESH)

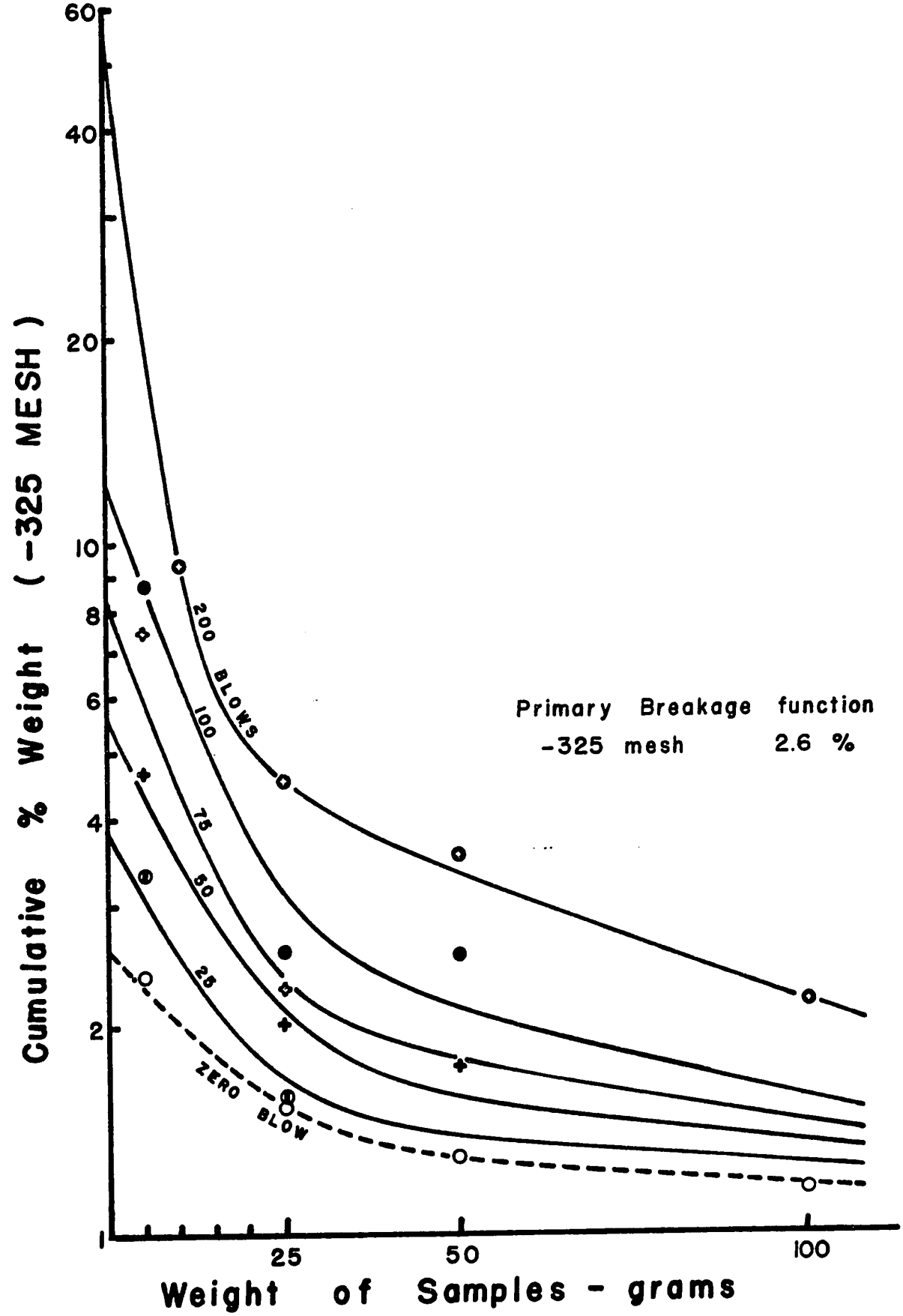

Fig.5.11-7 EXTRAPOLATION TO ZERO GRAM

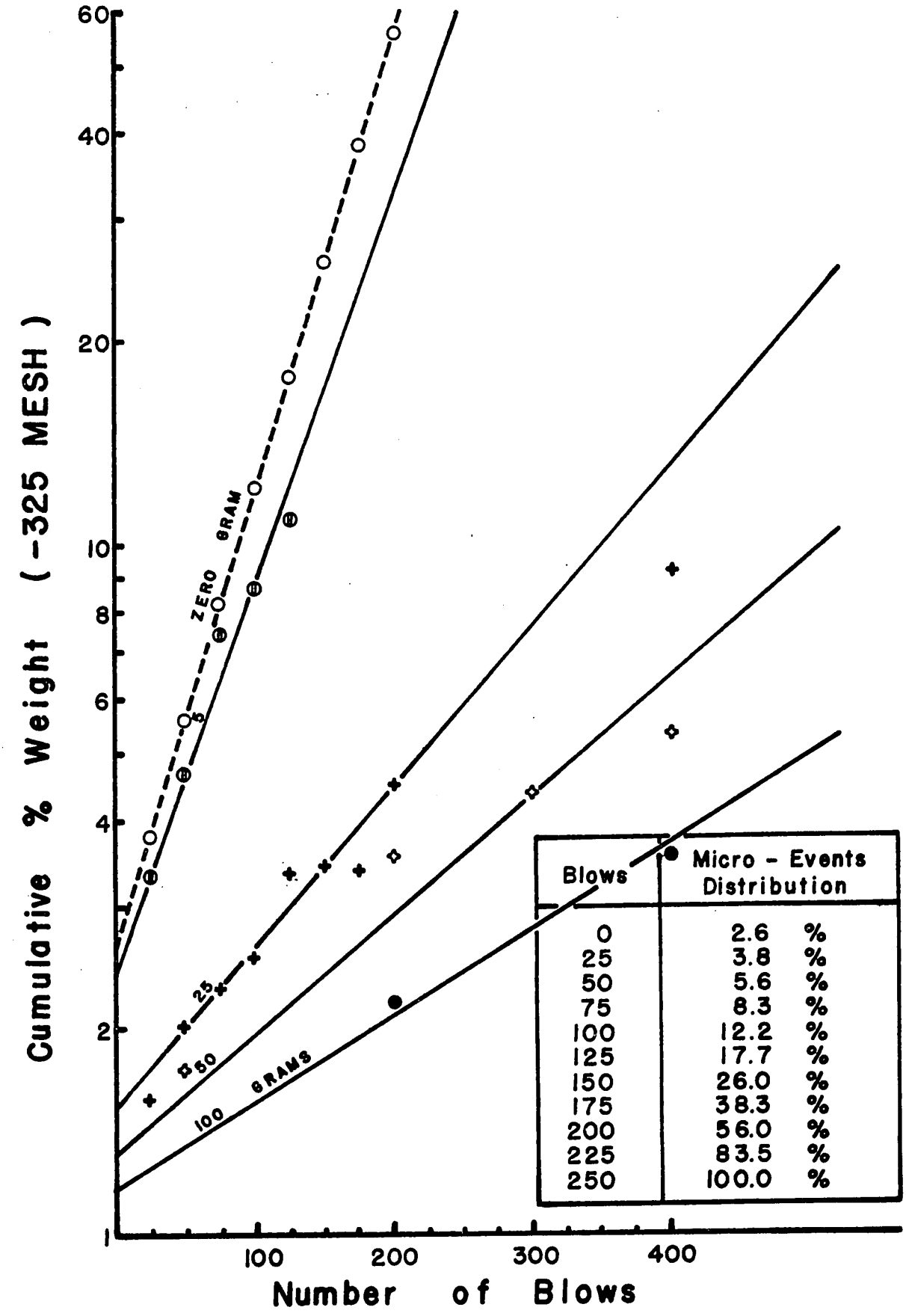

Fig.5.12-7 EXTRAPOLATION TO ZERO BLOW

APPENDIX D

ADDITIONAL DATA ON

SPECIFIC DRILLING VARIABLES

N.B. The number of the figures in the Appendix corresponds to a related figure in the main text of this thesis.

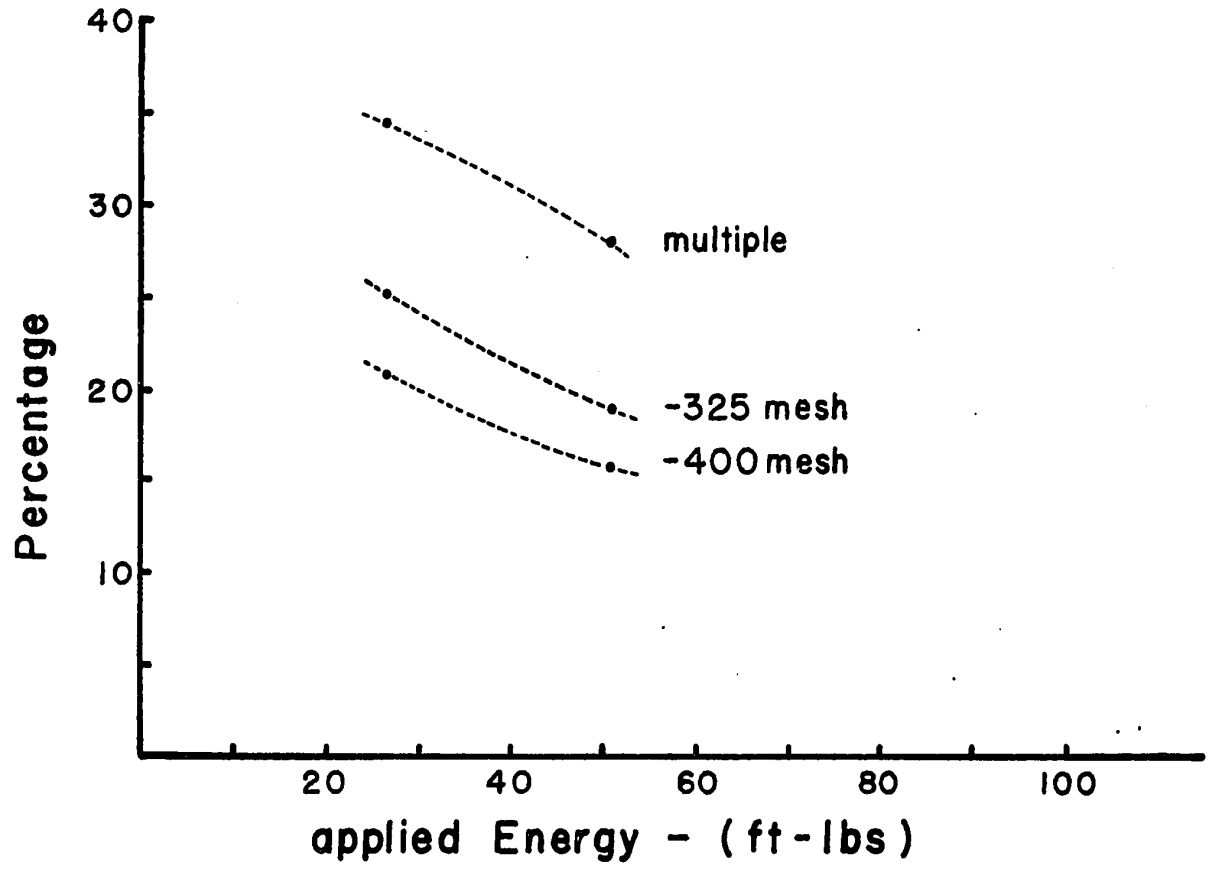

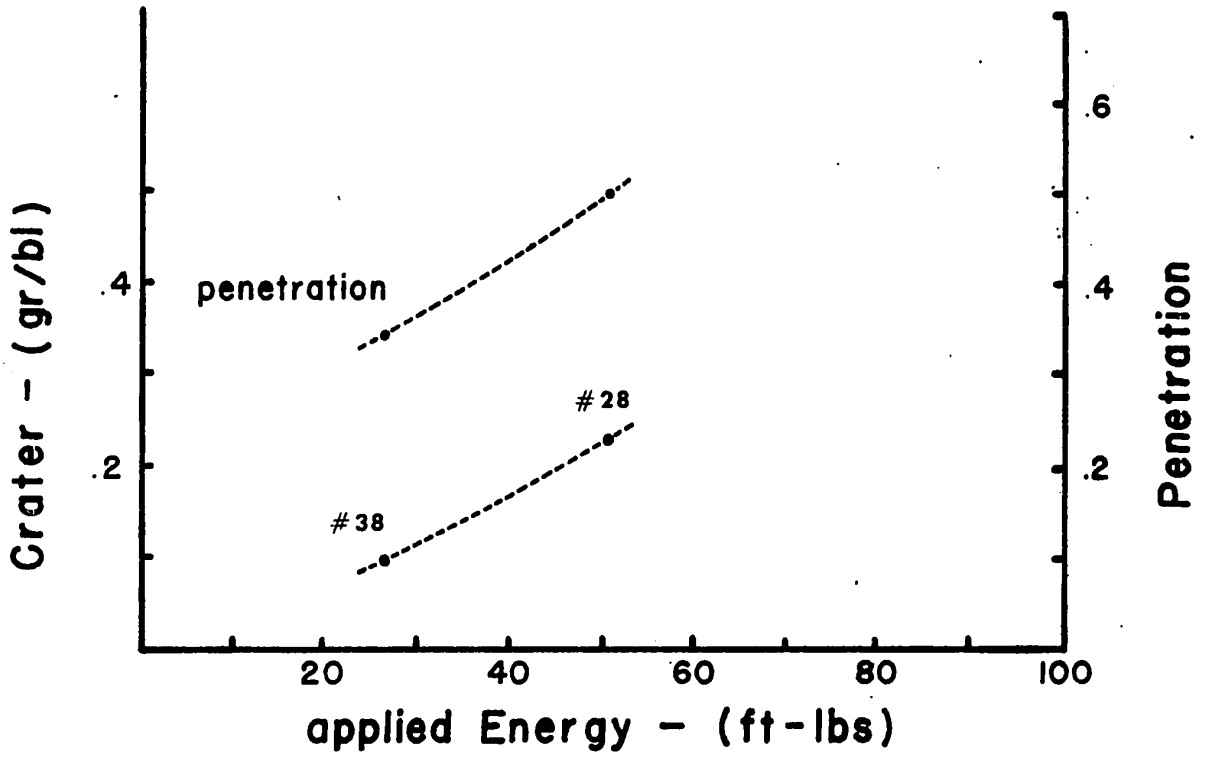

Fig. 6.7-1, ENERGY SERIES - CONSTANT IMPACT WEIGHT

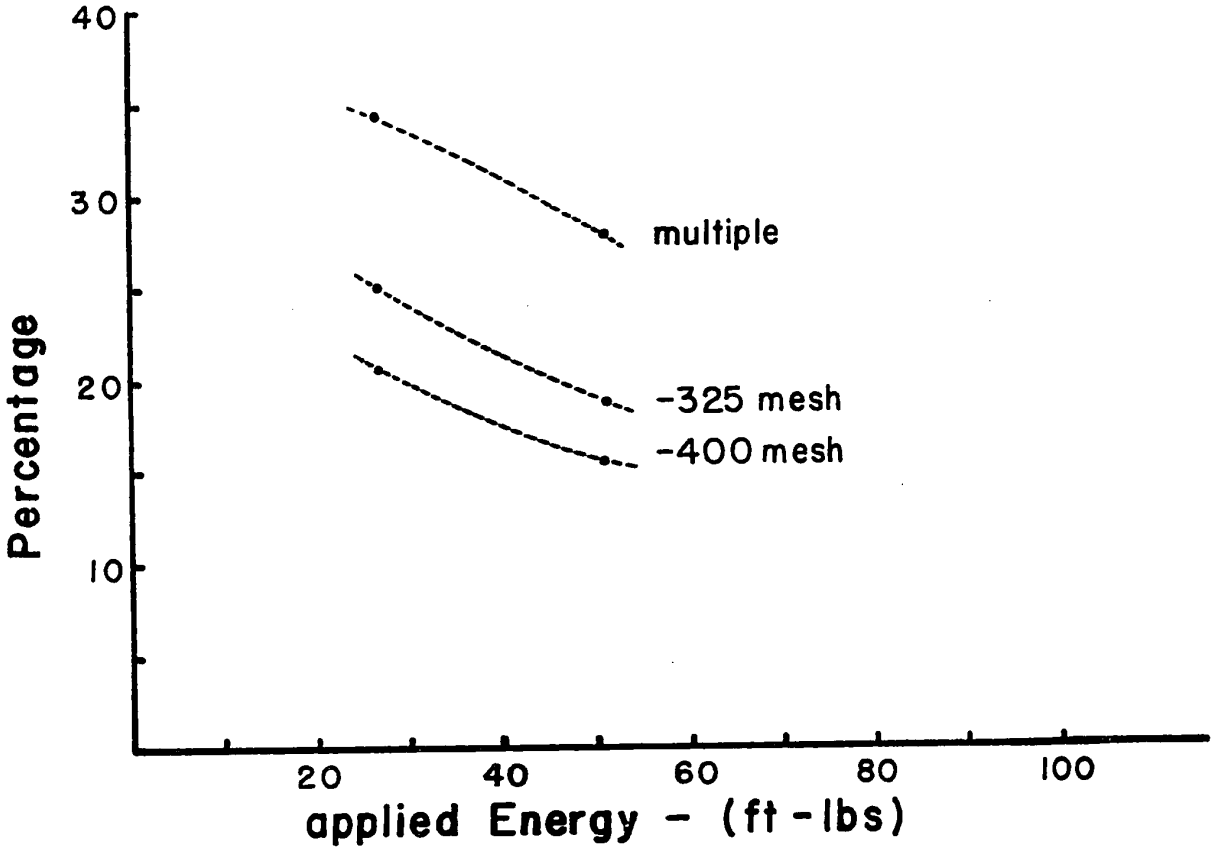

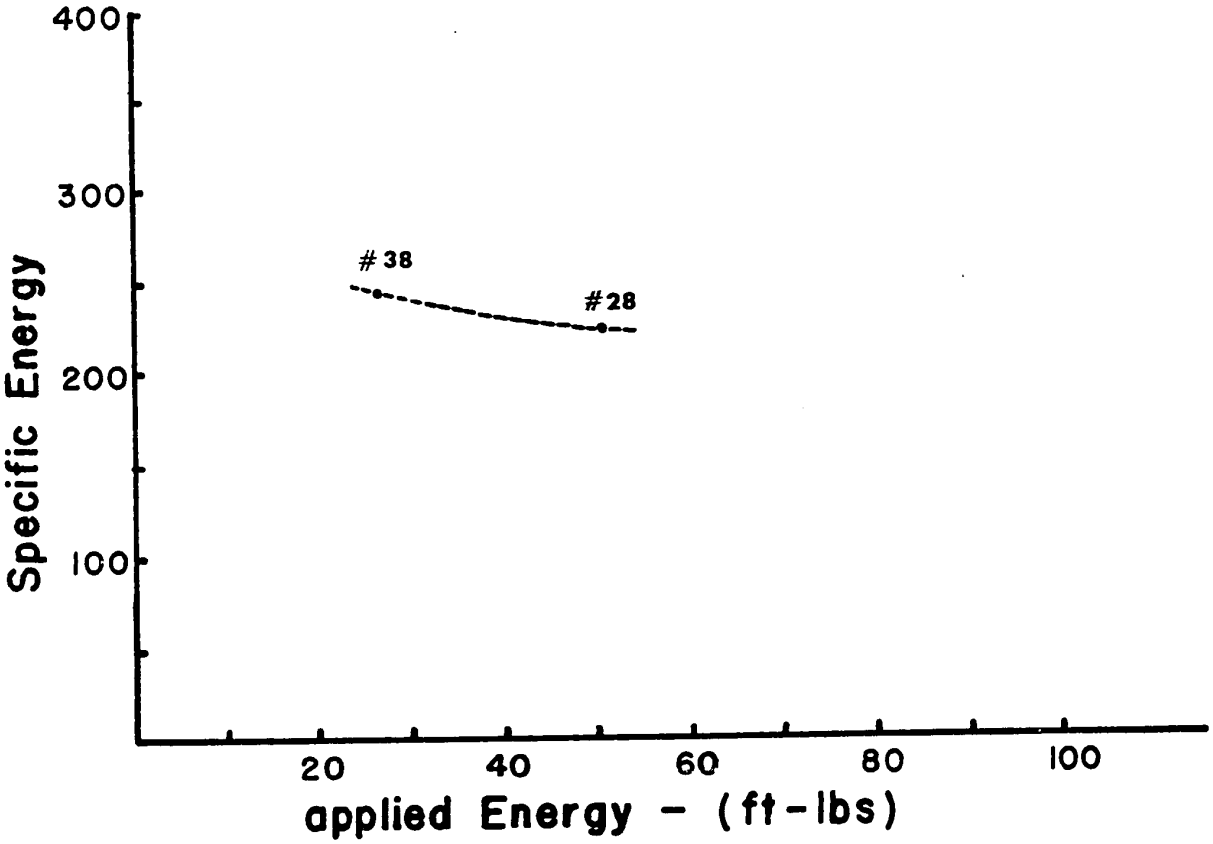

Fig.6.8-1, ENERGY SERIES - CONSTANT IMPACT WEIGHT

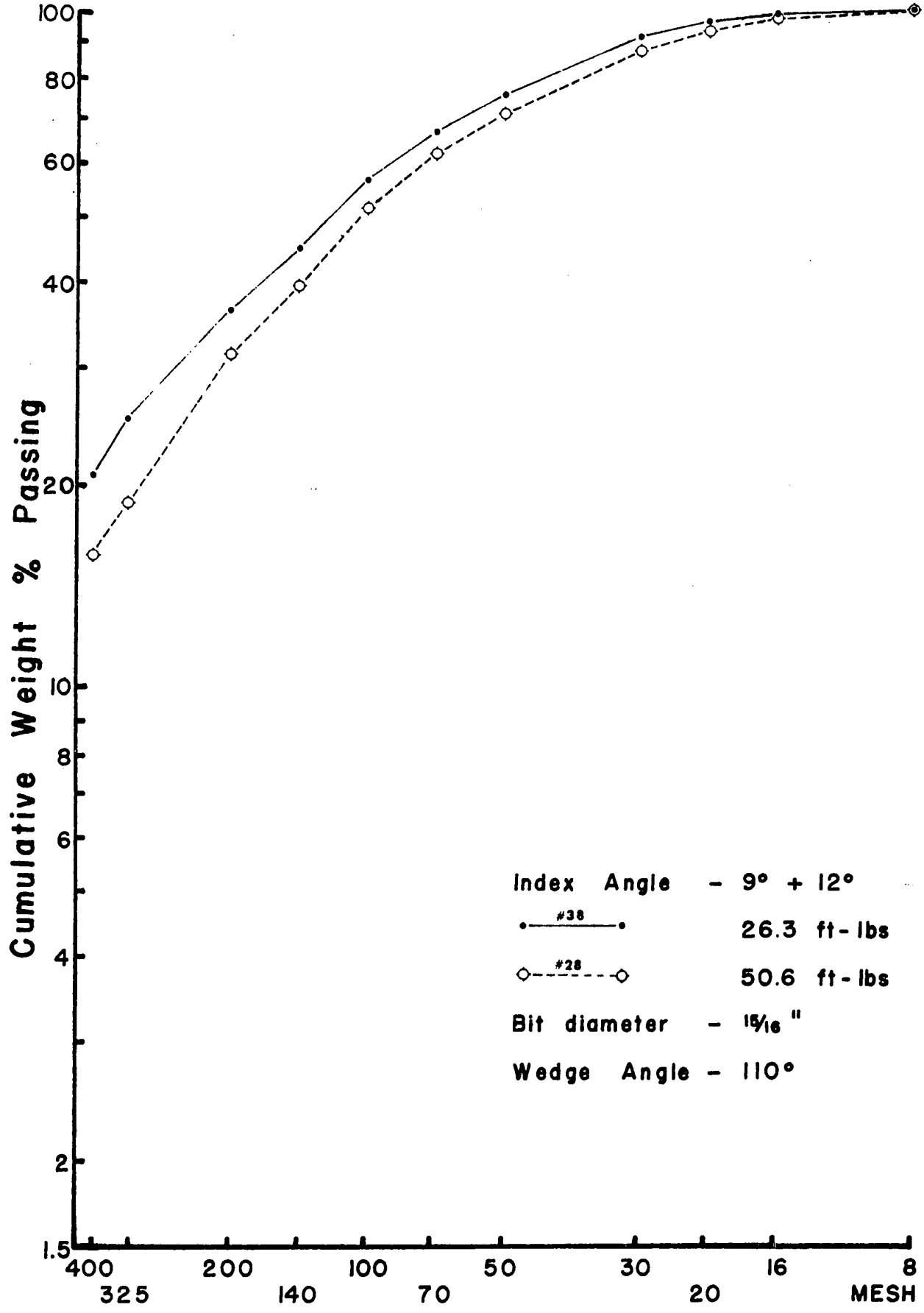

Fig. 6.13-1 ENERGY SERIES - CONSTANT IMPACT WEIGHT

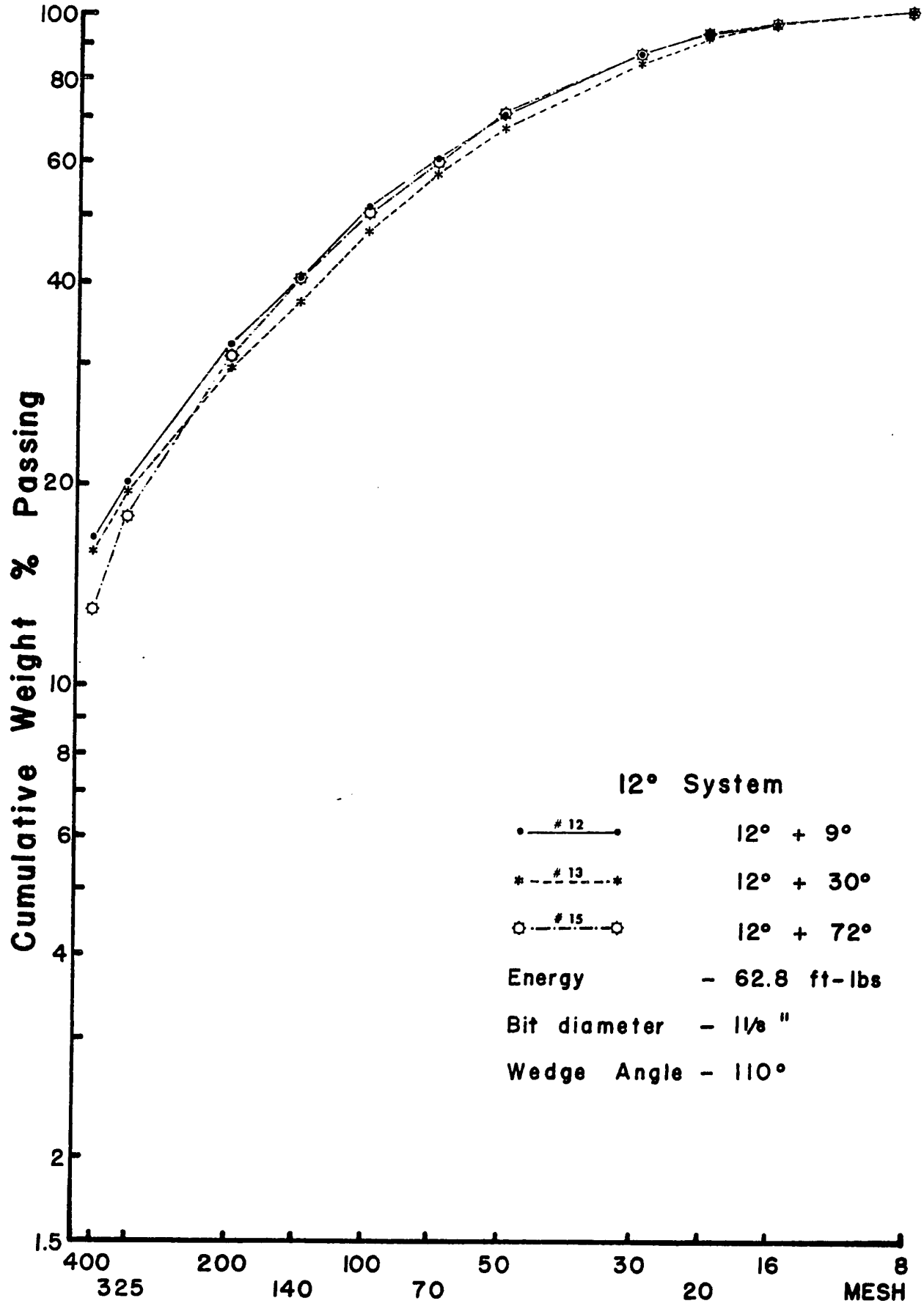

Fig. 6.15-1 INDEX ANGLE SERIES

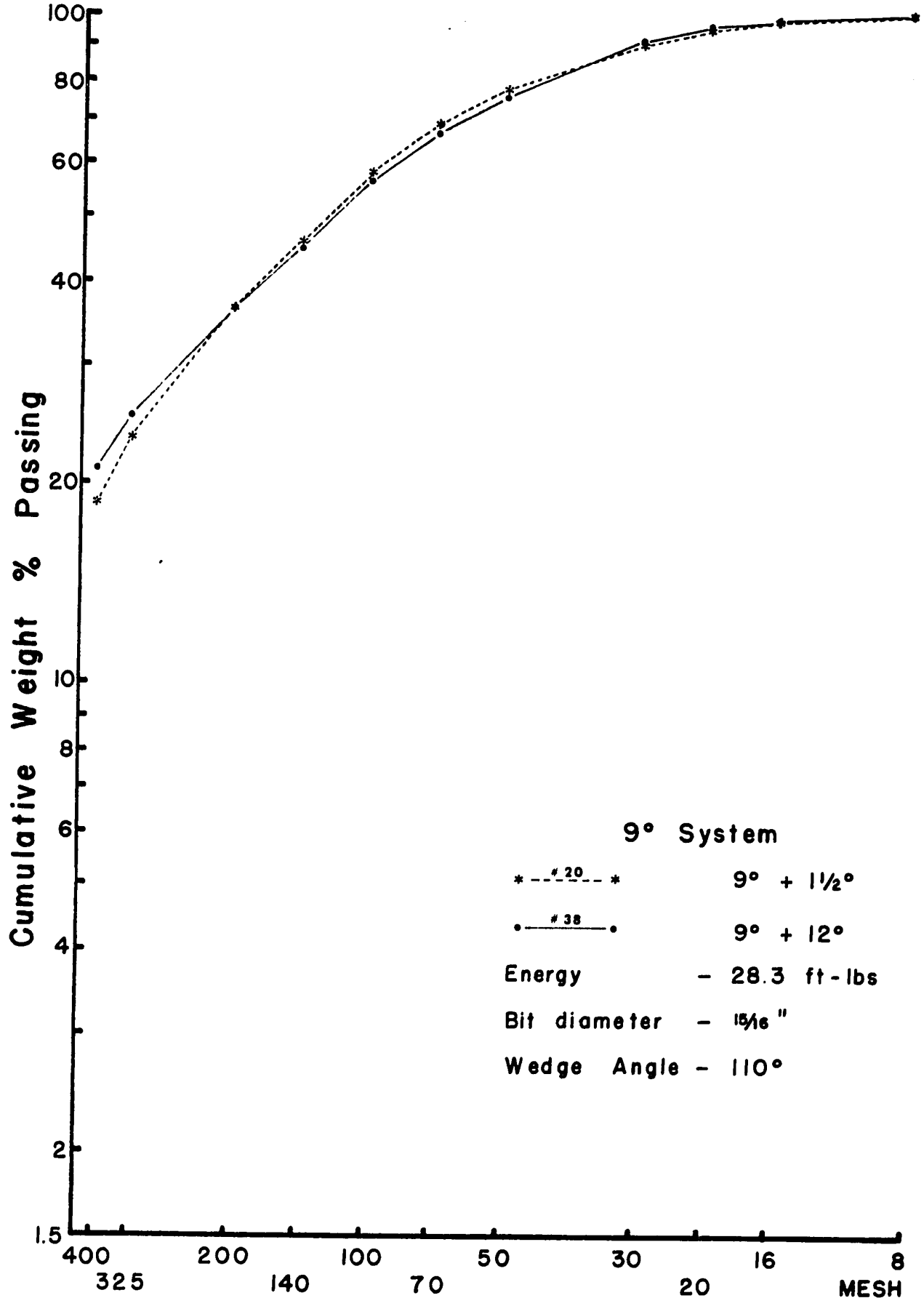

Fig.6.15-2, INDEX ANGLE SERIES

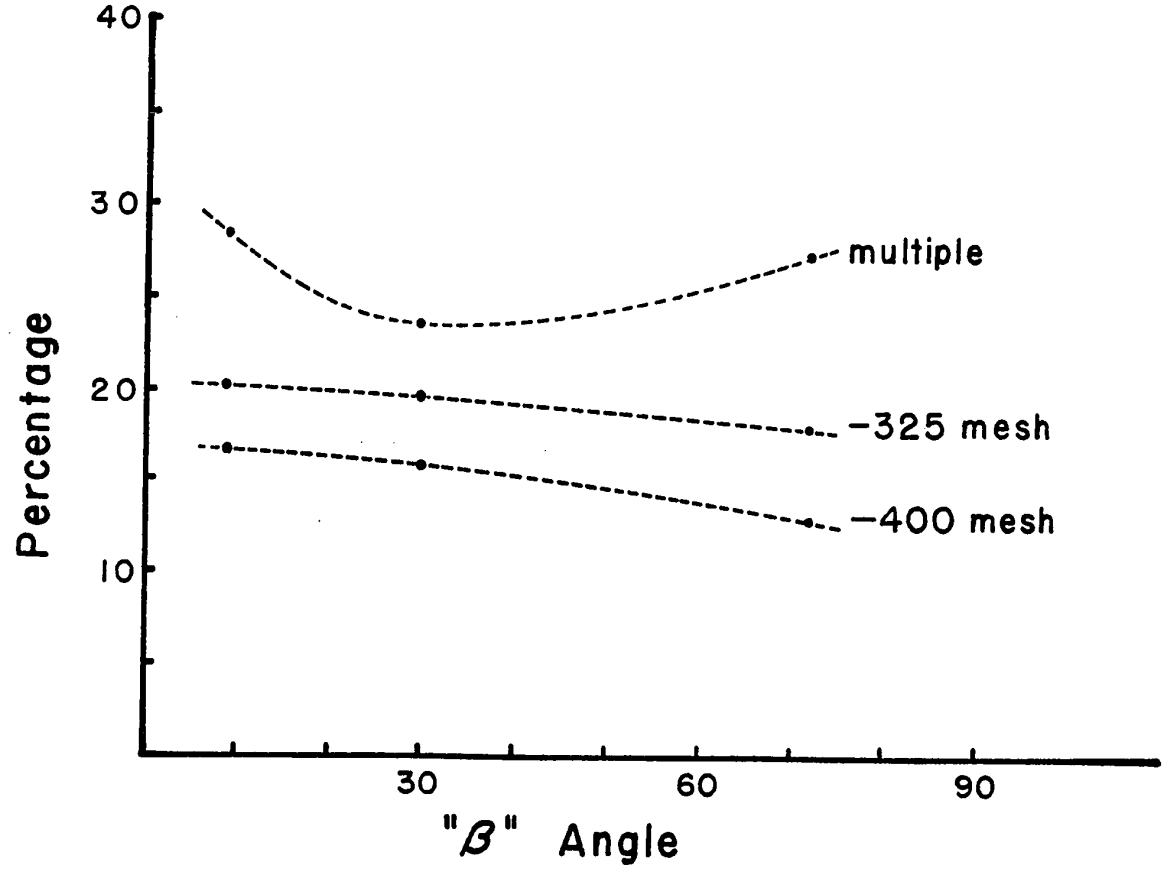

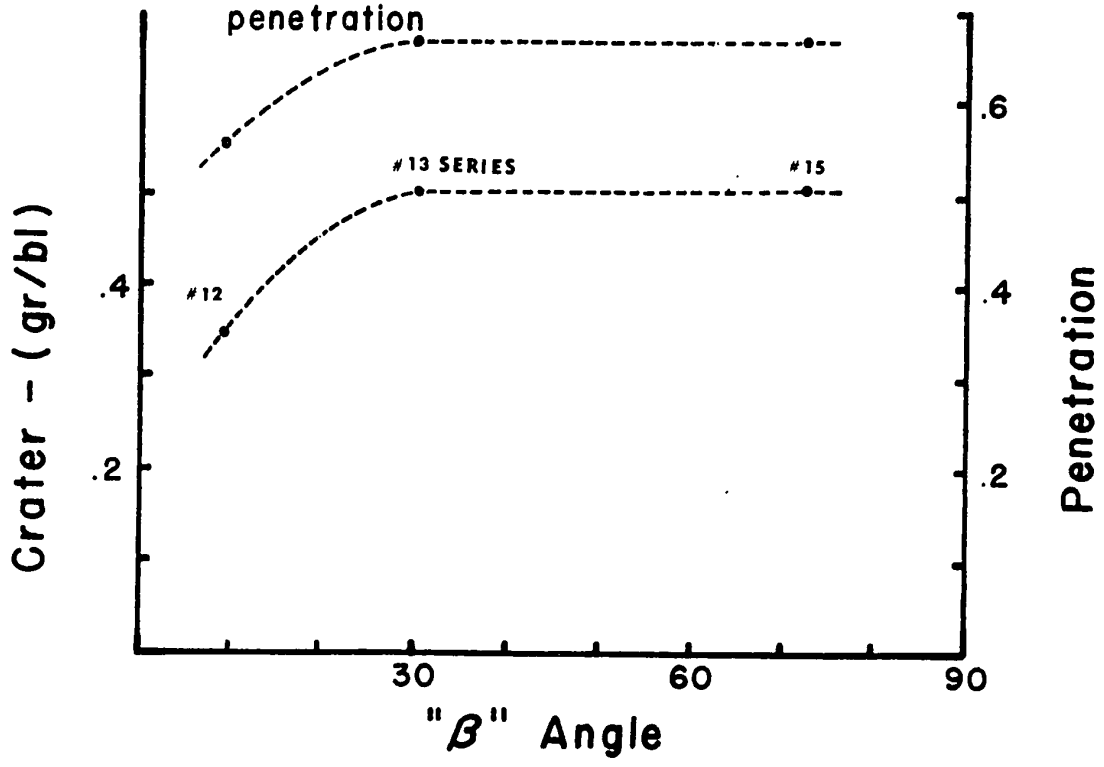

Fig. 6.16-1 INDEX ANGLE SERIES - 12° SYSTEM

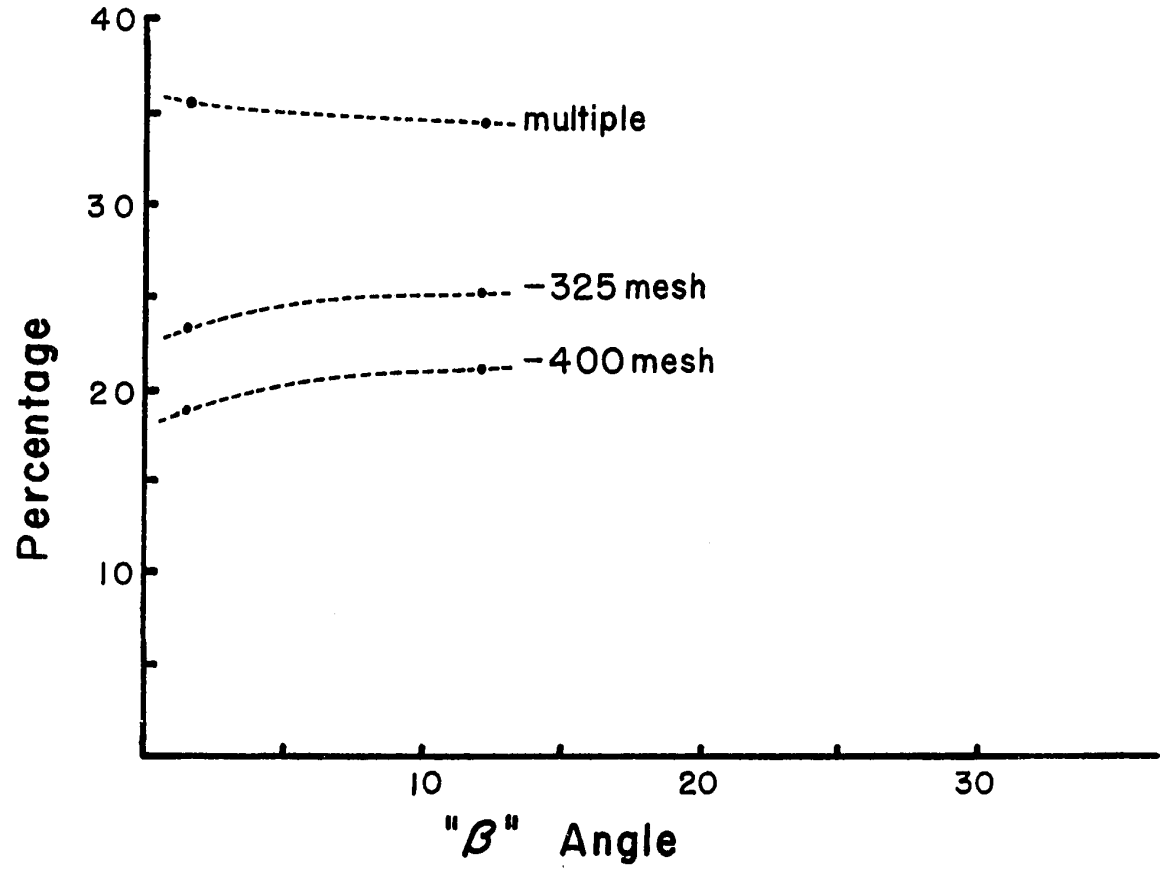

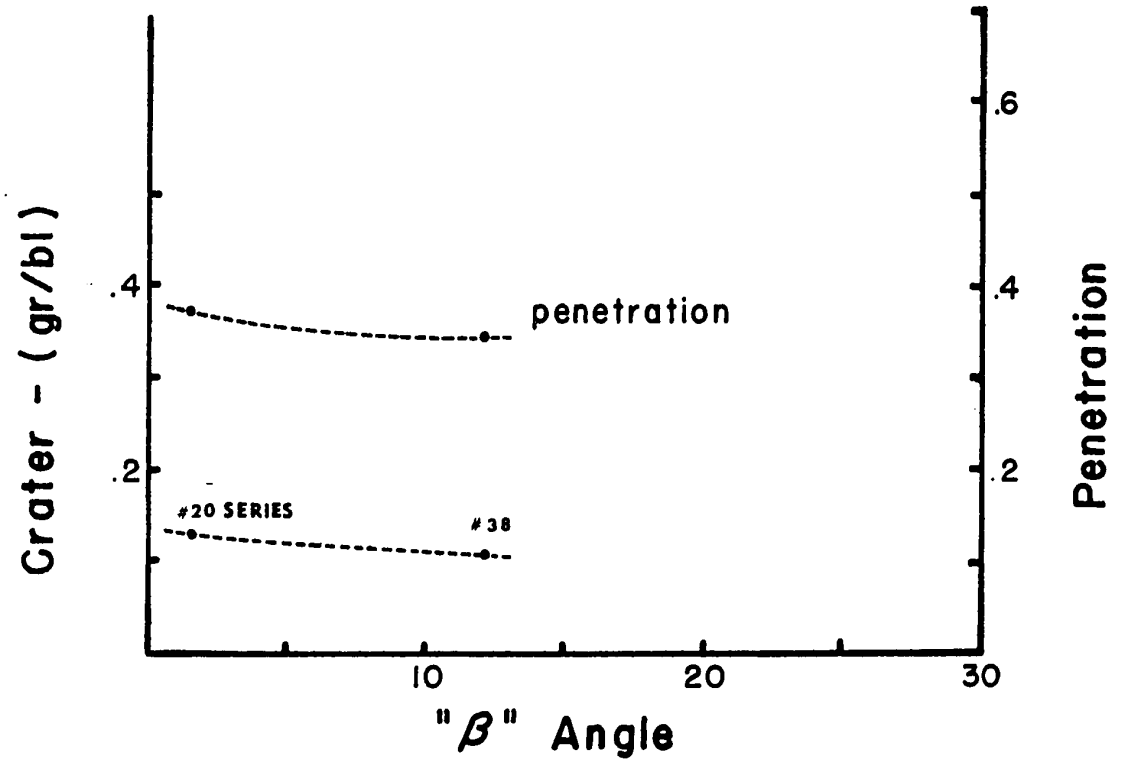

Fig.6.16-2,INDEX ANGLE SERIES - 9° SYSTEM

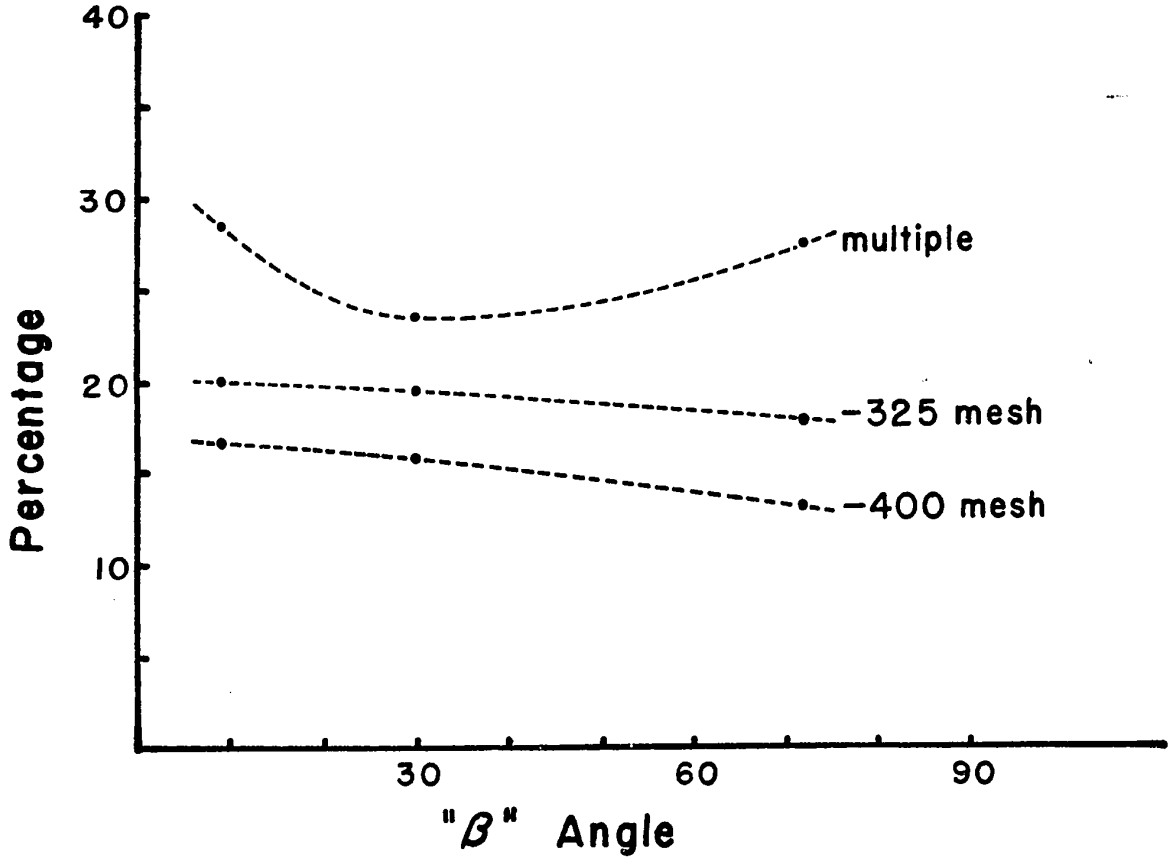

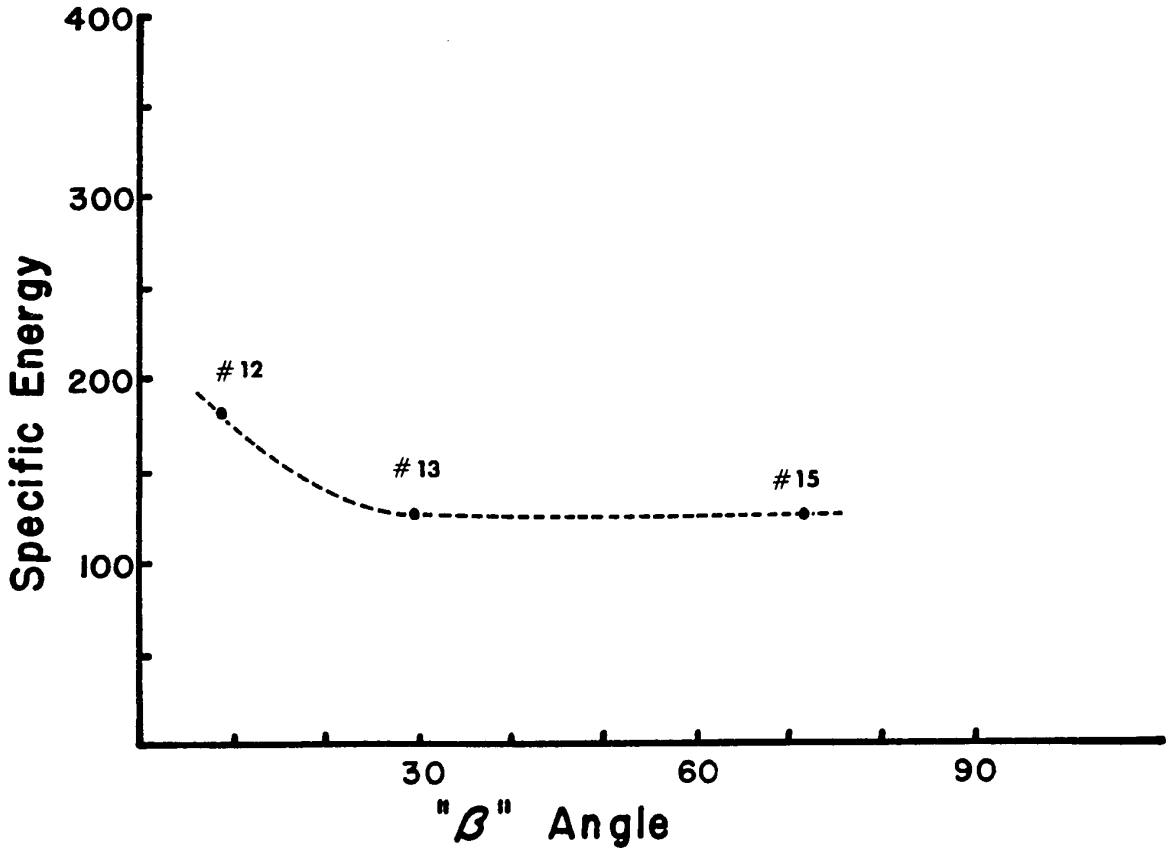

Fig.6.17-1 INDEX ANGLE SERIES - 12° SYSTEM

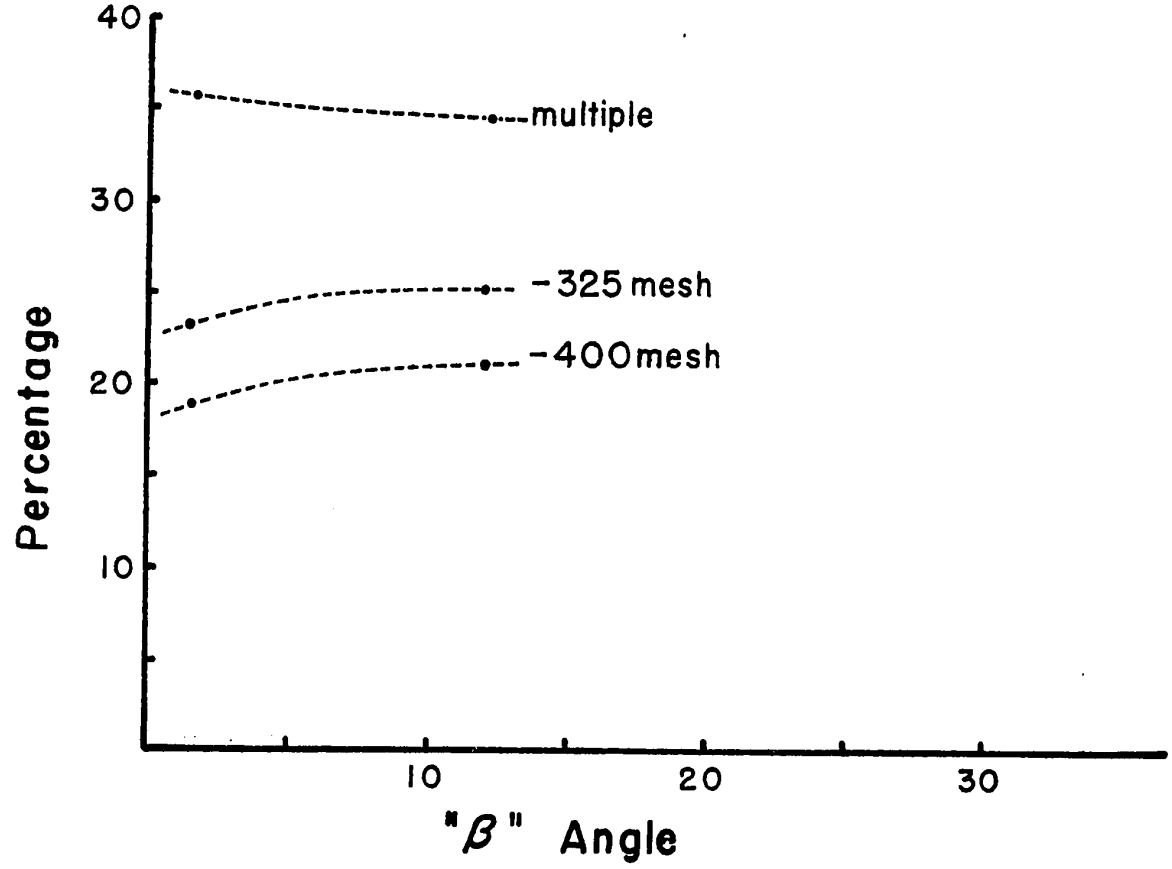

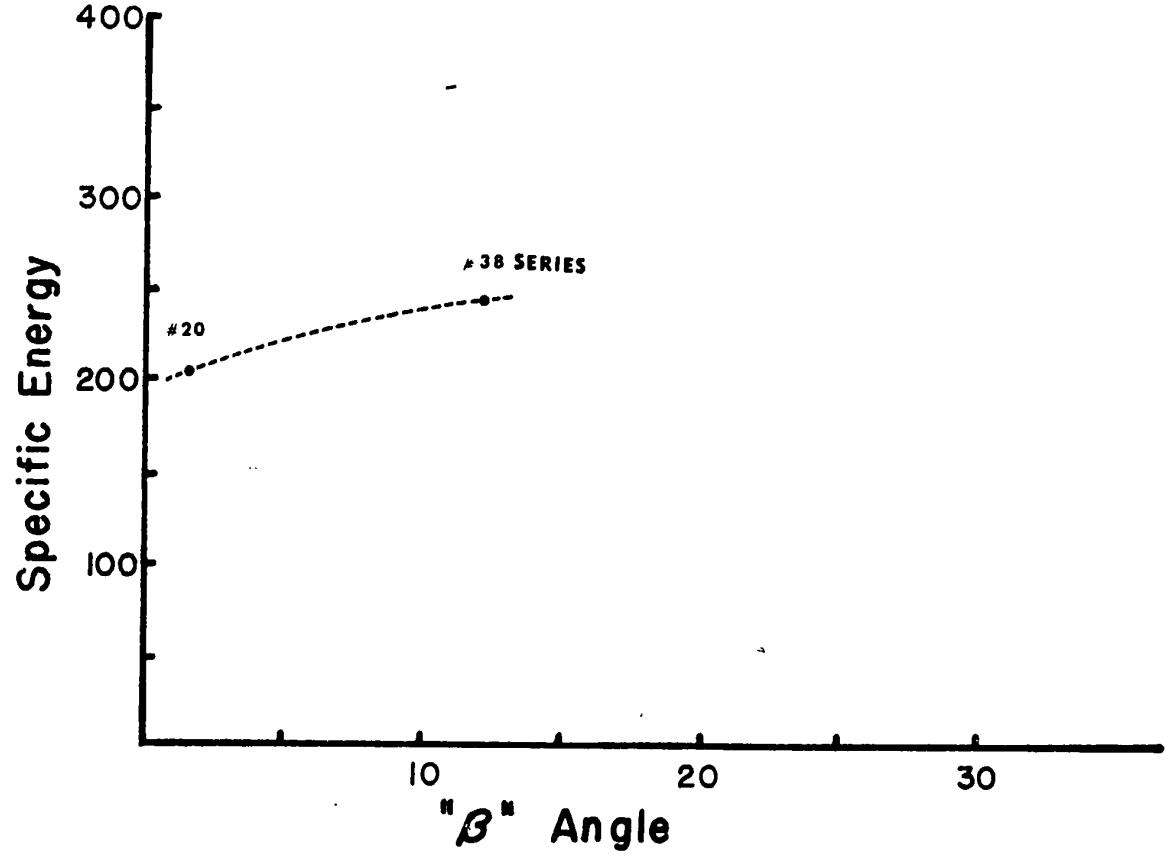

Fig.6.17-2 INDEX ANGLE SERIES - 9° SYSTEM

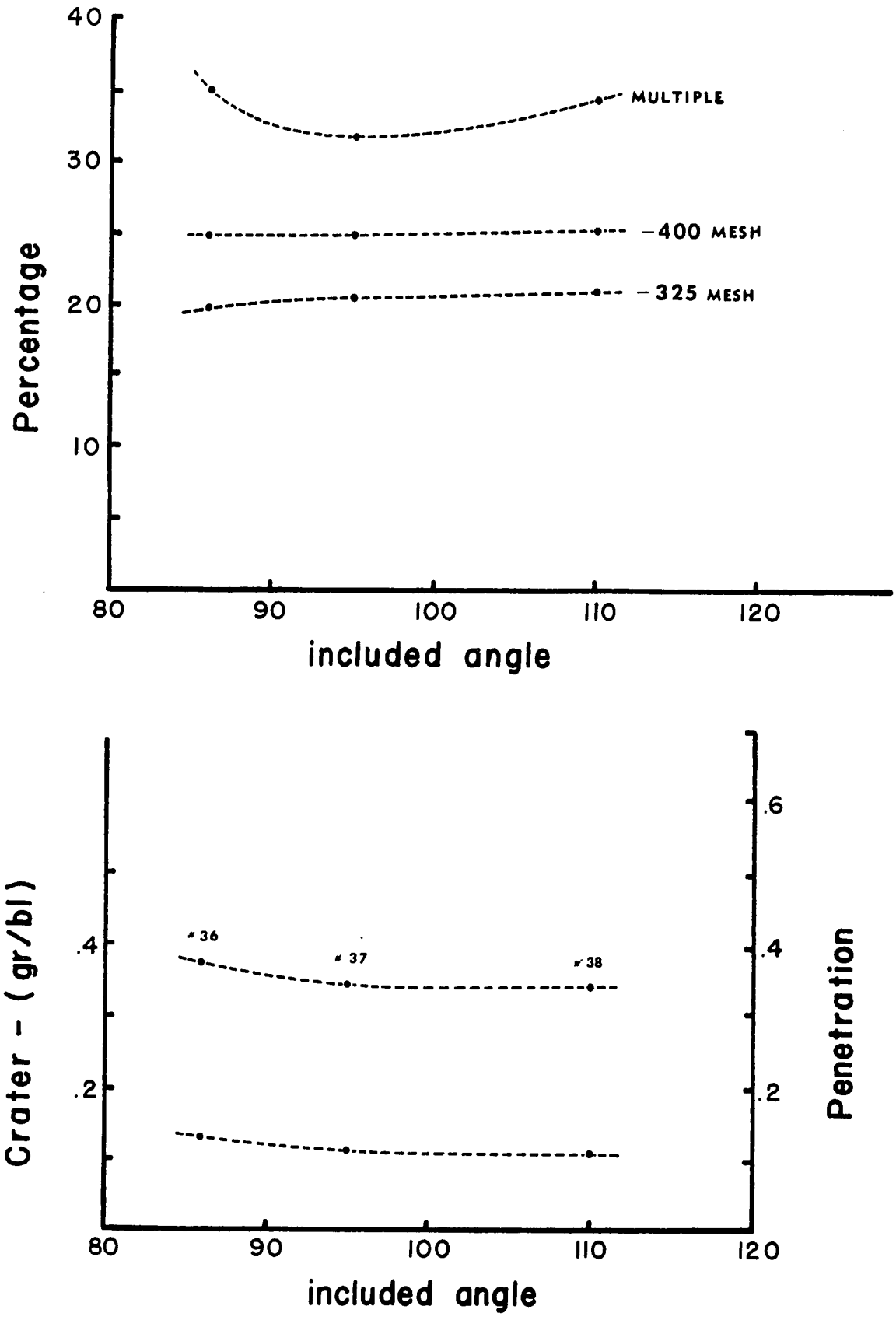

Fig.6.19-1 BIT INCLUDED ANGLE SERIES

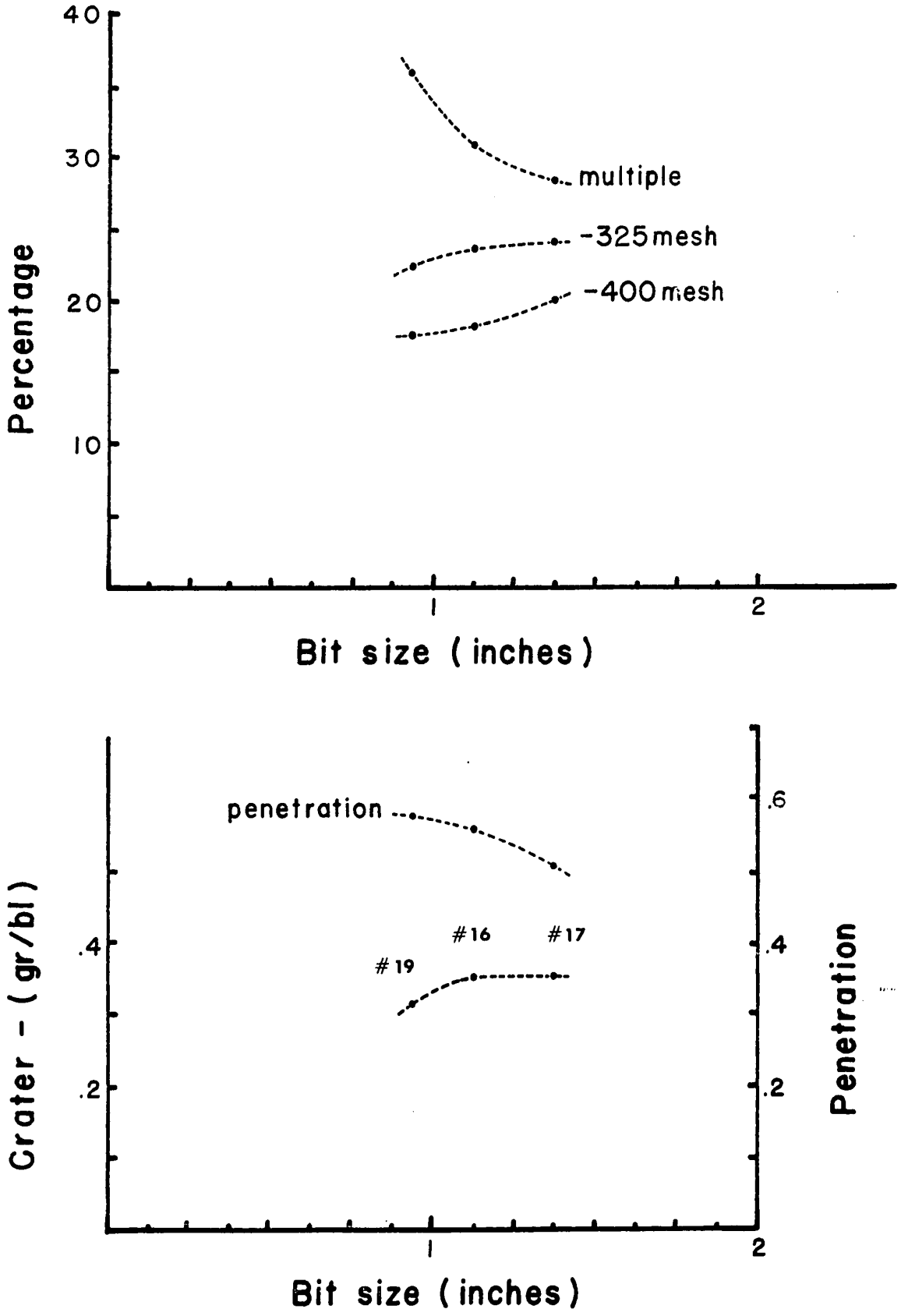

Fig. 6.22-1 BIT SIZE SERIES

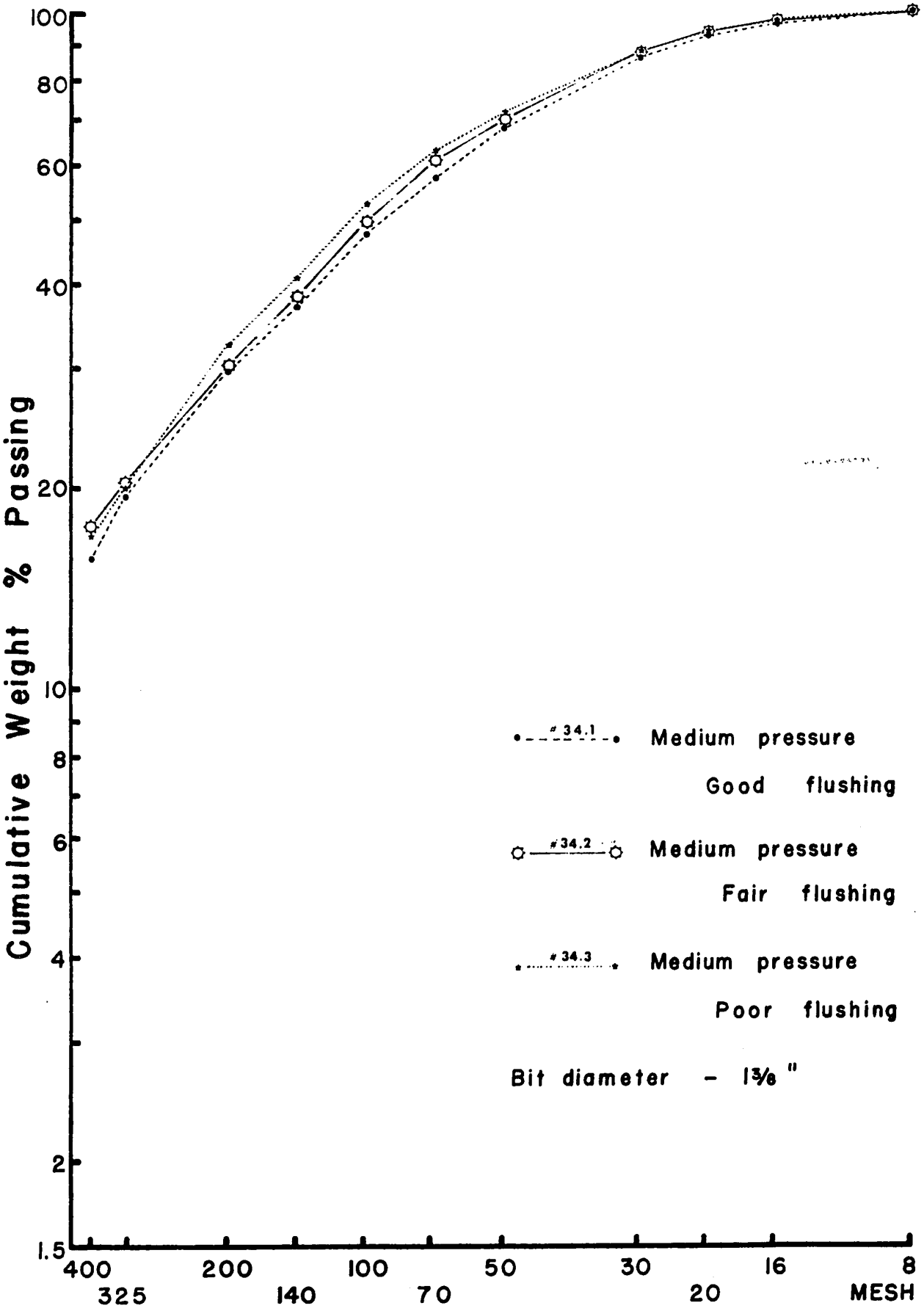

Fig. 6.24-1 ACTUAL DRILLING TESTS

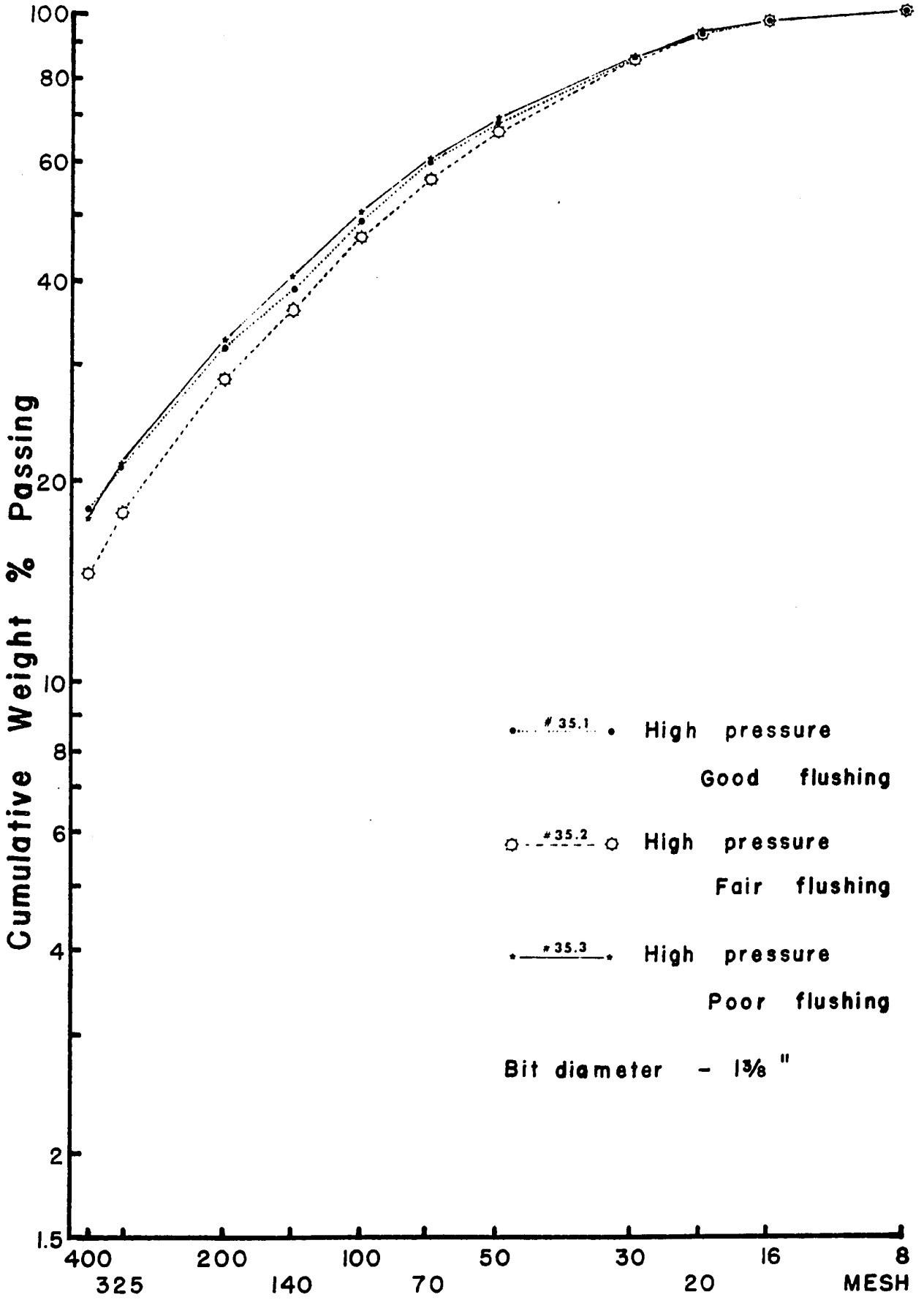

Fig. 6.24-2 ACTUAL DRILLING TESTS